GeoStudio

Stability Modeling with GeoStudio

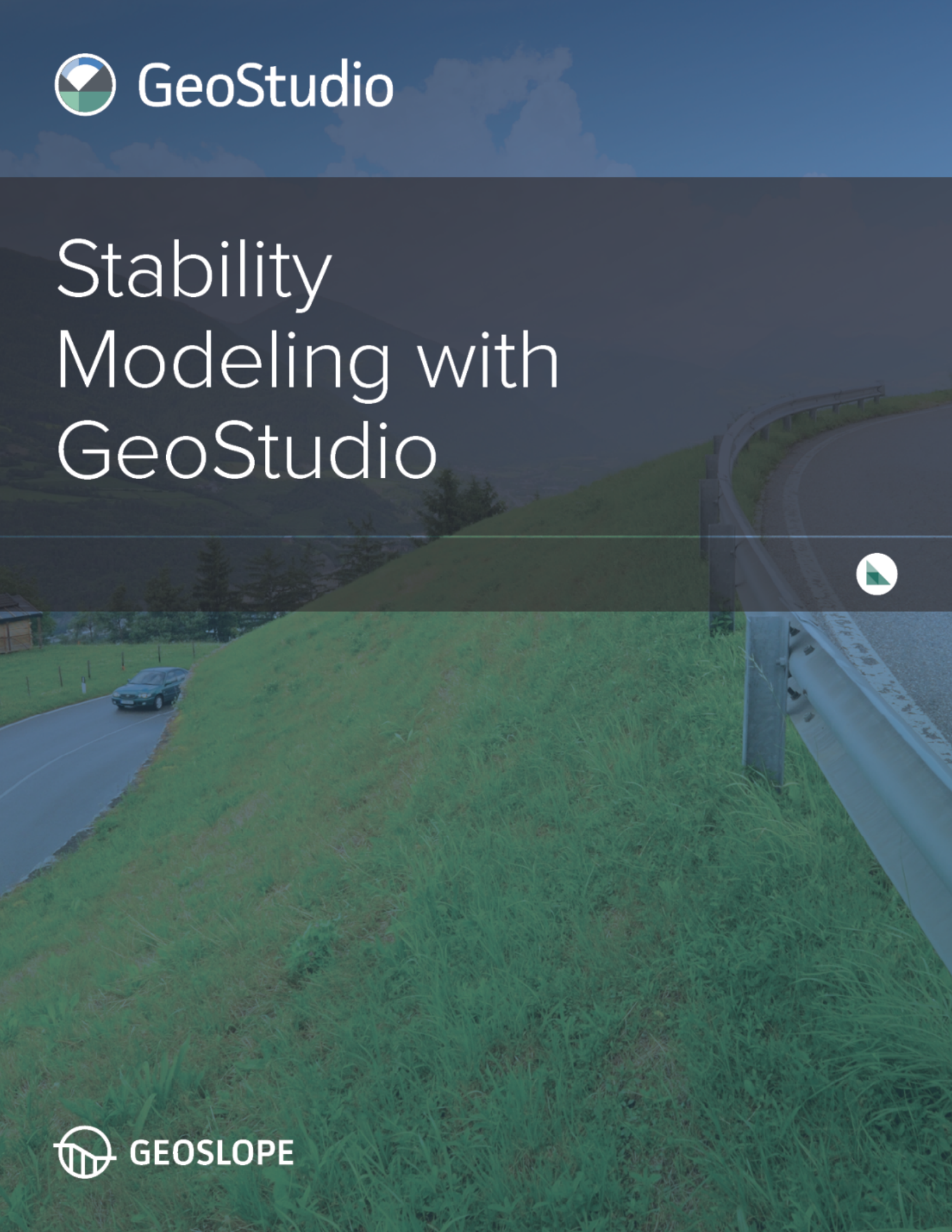

GEOSLOPE

Copyright © 2004-2020 by GEO-SLOPE International, Ltd.

All rights reserved. No part of this work may be reproduced or transmitted in any form or by any means, electronic or mechanical, including photocopying, recording, or by any information storage or retrieval system, without the prior written permission of GEO-SLOPE International, Ltd.

Trademarks: GEO-SLOPE, GeoStudio, SLOPE/W, SEEP/W, SIGMA/W, QUAKE/W, CTRAN/W, TEMP/W, AIR/W and VADOSE/W are trademarks or registered trademarks of GEO-SLOPE International Ltd. in Canada and other countries. Other trademarks are the property of their respective owners.

GEO-SLOPE International Ltd

1200, 700 - 6th Ave SW,

Calgary, AB, Canada T2P 0T8

E-mail: info@geo-slope.com

Web: http://www.geo-slope.com

Table of Contents

1 Introduction 1

2 Limit Equilibrium Fundamentals 5

2.1 Introduction 5
2.2 Background and history 5
2.3 Method basics 6
2.4 General limit equilibrium formulation 7
2.5 Interslice force functions 11
2.6 Slip surface shapes 11
Circular slip surface 11
Planar slip surface 12
Composite slip surface 13
Block slip surface 13
Shoring wall 14
2.7 Stress distributions 15
2.8 Limit equilibrium forces and stresses 20
2.9 Janbu generalized method 20
2.10 Missing physics 21
2.11 Other limitations 21
2.12 Slip surface shapes 22
2.13 Seepage forces 23
2.14 Concluding remarks 24

3 Factor of Safety Methods 27

3.1 Introduction 27
3.2 General limit equilibrium Formulation 27
3.3 Ordinary or Fellenius method 31
3.4 Bishop's simplified method 34
3.5 Janbu's simplified method 36
3.6 Spencer method 37
3.7 Morgenstern-Price method 40
3.8 Corps of Engineers method 43
Interslice assumption one 43
Interslice assumption two 44
3.9 Lowe-Karafiath method 46

3.10 Sarma method....48
3.11 Janbu's Generalized method....49
3.12 Finite element stress-based method....51
3.13 Commentary on finite element stress-based method....56
3.14 Selecting an appropriate method....57
3.15 Rapid Drawdown Analysis Methods....58
The Simple Effective Strength Method....59
The Rigorous Effective Strength Method....59
The Staged Undrained Strength Method....60

4 Slip Surface Shapes....63
4.1 Introduction and background....63
4.2 Grid and radius for circular slips....63
Single radius point....65
Multiple radius points....66
Lateral extent of radius lines....66
Factor of Safety contours....67
4.3 Composite slip surfaces....68
4.4 Fully specified slip surfaces....71
4.5 Block specified slip surface....73
General cross-over form....73
Specific parallel form....75
4.6 Entry and exit specification....77
4.7 Optimization....79
4.8 Effect of soil strength....82
Purely frictional case....82
Undrained strength case....84
Cause of unrealistic response....84
Minimum depth....86
Most realistic slip surface position....86
4.9 Tension cracks and exit projections....86
Tension crack angle....86
Constant tension crack depth....87
Tension crack fluid pressures....87
Toe projection....87
4.10 Physical admissibility....88
4.11 Invalid slip surfaces and factors of safety....89

4.12 Concluding remarks 93

5 Geometry 95

5.1 Introduction 95

5.2 Regions 95

5.3 Slice discretization 97

5.4 Ground surface line 99

5.5 Tension crack line 100

5.6 Concentrated point loads 100

5.7 Ponded water 102

5.8 Surface surcharge loads 103

6 Functions in GeoStudio 109

6.1 Spline functions 109

Slopes of spline functions 110

6.2 Linear functions 111

6.3 Step functions 111

6.4 Closed form curve fits for water content functions 112

6.5 Add-in functions 112

6.6 Spatial functions 112

7 Material Strength 115

7.1 Introduction 115

7.2 Mohr-Coulomb 115

7.3 Spatial Mohr-Coulomb model 116

7.4 Undrained strength 117

7.5 High strength 117

7.6 Impenetrable (Bedrock) 117

7.7 Bilinear 117

7.8 General data-point strength function 118

7.9 Anisotropic strength 119

7.10 Strength using an anisotropic function 120

7.11 Strength as a function of depth 121

Relative to top of soil layer 121

Relative to specified datum 121

7.12 Frictional-undrained combined models 122

7.13 SHANSEP: Strength as a function of overburden stess 122

7.14 Hoek and Brown model 124

7.15 Unsaturated shear strength....129
7.16 Soil unit weight....130
7.17 Other soil parameters....132

8 Pore-water....133
8.1 Introduction....133
8.2 Piezometric surfaces....133
Single piezometric line....133
Multiple piezometric lines....134
Phreatic correction....134
8.3 R_u Coefficients....135
8.4 B-bar coefficients....136
8.5 Pore-water pressures head with spatial function....137
8.6 Negative pore-water pressures....138
8.7 Finite element computed pressures....138
8.8 Recommended practice....141

9 Reinforcement and Structural Components....143
9.1 Introduction....143
9.2 Fundamentals related to concentrated lateral loads....143
Mobilization of reinforcement forces....143
Slice forces and stress distributions....145
Reinforcement Anchorage....149
Convergence....150
Safety factors of the various components....151
Recommended analysis approach....151
Summary....151
9.3 Anchors and nails....152
9.4 Geosynthetic reinforcement....155
9.5 Piles....158
9.6 User defined reinforcement....159
9.7 Manufacturer Reinforcement....161
9.8 Sheet pile walls....162
9.9 Deep-seated instability....163
9.10 Mitigation of numerical problems....164
9.11 Finite element stress-based approach....164
Wall with nails....164
Tie-back wall....168

Soil-structure interaction safety factors 171
Shear wall 173
Key issues 175

10 Seismic and Dynamic Stability.....177
10.1 Introduction 177
10.2 Rapid loading strength 177
10.3 Pseudostatic analysis.....179
Staged Pseudostatic analysis.....182
10.4 Dynamic analysis 183
10.5 Permanent deformation.....185
10.6 Liquefaction stability.....187

11 Probabilistic and Sensitivity Analyses.....191
11.1 Introduction 191
11.2 Probability density functions.....191
Normal function 191
Lognormal function 193
Uniform function 196
11.3 Triangular probability function 197
11.4 General probability function 198
11.5 C – ϕ correlation 200
11.6 Probability of failure and reliability index 200
11.7 Spatial variability 202
11.8 Multiple statistical parameters.....207
11.9 Sensitivity analyses.....207

12 Partial Factors.....209
12.1 Favorable or unfavorable actions.....209
12.2 Pore-water pressures and ponded water 210
12.3 Shear strength.....211
12.4 Reinforcement loads 212

13 Illustrative Examples.....212
Analysis integration 213

14 Theory.....215
14.1 Introduction 215
14.2 Definition of variables.....215

14.3 General limit equilibrium Solution Scheme 219
14.4 Moment equilibrium factor of safety 220
14.5 Force equilibrium factor of safety 220
14.6 Slice normal force at the base.....220
14.7 M-alpha values.....221
14.8 Interslice forces 223
14.9 Effect of negative pore-water pressures 225
14.10 Factor of safety for unsaturated soil.....225
14.11 Use of unsaturated shear strength parameters.....226
14.12 Solving for the factors of safety.....227
Stage 1 solution.....227
Stage 2 solution.....227
Stage 3 solution.....227
14.13 Simulation of the various methods 228
14.14 Spline interpolation.....229
14.15 Moment axis.....231
14.16 Finite element stress method 231
Stability factor 231
Normal stress and mobilized shear stress.....232
14.17 Probabilistic slope stability analysis 234
Monte Carlo method 234
Parameter variability.....235
Random number generation.....235
Correlation coefficient.....235
Number of Monte Carlo trials.....236

References.....237

Index 241

1 Introduction

Analyzing the stability of earth structures is the oldest type of numerical analysis in geotechnical engineering. The idea of discretizing a potential sliding mass into slices was introduced early in the 20th Century. In 1916, Petterson (1955) presented the stability analysis of the Stigberg Quay in Gothenberg, Sweden where the slip surface was taken to be circular and the sliding mass was divided into slices. During the next few decades, Fellenius (1936) introduced the Ordinary or Swedish method of slices. In the mid-1950s Janbu (1954) and Bishop (1955) developed advances in the method. The advent of electronic computers in the 1960's made it possible to more readily handle the iterative procedures inherent in the method which led to mathematically more rigorous formulations such as those developed by Morgenstern and Price (1965) and by Spencer (1967). One of the reasons the limit equilibrium method was adopted so readily, is that solutions could be obtained by hand-calculations. Simplifying assumption had to be adopted to obtain solutions, but the concept of numerically dividing a larger body into smaller pieces for analysis purposes was rather novel at the time.

Even to this day, stability analyses are by far the most common type of numerical analysis in geotechnical engineering. This is in part because stability is obviously a key issue in any project – will the structure remain stable or collapse? This, however, is not the only reason. Concepts associated with the method of slices are not difficult to grasp and the techniques are rather easy to implement in computer software – the simpler methods can even be done on a spreadsheet. Consequently, slope stability software became available soon after the advent of computers. The introduction of powerful desktop personal computers in the early 1980s made it economically viable to develop commercial software products based on these techniques, and the ready availability today of such software products has led to the routine use of limit equilibrium stability analysis in geotechnical engineering practice.

Modern limit equilibrium software is making it possible to handle ever-increasing complexity within an analysis. It is now possible to deal with complex stratigraphy, highly irregular pore-water pressure conditions, various linear and nonlinear shear strength models, almost any kind of slip surface shape, concentrated loads, and structural reinforcement. Limit equilibrium formulations based on the method of slices are also being applied more and more to the stability analysis of structures such as tie-back walls, nail or fabric reinforced slopes, and even the sliding stability of structures subjected to high horizontal loading arising, for example, from ice flows.

While modern software is making it possible to analyze ever-increasingly complex problems, the same tools are also making it possible to better understand the limit equilibrium method itself. Computer-assisted graphical viewing of data used in the calculations makes it possible to look beyond the factor of safety. For example, graphically viewing all the detailed forces on each slice in the potential sliding mass, or viewing the distribution of a variety of parameters along the slip surface, helps greatly to understand the details of the technique.

While the graphical viewing of computed details has led to a greater understanding of the method, particularly the differences between the various methods available, it has also led to the exposure of limitations in the limit equilibrium formulations. Exposure of the limitations has revealed that the method is perhaps being pushed too far beyond its initial intended purpose. The method of slices was initially conceived for the situation where the normal stress along the slip surface is primarily influenced by gravity (weight of the slice). Including reinforcement in the analysis goes far beyond the initial intention. Even though the limitations do not necessarily prevent using the method in practice, understanding the limitations is vital to understanding and relying on the results.

Despite the extensive and routine use of stability analyses in practice, it seems the fundamentals of the limit equilibrium method of slices are not well understood. The fact that the limit equilibrium method of

slices is based on nothing more than statics often seems to be forgotten, and the significance of one factor of safety for all slices is not appreciated.

SLOPE/W, in one form, or another has been on the market since 1977. The initial code was developed by Professor D.G. Fredlund at the University of Saskatchewan. The first commercial version was installed on mainframe computers and users could access the software through software bureaus. Then in the 1980s when Personal Computers (PCs) became available, the code was completely re-written for the PC environment. Processing time was now available at the relatively low fixed cost of the computer, but computer memory was scarce and so the code had to be re-structured for this hardware environment. The product was renamed PC-SLOPE and released in 1983. Later in the 1980s it became evident that graphical interaction with PC software was going to be the wave of the future, and consequently a graphical CAD-like user interface was developed. The software was again renamed as SLOPE/W to reflect the Microsoft Windows environment and that it now had a graphical user interface. SLOPE/W was the very first geotechnical software product available commercially for analyzing slope stability. Currently, SLOPE/W is being used by thousands of professionals both in education and in practice.

Over the years, as computer technology has advanced, SLOPE/W has continually been enhanced and upgraded. This book is based on Version 8 of the program.

When using software like SLOPE/W with its myriad of options, it is often necessary to look at more than just the factor of safety. Other issues to consider include, but are not limited to: Was the intended data correctly specified? Was the data used correctly by the software? Why are there differences between factors of safety from the various methods? To help answer these types of questions, SLOPE/W has many tools for inspecting the input data and evaluating the results – tools like allowing you to graph a list of different variables along the slip surface or to display the detail forces on each slice, for example. These types of tools are vitally important to judging and being confident in the results.

Earlier it was noted that despite the extensive use of limit equilibrium methods in routine practice, the fundamentals of the formulations and the implications of the inherent assumptions are not well understood. An entire chapter is consequently devoted to a review of the fundamentals of limit equilibrium as a method of analysis. The chapter looks at the consequences of a pure statics formulation, what are the differences between the various methods, why are interslice forces important, what effect does the shape of the slip surface have, and so forth. In addition, the chapter discusses the limitations of the limit equilibrium method and discusses ways of overcoming the limitations. Gaining a thorough understanding of these fundamentals is essential to effective use of SLOPE/W.

SLOPE/W is one component in a complete suite of geotechnical products called GeoStudio. One of the powerful features of this integrated approach is that it opens the door to types of analyses of a much wider and more complex spectrum of problems, including the use of finite element computed pore-water pressures and stresses in a stability analysis. Not only does an integrated approach widen the analysis possibilities, it can help overcome some limitations of the purely limit equilibrium formulations. Although, it is not necessary to use this advanced feature as SLOPE/W can be used as an individual product, there is certainly an increase in the capability of the program by using it as one component of a complete suite of geotechnical software programs.

The very large number of options in SLOPE/W can be somewhat confusing, especially when you are using the software for the first time. Some semblance of order can be made of these options by thinking of a problem in terms of five components. They are:

- Geometry – description of the stratigraphy and shapes of potential slip surfaces.
- Soil strength - parameters used to describe the soil (material) strength
- Pore-water pressure – means of defining the pore-water pressure conditions

- Reinforcement or soil-structure interaction – fabric, nails, anchors, piles, walls and so forth.
- Imposed loading – surcharges or dynamic earthquake loads

Separate chapters are devoted to each of these main components.

More and more engineers are interested in conducting probabilistic types of stability. An entire chapter is devoted to the special subject of probabilistic analysis and sensitivity studies.

Examples are included throughout the book to illustrate features and explain behavior. In addition there is a special section devoted to illustrative examples, which are intended to provide ideas on how to model various situations. The examples are not intended to be complete case histories, but instead are intended to be simple illustrations used to highlight possible situations including complete submergence, stability on a synthetic liner, and bearing pressure.

At the end of the book is a chapter on theory. This chapter is included primarily as a reference, as a connection to the past and as information for those who are curious about the fundamental details used in SLOPE/W. Generally, it should not be necessary to spend too much time in this chapter to use SLOPE/W effectively.

This book is aimed at highlighting engineering concepts and stability analysis modeling techniques. This book is not aimed at describing all the software interaction commands and the meaning of all the various parameters in the dialogs boxes. These details are provided in the online help.

SLOPE/W has been designed and developed to be a general software tool for the stability analysis of earth structures. SLOPE/W is not designed for certain specific cases. SLOPE/W was not created specifically to design retaining walls, although SLOPE/W can certainly be used to assess the sliding stability of a gravity retaining wall, or to find the active earth forces on the wall. Likewise, SLOPE/W was not specifically designed for earth-reinforced retaining walls, but SLOPE/W can be used to analyze the stability of a wedge of soil that has been reinforced with a structural component such as a pre-stressed anchor, a soil nail, geo-fabric or some other material. Using a general tool such as SLOPE/W sometimes requires careful thought as to how to model a certain situation, but at the same time it greatly expands the range of possible situations you can model, which has been our main intention. The general nature allows for much greater creativity. Once you understand how the general features function, the types of problems that can be analyzed are primarily limited by your creativity. The main purpose of this book is to help you be creative, not to outline an endless list of rules you must follow.

2 Limit Equilibrium Fundamentals

2.1 Introduction

In 2003, at the Canadian Geotechnical Conference in Calgary, Alberta, Krahn (2003) presented the R.M. Hardy Lecture. The title of the lecture was, *The Limits of Limit Equilibrium Analyses*. This chapter is in large part a replication of this Lecture and as published in the Canadian Geotechnical Journal, Vol. 40, pages 643 to 660.

The main message of the lecture was that limit equilibrium methods for assessing the stability of earth structures are now used routinely in practice. In spite of this extensive use, the fundamentals of the methods are often not that well understood and expectations exceed what the methods can provide. The fact and implications that limit equilibrium formulations are based on nothing more than equations of statics with a single, constant factor of safety is often not recognized. A full appreciation of the implications reveals that the method has serious limitations.

To use limit equilibrium methods effectively, it is important to understand and comprehend the inherent limitations. This chapter discusses the fundamentals of limit equilibrium formulations, points out the limitations, explores what can be done to overcome the limitations, and ends with general guidelines on the continued use of the method in practice.

2.2 Background and history

Limit equilibrium types of analyses for assessing the stability of earth slopes have been in use in geotechnical engineering for many decades. The idea of discretizing a potential sliding mass into vertical slices was introduced early in the 20th century and is consequently the oldest numerical analysis technique in geotechnical engineering.

In 1916, Petterson (1955) presented the stability analysis of the Stigberg Quay in Gothenberg, Sweden where the slip surface was taken to be circular and the sliding mass was divided into slices. During the next few decades, Fellenius (1936) introduced the Ordinary or Swedish method of slices. In the mid-1950s Janbu (1954) and Bishop (1955) developed advances in the method. The advent of electronic computers in the 1960's made it possible to more readily handle the iterative procedures inherent in the method, which led to mathematically more rigorous formulations such as those developed by Morgenstern and Price (1965) and by Spencer (1967). The introduction of powerful desktop personal computers in the early 1980s made it economically viable to develop commercial software products based on these techniques, and the ready availability today of such software products has led to the routine use of limit equilibrium stability analysis in geotechnical engineering practice.

Modern limit equilibrium software such as SLOPE/W is making it possible to handle ever-increasing complexity in the analysis. It is now possible to deal with complex stratigraphy, highly irregular pore-water pressure conditions, a variety of linear and nonlinear shear strength models, virtually any kind of slip surface shape, concentrated loads, and structural reinforcement. Limit equilibrium formulations based on the method of slices are also being applied more and more to the stability analysis of structures such as tie-back walls, nail or fabric reinforced slopes, and even the sliding stability of structures subjected to high horizontal loading arising, for example, from ice flows.

While modern software is making it possible to analyze ever-increasingly complex problems, the same tools are also making it possible to better understand the limit equilibrium method. Computer-assisted graphical viewing of data used in the calculations makes it possible to look beyond the factor of safety. For example, graphically viewing all the detailed forces on each slice in the potential sliding mass, or

viewing the distribution of a variety of parameters along the slip surface, helps greatly to understand the details of the technique. From this detailed information, it is now becoming evident that the method has its limits and that it is perhaps being pushed beyond its initial intended purpose. Initially, the method of slices was conceived for the situation where the normal stress along the slip surface is primarily influenced by gravity (weight of the slice). Including reinforcement in the analysis goes far beyond the initial intention.

2.3 Method basics

Many different solution techniques for the method of slices have been developed over the years. Basically, all are very similar. The differences between the methods are depending on: what equations of statics are included and satisfied and which interslice forces are included and what is the assumed relationship between the interslice shear and normal forces? Figure 2-1 illustrates a typical sliding mass discretized into slices and the possible forces on the slice. Normal and shear forces act on the slice base and on the slice sides.

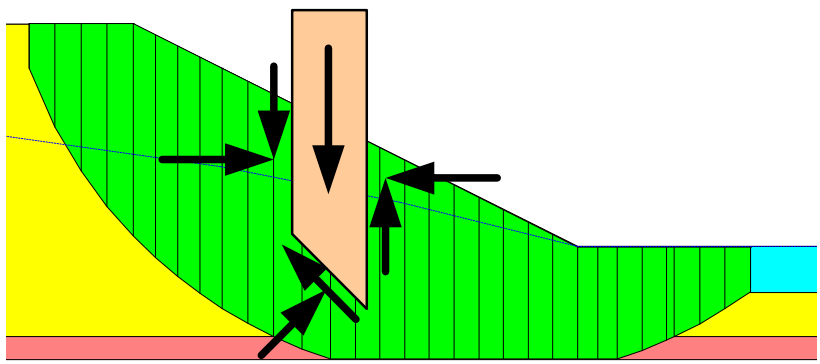

Figure 2-1 Slice discretization and slice forces in a sliding mass

The Ordinary, or Fellenius method was the first method developed. The method ignored all interslice forces and satisfied only moment equilibrium. Adopting these simplified assumptions made it possible to compute a factor of safety using hand calculations, which was important since there were no computers available.

Later Bishop (1955) devised a scheme that included interslice normal forces, but ignored the interslice shear forces. Again, Bishop's Simplified method satisfies only moment equilibrium. Of interest and significance with this method is the fact that by including the normal interslice forces, the factor of safety equation became nonlinear and an iterative procedure was required to calculate the factor of safety. The Janbu's Simplified method is similar to the Bishop's Simplified method in that it includes the normal interslice forces and ignores the interslice shear forces. The difference between the Bishop's Simplified and Janbu's Simplified methods is that the Janbu's Simplified method satisfies only horizontal force equilibrium, as opposed to moment equilibrium.

Later, computers made it possible to more readily handle the iterative procedures inherent in the limit equilibrium method, and this lead to mathematically more rigorous formulations which include all interslice forces and satisfy all equations of statics. Two such methods are the Morgenstern-Price and Spencer methods.

Table 2-1 lists the methods available in SLOPE/W and indicates what equations of statics are satisfied for each of the methods. Table 2-2 gives a summary of the interslice forces included and the assumed relationships between the interslice shear and normal forces.

Further details about all the methods are presented elsewhere.

Table 2-1 Equations of Statics Satisfied

Method	Moment Equilibrium	Force Equilibrium
Ordinary or Fellenius	Yes	No
Bishop's Simplified	Yes	No
Janbu's Simplified	No	Yes
Spencer	Yes	Yes
Morgenstern-Price	Yes	Yes
Corps of Engineers – 1	No	Yes
Corps of Engineers – 2	No	Yes
Lowe-Karafiath	No	Yes
Janbu Generalized	Yes (by slice)	Yes
Sarma – vertical slices	Yes	Yes

Table 2-2 Interslice force characteristics and relationships

Method	Interslice Normal (E)	Interslice Shear (X)	Inclination of X/E Resultant, and X-E Relationship
Ordinary or Fellenius	No	No	No interslice forces
Bishop's Simplified	Yes	No	Horizontal
Janbu's Simplified	Yes	No	Horizontal
Spencer	Yes	Yes	Constant
Morgenstern-Price	Yes	Yes	Variable; user function
Corps of Engineers – 1	Yes	Yes	Inclination of a line from crest to toe
Corps of Engineers – 2	Yes	Yes	Inclination of ground surface at top of slice
Lowe-Karafiath	Yes	Yes	Average of ground surface and slice base inclination
Janbu Generalized	Yes	Yes	Applied line of thrust and moment equilibrium of slice
Sarma – vertical slices	Yes	Yes	$X = C + E \tan \phi$

2.4 General limit equilibrium formulation

A general limit equilibrium (GLE) formulation was developed by Fredlund at the University of Saskatchewan in the 1970's (Fredlund and Krahn 1977; Fredlund et al. 1981). This formulation encompasses the key elements of all the methods listed in Table 1. The GLE formulation is based on two factors of safety equations and allows for a range of interslice shear-normal force conditions. One equation gives the factor of safety with respect to moment equilibrium (F_m) while the other equation gives

the factor of safety with respect to horizontal force equilibrium (F_f). The idea of using two factor of safety equations was actually first published by Spencer (1967).

The interslice shear forces in the GLE formulation are handled with an equation proposed by Morgenstern and Price (1965). The equation is:

$$X = E\,\lambda\,f(x)$$

where:

f(x)	=	a function,
λ	=	the percentage (in decimal form) of the function used,
E	=	the interslice normal force, and
X	=	the interslice shear force.

Figure 2-2 shows a typical half-sine function. The upper curve in this figure is the actual specified function. The lower curve is the function used. The ratio between the two curves represents λ. Lambda (λ) in Figure 2-2 is 0.43. At Slice 10, f(x) = 0.83. If, for example, E = 100 kN, then X = E f(x) λ = 100 x 0.43 x 0.83 = 35.7 kN. Arc tan (35.7/100) = 19.6 degrees. This means the interslice resultant force is inclined at 19.6 degrees from the horizontal at Slice 10. One of the key issues in the limit equilibrium formulation, as will be illustrated later, is knowing how to define this interslice function.

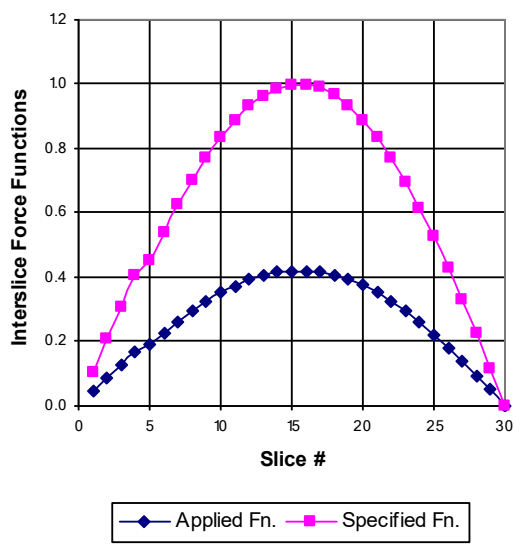

Figure 2-2 Half-sine interslice force function

The GLE factor of safety equation with respect to moment equilibrium is:

$$F_m = \frac{\sum (c'\beta R + (N - u\beta)R\ \tan\phi')}{\sum Wx - \sum Nf \pm \sum Dd}$$

The factor of safety equation with respect to horizontal force equilibrium is:

$$F_f = \frac{\sum (c'\beta \cos\alpha + (N - u\beta)\tan\phi' \cos\alpha)}{\sum N \sin\alpha - \sum D \cos\omega}$$

The terms in the equations are:

c'	=	effective cohesion
ϕ'	=	effective angle of friction
u	=	pore-water pressure
N	=	slice base normal force
W	=	slice weight
D	=	concentrated point load
β, R, x, f, d, ω	=	geometric parameters
α	=	inclination of slice base

(There are additional terms in the factor of safety equations, but they are not required for the discussion on limit equilibrium fundamentals; the complete equations are presented in the theory chapter.)

One of the key variables in both equations is *N*, the normal at the base of each slice. This equation is obtained by the summation of vertical forces, thus vertical force equilibrium is consequently satisfied. In equation form, the base normal is defined as:

$$N = \frac{W + (X_R - X_L) - \dfrac{(c'\beta \sin\alpha + u\beta \sin\alpha \tan\phi')}{F}}{\cos\alpha + \dfrac{\sin\alpha \tan\phi'}{F}}$$

F is F_m when *N* is substituted into the moment factor of safety equation and *F* is F_f when *N* is substituted into the force factor of safety equation. The literature on slope stability analysis often refers to the denominator of this equation as m_α.

A very important point to make here is that the slice base normal is dependent on the interslice shear forces X_R and X_L on either side of a slice. The slice base normal is consequently different for the various methods, depending on how each method deals with the interslice shear forces.

The GLE formulation computes F_m and F_f for a range of lambda (λ) values. With these computed values, a plot similar to Figure 2-3 can be drawn which shows how F_m and F_f vary with lambda (λ).

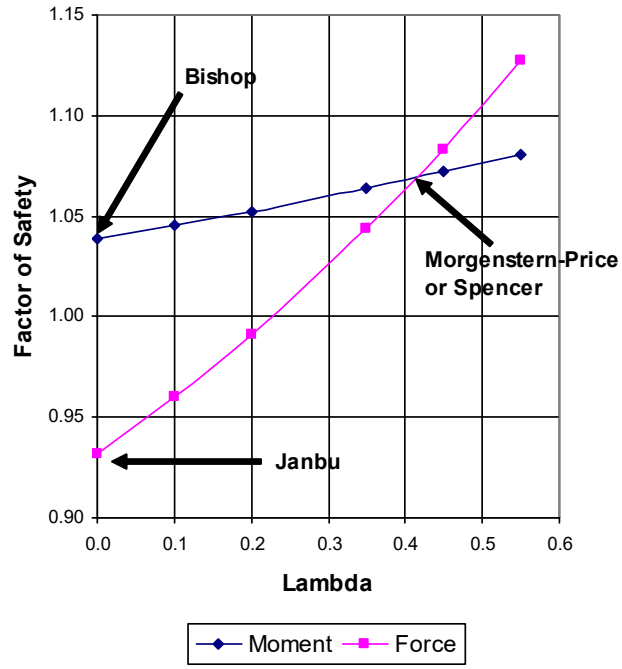

Figure 2-3 A factor of safety versus lambda (λ) plot

As listed in Table 2-1 and Table 2-2, Bishop's Simplified method ignores interslice shear forces and satisfies only moment equilibrium. In the GLE terminology, neglecting interslice shear forces means λ is zero. As a result, the Bishop's Simplified factor of safety falls on the moment curve in Figure 2-3 where lambda is zero. Janbu's Simplified method also ignores interslice shear forces and only satisfies force equilibrium. The Janbu's Simplified factor of safety consequently falls on the force curve in Figure 2-3 where λ is zero. The Spencer and Morgenstern-Price (M-P) factors of safety are determined at the point where the two curves cross in Figure 2-3. At this point, the factor of safety satisfies both moment and force equilibrium. Whether the crossover point is the Spencer or M-P factor of safety depends on the interslice force function. Spencer only considered a constant *X/E* ratio for all slices. The M-P method can utilize any general appropriate function. The Corp of Engineers and Lowe-Karafiath factors of safety fall on the force curve in Figure 2-3. The position on the force curve depends on the procedure used to establish the inclinations of the interslice resultant. The inclination of the interslice resultant is arc tan(λ) when *f(x)* is a constant 1.0 as in the Spencer method.

The GLE formulation is very useful for explaining the differences between the various methods and for determining how the interslice force functions influence the computed factor of safety, as discussed in more detail below.

There is one characteristic in the two factor of safety equations and the base normal equation that have a profound consequence. In the end there is only one factor of safety for the overall slope. F_m and F_f are the same when both moment and force equilibrium are satisfied. This same value appears in the equation for the normal at the slice base. This means the factor of safety is the same for each and every slice. As we will see later, this has a significant effect on the resulting computed stress distributions within the sliding mass and along the slip surface.

Another important point about the GLE formulation is that it is not restricted by the shape of the slip surface. The Bishop's Simplified method was initially developed for circular slip surfaces, but the assumptions inherent in the Bishop's Simplified method can be applied to any noncircular slip surface. In

fact, with the GLE formulation, all methods listed in Table 2-1 can be applied to any kinematicly admissible slip surface shape.

2.5 Interslice force functions

How the interslice shear forces are handled and computed is a fundamental point with most of the methods listed in Table 2-1. The Spencer method, for example, uses a constant function which infers that the ratio of shear to normal is a constant between all slices. You do not need to select the function; it is fixed to be a constant function in the software when the Spencer method is selected.

Only the Morgenstern-Price allows for user-specified interslice functions. Some of the functions available are the constant, half-sine, clipped-sine, trapezoidal and data-point specified. The most commonly used functions are the constant and half-sine functions. A Morgenstern-Price analysis with a constant function is the same as a Spencer analysis.

SLOPE/W by default uses the half-sine function for the M-P method. The half-sine function tends to concentrate the interslice shear forces towards the middle of the sliding mass and diminishes the interslice shear in the crest and toe areas. Defaulting to the half-sine function for these methods is based primarily on experience and intuition and not on any theoretical considerations. Other functions can be selected if deemed necessary.

The Sarma method deals with the interslice shear-normal relationship somewhat differently. Most methods use a specified function or a specified direction to establish the relationship between the interslice shear and normal. The Sarma method uses a shear strength equation as noted in Table 2-2. This approach does not offer any particular advantages over the other approaches, for reasons that will become clear later in this chapter. In the end, this is just another mechanism to compute interslice shear forces from the normal forces, and is included primarily for completeness and to accommodate user preferences.

The influence and importance of the interslice forces is discussed in the next section.

2.6 Slip surface shapes

The importance of the interslice force function depends to a large extent on the amount of contortion the potential sliding mass must undergo to move. The function is not important for some kinds of movement while the function may significantly influence the factor of safety for other kinds of movement. The following examples illustrate this sensitivity.

Circular slip surface

Figure 2-4 presents a simple circular slip surface together with the associated FS vs λ plot. In this case the moment equilibrium is completely independent of the interslice shear forces, as indicated by the horizontal moment equilibrium curve. The force equilibrium, however, is dependent on the interslice shear forces.

The moment equilibrium is not influenced by the shear forces because the sliding mass as a free body can rotate without any slippage between the slices. However, substantial interslice slippage is necessary for the sliding mass to move laterally. As a consequence the horizontal force equilibrium is sensitive to interslice shear.

Since the moment equilibrium is completely independent of interslice shear, any assumption regarding an interslice force function is irrelevant. The interslice shear can be assumed to be zero, as in the Bishop's Simplified method, and still obtain an acceptable factor of safety, provided the method satisfies moment

equilibrium. This is, of course, not true for a method based on satisfying only horizontal force equilibrium such as the Janbu's Simplified method. Ignoring the interslice shear when only horizontal force equilibrium is satisfied for a curved slip surface results in a factor of safety significantly different than when both force and moment equilibrium is satisfied.

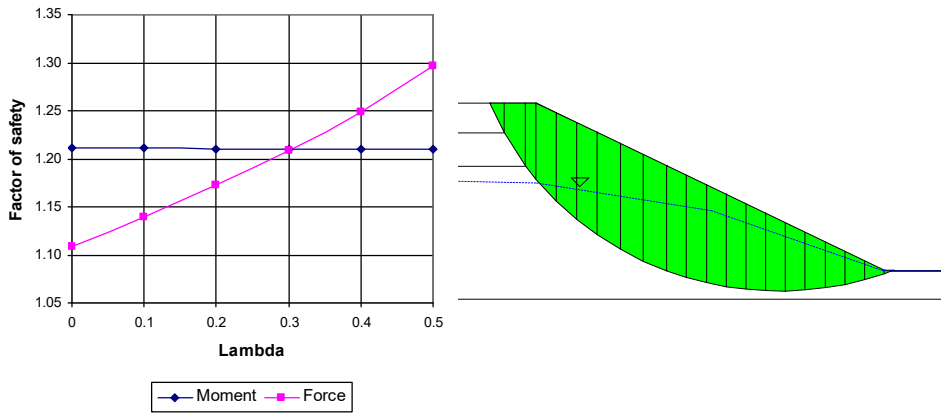

Figure 2-4 Conditions for a simple circular slip surface

The moment equilibrium curve is not always perfectly horizontal for circular slip surfaces. The moment curve in Figure 2-4 was obtained from a circular slip surface analysis and it is slightly inclined. Usually, however, the slope of the moment curve is nearly horizontal. This is why the Bishop and Morgenstern-Price factors of safety are often similar for circular slip surfaces.

Planar slip surface

Figure 2-5 illustrates a planar slip surface. The moment and force equilibrium curves now have reverse positions from those for a circular slip surface. Now force equilibrium is completely independent of interslice shear, while moment equilibrium is fairly sensitive to the interslice shear. The soil wedge on the planar slip surface can move without any slippage between the slices. Considerable slippage is, however, required for the wedge to rotate.

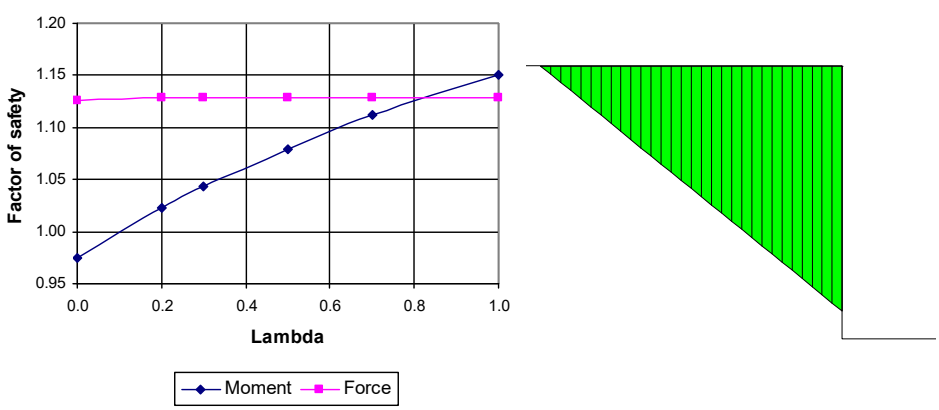

Figure 2-5 Situation for a planar slip surface

Composite slip surface

A composite slip surface is one where the slip surface is partly on the arc of a circle and partly on a planar surface, as illustrated in Figure 2-6. The planar portion in this example follows a weak layer, a common situation in many stratigraphic settings. In this case, both moment and force equilibrium are influenced by the interslice shear forces. Force equilibrium factors of safety increase, while moment equilibrium factors of safety decrease as the interslice shear forces increase (higher lambda values).

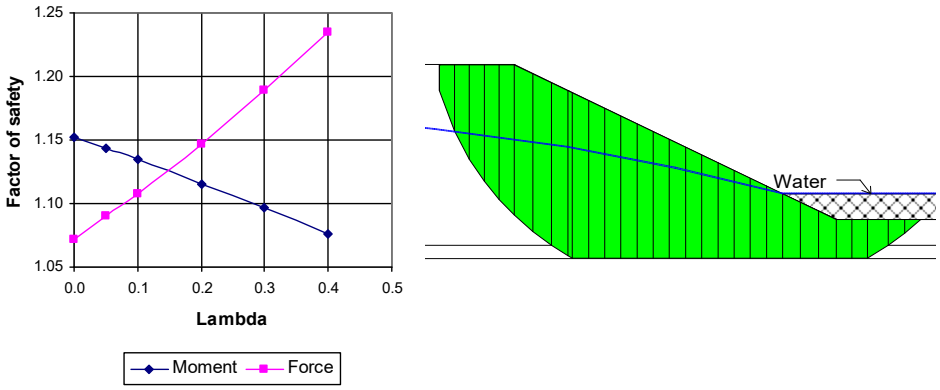

Figure 2-6 Situation for a typical composite slip surface

This illustrates that a Bishop's Simplified type of analysis does not always err on the safe side. A more rigorous formulation such as the Morgenstern-Price or Spencer method will give a lower factor of safety than a Bishop Simplified factor of safety. This is not necessarily true for all composite slip surfaces. For some composite slip surfaces, a mathematically more rigorous factor of safety may be higher than the Bishop's Simplified. It is not possible to generalize as to when a more simplified factor of safety will or will not err on the safe side.

Slippage between the slices needs to occur for both moment and force equilibrium for a slip surface of this shape and, consequently, the interslice shear is important for both types of equilibrium.

Block slip surface

Figure 2-7 shows a block-type slip surface. As with the previous composite slip surface, the moment and force equilibrium are both influenced by the interslice shear. The force equilibrium is more sensitive to the shear forces than the moment equilibrium, as indicated by the curve gradients in Figure 2-7. Once again it is easy to visualize that significant slippage is required between the slices for both horizontal translation and rotation, giving rise to the importance of the shear forces.

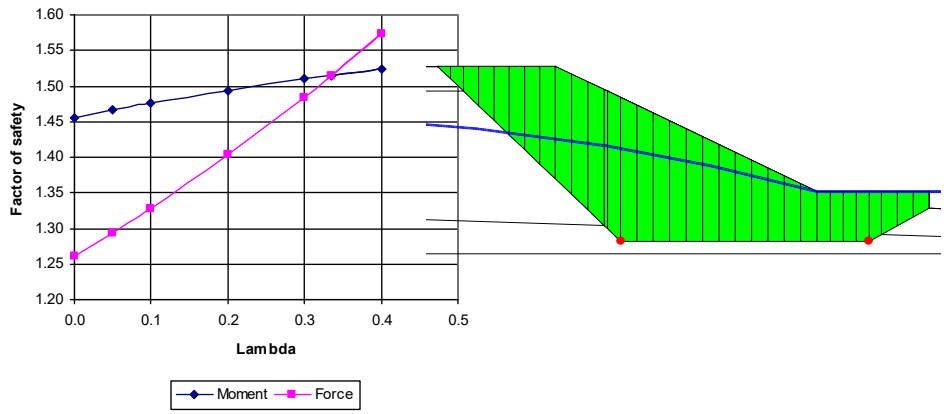

Figure 2-7 Typical situation for a block slip surface

Shoring wall

Figure 2-8 provides an example that examines the deep-seated stability of a shoring wall. The slip surface is beneath the lower tip of the sheet piling. This example comes from the analysis of a deep excavation in downtown Calgary. The *FS* vs λ plot shows that the moment and force equilibrium curves are similar in this case. They are both very sensitive to the interslice shear forces. Ignoring the interslice shear forces for this case results in a significant underestimation of the factor of safety. Without including the interslice shear forces, the factor of safety is less than 1.0 indicating an unstable situation. Including the shear forces increases the factor of safety to 1.22. The difference again is due to the contortion the potential failing mass would have to undergo to rotate or move laterally.

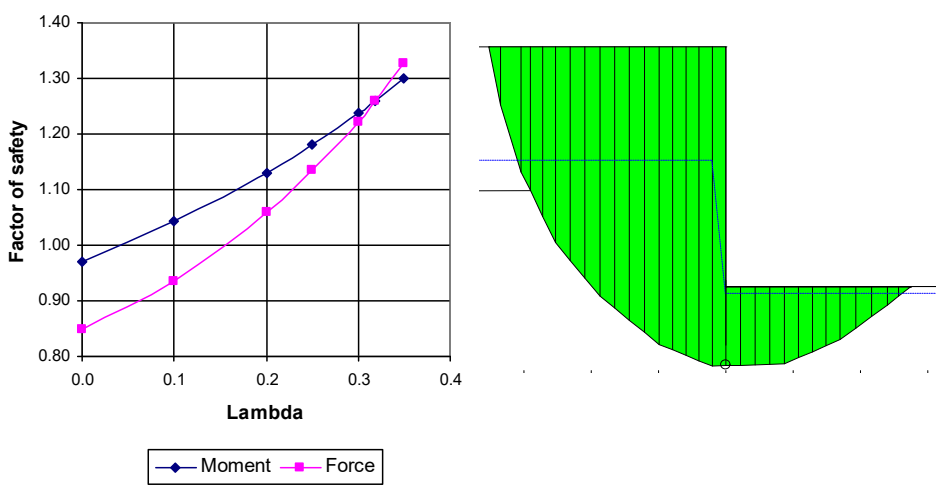

Figure 2-8 A deep stability analysis of a shoring wall

These examples show that the importance of the interslice force functions is strongly related to the shape of the potential slip surface, which in turn is related to the amount of contortion the sliding mass needs to undergo to rotate or move laterally.

When the adopted interslice force function becomes critical in a stability analysis, the limit equilibrium method of slices is approaching the limits of its applicability. Alternative approaches such as described later may then be required.

2.7 Stress distributions

The primary unknown in a limit equilibrium formulation is the normal at the base of the slice. Plotting the stresses along a slip surface gives an indication of the stress distribution in the slope. The computed stresses are, however, not always representative of the true stresses in the ground.

Consider the simple 45-degree slope in Figure 2-9 and Figure 2-10 with a slip surface through the toe and another deeper slip surface below the toe. The normal stress distribution along the slip surface from a limit equilibrium Morgenstern-Price analysis with a constant interslice force function is compared with the normal stress distribution from a linear-elastic finite element stress analysis. For the toe slip surface, the normal stresses are quite different, especially in the toe area. The normal stress distributions for the deeper slip surface are closer, but still different for a good portion of the slip surface.

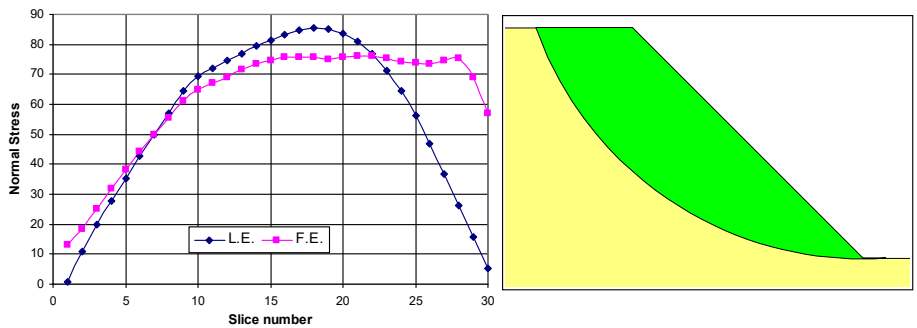

Figure 2-9 Normal stress distribution along a toe slip surface

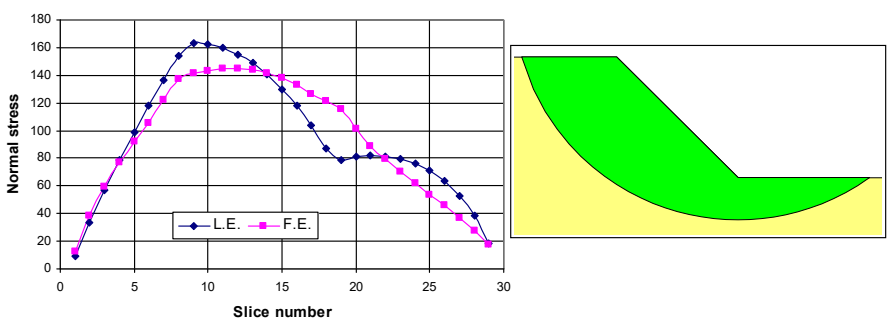

Figure 2-10 Normal stress distribution along a deep slip surface

Figure 2-11 presents a case with reinforcement. The reinforcement loads are applied at the point where the slip surface intersects the line of action. Again there are significant differences between the limit equilibrium normal stresses and the finite element stresses, particularly for the slices which include the reinforcement loads. The finite element stresses show some increase in normal stresses due to the nails, but not as dramatic as the limit equilibrium stresses.

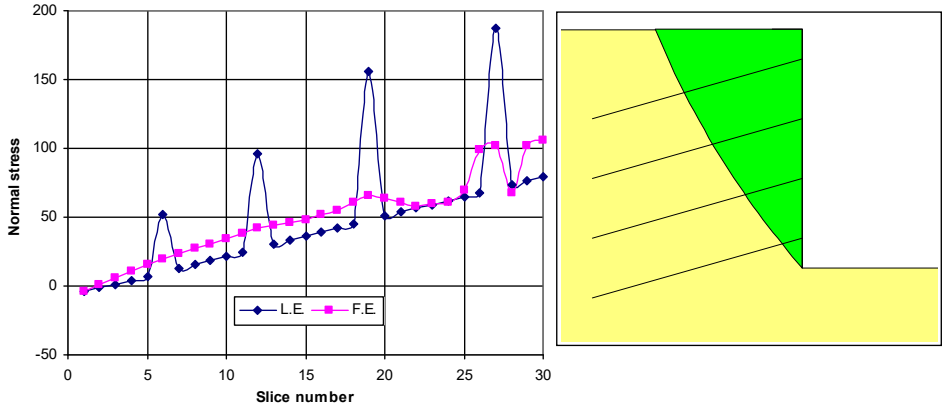

Figure 2-11 Normal stress distributions with reinforcement

These examples show that the stress conditions as computed from a limit equilibrium analysis may be vastly different from finite element computed stresses. The finite element stresses are more realistic and are much closer to the actual conditions in the ground. The implication is that the limit equilibrium computed stresses are not representative of actual field conditions.

The sliding mass internal stresses are also not necessarily representative of actual field conditions. Figure 2.12 presents the case of a tie-back wall with two rows of anchors. The anchor forces are applied where the slip surface intersects the anchor.

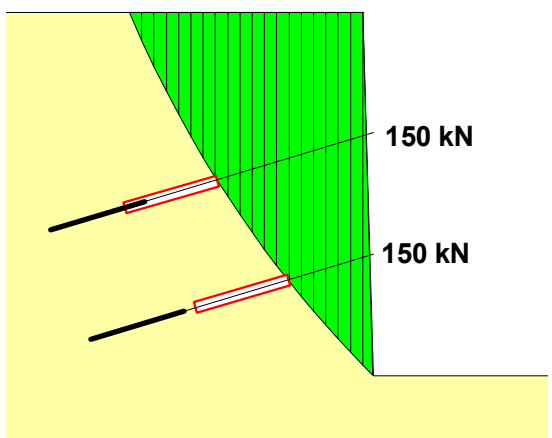

Figure 2-12 Tie-back wall example

The free body diagrams and force polygons for two different slices are presented in Figure 2-13 and Figure 2-14.

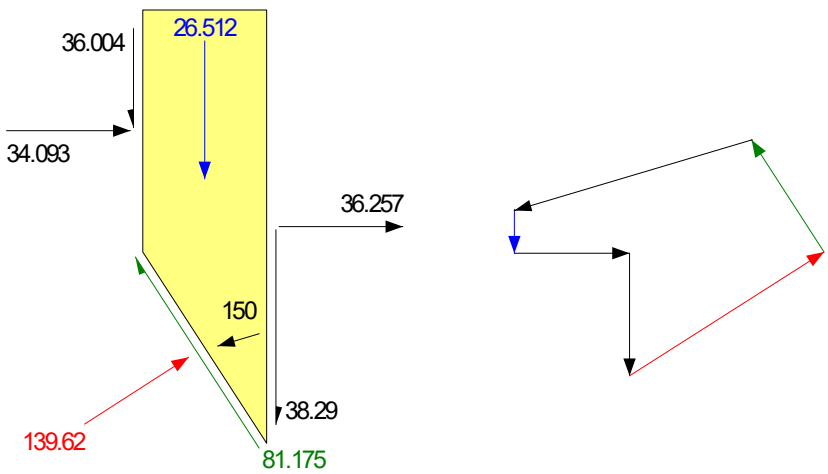

Figure 2-13 Free body and force polygon for upper anchor

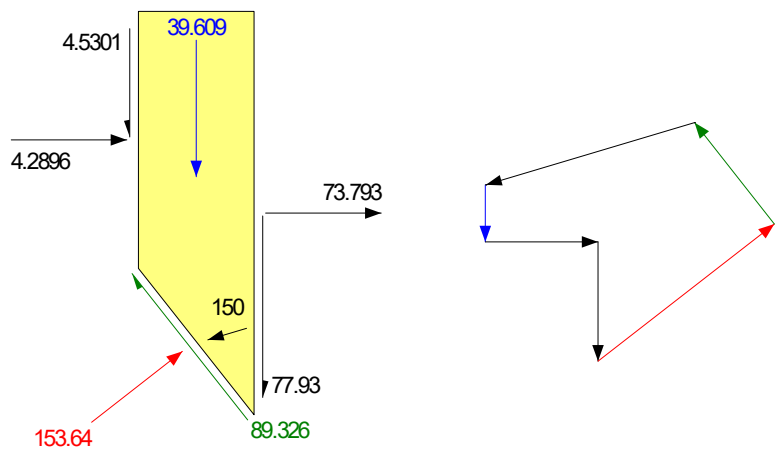

Figure 2-14 Free body and force polygon for lower anchor

Note that the interslice normals point away from the slice on the right side. This indicates tension between the slides, which is obviously not the case in the field. Plotting the interslice forces as in Figure 2-15 further highlights this difficulty. At each of the anchor locations, the interslice normals become negative and the interslice shear forces reverse direction. Of great significance, however, is the fact that the force polygons close signifying that the slices are in equilibrium. In this sense, the results fulfill in part the objectives of the limit equilibrium formulation.

When looking at the exact same situation, but with the anchor loads applied at the wall, the interslice forces are now completely different. Figure 2-16 again shows the interslice shear and normal forces. The normal force increases evenly and gradually except for the last two slices. Of interest is the interslice shear force. The direction is now the reverse of that which usually occurs when only the self weight of the slices is included (simple gravity loading). The shear stress reversal is a reflection of a negative lambda (λ).

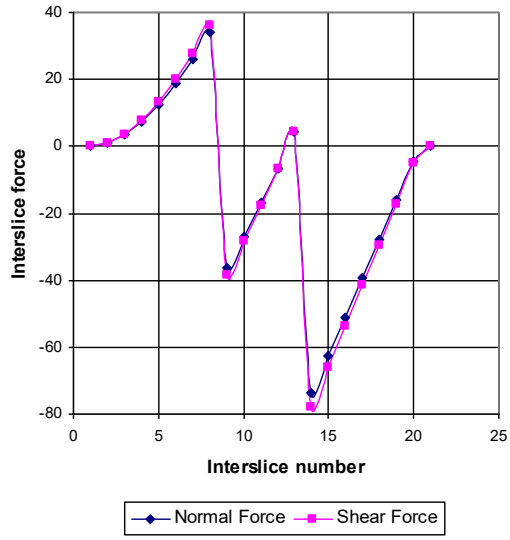

Figure 2-15 Interslice shear and normal forces with anchor loads applied at the slip surface

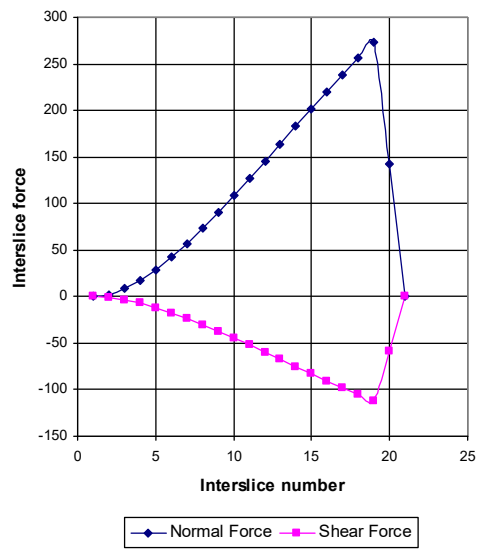

Figure 2-16 Interslice shear and normal forces with anchor loads applied at face of wall

The large differences in the interslice forces also lead to significantly different normal stress distributions along the slip surface, as shown in Figure 2-17. It was noted earlier that the equation for the normal at the base of the slices includes terms for the interslice shear forces. This example vividly illustrates this effect.

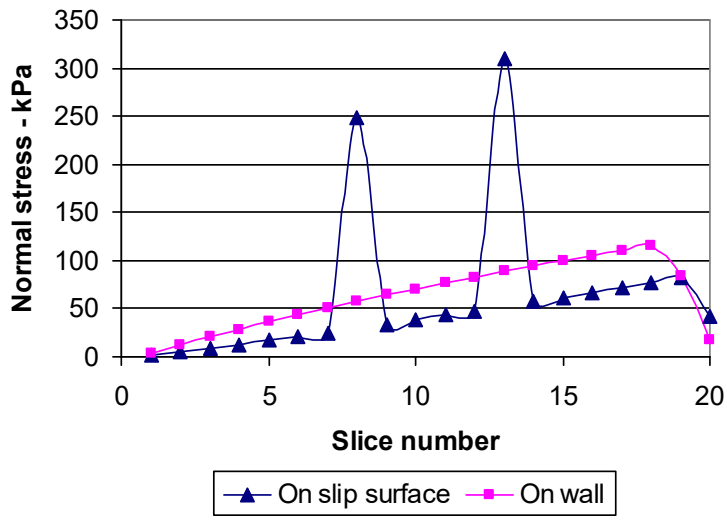

Figure 2-17 Comparison of normal stress distributions

Interestingly, in spite of the vastly different stresses between the slices and along the slip surface, the factors of safety are nearly identical for these two approaches of applying the anchor loads. With the anchors applied at the slip surface location, the factor of safety is 1.075 and when they are applied at the wall, the factor of safety is 1.076. The following table highlights this important and significant result.

Anchor Force Location	Factor of Safety
On slip surface	1.075
On wall	1.076

For all practical purposes they are the same. The reason for this is discussed later.

Another reason why the stresses do not represent field conditions is that in the limit equilibrium formulation the factor of safety is assumed to be the same for each slice. In reality this is not correct. In reality the local factor of safety varies significantly, as demonstrated in Figure 2-18.

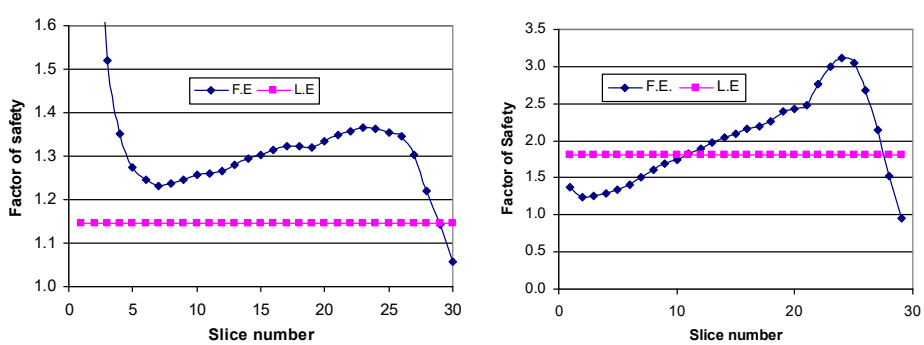

Figure 2-18 Local variation safety factors

Forcing the factor of safety to be the same for all slices over-constrains the problem, with the result that computed stresses are not always real.

2.8 Limit equilibrium forces and stresses

Why can such unrealistic stresses as discussed in the previous section give a seemingly reasonable factor of safety? The answer lies in the fundamental assumption that the factor of safety is the same for each slice. The limit equilibrium method of slices requires iterative techniques to solve the nonlinear factor of safety equations. In the Morgenstern-Price or Spencer methods, a second level of iterations is required to find the slice forces that result in the same F_m and F_f. Fundamentally, the iterations are required to meet two conditions, namely:

- To find the forces acting on each slice so the slice is in force equilibrium, and
- To find the forces on each slice that will make the factor of safety the same for each slice.

This means that interslice and slip surface forces are not necessarily representative of the actual insitu conditions, but they are the forces that satisfy the above two conditions for each slice.

If the slice forces are not representative of actual insitu ground conditions, then it is also not possible to determine a realistic line of thrust for the interslice shear-normal resultant. The forces on each slice that meet the above two conditions can result in a line of thrust outside the slice, a further indication that the slice forces are not always realistic.

Fortunately, even though the limit equilibrium statics formulation does not give realistic slice forces locally, the global factor of safety is nonetheless realistic. Once all the mobilized driving forces and base resisting shear forces are integrated, the local irregularities are smoothed out, making the overall factor of safety for the entire sliding mass quite acceptable.

As a footnote, it is interesting that the early developers of the method of slices recognized the limitations of computing realistic stresses on the slip surface. Lambe & Whitman (1969) in their text book *Soil Mechanics* point out that the normal stress at a point acting on the slip surface should be mainly influenced by the weight of the soil lying above that point. This, they state, forms the basis of the method of slices. Morgenstern and Sangrey (1978) state that one of the uses "… of the factor of safety is to provide a measure of the average shear stress mobilized in the slope." They go on to state that, "This should not be confused with the actual stresses." Unfortunately, these fundamental issues are sometimes forgotten as use of a method is gradually adopted in routine practice.

While the early developers of the method of slices intuitively recognized that the slice stress may not be real, they did not have finite element tools to demonstrate the way in which they differ from the actual ground stresses. Now, with the help of finite element analyses, it is possible to show that the difference is quite dramatic.

2.9 Janbu generalized method

In the context of stress distributions, it is of interest to examine the Janbu Generalized formulation (Janbu, 1954; Janbu, 1957). The Janbu Generalized method imposes a stress distribution on each slice. The interslice stress distribution is often assumed hydrostatic and the resultant is assumed to act on the lower third point along the side of the slice. A line which passes through the interslice force resultants on either side of the slice is known as the line of thrust. Assuming a line of thrust and taking moments about the base of each slice makes it possible to determine the magnitudes of the interslice force.

This approach works reasonably well provided the actual stress distribution in the ground is close to the imposed stress distribution, such as when the slip surface does not have sharp corners and the sliding mass is long relative to the slide depth. More generally, the approach works well when the potential sliding mass does not have significant stress concentrations. If stress concentrations exist which deviate

significantly from the Janbu Generalized imposed stress distribution, the problem is over-constrained. This leads to convergence problems and lack of force equilibrium for some slices. This is particularly true when features like anchors or nails are included in the analysis. As Abramson et al. (2002) points out, the calculations for the Janbu Generalized method are very sensitive to the line of thrust location.

Earlier it was mentioned that the line of thrust could potentially fall outside the slice. In a rigorous limit equilibrium method, the slices are always in force equilibrium, but it is possible that the interslice forces would have to act outside the slice for the slice itself to be in moment equilibrium. The Janbu Generalized approach, on the other hand, forces the line of thrust to be at a particular point on the side of the slice, but this may lead to the slice not being in force equilibrium. So it is not always possible to achieve both conditions. Sometimes the line of thrust needs to be outside the slice to have slice force equilibrium, or the slice cannot be in force equilibrium if the line of thrust is fixed at a particular point on the slice.

The behavior of the Janbu Generalized method reinforces the earlier observation that limit equilibrium methods based purely on statics can, in some circumstances, over-constrain the problem, resulting in unrealistic stress conditions. In this sense the Janbu Generalized approach is no different than any other limit equilibrium method. The inherent interslice force assumptions are different, but in the end the limitations are similar.

2.10 Missing physics

The limit equilibrium method of slices is based purely on the principle of statics; that is, the summation of moments, vertical forces, and horizontal forces. The method says nothing about strains and displacements, and as a result it does not satisfy displacement compatibility. It is this key piece of missing physics that creates many of the difficulties with the limit equilibrium method.

The missing physics in a limit equilibrium formulation is the lack of a stress-strain constitutive relationship to ensure displacement compatibility.

Overcoming the gap left by the missing piece of physics means somehow incorporating a stress-strain constitutive relationship into the formulation. One way of doing this is to use finite element computed stresses instead of determining the stresses from equations of statics. This type of scheme has been implemented in GeoStudio. Stresses computed by SIGMA/W, for example, can be used in SLOPE/W to compute a factor of safety. The details are presented in the Factor of Safety Methods chapter of this book.

2.11 Other limitations

Besides unrealistic stress distributions, limit equilibrium formulations have other limitations. One of the most primary limitations is the difficulty with convergence under certain conditions. Most of the convergence problems arise with lateral loads representing anchors, nails, fabrics and so forth. Earth structures requiring reinforcement usually have a steep face and, consequently, the critical slip surface position is inclined at a steep angle. The lateral forces, together with a steep slip surface, make it difficult to obtain a converged solution. In addition, the minimum obtainable factor of safety is often directly adjacent to trial slip surfaces for which a converged solution cannot be computed. This casts doubt on the validity of the obtainable factors of safety. This problem is discussed further in the chapter on modeling reinforcement in SLOPE/W.

Soil-structure interaction also creates some difficulties in a limit equilibrium analysis. Consider the case of a sheet pile wall as illustrated in Figure 2-19.

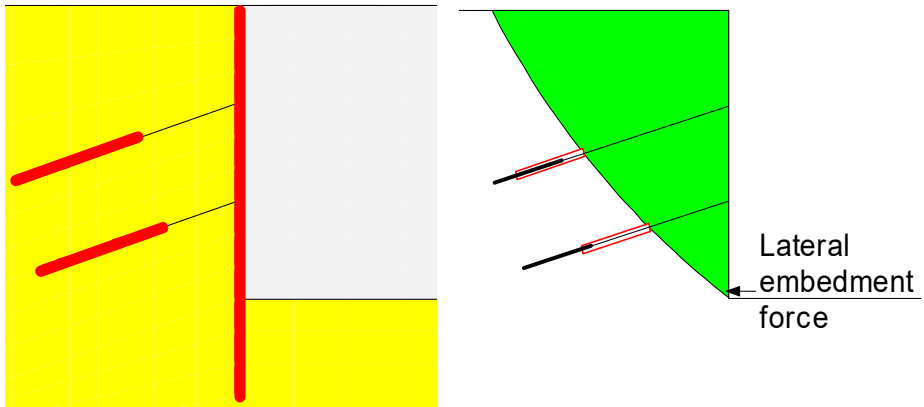

Figure 2-19 Inclusion of pile embedment in a limit equilibrium analysis

When structural components are included in a limit equilibrium analysis, the influence of the structure can extend outside the potential sliding mass. The issue is how to include the lateral resistance provided by the buried portion of the sheet piling when looking at a potential mode of failure, where the slip surface exits at the excavation base. The passive resistance in front of the pile is an integral part of the stability of the system, but it is outside the free body of the sliding mass.

One way of including the passive resistance in front of the wall is to do an independent analysis. This could be done with closed form solutions or even with a limit equilibrium analysis. The computed available force can then be included in the wall stability analysis as a concentrated point load just above the slip surface exit point as shown in the diagram on the right side of Figure 2-19.

The issue is further complicated by the fact that the passive resistance is sensitive to the friction between the wall and the soil. The passive earth pressure coefficient can vary greatly depending on the assumed friction between the soil and the steel. Also, large movement is sometimes required to develop the complete passive resistance. To account for this, only a portion of the passive resistance can be relied upon in the wall stability analysis. In other words, the passive resistance needs its own factor of safety which is likely much higher than the factor of safety for the wall stability.

2.12 Slip surface shapes

Inherent in limit equilibrium stability analyses is the requirement to analyze many trial slip surfaces and find the slip surface that gives the lowest factor of safety. Included in this trial approach is the form of the slip surface; that is, whether it is circular, piece-wise linear or some combination of curved and linear segments. SLOPE/W has a variety of options for specifying trial slip surfaces.

Often the slip surface shape is controlled, at least in part by stratigraphic boundaries or geologic features such as faults or pre-sheared surfaces. Defining these features becomes part of forming trial slip surfaces. The point is that even with such structural controls, there is still a need to examine many trial slip surfaces since the slip surface is not completely defined by the stratigraphic boundaries.

The position of the critical slip surface is affected by the soil strength properties. The position of the critical slip surface for a purely frictional soil ($c = 0$) is radically different than for a soil assigned an undrained strength ($\phi = 0$). This complicates the situation, because it means that in order to find the position of the critical slip surface, it is necessary to accurately define the soil properties in terms of effective strength parameters.

Recent research has shown that assumed user-specified slip surface shapes do not necessarily give the lowest possible factor of safety. Algorithms that alter the slip surface shape in some systematic manner tend to give lower safety factors than for a predetermined slip surface shape. For example, say a minimum factor of safety has been found for a circular slip surface. Further refinement of the shape can lead to a non-circular slip surface with a lower factor of safety. In SLOPE/W this is called optimization the slip surface shape and position.

Finding the critical slip surface shape and position still remains one of the key issues in any limit equilibrium stability analysis, in spite of all the advanced techniques available. It is not as yet a black box solution. Guidance from the user still remains an essential ingredient, and to help you with providing this guidance, a complete chapter is devoted to this topic.

2.13 Seepage forces

Seepage forces in a stability analysis can create considerable confusion. The concept of seepage forces is easy to comprehend, but including seepage forces in a limit equilibrium stability analysis is fraught with misunderstanding.

Consider the slice in Figure 2-20 where the phreatic surface passes through the slice at a steep angle relative to the slice base. The water force on the left side of the slice is larger than on the right side. The difference in water forces from one side to other side of the slice is known as a seepage force. Energy is lost or dissipated as water flows across the slice and the seepage force is proportional to the energy loss.

Now if the seepage force is to be considered in a limit equilibrium formulation, it is necessary to deal with multiple interslice forces. Below the phreatic surface we need a water force and a soil force, where the soil force is determined from the submerged or buoyant unit weight. Above the phreatic surface, the soil force is determined from the total unit weight. This is illustrated in Figure 2-20.

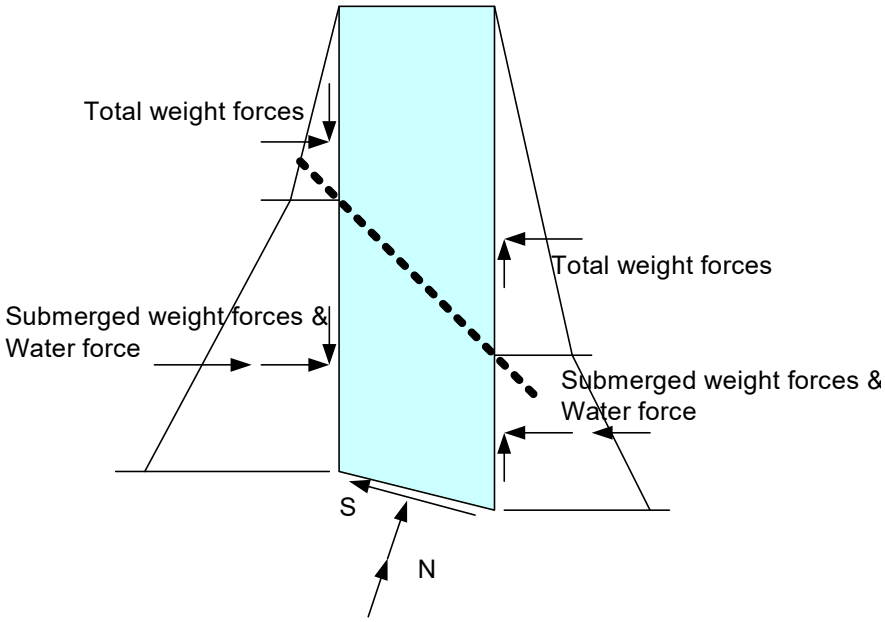

Figure 2-20 Interslice forces when seepage forces are considered

Breaking out the interslice force components unnecessarily complicates the formulation. One normal and one shear force on each side is adequate for satisfying the inherent equations of statics. As discussed above, the prime objective is to ensure force equilibrium of each slice. Also, attempting to apply interslice

forces at specific locations on the sides of slices as in the Janbu Generalized method can over constrain the problem. As noted earlier, the Janbu Generalized approach may satisfy slice moment equilibrium, but by doing so the slice may not be in force equilibrium. It was pointed out earlier that limit equilibrium formations based purely on satisfying equations of statics do not necessarily lead to computed stresses representative of actual field conditions. This being the case, there is no benefit to refining the interslice forces. Fortunately, unrealistic stress distributions do not invalidate the resulting factor of safety. The factor of safety is valid provided the overall potential sliding mass is in force and moment equilibrium – the forces internal to the sliding mass are of secondary importance. The internal forces need to be such that each slice is in force equilibrium and the factor of safety is the same for each slice. This can be accomplished without the complication of subdividing the interslice forces into submerged soil forces, total soil forces and seepage forces.

Lambe and Whitman (1968, p. 261) argue the point from a different perspective, but reach the same conclusion. They point out that to analyze the forces acting on an element we can use either *boundary water* forces with *total* weights or *seepage* forces with *submerged* weights. Then they go on to state that, although the two methods give exactly the same answer, the use of boundary forces and total weights is nearly always the more convenient method. This is certainly true in the SLOPE/W formulation. The SLOPE/W formulation uses the concept of boundary forces and total weights - SLOPE/W does **not** use the alternative concept of seepage forces and submerged or buoyant unit weights.

It is important to be aware of the SLOPE/W formulation when viewing slice forces. The slice forces are all total forces. SLOPE/W does not break out any water forces when displaying the slice forces and the force polygons. Water pressures come into play in the base shear force calculation, but water forces *per se* do not come into play in the slice equilibrium calculations.

It is critical not to mix submerged weights and seepage forces with boundary water forces and total weights. SLOPE/W uses total weights throughout and no attempt should be made to manually add seepage forces via concentrated point loads.

2.14 Concluding remarks

Geotechnical limit equilibrium stability analysis techniques have limitations. The limitations arise principally because the method does not consider strain and displacement compatibility. This has two serious consequences. One is that local variations in safety factors cannot be considered, and the second is that the computed stress distributions are often unrealistic. To allow for variations in local safety factors along the slip surface and to deal with somewhat realistic stresses, the formulation and analysis technique needs to include a stress-strain constitutive relationship. It is the absence of a stress-strain relationship in conventional limit equilibrium analysis methods that is the fundamental piece of missing physics.

The limit equilibrium method for analyzing stability of earth structures remains a useful tool for use in practice, in spite of the limitations inherent in the method. Care is required, however, not to abuse the method and apply it to cases beyond its limits. To effectively use limit equilibrium types of analyses, it is vitally important to understand the method, its capabilities and its limits, and not to expect results that the method is not able to provide. Since the method is based purely on the principles of statics and says nothing about displacement, it is not always possible to obtain realistic stress distributions. This is something the method cannot provide and consequently should not be expected to provide. Fortunately it does not mean the overall factor of safety is necessarily unacceptable just because some unrealistic stresses exist for some slices. The greatest caution and care is required when stress concentrations exist in the potential sliding mass due to the slip surface shape or due to soil-structure interaction.

A full understanding of the method and its limits leads to greater confidence in the use and in the interpretation of the results. In order to obtain this level of understanding, it is important to look at more than just the factor of safety. To use the limit equilibrium method effectively, it is also important to examine the detailed slice forces and the variation of parameters along the slip surface during the course of a project. Looking at a FS versus lambda plot can be of significant help in deciding how concerned one needs to be about defining an interslice force function.

Finally, limit equilibrium analyses applied in practice should as a minimum use a method that satisfies both force and moment equilibrium such as the Morgenstern-Price or Spencer methods. With software such as SLOPE/W, it is just as easy to use one of the mathematically more rigorous methods than to use the simpler methods that only satisfy some of the statics equations.

3 Factor of Safety Methods

3.1 Introduction

Over the years, many different methods have been developed for computing factors of safety. This chapter describes each of the methods available in SLOPE/W. All the methods are based on limit equilibrium formulations except for one method, the finite element method, which uses finite element computed stresses.

The final section of the chapter contains suggestions on how to select an appropriate method for use in practice.

3.2 General limit equilibrium Formulation

A general limit equilibrium (GLE) formulation was developed by Fredlund at the University of Saskatchewan in the 1970s (Fredlund and Krahn 1977; Fredlund et al. 1981). This formulation encompasses the key elements of all the limit equilibrium methods available in SLOPE/W. The GLE formulation provides a framework for discussing, describing and understanding all the other methods.

The GLE formulation is based on two factor of safety equations and allows for a range of interslice shear-normal force assumptions. One equation gives the factor of safety with respect to moment equilibrium (F_m), while the other equation gives the factor of safety with respect to horizontal force equilibrium (F_f). The idea of using two factor of safety equations follows from the work of Spencer (1967).

The interslice shear forces in the GLE formulation are handled with an equation proposed by Morgenstern and Price (1965). The equation is:

$$X = E \lambda f(x)$$

where, $f(x)$ is a function, λ is the percentage (in decimal form) of the function used, E is the interslice normal force and X is the interslice shear force. Figure 3-1 shows a typical half-sine function. The upper curve in this figure is the actual specified function, while the lower curve is the function used in the solution. The ratio between the two curves is called lambda (λ). The lambda value (λ) in Figure 3-1 is 0.43, which becomes apparent by looking at the value of the applied function where the specified function is 1.0. At Slice 10, $f(x)$ = 0.83. If, for example, the interslice normal force, E = 100 kN, then the interslice shear force, $X = E\, f(x)\, \lambda$ = 100 x 0.43 x 0.83 = 35.7 kN. Arc tan (35.7/100) = 19.6 degrees. This means the interslice resultant force is inclined at 19.6 degrees from the horizontal at Slice 10.

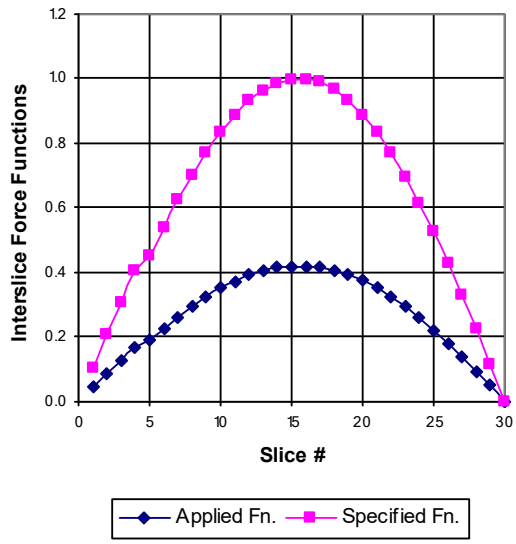

Figure 3-1 Interslice applied and specified functions

The GLE factor of safety equation with respect to moment equilibrium is:

$$F_m = \frac{\sum (c'\beta R + (N - u\beta)R \ \tan\phi')}{\sum Wx - \sum Nf \pm \sum Dd}$$

The factor of safety equation with respect to horizontal force equilibrium is:

$$F_f = \frac{\sum (c'\beta \cos\alpha + (N - u\beta) \tan\phi' \cos\alpha)}{\sum N \sin\alpha - \sum D \cos\omega}$$

The terms in the equations are:

c'	=	effective cohesion
ϕ'	=	effective angle of friction
U	=	pore-water pressure
N	=	slice base normal force
W	=	slice weight
D	=	concentrated point load
β, R, x, f, d, ω	=	geometric parameters
α	=	inclination of slice base

There are additional terms in these equations, but their definition is not required here for this discussion. The complete equations are presented in the theory chapter.

One of the key variables in both equations is *N*, the normal at the base of each slice. This equation is obtained by the summation of vertical forces. Vertical force equilibrium is consequently satisfied. In equation form, the base normal is defined as:

$$N = \frac{W + (X_R - X_L) - \dfrac{c'\beta \sin\alpha + u\beta \sin\alpha \tan\phi'}{F}}{\cos\alpha + \dfrac{\sin\alpha \tan\phi'}{F}}$$

F is F_m when N is substituted into the moment factor of safety equation and F is F_f when N is substituted into the force factor of safety equation. The literature on slope stability analysis often refers to the denominator as m_α. Later we will return to this term in the discussion on the Bishop method.

An important point to note here is that the slice base normal is dependent on the interslice shear forces X_R and X_L on either side of a slice. The slice base normal is consequently different for the various methods, depending on how each method deals with the interslice shear forces.

The GLE formulation computes F_m and F_f for a range of lambda (λ) values. With these computed values, a plot such as in Figure 3-2 can be drawn that shows how F_m and F_f vary with lambda (λ). This type of plot is a useful feature of the GLE formulation. Such a plot makes it possible to understand the differences between the factors of safety from the various methods, and to understand the influence of the selected interslice force function.

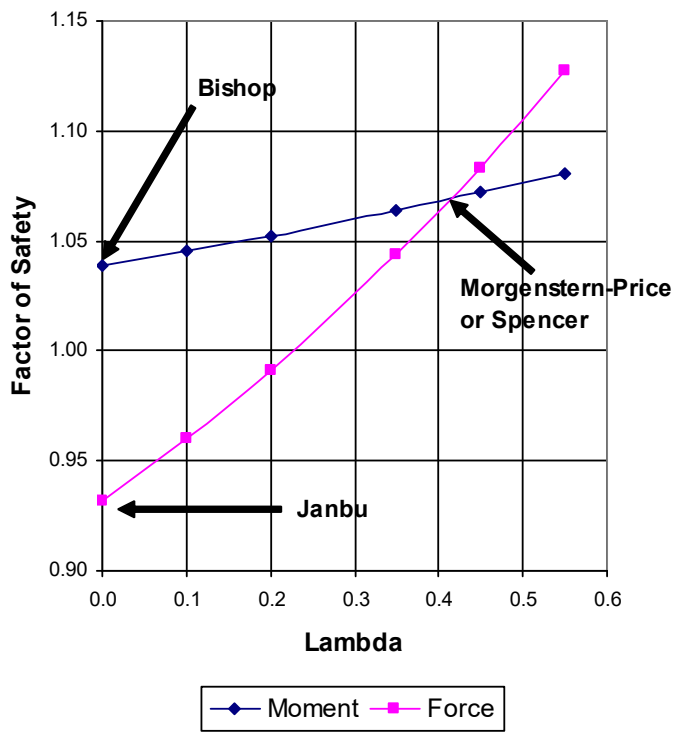

Figure 3-2 A factor of safety versus lambda (λ) plot

Two of the primary assumptions of the Bishop's Simplified method are that it ignores interslice shear forces and satisfies only moment equilibrium. In the GLE terminology, not considering shear forces means λ is zero. As a result, the Bishop's Simplified factor of safety falls on the moment curve in Figure 3-2 where lambda is zero. Janbu's Simplified method also ignores interslice shear forces and only satisfies force equilibrium. The Janbu's Simplified factor of safety consequently falls on the force curve in Figure 3-2 where λ is zero. The Spencer and Morgenstern-Price (M-P) factors of safety are determined at the point where the two curves cross. At this point the factor of safety satisfies both moment and force

equilibrium. Whether the crossover point is the Spencer or M-P factor of safety depends on the interslice force function. Spencer only considered a constant X/E ratio for all slices. The M-P method can utilize any general appropriate function. Methods like the Corps of Engineers and Lowe-Karafiath factors of safety fall on the force curve, since they only satisfy force equilibrium. The position on the force curve depends on the procedure used to establish the inclinations of the interslice force resultant. This is discussed in further detail below for each of the method.

The GLE formulation can be applied to any kinematically admissible slip surface shape. By implication, the Bishop method, for example, can consequently be used to analyze non-circular as well as circular slip surfaces. All the methods discussed here are characterized more by the equations of statics satisfied and the manner in which the interslice forces are handled than by the shape of the slip surface. The importance of the interslice force function is related to the slip surface shape, as noted in the previous chapter, but no method is restricted to a particular slip surface shape. As it turns out, the moment factor of safety is not sensitive to the assumed interslice force function when the slip surface is circular. Consequently, the Bishop's Simplified factor of safety for a circular slip surface is often close to a Spencer or Morgenstern-Price factor of safety. In this sense, the Bishop's Simplified method is suitable for a circular slip surface analysis. The assumptions inherent in the Bishop's Simplified method, however, can equally be applied to non-circular slip surfaces. So the GLE formulation encompasses all the other methods regardless of slip surface shape.

SLOPE/W can accommodate a wide range of different interslice force functions. The following is a summary list.

- Constant
- Half-sine
- Clipped-sine
- Trapezoidal
- Data point fully specified

A rigoruous method such a M-P or Spencer's method satisfies both moment and force equilibrium by finding the cross- over point of the F_m and F_f curves. The factor of safety versus lambda plots are mirrored for right-left and left-right problems, as illustrated in Figure 3-3. The safety factors are the same (1.283), but lambda has the opposite sign. This is required to keep all the forces in the correct direction. Lambda values can sometimes also take on opposite signs, for example, when large lateral forces are applied.

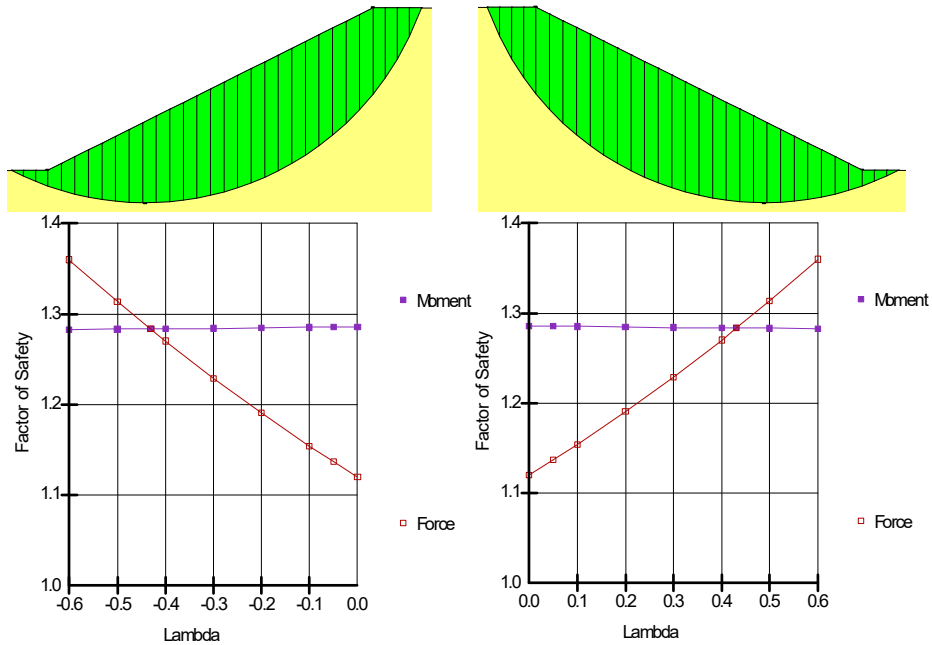

Figure 3-3 Effect of sliding direction on lambda

SLOPE/W by default uses lambda values that varying from -1.25 to +1.25. This range sometimes needs to be narrowed, since it is not always possible to obtain a converged solution at the extremities of the range. For presentation in Figure 3-3 the lambda range was set to a range from 0.0 to 0.6.

The GLE formulation is very useful for understanding what is happening behind the scenes and understanding the reasons for differences between the various methods. It is not necessarily a method for routine analyses in practice, but it is an effective supplementary method useful for enhancing your confidence in the selection and use of the other more common methods.

3.3 Ordinary or Fellenius method

This method is also sometimes referred to as the Swedish method of slices.

This is the first method of slices developed and presented in the literature. The simplicity of the method made it possible to compute factors of safety using hand calculations.

In this method, all interslice forces are ignored. The slice weight is resolved into forces parallel and perpendicular to the slice base. The force perpendicular to the slice base is the base normal force, which is used to compute the available shear strength. The weight component parallel to the slice base is the gravitational driving force. Summation of moments about a point used to describe the trial slip surface is also used to compute the factor of safety. The factor of safety is the total available shear strength along the slip surface divided by the summation of the gravitational driving forces (mobilized shear).

The simplest form of the Ordinary factor of safety equation in the absence of any pore-water pressures for a circular slip surface is:

$$FS = \frac{\sum [c\beta + N \tan \phi]}{\sum W \sin \alpha} = \frac{\sum S_{resistance}}{\sum S_{mobilized}}$$

where:

c	=	cohesion,
β	=	slice base length,
N	=	base normal (W cos α),
ϕ	=	friction angle,
W	=	slice weight, and
α	=	slice base inclination.

The Ordinary factor of safety can be fairly easily computed using a spreadsheet. Using a spreadsheet is of course not necessary when you have SLOPE/W, but doing a simple manual analysis periodically is a useful learning exercise.

Consider the simple problem in Figure 3-4. There are 14 slices numbered from left to right. The cohesive strength is 5 kPa and the soil friction angle ϕ is 20 degrees.

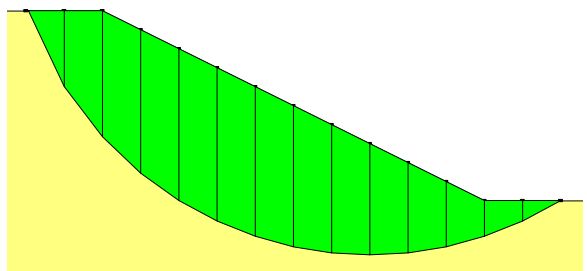

Figure 3-4 Case for hand-calculations

The following two tables illustrate how the Ordinary factor of safety can be easily calculated. The most difficult part is specifying the slice dimensions.

Slice #	Width (m)	Mid-height (m)	Weight (kN)	Alpha (degrees)	β (m)
1	1.9	2.3	86.9	64.7	4.42
2	2.0	5.4	217.8	52.9	3.32
3	2.0	7.2	287.0	43.7	2.77
4	2.0	7.8	313.2	35.8	2.46
5	2.0	8.1	323.3	28.5	2.28
6	2.0	8.0	320.9	21.8	2.15
7	2.0	7.7	307.7	15.4	2.07
8	2.0	7.1	285.1	9.2	2.03
9	2.0	6.3	253.7	3.0	2.00
10	2.0	5.3	213.7	-3.0	2.00
11	2.0	4.1	165.1	-9.2	2.03
12	2.0	2.7	107.7	-15.4	2.07
13	2.0	1.5	60.9	-21.8	2.15
14	2.0	0.6	23.3	-28.5	2.28

Slice #	C β	N	N tan ϕ	W sin α	C β + N tan ϕ
1	22.12	37.09	13.50	78.56	35.62
2	16.60	131.25	47.77	173.84	64.37
3	13.83	207.49	75.52	198.27	89.35
4	12.32	254.18	92.51	182.98	104.83
5	11.38	284.02	103.37	154.50	114.76
6	10.77	297.88	108.42	119.23	119.19
7	10.37	296.70	107.99	81.67	118.36
8	10.13	281.48	102.45	45.40	112.58
9	10.01	253.30	92.19	13.46	102.21
10	10.01	213.35	77.65	-11.34	87.67
11	10.13	163.01	59.33	-26.29	69.46
12	10.37	103.87	37.81	-28.59	48.18
13	10.77	56.50	20.56	-22.61	31.33
14	11.38	20.49	7.46	-11.15	18.84
Σ	–	–	–	947.93	1116.75

From the summations listed above, the factor of safety can be computed to be:

$$FS = \frac{\sum[c\beta + N\tan\phi]}{\sum W\sin\alpha} = \frac{1116.75}{947.93} = 1.18$$

SLOPE/W gives the same factor of safety as shown in Figure 3-5.

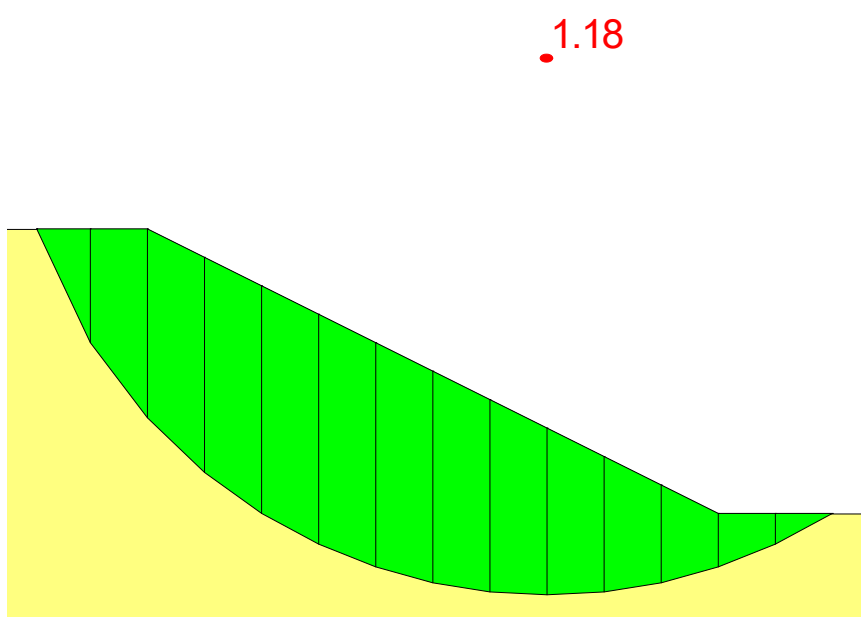

Figure 3-5 SLOPE/W computed Ordinary factor of safety

The most noteworthy aspects of this method are the slice forces and force polygons. Figure 3-6 shows free body diagrams and force polygons for Slice 3 and Slice 13. Slice 3 is just below the slope crest and Slice 13 is just below the slope toe. First of all, note that there are no interslice shear and no interslice normal forces. Secondly, note the extremely poor force polygon closure. The lack of force polygon closure indicates the slices are not in force equilibrium. With no interslice normal forces, there is nothing available to counterbalance the lateral components of the base shear and normal, particularly when the slice base is close to being horizontal.

When interpreting the free body diagram and force polygons, it is important to note that the shear at the slice base is the mobilized shear, not the available shear strength resistance. The available shear resistance is equal to the mobilized shear times the factor of safety. The last column in the above table lists the available shear resistance, which has to be divided by the factor of safety in order to match the base shear values shown on the slice free bodies.

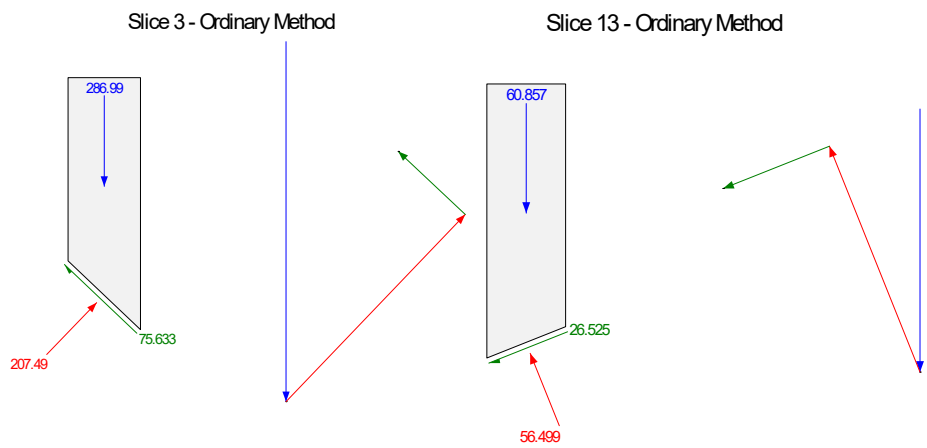

Figure 3-6 Free body diagram and force polygon for the Ordinary method

Due to the poor force polygon closure, the Ordinary method can give unrealistic factors of safety and consequently should not be used in practice. A more realistic Factor of Safety for this simple problem is around 1.36, which is about 15% higher than the 1.18 obtained from the Ordinary method.

The Ordinary method is included in SLOPE/W only for historic reasons and for teaching purposes. It is a useful learning exercise to compare a SLOPE/W analysis with hand calculations. Also, this method is where it all started, so in this sense, it is a good historic reference point.

The Ordinary factor of safety cannot be plotted on a GLE Factor of Safety versus Lambda graph since lambda is undefined.

The Ordinary method should not be used in practice, due to potential unrealistic factors of safety.

3.4 Bishop's simplified method

In the 1950's Professor Bishop at Imperial College in London devised a method which included interslice normal forces, but ignored the interslice shear forces. Bishop developed an equation for the normal at the slice base by summing slice forces in the vertical direction. The consequence of this is that the base normal becomes a function of the factor of safety. This in turn makes the factor of safety equation nonlinear (that is, FS appears on both sides of the equation) and an iterative procedure is consequently required to compute the factor of safety.

A simple form of the Bishop's Simplified factor of safety equation in the absence of any pore-water pressure is:

$$FS = \frac{1}{\sum W \sin\alpha} \sum \left[\frac{c\beta + W \tan\phi - \frac{c\beta}{FS} \sin\alpha \tan\phi}{m_\alpha} \right]$$

FS is on both sides of the equation as noted above. The equation is not unlike the Ordinary factor of safety equation except for the m_α term, which is defined as:

$$m_\alpha = \cos\alpha + \frac{\sin\alpha \tan\phi}{FS}$$

To solve for the Bishop's Simplified factor of safety, it is necessary to start with a guess for FS. In SLOPE/W, the initial guess is taken as the Ordinary factor of safety. The initial guess for FS is used to compute m_α and then a new FS is computed. Next the new FS is used to compute m_α and then another new FS is computed. The procedure is repeated until the last computed FS is within a specified tolerance of the previous FS. Fortunately, usually it only takes a few iterations to reach a converged solution.

Now if we examine the slice free body diagrams and forces polygons for the same slices as for the Ordinary method above, we see a marked difference (Figure 3-7). The force polygon closure is now fairly good with the addition of the interslice normal forces. There are no interslice shear forces, as assumed by Bishop, but the interslice normal forces are included.

In a factor of safety versus lambda plot, as in Figure 3-8, the Bishop's Simplified factor of safety falls on the moment equilibrium curve where lambda is zero (FS = 1.36). Recall that

$$X = E\lambda f(x)$$

The interslice shear is not included by making lambda zero.

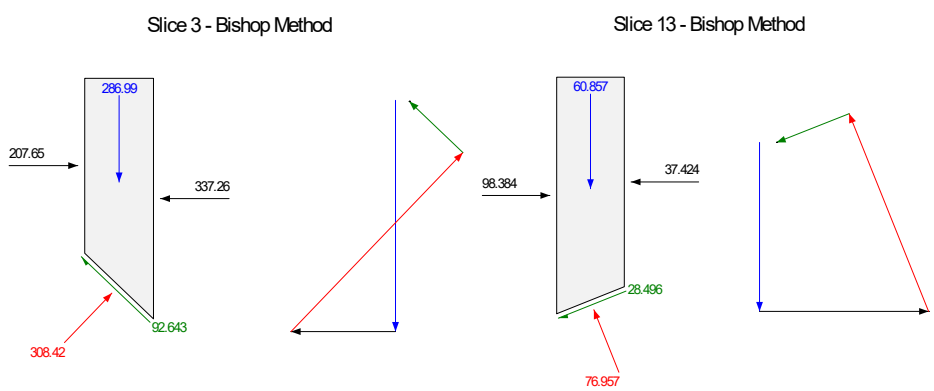

Figure 3-7 Free body diagram and force polygon for the Bishop's Simplified method

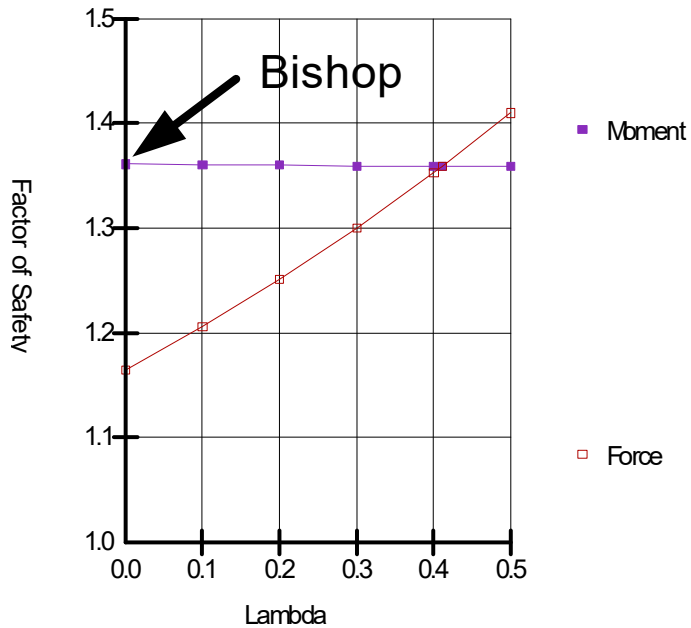

Figure 3-8 Bishop's Simplified factor of safety

Note that in this case the moment factor of safety (F_m) is insensitive to the interslice forces. The reason for this, as discussed in the previous chapter, is that no slippage is required between the slices for the sliding mass to rotate. This is not true for force equilibrium and thus the force factor of safety (*Ff*) is sensitive to the interslice shear.

In summary, the Bishop's Simplified method, (1) considers normal interslice forces, but ignores interslice shear forces, and (2) satisfies over all moment equilibrium, but not overall horizontal force equilibrium.

3.5 Janbu's simplified method

The Janbu's Simplified method is similar to the Bishop's Simplified method except that the Janbu's Simplified method satisfies only overall horizontal force equilibrium, but not overall moment equilibrium.

Figure 3-9 shows the free body diagrams and force polygons of the Janbu's Simplified method. The slice force polygon closure is actually better than that for the Bishop's Simplified method. The factor of safety, however, is 1.16 as opposed to 1.36 by Bishop's Simplified method. This is a significant difference. The Janbu's Simplified factor of safety is actually too low, even though the slices are in force equilibrium.

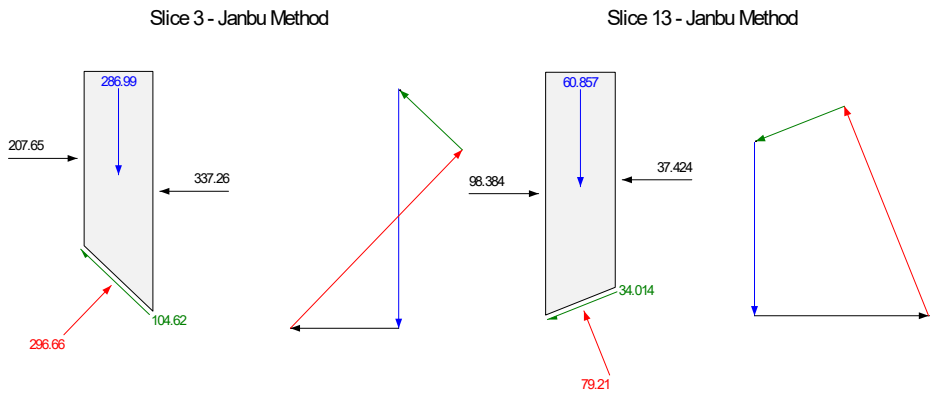

Figure 3-9 Free body diagram and force polygon for the Janbu method

As with the Bishop's Simplified method, lambda (λ) is zero in the Janbu's Simplified method, since the interslice shear is ignored. Therefore, the Janbu's Simplified factor of safety falls on the force equilibrium curve where lambda is zero (Figure 3-10). Since force equilibrium is sensitive to the assumed interslice shear, ignoring the interslice shear, as in the Janbu's Simplified method, makes the resulting factor of safety too low for circular slip surfaces.

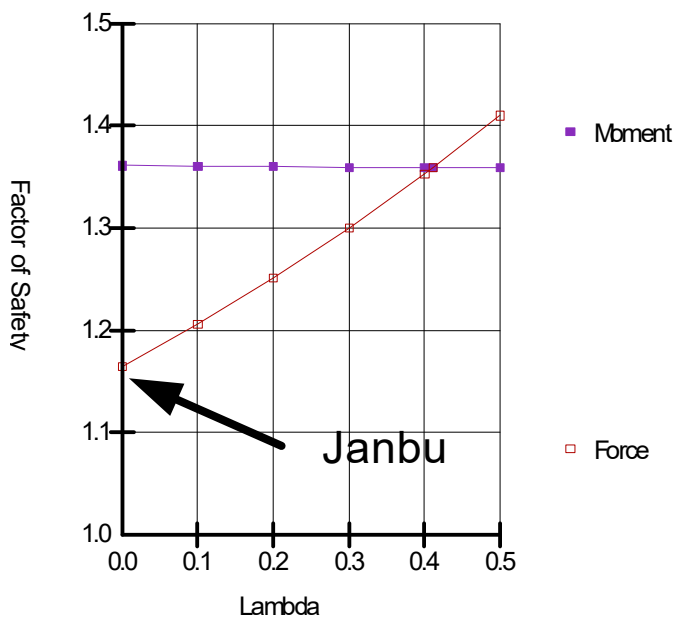

Figure 3-10 Janbu's Simplified factor of safety

In summary, the Janbu's Simplified method, (1) considers normal interslice forces, but ignores interslice shear forces, and (2) satisfies over all horizontal force equilibrium, but not over all moment equilibrium.

3.6 Spencer method

As discussed in the previous chapter, Spencer (1967) developed two factor of safety equations; one with respect to moment equilibrium and another with respect to horizontal force equilibrium. He adopted a constant relationship between the interslice shear and normal forces, and through an iterative procedure altered the interslice shear to normal ratio until the two factors of safety were the same. Finding the shear-

normal ratio that makes the two factors of safety equal, means that both moment and force equilibrium are satisfied.

SLOPE/W uses the following equation to relate the interslice shear (*X*) and normal (*E*) forces.

$$X = E\,\lambda\,f(x)$$

In the Spencer method, the function *f(x)* is a constant; that is, the interslice shear-normal ratio is the same between all slices.

Figure 3-11 shows a typical slope stability situation. The Spencer Factor of Safety is 1.140.

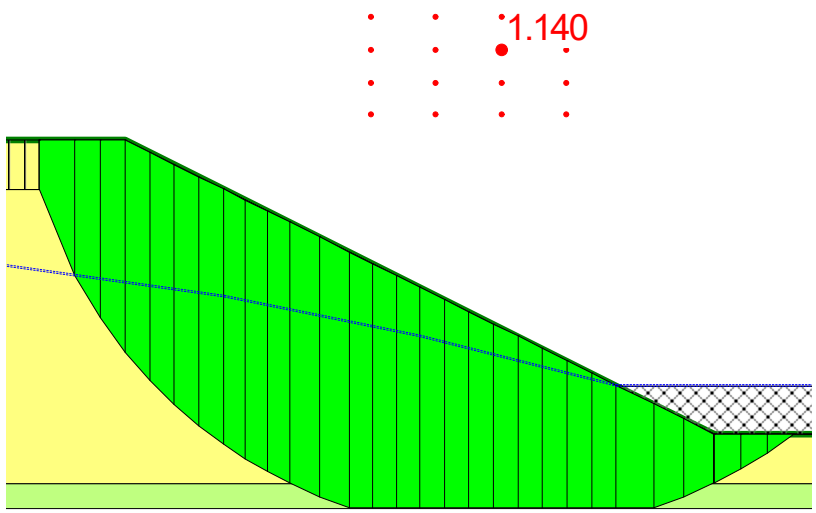

Figure 3-11 Typical slope stability situation

On a Factor of Safety versus Lambda plot as in Figure 3-12 the Spencer factor of safety is where the moment and force equilibrium curves cross.

Lambda at the crossover point is 0.12. The function *f(x)* is 1.0 for the Spencer method. This means that the equation relating the interslice shear and normal forces is,

$$X = E \times 0.12 \times 1.0$$
$$X = 0.12E$$

A graph of the specified function and the applied interslice function is shown in Figure 3-13. Note that the applied function is a constant at 0.12.

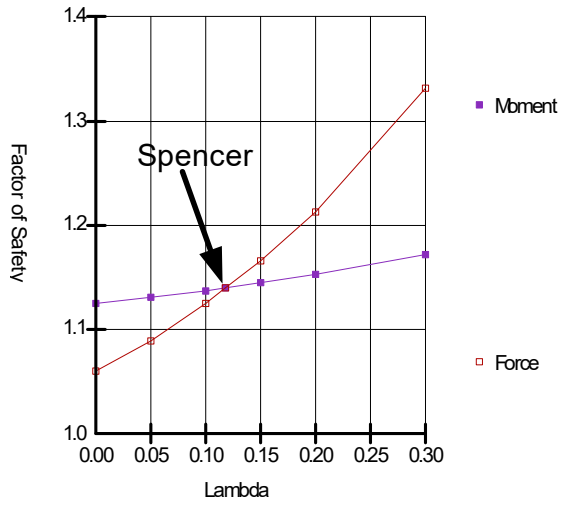

Figure 3-12 Spencer factor of safety

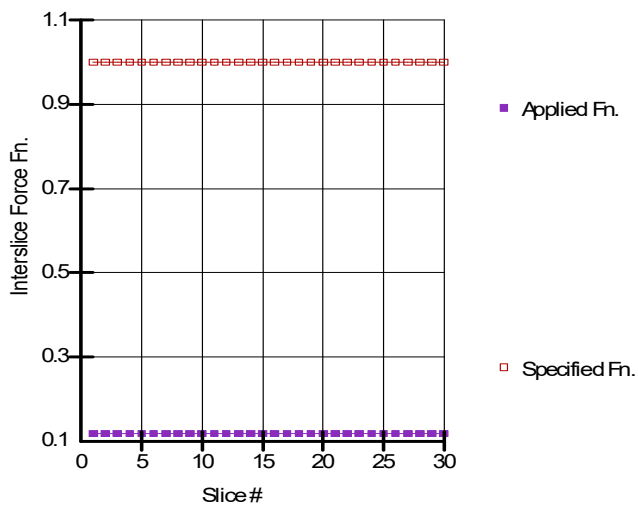

Figure 3-13 Interslice functions for the Spencer method

Further confirmation of the relationship between the interslice shear and normal forces is evident in the slice forces. Figure 3-14 shows a typical slice.

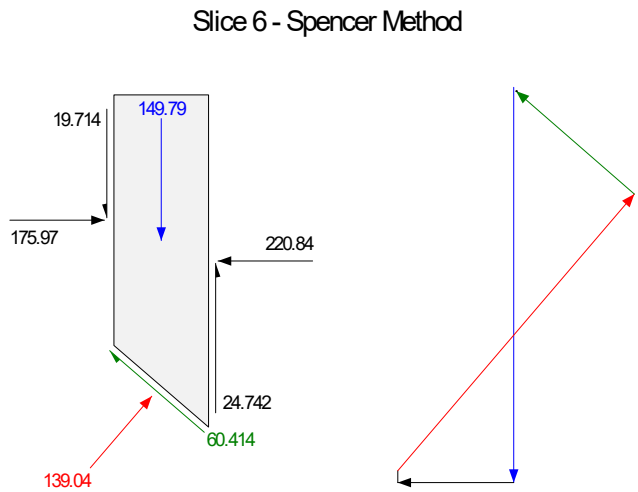

Figure 3-14 Free body diagram and force polygon for the Spencer method

On the left of the slice, the ratio of shear to normal is 19.714/175.97 which is 0.12. On the right side the ratio is 24.742/220.84 which is also 0.12.

A shear-normal ratio of 0.12 means that the interslice force resultant is inclined at an angle of arctan (0.12), which is 6.74 degrees.

Worth noting is that when both interslice shear and normal forces are included, the force polygon closure is very good.

In summary, the Spencer method:

- Considers both shear and normal interslice forces,
- Satisfies both moment and force equilibrium, and
- Assumes a constant interslice force function.

3.7 Morgenstern-Price method

Morgenstern and Price (1965) developed a method similar to the Spencer method, but they allowed for various user-specified interslice force functions. The interslice functions available in SLOPE/W for use with the Morgenstern-Price (M-P) method are:

- Constant
- Half-sine
- Clipped-sine
- Trapezoidal
- Data-point specified

Selecting the Constant function makes the M-P method identical to the Spencer method.

For illustrative purposes, let us look at a M-P analysis with a half-sine function for the same problem as was used to discuss the Spencer method. The result is presented in Figure 3-15.

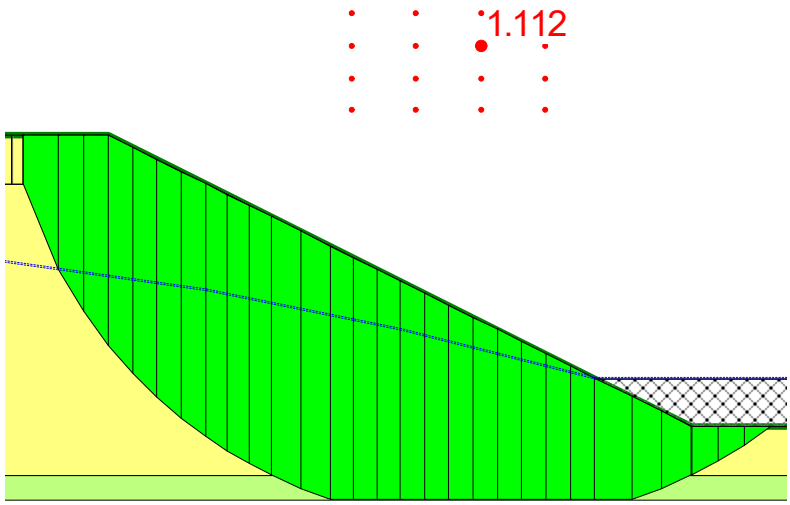

Figure 3-15 Result of Morgenstern-Price analysis

Figure 3-16 shows how the moment and force factors of safety vary with lambda. The M-P Factor of safety occurs where the two curves across.

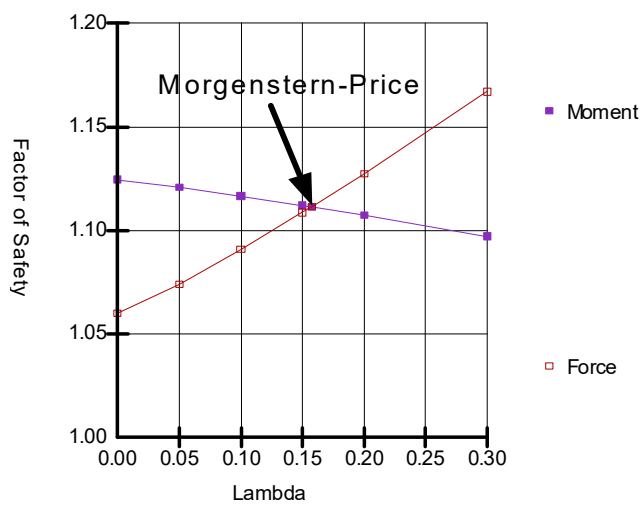

Figure 3-16 Morgenstern-Price safety factors with half-sine function

The specified and applied interslice force functions are shown in Figure 3-17. The specified function has the shape of a half-sine curve. The applied function has the same shape, but is scaled down by a value equal to lambda which is 0.145.

Consider the forces on Slice 10 (Figure 3-18). The specified function at Slice 10 is 0.86 and lambda is 0.146. The normal force on the right side of Slice 10 is 316.62. The corresponding interslice shear then is,

$$X = E\lambda f(x)$$

$$X = 316.62 \times 0.146 \times 0.86$$

$$X = 39.7$$

This matches the interslice shear value on the free body diagram in Figure 3-18.

As with the Spencer method, the force polygon closure is very good with the M-P method, since both shear and normal interslice forces are included.

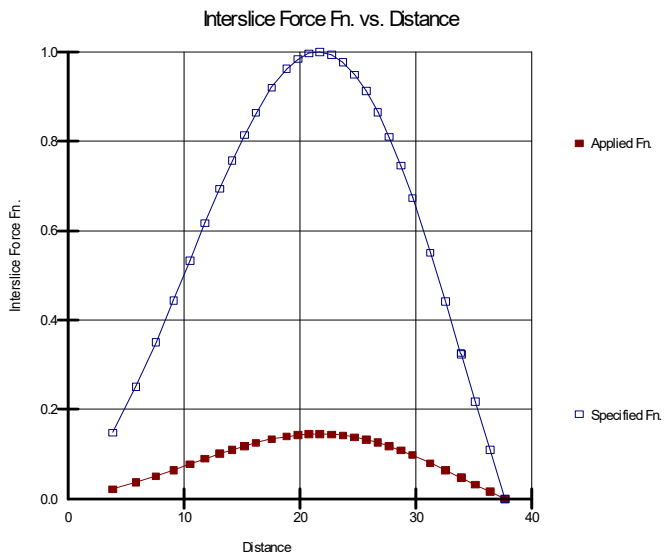

Figure 3-17 Interslice half-sine functions

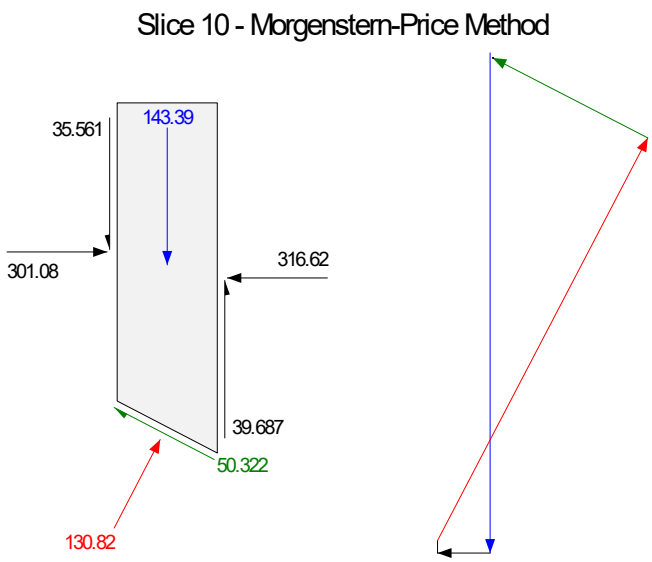

Figure 3-18 Free body and force polygon for Morgenstern-Price method

A significant observation in Figure 3-18 is that the M-P Factor of Safety (cross over point) is lower than the Bishop's Simplified Factor of Safety (moment equilibrium ay lambda zero). This is because the moment equilibrium curve has a negative slope. This example shows that a simpler method like Bishop's Simplified method that ignores interslice shear forces does not always err on the save side. A more rigorous method like the M-P method that considers both interslice shear and normal forces results in a lower factor of safety in this case.

Simpler methods that do not include all interslice forces and do not satisfy all equations of equilibrium sometimes can err on the unsafe side.

In summary, the Morgenstern-Price method:

- Considers both shear and normal interslice forces,
- Satisfies both moment and force equilibrium, and
- Allows for a variety of user-selected interslice force function.

3.8 Corps of Engineers method

The Corps of Engineers method is characterized by a specific interslice force function, and the method only satisfies overall horizontal force equilibrium. Overall moment equilibrium is not satisfied.

This method makes two different assumptions about the interslice forces. One uses the slope of a line from crest to toe (slip surface entrance and exit points) and the one uses the slope of the ground surface at the top of the slice.

Interslice assumption one

Figure 3-19 illustrates the first of the interslice force assumption for Corps of Engineers method. The dark line from crest to toe is the assumed direction of the interslice force resultant.

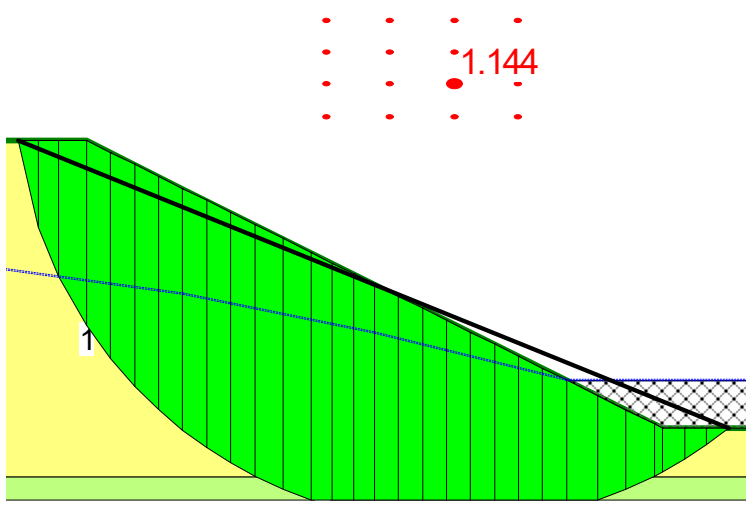

Figure 3-19 Corps of Engineers assumption #1

The slope of the line from crest to toe in Figure 3-19 is about 0.37. The SLOPE/W plot of the interslice force function, as shown in Figure 3-20, indicates a constant function of 0.37. In this case, the applied function is equal to the specified function, since the specified function is computed by the software.

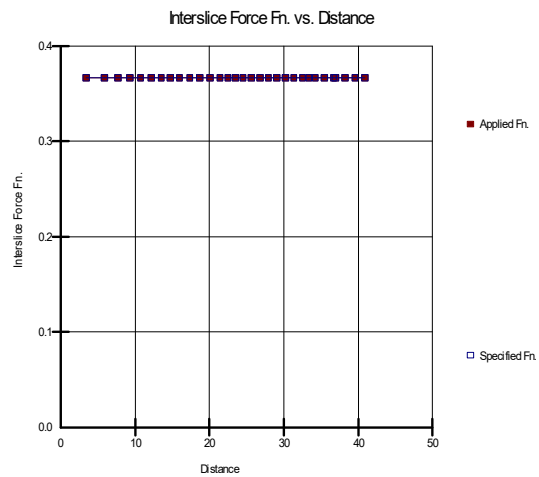

Figure 3-20 Corps of Engineers #1 interslice function

We can check the resultant direction by looking at the slice forces. Figure 3-21 shows the forces for Slice 6. The ratio of shear to normal on the side of the slice is about 0.37, confirming that the direction of the resultant is parallel to the line from crest to toe.

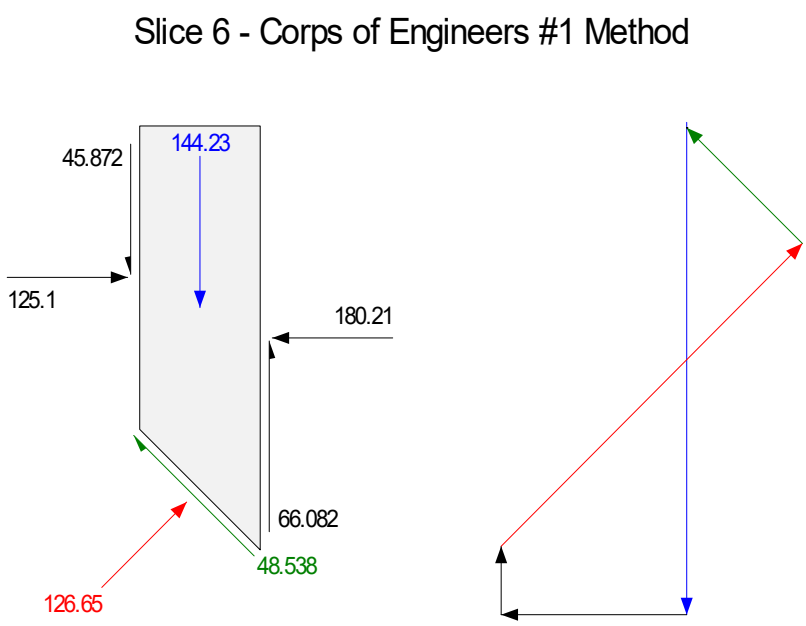

Figure 3-21 Free body and force polygon for Corps of Engineers Method Interslice Assumption One

Interslice assumption two

The second interslice assumption in the Corps of Engineers method is that the interslice resultant is equal to the ground surface slope at the top of the slice. The interslice function for the example in Figure 3-22 is shown in Figure 3-23. Where the ground surface is horizontal, the interslice force resultant is horizontal. Where the ground surface is at an incline, the resultant is parallel to the ground surface slope. The

inclination of the slope is at 2:1. This makes the ratio of shear to normal 0.5. This is consistent with the function in Figure 3-23.

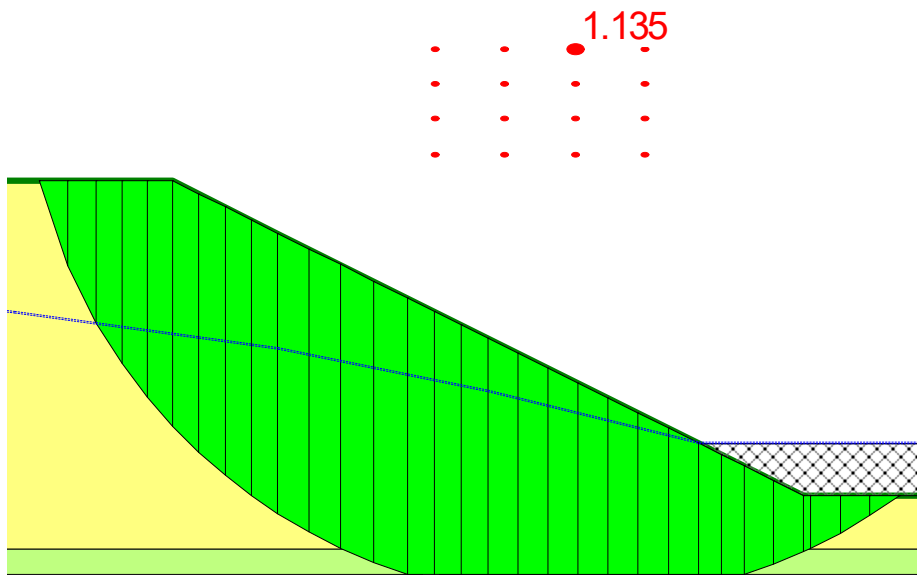

Figure 3-22 Corps of Engineers assumption #2

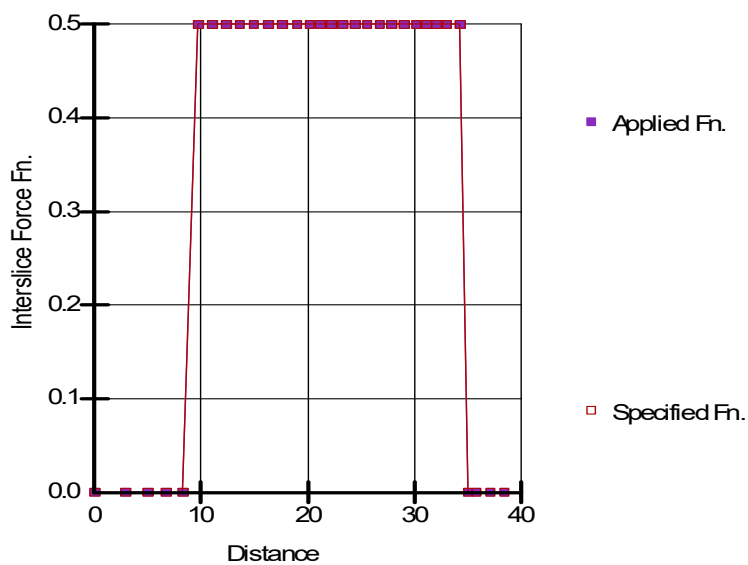

Figure 3-23 Corps of Engineers #2 interslice force function

A consequence of the second Corps of Engineers interslice force assumption is that the interslice shear is zero when the ground surface is horizontal.

Again, we can check the resultant direction by looking at the slice forces. Figure 3-24 shows the forces for Slice 6. The ratio of shear to normal on the side of the slice is about 0.5, confirming that the direction of the resultant is parallel to inclination of the slope.

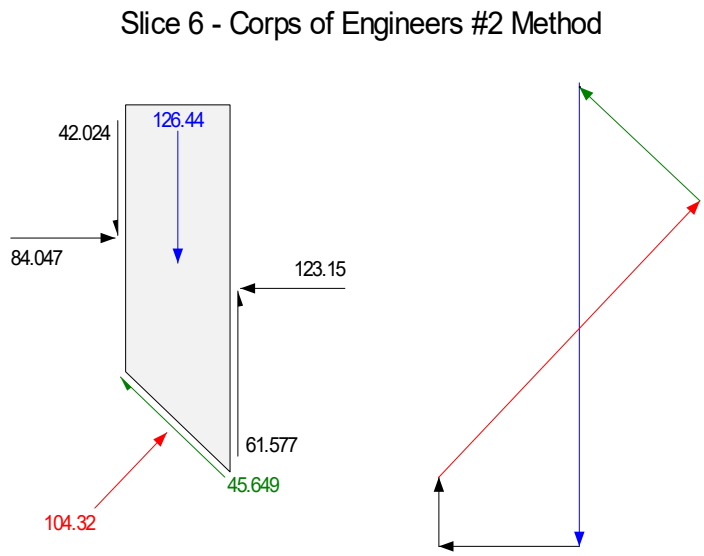

Figure 3-24 Free body and force polygon for Corps of Engineers Method Interslice Assumption Two

The Corps of Engineers factor of safety falls on the force equilibrium curve in a Factor of Safety versus Lambda plot, since this method only satisfies force equilibrium. Placing the computed safety factor on the plot is, however, somewhat misleading. There is no one single lambda value as in the Spencer or M-P method. If a Corps of Engineers factor of safety is plotted on such a graph, the corresponding lambda value would be a representation of an average lambda. Such an average value, however, can not be used to spot check the shear to normal ratio. The computed interslice function is all that is required to spot check that the correct shear forces have been computed.

In Summary, the Corps of Engineers method:

- Considers both interslice shear and normal forces,
- Satisfies overall horizontal force equilibrium, but not moment equilibrium, and
- Uses interslice force functions related to the slope and slip surface geometry.

3.9 Lowe-Karafiath method

The Lowe-Karafiath (L-K) method is essentially the same as the Corps of Engineers method, except that it uses another variation on the assumed interslice force function. The L-K method uses the average of the slice top (ground surface) and the base inclination. Figure 3-25 shows a case analyzed using the L-K method, and Figure 3-26 shows the corresponding computed interslice force function. The function is a reflection of the ground surface slope and the slice base inclination. Note that where the slice base is horizontal, the function is around 0.25, which is the average of the surface slope (0.5) and the base inclination (0.0).

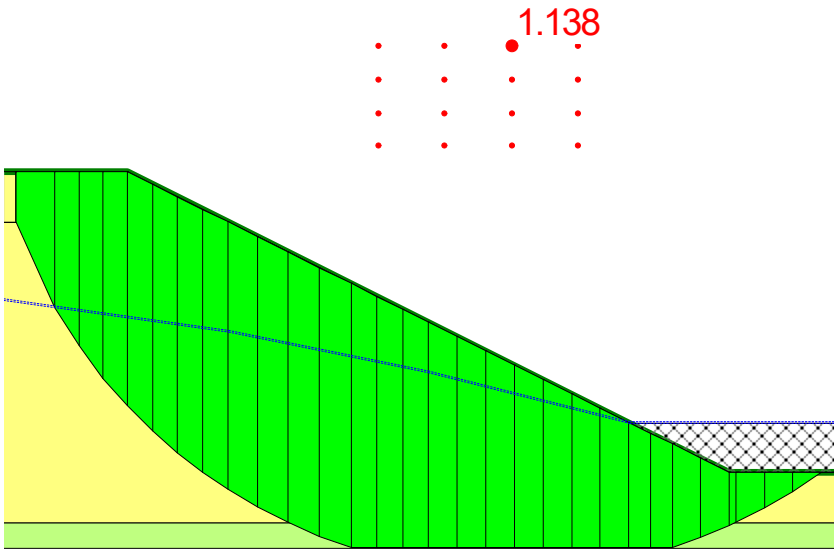

Figure 3-25 Lowe-Karafiath safety factor

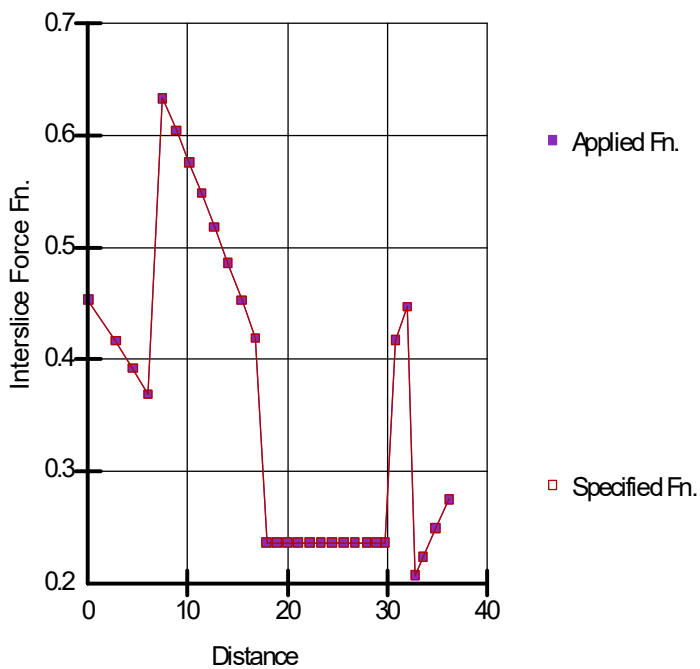

Figure 3-26 Lowe-Karafiath interslice function

We can check the resultant direction by looking at the slice forces. Figure 3-27 shows the forces for Slice 6. The ratio of shear to normal on the side of the slice is about 0.62, confirming that the direction of the resultant is parallel to inclination of the slope.

In Summary, the Lowe-Karafiath method:

- Considers both interslice shear and normal forces,
- Satisfies overall horizontal force equilibrium, but not moment equilibrium, and

- Uses interslice force functions related to the ground surface slope and slip surface inclination.

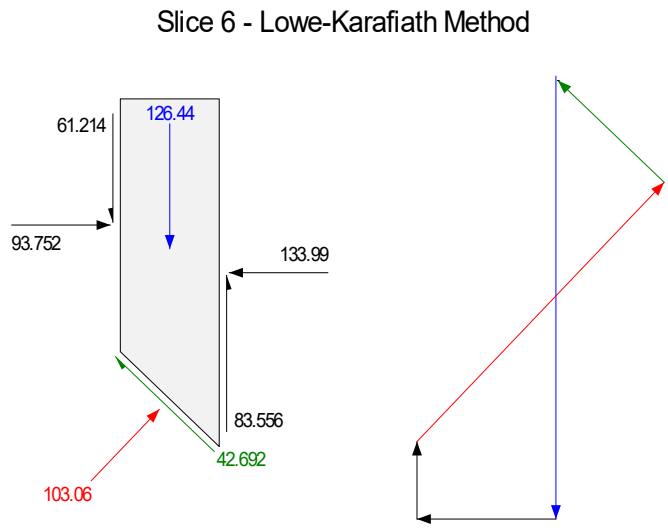

Figure 3-27 Free body and force polygon for Lowe-Karafiath Method

3.10 Sarma method

Sarma (1973) developed a stability analysis method for non-vertical slice or for general blocks. Only vertical slices are assumed in the current Sarma method implemented in SLOPE/W. The full Sarma method has as yet not been implemented. The geometric definition of the blocks does not fit into the general method of slices scheme in SLOPE/W for all the other methods, and therefore special software is required to define and visualize the results. The plan is to add the complete Sarma method at a future time.

The approach used by Sarma to relate the inter-block shear and normal forces can also be used to describe the relationship between the interslice shear and normal forces between slice.

Sarma adopted an equation similar to the Mohr-Coulomb shear strength equation to relate the interslice shear and normal forces. The equation (using SLOPE/W terminology) is:

$$X = c \times h + E \tan \phi$$

where, c is a cohesive strength component, h is the slice side height and ϕ is a material friction angle. The material properties are user-specified values.

The attraction of this approach is that the interslice forces are related by material properties that are intuitively perhaps easier to conceptualize than a specified function, but in the end it just another mechanism for specifying the interslice function.

This approach works best when the cohesion is zero or at least very small. When the cohesion is zero, the interslice shear is directly proportional to the normal as with all the other methods. When a cohesion value is specified, the interslice shear starts to become independent of the interslice normal, which can lead to convergence difficulties.

When using the Sarma interslice force approach, you should start with cohesion being zero. Later you can add a small amount to cohesion and investigate the effect of adding this component, but is has to be done care and caution. Considering how insensitive the resulting factor of safety is to interslice forces, it is likely best to always leave the cohesion as zero.

Other than the manner in which the interslice forces are related, the Sarma method in SLOPE/W is the same as the Spencer and the Morgenstern-Price methods. The computed interslice shear forces are adjusted with a global factor (similar to Lambda) until overall force and moment equilibrium are satisfied.

Figure 3-28 shows the free body diagram and the force polygon when $c = 0$ and $\phi = 30$ degrees. The final lambda value when converged is 0.197. The interslice shear force on the right side of the slice is 0.197 x 221.51 tan 30 = 25.1 as shown in Figure 3-28. The force polygon closes, showing force equilibrium in the Sarma method.

In summary, the Sarma method in SLOPE/W:

- Considers both shear and normal interslice forces,
- Satisfies both moment and force equilibrium, and
- Relates the interslice shear and normal forces by a quasi-shear strength equation.

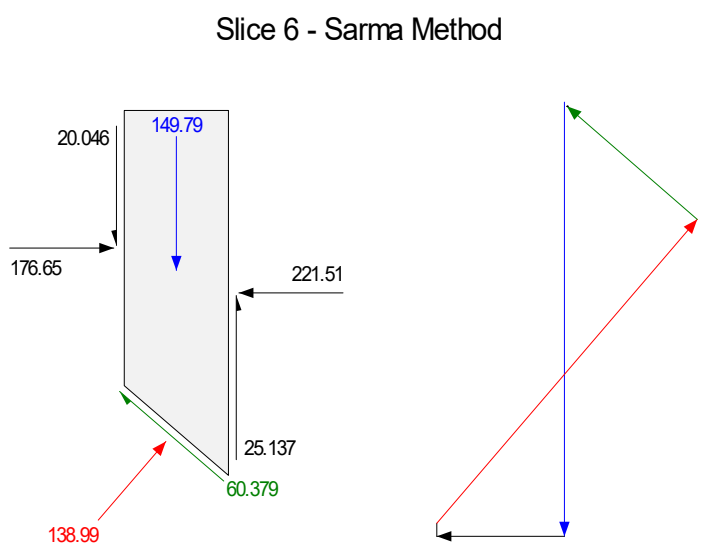

Figure 3-28 Free body and force polygon for Sarma Method

3.11 Janbu's Generalized method

The Janbu Generalized method is somewhat different than all the other limit equilibrium methods discussed above. This method imposes a stress distribution on the potential sliding mass by defining a line of thrust. The interslice shear-normal resultant is assumed to act where the line of thrust intersects the slices, which typically is at the lower ⅓ point along the sides of the slices to represent a hydrostatic stress distribution. Assuming the position of the resultant makes it possible to compute the interslice shear forces by taking moments about the slice base center, the interslice normals are first computed using the

Janbu's Simplified method, which has been discussed earlier. Next the interslice shear forces are determined by taking moments about the base of the slice.

The Janbu's Generalized method only satisfies overall force equilibrium, which is the same as the Janbu's Simplified. Moment equilibrium is only satisfied at the slice level. In SLOPE/W, the Janbu's Generalized method only computes the force equilibrium factor of safety (F_f). The overall moment equilibrium factor of safety (F_m) is not computed.

The Janbu Generalized method is actually similar to the Corps of Engineers and Lowe-Karafiath methods. All these methods consider both interslice shear and normal forces, but satisfy only force equilibrium. The Janbu Generalized method just uses a different technique to relate the interslice shear forces to the normal forces.

The previous chapter on Limit Equilibrium Fundamentals discusses the consequence of imposing a stress distribution on the potential sliding mass. Limit equilibrium formulations do not necessarily result in realistic stress distributions. Limit Equilibrium formulations find the slice forces that ensure force equilibrium of each slice and that ensure a constant factor of safety for each slice. These inherent characteristics can result in unrealistic stresses, and if the stresses are unrealistic, the slice itself may not satisfy moment equilibrium. Numerically this means the application point of the interslice resultant may be outside the slice. Conversely, if we find the slice forces that ensure moment equilibrium of each slice, then it may not be possible to ensure force equilibrium of each slice if the factor of safety is assumed the same for each slice. In a sense, assuming on a constant factor of safety overconstrains the problem at some level. To overcome this difficulty it is necessary to have a variable local factor of safety. In a limit equilibrium formulation, this is not possible. A method such as the Finite Element Stress based method discussed in the next section is required to have a variable local slice factor of safety.

Stress concentrations arising from sharp corners in a piece-wise linear slip surface or from concentrated forces representing reinforcement can create convergence difficulties in the Janbu's Generalized method. Also, the method may exhibit poor force polygon closure. Enforcing slice moment equilibrium means that it is not always possible to achieve slice force equilibrium.

Figure 3-29 shows the free body diagram and the force polygon of a slice using the Janbu's Generalized method. The interslice forces, although shown to be applied to the middle of the slice, are actually applied at the lower 1/3 of the slice sides in SLOPE/W. Although moment equilibrium is achieved in the slice, force equilibrium is not necessarily achieved, as indicated by the force polygon in Figure 3-29.

You will note in publications on the Janbu's Generalized method that the illustrated potential sliding masses are often long relative to the depth. In a relatively long shallow slide, the stress distribution is likely close to being hydrostatic with depth, similar to that assumed in the method. The Janbu's Generalized method of course works the best when the actual stress distribution is close to the imposed stress distribution.

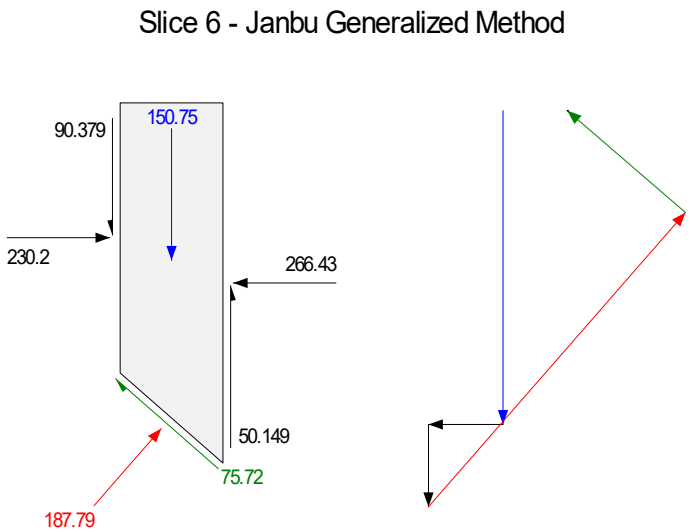

Figure 3-29 Free body and force polygon for Janbu's Generalized Method

So in summary, Janbu's Generalized method is just another approach to a limit equilibrium formulation. It is not necessarily better or worse than any of the other methods, as it has limitations just like all the other methods. The Janbu's Generalized method factors of safety will be similar to those methods that consider both shear and normal interslice forces, particularly if there are no sharp corners along the slip surface or high concentrated loads that cause stress concentrations.

3.12 Finite element stress-based method

The chapter on Limit Equilibrium Fundamentals discusses stress distributions obtained from limit equilibrium formulations, and shows that these stress distributions are not necessarily representative of the actual field stresses. To repeat, the limit equilibrium formulations give stresses and forces that:

- Aim to provide for force equilibrium of each slice
- Make the factor of safety the same for each slice

These inherent concepts and assumptions mean that it is not always possible to obtain realistic stress distributions along the slip surface or within the potential sliding mass. Some other piece of physics has to be added to the stability analysis to over come these limitations. The missing piece of physics is a stress-strain relationship. Including such a relationship means displacement compatibility is satisfied, which in turn leads to much more realistic stress distributions.

One way of including a stress-strain relationship in a stability analysis is to first establish the stress distribution in the ground using a finite element analysis and then use these stresses in a stability analysis. This idea has been implemented in SLOPE/W. The ground stresses can be computed using SIGMA/W, and SLOPE/W uses the SIGMA/W stresses to compute safety factors. The following is a description of the implemented procedure.

Figure 3-30 shows a simple 45-degree slope discretized into finite elements. Using a simple gravity turn-on technique, the stresses in the ground can be computed. Using a linear-elastic constitutive relationship, the vertical stresses are as presented in Figure 3-31. This is typical of the information available from a

finite element analysis. The basic information obtained from a finite element stress analysis is σ_x, σ_y and τ_{xy} within each element.

Worth noting at this stage is the 50 kPa contour, which is not a constant distance from the ground surface. The contour is closer to the surface under the toe. This means that the vertical stress is not just influenced by the overburden weight. It is also affected by the shear stress.

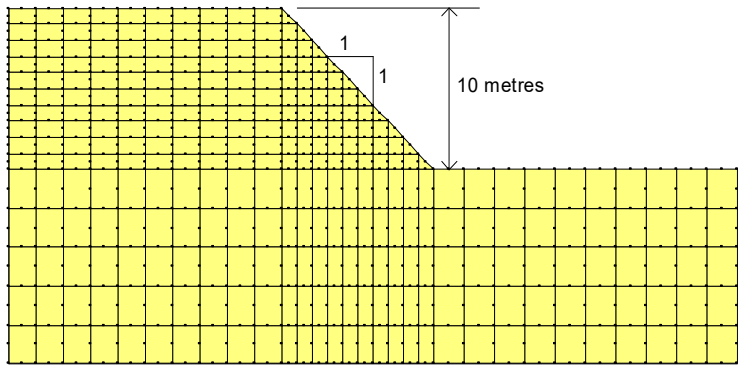

Figure 3-30 Finite element mesh for computing insitu stresses

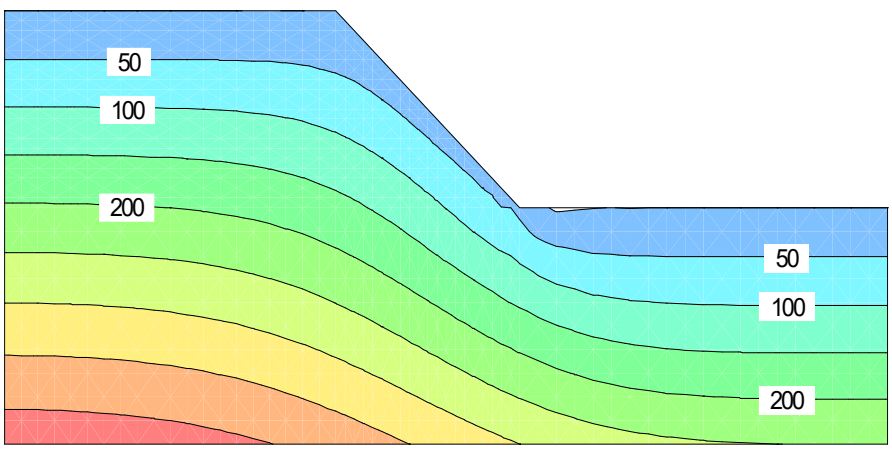

Figure 3-31 Vertical stress contours computed with SIGMA/W

The finite element-computed stresses can be imported into a conventional limit equilibrium analysis. The stresses σ_x, σ_y τ_{xy} are known within each element, and from this information the normal and mobilized shear stresses can be computed at the base mid-point of each slice. The procedure is as follows:

1. The known σ_x, σ_y and τ_{xy} at the Gauss numerical integration point in each element are projected to the nodes and then averaged at each node. With the σ_x, σ_y and τ_{xy} known at the nodes, the same stresses can be computed at any other point within the element.
2. For Slice 1, find the element that encompasses the x-y coordinate at the base mid-point of the slice.
3. Compute σ_x, σ_y and τ_{xy} at the mid-point of the slice base.
4. The inclination (α) of the base of the slice is known from the limit equilibrium discretization.
5. Compute the slice base normal and shear stress using ordinary Mohr circle techniques.
6. Compute the available shear strength from the computed normal stress,

7. Multiply the mobilized shear and available strength by the length of the slice base to convert stress into forces.
8. Repeat process for each slice in succession up to Slice # n

Once the mobilized and resisting shear forces are available for each slice, the forces can be integrated over the length of the slip surface to determine a stability factor. The stability factor is defined as:

$$FS = \frac{\sum S_r}{\sum S_m}$$

where, S_r is the total available shear resistance and S_m is the total mobilized shear along the entire length of the slip surface. Similar stability factor expressions have been presented by others (Kulhawy 1969; Naylor, 1982).

Figure 3-32 shows a potential sliding mass discretized into slices superimposed on the finite element mesh. Following the procedure listed above, the stability factor for this slip surface is 1.318. This compares with a Morgenstern-Price factor of safety of 1.145 (constant interslice function). This is about a 15% difference.

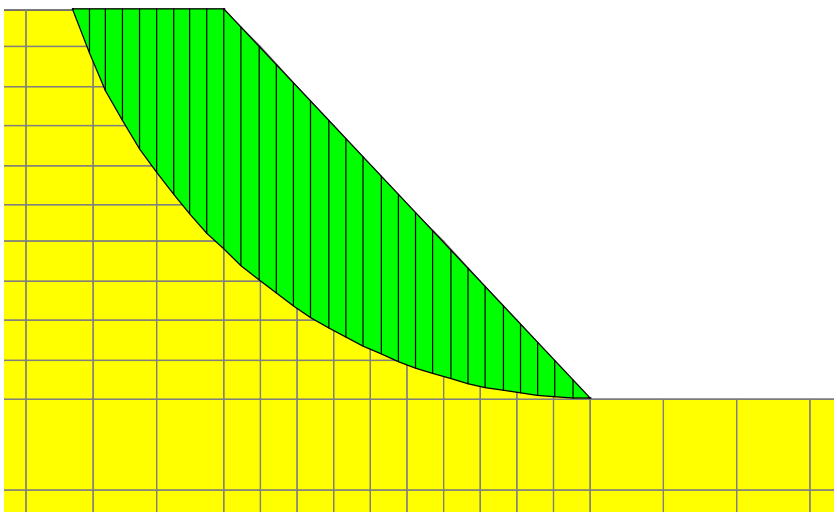

Figure 3-32 Toe slip surface on a finite element mesh

The reason for the difference in the margin of safety is primarily related to the normal stress distribution along the slip surface. The finite element and limit equilibrium normal stress distributions for this particular slip surface were presented earlier in Figure 3-33. The significantly different normal stresses in the toe area result from the shear stress concentration in this part of the section. Localized shear stress concentrations are, of course, not captured in a limit equilibrium formation where the slice base normal is derived primarily from the slice weight. This is one of the limitations of the limit equilibrium method.

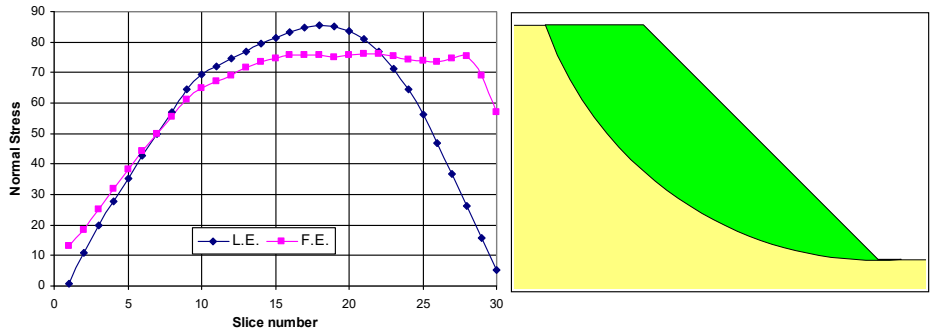

Figure 3-33 Normal stress distribution along a toe slip surface

The situation is somewhat different for a deeper slip, as shown in Figure 3-34. The finite element and limit equilibrium normal stress distributions along the slip surface are much closer for this case. Consequently the stability factor based on finite element stresses is almost the same as the Morgenstern-Price factor of safety. The stress-based stability factor is 1.849 while the Morgenstern-Price factor of safety is 1.804. This shows that, when the normal stress distribution along the slip surface is fairly representative of the actual ground stresses, the limit equilibrium factor of safety is as good as a stress-based factor of safety.

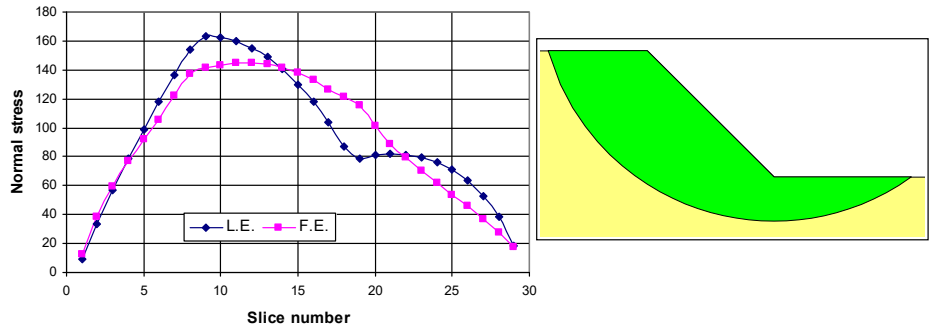

Figure 3-34 Normal stress distribution along a deep slip surface

An added advantage of the finite element stressbased approach is that it creates the possibility of looking at local safety factors for each slice. Figure 3-35 shows the variation of the local safety factor for the toe and deep slip surfaces. Included in the figure is the limit equilibrium factor of safety, which is the same for each slice.

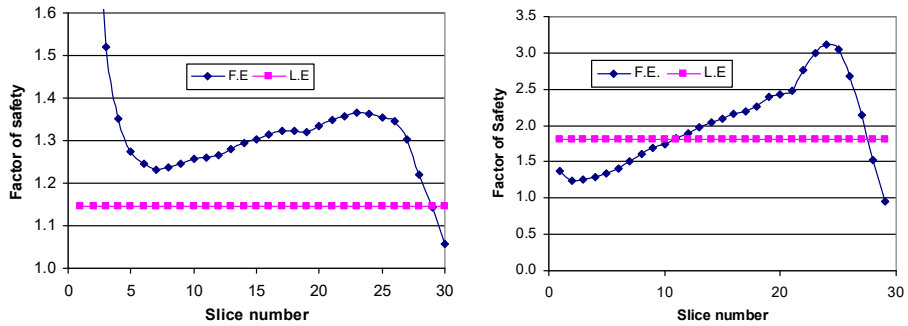

Figure 3-35 Local safety factors for toe (left) and deep (right) slip surfaces

For the deep slip surface the two global factors of safety are almost identical. Locally, however, the safety factors are either smaller or greater than the global value represented in this figure by the constant limit equilibrium factor of safety. Integrating the total available shear resistance and total mobilized shear along the slip surface averages the variation, making the two factors of safety the same.

The finite element stress-based approach overcomes some other limitations, such highlighted in the previous chapter. Convergence is problematic in a LE formation, particularly when the critical slip surface is steep, as behind a tie-back wall. Using FE stresses overcomes these convergence difficulties, as is further illustrated in the chapter on analyzing walls and steep slopes with reinforcement. Also, using FE stresses overcomes many of the difficulties with soil-structure problems. One of the very attractive features of doing a stability analysis based on finite element computed stresses is that soil-structure interaction can be handled in a direct manner. The difficulty of dealing with forces outside the sliding mass in a LE analysis was discussed in the previous chapter in the discussion on dealing with sheet piling embedment below the slip surface. Another similar situation is the use of a shear key wall placed across a slip surface to stabilize a slope, as illustrated in Figure 3-36. In this case, there is no need to try and represent the wall resistance with a point load as in a limit equilibrium analysis, and there is no need to independently determine the point load magnitude. The stiffness of the structure is included in the finite element analysis, which alters the stress state and which in turn increases the margin of safety.

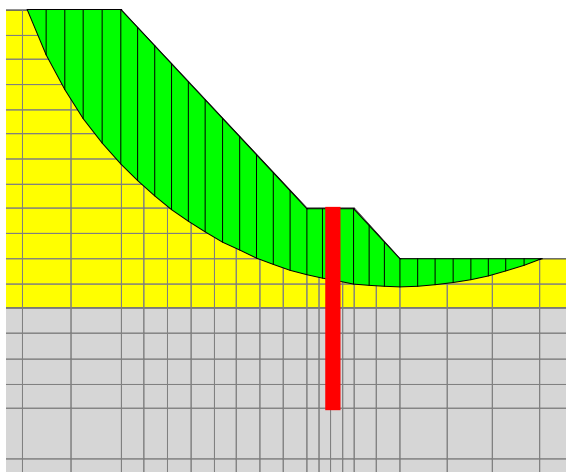

Figure 3-36 A shear-key wall for slope stabilization

The finite element stress-based approach also opens the door to looking at stability variations due to ground shaking during an earthquake. The stresses can come from a QUAKE/W dynamic finite element analysis the same as they can from a static stress analysis. The stresses computed during a dynamic earthquake analysis can be saved at regular intervals during the shaking. A factor of safety then can be computed for each moment in time that the stresses are available, and in the end a plot of factor of safety versus time graph can be created, as shown in Figure 3-38. This type of plot can be readily created for each and every trial slip surface. This is a great improvement over the historic pseudo-static approach still used so routinely in practice. This is discussed further in the chapter on Seismic and Dynamic stability.

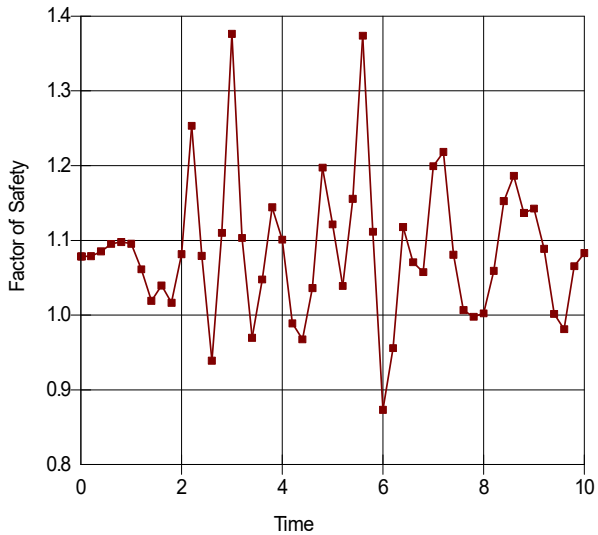

Figure 3-37 Factors of safety variations during earthquake shaking

3.13 Commentary on finite element stress-based method

The use of finite element computed stresses inside a limit equilibrium framework to assess stability has many advantages. Some are as follows:

- There is no need to make assumptions about interslice forces.
- The stability factor is deterministic once the stresses have been computed, and consequently, there are no iterative convergence problems.
- The issue of displacement compatibility is satisfied.
- The computed ground stresses are much closer to reality.
- Stress concentrations are indirectly considered in the stability analysis.
- Soil-structure interaction effects are readily handled in the stability analysis
- Dynamic stresses arising from earthquake shaking can be directly considered in a stability analysis.

The finite element based approach overcomes many of the limitations inherent in a limit equilibrium analysis. At the same time, it does raise some new issues.

It is necessary to first carry out a finite element stress analysis with the proposed approach. Fortunately, the necessary software tools are now readily available and relatively easy to use. However, it does mean that the analyst must become familiar with finite element analysis techniques.

Fortunately, a finite element stress analysis is fairly straightforward if the material properties are restricted to simple linear-elastic behavior. Besides being relatively simple, using only linear-elastic soil models always ensures a solution, since there are no convergence difficulties, which can be a problem with nonlinear constitutive models. A linear-elastic analysis is adequate in many cases to obtain a reasonable picture of the stress conditions. It certainly gives a much better stress distribution picture than that obtained from a limit equilibrium analysis. Nonlinear constitutive relationships are often essential if

the main interest is deformation, but not if the main interest is a stress distribution. Furthermore, even approximate linear-elastic properties are adequate to get a reasonable stress distribution and, consequently, not a great deal of effort is required to define the linear-elastic parameters.

The results from a simple linear-elastic analysis may mean that the computed stresses in some zones are higher than the available soil strength. This manifests itself as a local factor of safety of less than 1.0 for some slices, which is not physically possible. Ideally, nonlinear constitutive models should be used to redistribute the stresses such that the applied stresses do not exceed the strength. However, using nonlinear constitutive relationships greatly complicates the analysis, primarily because of the associated numerical convergence issues. Ignoring local safety factors that are less than unity is not all that serious. Physically, it means that neighboring slices have a local safety factor that is too high. Since all the mobilized and resisting shear forces are tallied along the entire slip surface, local irregularities are smoothed out and therefore have little effect on the total forces which are used in computing the global factor of safety for the entire sliding mass. This is an indirect form of averaging, but not nearly to the extent that is inherent in the limit equilibrium formulation, where the factor of safety is the same for all slices.

Figure 3-38 shows the local factor of safety distribution for a simple 2h:1v slope when the stresses are determined using a linear-elastic analysis and an elastic-plastic analysis. The linear-elastic stresses result in local safety factors less than 1.0. The elastic-plastic analysis redistributes the stresses and then none of the local safety factors are less than 1.0. The global factors of safety are, however, nearly identical. For the linear-elastic case, the global factor of safety is 1.206 and for the elastic-plastic case the global factor of safety is 1.212, less than half a percent difference.

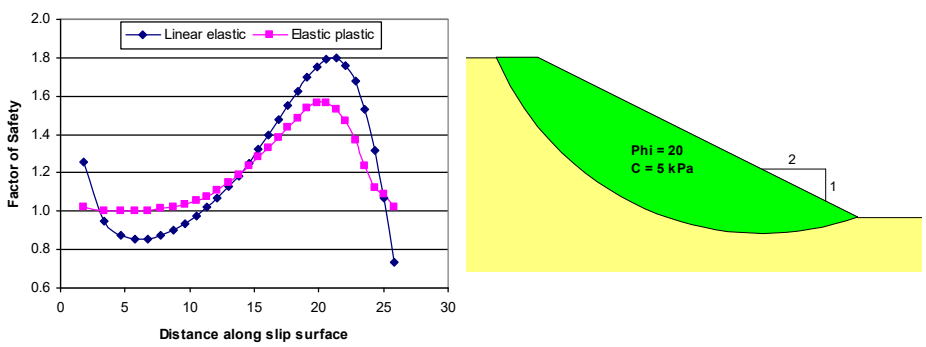

Figure 3-38 Local safety factors for linear-elastic & elastic-plastic stresses

Using the finite element computed stresses means that the stability calculations now involve the horizontal stresses as well as the vertical stresses. This is good and bad. The good part is that various K_o (σ_x / σ_y ratio) conditions can be considered in a stability analysis. The bad part is that the K_o must be defined In a linear-elastic gravity turn-on analysis, the ratio of σ_x / σ_y is reflected through Poisson's ratio (v). For level ground, K_o equals $v/(1- v)$. Different K_o conditions will give different safety factors. Fredlund et al. (1999) studied the effect of varying Poisson's ratio on the factor of safety. Fortunately, defining appropriate K_o conditions is not an impossibility. It is certainly not so difficult as to prevent the use of finite element stresses in assessing stability.

3.14 Selecting an appropriate method

The limit equilibrium method for analyzing stability of earth structures remains a useful tool for use in practice, in spite of the limitations inherent in the method. Care is required, however, not to abuse the method and apply it to cases beyond its limits. To effectively use limit equilibrium types of analyses, it is

vitally important to understand the method, its capabilities and its limits, and not to expect results that the method is not able to provide. Since the method is based purely on the principles of statics and says nothing about displacement, it is not always possible to obtain realistic stress distributions. This is something the method cannot provide and consequently should not be expected. Fortunately, just because some unrealistic stresses perhaps appear for some slices, does not mean the overall factor of safety is necessarily unacceptable. The greatest caution and care is required when stress concentrations exist in the potential sliding mass due to the slip surface shape or due to soil-structure interaction.

A detailed understanding of the method and its limits leads to greater confidence in the use and in the interpretation of the results. Getting to this position means you have to look at more than just factors of safety. To use the limit equilibrium method effectively, it is also important to examine the detailed slice forces and the variation of parameters along the slip surface, at least sometime during the course of a project. Looking at a FS versus lambda plots, for example, is a great aid in deciding how concerned one needs to be about defining an interslice force function.

Also, limit equilibrium analyses applied in practice should as a minimum use a method that satisfies both force and moment equilibrium, such as the Morgenstern-Price or Spencer methods. With the software tools now available, it is just as easy to use one of the mathematically more rigorous methods than to use the simpler methods that only satisfy some of the statics equations.

In practice you should use a method that meets two criteria. One, the method should satisfy all equations of statics, and two, the method should consider both shear and normal interslice forces.

At this stage the SIGMA/W-SLOPE.W integrated method is the most applicable where conventional limit equilibrium methods have numerical difficulties as in vertical or near vertical walls with some kind of reinforcement. The method is perhaps not all that applicable in the stability of natural slopes where it is not easy to accurately determine the stresses in the slope due to the complex geological processes that created the slope. In the analysis of natural slopes where the potential slip surface does not have sharp corners and there are no high stress concentrations, the conventional limit equilibrium method is more than adequate in spite of its limitations.

The tools required to carry out geotechnical stability analyses based on finite element computed stresses are today readily available. Applying the tools is now not only feasible, but also practical. Unforeseen issues will possibly arise in the future, but such details will likely be resolved with time as the method is used more and more in geotechnical engineering practice.

Using finite element computed stresses inside a limit equilibrium framework to analyze the stability of geotechnical structures is a major step forward since it overcomes many of the limitations of traditional limit equilibrium methods and yet it provides an anchor to the familiarity of limit equilibrium methods so routinely used in current practice.

3.15 Rapid Drawdown Analysis Methods

Stability analysis during rapid drawdown is an important consideration in the design of embankment dams. During rapid drawdown, the stabilizing effect of the water on the upstream face is lost, but the pore water pressures within the embankment may remain high. As a result, the stability of the upstream face of the dam can be much reduced. The dissipation of pore water pressure in the embankment is largely influenced by the permeability and the storage characteristic of the embankment materials. Highly permeable materials drain quickly during rapid drawdown, but low permeability materials take a long time to drain.

Using SLOPE/W, stability during rapid drawdown can be modeled in two approaches, namely the "effective strength" approach (simple and rigorous) and the "staged undrained strength" approach.

In the effective strength approach, the effective stress parameters are used to compute the effective shear strength of the embankment during rapid drawdown. The advantage of this approach is that effective shear strength parameters are used which are fundamentally better. The disadvantage of this approach is the extra work required to estimate the pore water pressures within materials during the drawdown process.

In the staged undrained strength method, the shear strength is evaluated based on the total stress parameters and consequently, the requirements associated with the estimation of the pore water pressure conditions for effective stress analysis can be avoided. The disadvantage of this approach is that total stress parameters are used and these total stress parameters are not commonly available. Furthermore, the hydraulic properties of the materials are ignored and the stability of the embankment dam at different times during the drawdown process cannot be evaluated.

The Simple Effective Strength Method

One simple and conservative approach is to assume that the rapid drawdown process occurs instantaneously. With this assumption, the stabilizing force due to the upstream water is immediately reduced but the piezometric surface follows the upstream slope surface and remains unchanged within the embankment dam as shown in Figure 3-39. It is the piezometric surface that is used to compute the pore water pressures along the slip surface.

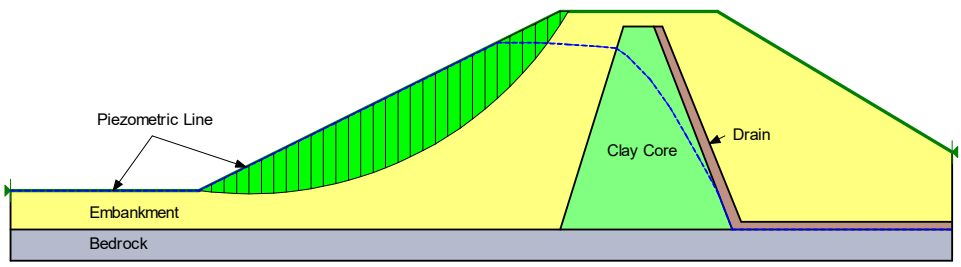

Figure 3-39 Define piezometric line along upstream surface in a rpaid drawdown analysis

This simple effective strength approach is similar to the idea of using a B-bar pore water pressure parameter of 1.0. In other words, when the water level in the reservoir is lowered, the pore water pressure in the materials directly below is reduced by 100% of the weight of the water. This is a reasonable assumption since the upstream slopes are usually constructed with free draining, highly permeable materials. In addition, the materials are usually fully saturated before drawdown occurs and the water within the materials are likely connected to the reservoir.

In general, the simple effective strength approach represents the worst case scenario. This is because rapid drawdown seldom occurs instantaneously and pore water pressures in the upstream material tends to dissipate quite readily during the drawdown process.

The Rigorous Effective Strength Method

A more sophisticated approach is to model the rapid drawdown and evaluate the pore water pressure conditions by doing a finite element transient seepage analysis with SEEP/W. The advantage of this

approach is that the hydraulic properties of the materials are appropriately considered and a time component can be included in the analysis. With this approach, rapid drawdown is not just instantaneous but can be modeled as a process. The factor of safety of the embankment dam at different times during the entire drawdown process can be evaluated as shown in Figure 3-40. The down side of this method is the extra work required to develop a transient finite element seepage analysis with SEEP/W. However, in the design of an embankment dam, the hydraulic properties of the materials have usually been evaluated and are available since a finite element seepage analysis of the embankment is likely required in any case.

GeoStudio allows easy integration between SLOPE/W and SEEP/W making the rigorous effective strength method an attractive alternative in conducting a rapid drawdown analysis.

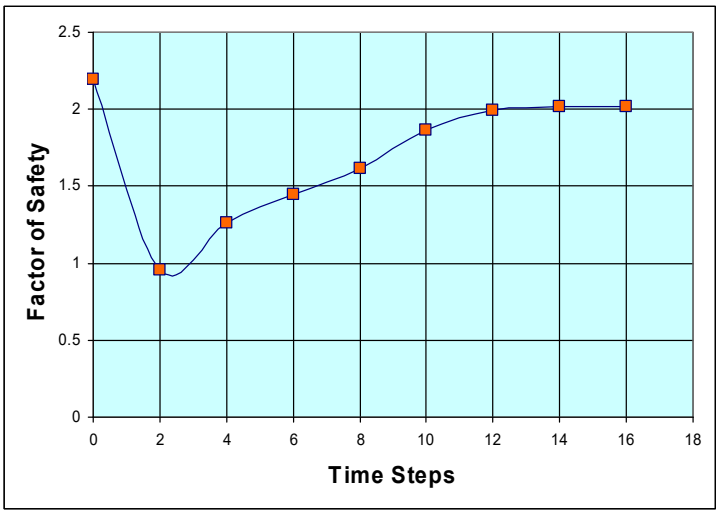

Figure 3-40 Factors of safety of the embankment dam at different times during rapid drawdown

The Staged Undrained Strength Method

Duncan, Wright and Wong (1990) proposed a three-stage procedure for analyzing the rapid drawdown case. The procedure assures that the undrained strength, calculated prior to drawdown, does not exceed the drained strength calculated post drawdown. The following inputs are required to complete the anlaysis in SLOPE/W:

- Effective stress strength parameters c' and ϕ' (via Mohr-Coulomb or spatial Mohr-Coulomb soil strength models);
- The intercept c_R and slope ϕ_R of the R (total stress) undrained strength envelope taken as the tangent to Mohr circles plotted using the minor principle stress at consolidation and principle stress difference at failure (diameter of circle).
- A piezometric line defining the pore-water pressure condition prior to drawdown.
- A piezometric line defining the pore-water pressure condition after drawdown.

Drained materials should have $c_R = 0$ and $\phi_R = 0$. SLOPE will verify that c_R and ϕ_R are larger than the effective stress strength properties.

Two piezometric lines must be defined to complete a staged rapid drawdown analysis. The higher piezometric line characterizes the pore-water pressure conditions prior to drawdown. The lower piezometric line characterizes the pore-water pressure conditions after drawdown.

The publications should be consulted for the details of the procedure. The following is a synopsis of the calculation stages:

1. **Stage 1**: The first stage involves a conventional limit equilibrium stability analysis using the long-term effective stress strengths and pore-water pressure conditions prior to rapid drawdown. The computed effective normal and shear stresses along the slip surface are retained. These effective stresses are assumed to represent those that exist on a potential failure plane at the time of consolidation and are referred to as the consolidation stresses. The consolidation stresses are used to estimate the undrained shear strengths for materials that do not drain freely.

2. **Stage 2**: The second stage involves a stability analysis after drawdown when the water level is low. The effective strength parameters are used for the freely drained materials. Undrained strengths are calculated for the poorly drained materials from the computed effective normal and shear stresses from Stage 1. Parameters $(d_{K_c=1}$ and $\psi_{K_c=1})$ that define the isotropic consolidation strength envelope are calculated from the effective ($c'$and ϕ') and total (c_R and ϕ_R) strength parameters by:

$$d_{K_c=1} = c_R \frac{cos\phi_R cos\phi'}{1 - sin\phi_R}$$

$$\psi_{K_c=1} = arctan \frac{sin\phi_R cos\phi'}{1 - sin\phi_R}$$

   The isotropic consolidation strength envelope relates the strength on the failure plane to the effective consolidation pressure; that is, the isotropic pressure on a triaxial specimen prior to shearing. Subsequently, a procedure is used to interpolate the undrained shear strength between the effective stress and isotropic consolidation shear strength envelopes. The procedure attempts to account for the fact that anisotropically consolidated undrained strengths might be lower than isotropically consolidated undrained strengths. The undrained strength at the base of each slice is compared with the drained strength, and the smaller strength is used in the third stage.

3. **Stage 3**: The third stage involves a stability analysis using the lesser of the effective stress strengths corresponding to the low water level or the total stress strengths from Stage 2. The factor of safety computed from the third stage analysis is used to represent the stability after rapid drawdown. The factor of safety computed from Stage 3 will be the same as the factor of safety from Stage 2 if the undrained strengths were less than the effective stress strengths.

A total of four rapid drawdown examples published by Duncan, Wright and Wong (1990) and by the Corps of Engineers (2003) have been repeated with SLOPE/W. As illustrated in table below, essentially the same factors of safety can be obtained using SLOPE/W.

Figure 3-41 shows the SLOPE/W result of the Walter Bouldin Dam. Please refer to the illustrated example called "Rapid drawdown with Multi-stage" for the detailed documentation of the referenced drawdown examples.

Example	SLOPE/W FOS	Publication FOS	Reference
Walter Bouldin Dam	1.03	1.04	Duncan, Wright and Wong (1990)
Pumed storage project dam	1.55	1.56	Duncan, Wright and Wong (1990)
Pilarcitos Dam	1.05	1.05	Duncan, Wright and Wong (1990)
USACE bench mark	1.46	1.44	Corps of Engineers (2003) EM 1110-2-1902

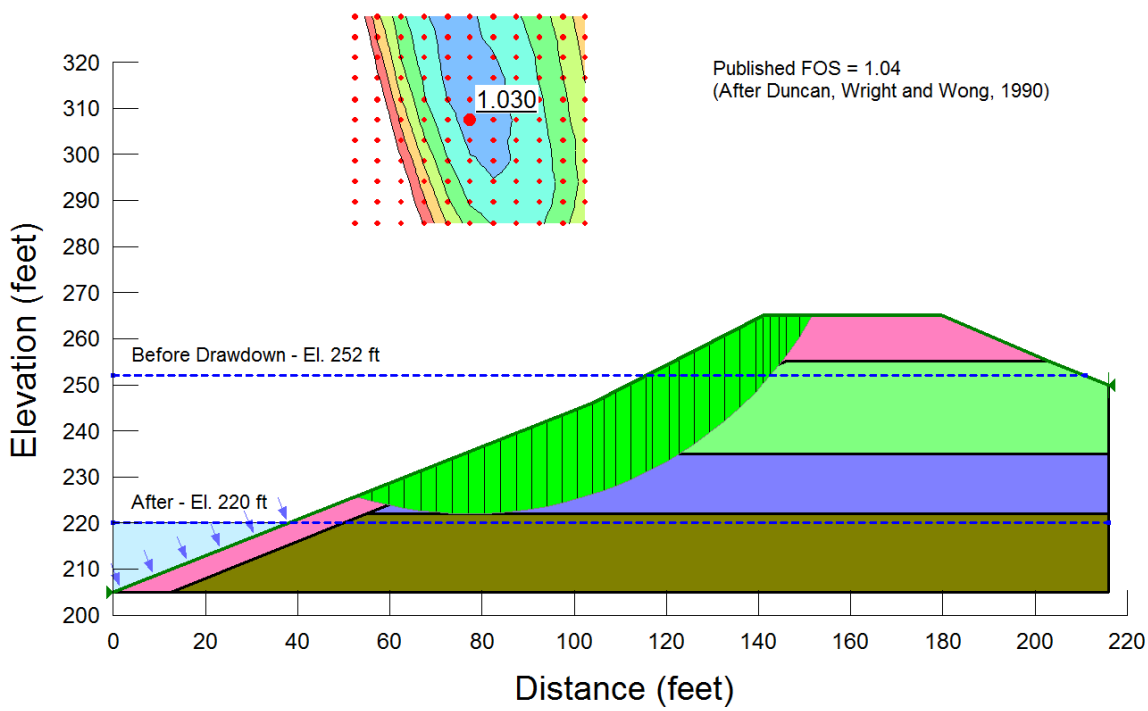

Figure 3-41 SLOPE/W solution showing the Walter Bouldin Dam after rapid drawdown

4 Slip Surface Shapes

4.1 Introduction and background

Determining the position of the critical slip surface with the lowest factor of safety remains one of the key issues in a stability analysis. As is well known, finding the critical slip surface involves a trial procedure. A possible slip surface is created and the associated factor of safety is computed. This is repeated for many possible slip surfaces and, at the end, the trial slip surface with the lowest factor of safety is deemed the governing or critical slip surface.

There are many different ways for defining the shape and positions of trial slip surfaces. This chapter explains all the procedures available in SLOPE/W, and discusses the applicability of the methods to various situations.

Finding the critical slip surface requires considerable guidance from the analyst in spite of the advanced capabilities of the software. The soil stratigraphy may influence the critical mode of potential failure and the stratigraphy therefore must be considered in the selected shape of the trial slip surfaces. In the case of a tie-back wall, it may be necessary to look separately at a toe failure and a deep seated failure. In an open pit mine the issue may be bench stability or overall high wall stability and each needs to be considered separately. Generally, not all potential modes of failure can necessarily be investigated in one analysis. In such cases the positions of the trial slip surfaces needs to be specified and controlled to address specific issues.

A general procedure for defining trial slips may result in some physically inadmissible trial slip surfaces; that is, the trial slip surface has a shape which cannot exist in reality. Often it is not possible to compute a safety factor for such unrealistic situations, due to lack of convergence. Sometimes, however, safety factors can be computed for unrealistic slips, and then it is the responsibility of the analyst to judge the validity of the computed factor of safety. The software cannot necessarily make this judgment. This is an issue that requires guidance and judgment from the analyst. This issue is discussed further toward the end of the chapter.

Another key issue that comes into play when attempting to find the position of the critical slip surface is the selection of soil strength parameters. Different soil strength parameters can result in different computed positions of the critical slip surface. This chapter discusses this important issue.

Presenting the results of the many trial slip surfaces has changed with time. This chapter also addresses the various options available for presenting a large amount of data in a meaningful and understandable way. These options are related to various slip surface shapes, and will consequently be discussed in the context of the trial slip surface options.

4.2 Grid and radius for circular slips

Circular trial slip surfaces were inherent in the earliest limit equilibrium formulations and the techniques of specifying circular slip surfaces has become entrenched in these types of analyses. The trial slip surface is an arc of circle. The arc is that portion of a circle that cuts through the slope. A circle can be defined by specifying the x-y coordinate of the centre and the radius. A wide variation of trial slip surfaces can be specified with a defined grid of circle centers and a range of defined radii. In SLOPE/W, this procedure is called the Grid and Radius method. Figure 4-1 shows a typical example.

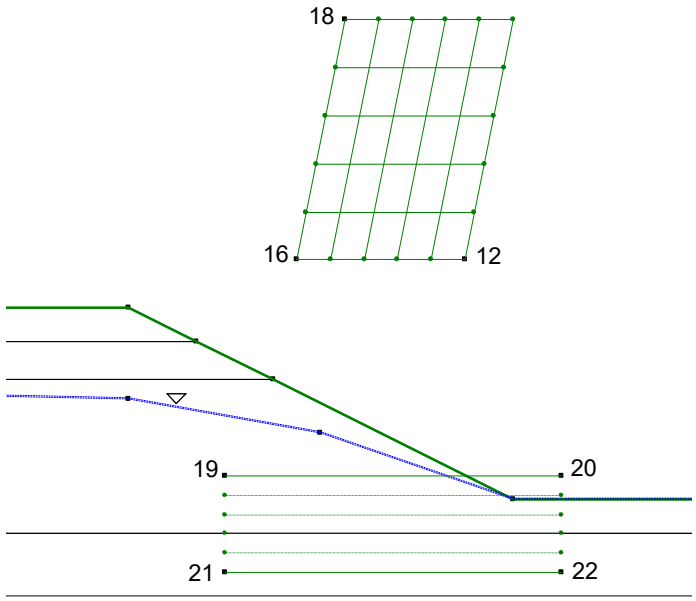

Figure 4-1 The grid and radius method of specifying trial slip surfaces

The grid above the slope is the grid of rotation centers. Each grid point is the circle center for the trial slips. In this example there are 36 (6 x 6) grid points or circle centers. In SLOPE/W, the grid is defined by three points; they are upper left (18), lower left (16) and lower right (12).

The trial circle radii are specified with radius or tangent lines. The lines are specified by the four corners of a box. In the above example, the four corners are 19 (upper left), 21 (lower left), 22 (lower right) and 20 (upper right). For the SLOPE/W main processor to interpret the radius line specification correctly, the four points need to start at the upper left and proceed in a counter-clockwise direction around the box. The number of increments between the upper and lower corners can be specified. In the above example there are five increments making the total number of radius lines equal to 6.

To start forming the trial slip surfaces, SLOPE/W forms an equation for the first radius line. Next SLOPE/W finds the perpendicular distance between the radius line and a grid centre. The perpendicular distance becomes the radius of the trial slip surface. The specified radius lines are actually more correctly tangent lines; that is, they are lines tangent to the trial circles. Figure 4-2 shows one imaginary circle. Note that the specified radius line is tangent to the circle. The trial slip surface is where the circle cuts the soil section. For this example, SLOPE/W will compute safety factors for 216 (36 x 6) trial slip surfaces.

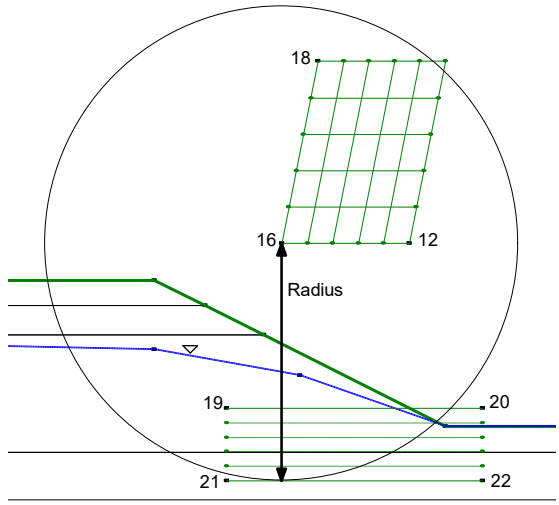

Figure 4-2 Imaginary trial slip surface

The radius line "box" (points 19, 21, 22, 20) can be located at any convenient position and can form any quadrilateral shape. The illustration in Figure 4-3 is entirely acceptable. Also, the position of the radius box does not necessarily need to be on the soil section. Usually it is most convenient for the box to be on the slope section, but this is not a requirement in the SLOPE/W formulation. It becomes useful when the trial slip surfaces have a composite shape as discussed below.

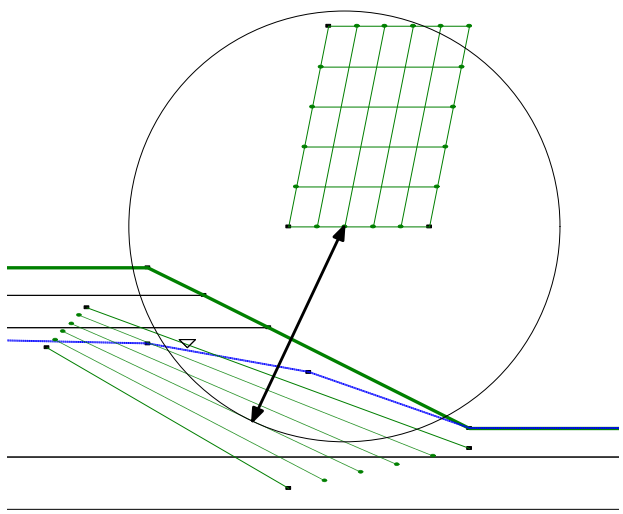

Figure 4-3 Specification of radius lines

Single radius point

The radius line box can be collapsed to a point. All four corners can have the same point or the same x-y coordinate. If this is the case, all trial slip surfaces will pass through a single point (Figure 4-4). This technique is useful when you want to investigate a particular mode of failure, such as the potential failure through the toe of a wall.

The grid of centers can also be collapsed to a single point. This makes it possible to analyze just one slip surface, which can be very useful for doing comparisons of various features or options.

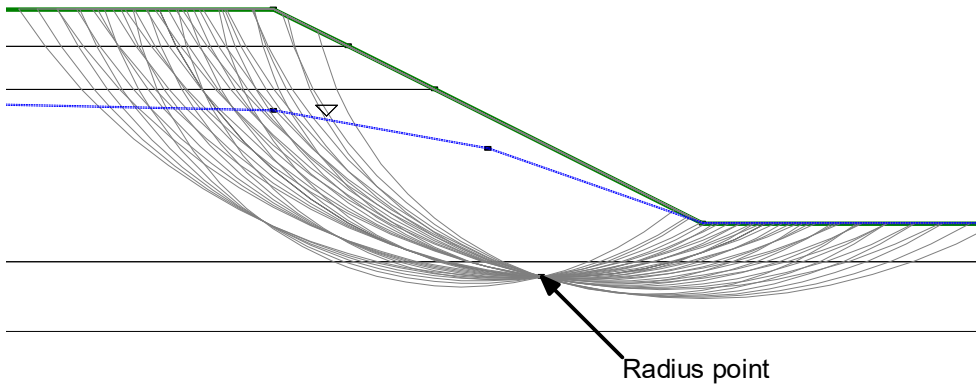

Figure 4-4 All slip surfaces through a point

Multiple radius points

The radius box can also be collapsed to a line with radius increments. This makes it possible to analyze trial slips that pass through a series if points. This can be done by making the upper two corners the same and the lower two corners the same. This is illustrated in Figure 4-5.

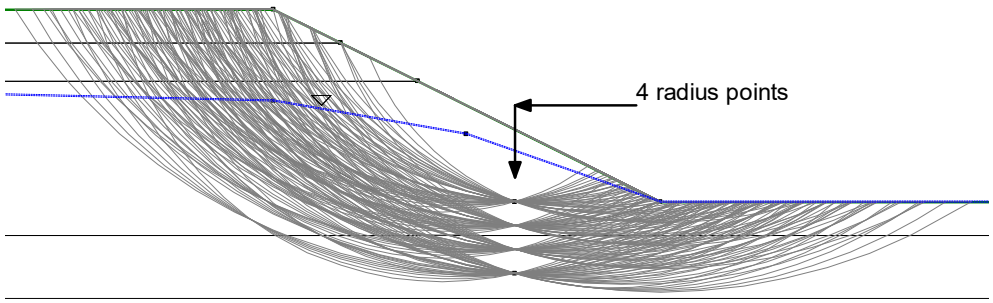

Figure 4-5 Slip surfaces though a series of radius points

Lateral extent of radius lines

The tangent or radius lines in SLOPE/W do not have lateral extents. The tangent lines are used to form the equation of a line, but the equation lines are not limited by the lateral extents of the specified lines. The two cases illustrated in Figure 4-6 result in exactly the same trial slip surfaces. This can sometimes result in unexpected trial slip surfaces that fall outside the intended range. A typical example may be a shallow slip that just cuts through the crest of the section as in a near vertical wall. This undesired outcome is one of the weaknesses of the Grid-Radius technique and the reason for other options for specifying trial slip surfaces. The Enter-Exit method, for example, discussed below does not have this shortcoming.

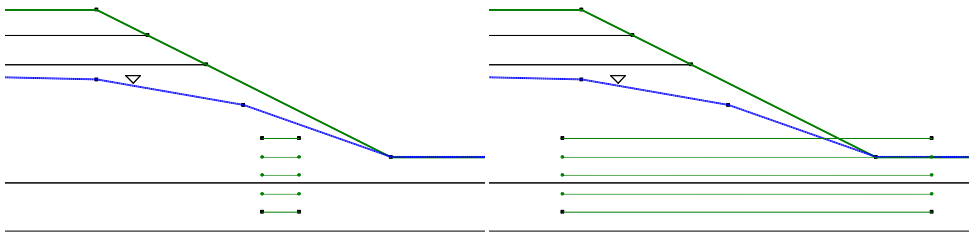

Figure 4-6 Effect of radius line lengths

Another side effect of the Grid-Radius method is that trial slips can fall outside the extents of the geometry. All trial slips must enter and exit along the Ground Surface line. If trial slips enter or exit outside the Ground Surface line, they are considered invalid and no factor of safety is computed. A typical case may be a trial slip that enters or exits the vertical ends of the defined geometry. Such trial slips are invalid. No safety factors are displayed at the Grid centers for which no valid trial slip surface exists.

Factor of Safety contours

In the early days of limit equilibrium stability analyses, the only way to graphically portray a summary of all the computed safety factors was to contour the factors of safety on the Grid, as illustrated in Figure 4-7. The contours provide a picture of the extent trial slip surfaces analyzed, but more importantly the contours indicate that the minimum safety factor has been found. The ideal solution is when the minimum falls inside a closed contour like the 1.240 contour in Figure 4-7.

The technique of contouring the safety factors on the Grid has become deeply entrenched in slope stability analyses. This has come about partly because of early developments and presentations, and partly because all related textbooks present this as an inherent requirement.

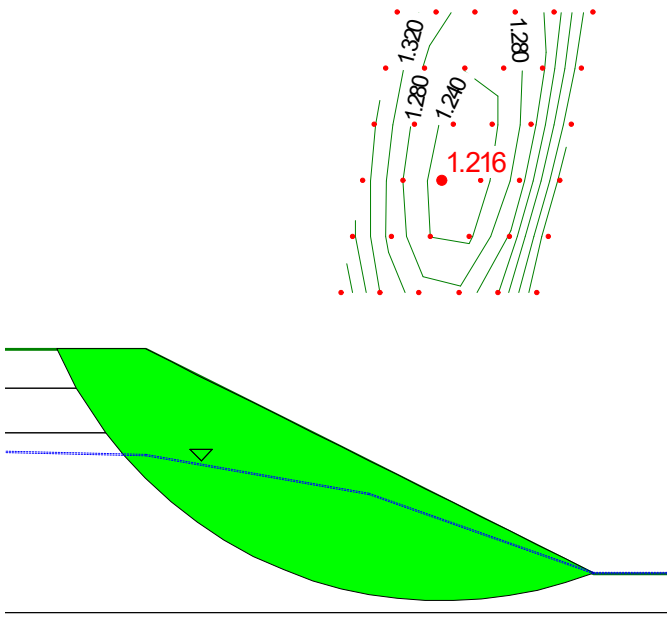

Figure 4-7 Factor of safety contours on grid of rotation centers

Unfortunately, the ideal solution illustrated in Figure 4-7 is not always attainable; in fact the number of situations where the ideal contour picture can be attained is considerably less than the situations where it is not attainable. The ideal solution can usually be obtained for conventional analyses of fairly flat slopes (2h:1v or flatter), with no concentrated point loads, and with c and ϕ effective strength parameters. A common case where the ideal cannot be attained is for purely frictional material ($c = 0;\ \phi > 0$) as discussed in detail further on in this Chapter. Another typical case is the stability analysis of vertical or near vertical walls.

Recognizing that the ideal textbook case of the minimum safety factor falling in the middle of the Grid is not always attainable is vitally important in the effective use of a tool like SLOPE/W.

Now there are other ways of graphically portraying a summary of computed safety factors. One way is to display all the trial slip surfaces as presented in Figure 4-8. This shows that the critical slip surface falls inside the range of trial slips and it shows the extent of the trial slips.

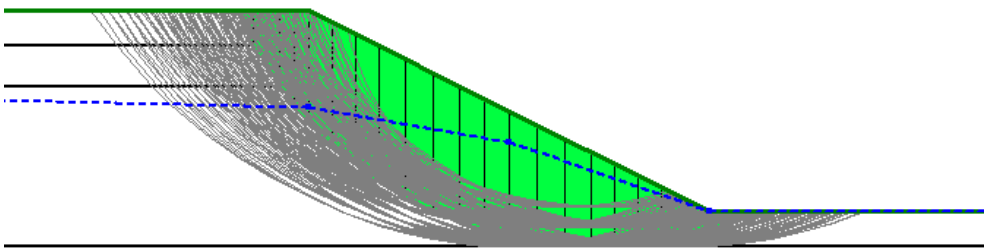

Figure 4-8 Display of multiple trial slip surfaces

Another effective way of graphically viewing a summary of the trial slip surfaces is with what is called a safety map. All the valid trial slip surfaces are grouped into bands with the same factor of safety. Starting from the highest factor of safety band to the lowest factor of safety band, these bands are painted with a different color. The result is a rainbow of color with the lowest factor of safety band painted on top of the rest of the color bands. Figure 4-9 illustrates an example of the safety map.

In this example, the red color is the smallest factor of safety band, and the white line is the critical slip surface. This type of presentation clearly shows the location of the critical slip surface with respect to all trial slip surfaces. It also shows zone of potential slip surfaces within a factor of safety range.

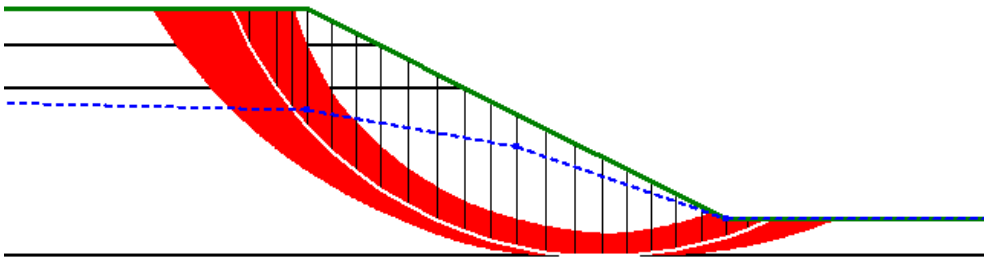

Figure 4-9 Display of safety map

4.3 Composite slip surfaces

Stratigraphic conditions have a major influence on potential slip surfaces. Circular slip surfaces are fairly realistic for uniform homogeneous situations, but this is seldom the case in real field cases. Usually there

are multiple layers with varying strength and varying pore-water pressure conditions which can have an effect on the shape of the critical slip surface.

A common situation is where surficial soils overlie considerably stronger material at depth. There is the potential for the surficial soils to slide along the contact between the two contrasting materials. This type of case can be analyzed with what is called a composite slip surface. The stronger underlying soil is flagged as being impenetrable (or bedrock). The trial slip surface starts as an arc of the circle until it intersects the impenetrable surface. The slip surface then follows the impenetrable surface until it intersects the circle, and then again follows the arc of a circle up to the surface as illustrated in Figure 4-10. The circular portion of the trial slip surfaces is controlled by the Grid and Radius method discussed above.

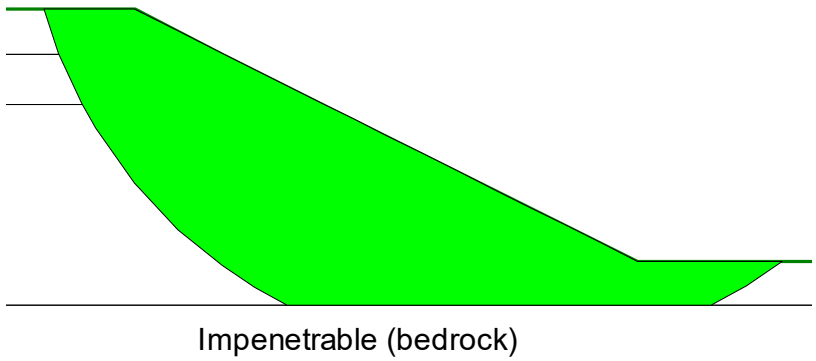

Figure 4-10 Composite slip surface controlled by impenetrable layer

The portion of the slip surface that follows the impenetrable material takes on the soil strength of the material just above the impenetrable layer. This can always be verified by graphing the strength along the slip surface.

The impenetrable surface does not have to be a straight line – it can have breaks as in Figure 4-11. However, extreme breaks may make the slip surface inadmissible, and it usually results in an unconverged solution.

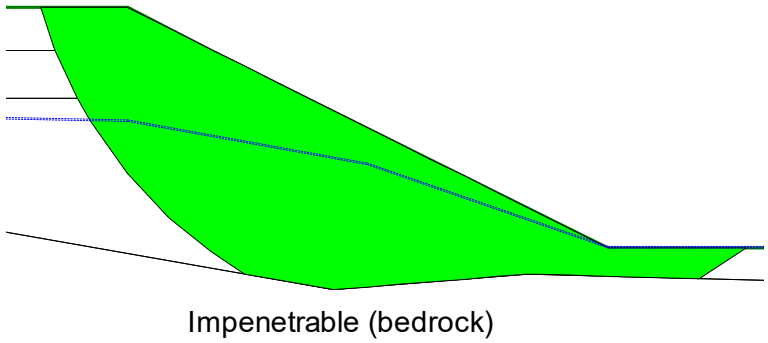

Figure 4-11 Irregular impenetrable layer

The impenetrable material feature is useful for analyzing cases with a weak, relatively thin layer at depth. Figure 4-12 shows such an example. In this case, the portion of the slip surface that follows the impenetrable takes on the strength assigned to the weak layer.

For practical reasons, there is no need to make the weak layer too thin. The portion of the slip surface in the weak layer that does not follow the impenetrable contact is relatively small and therefore has little

influence on the computed factor of safety. The effort required in making the weak layer very thin is usually not warranted.

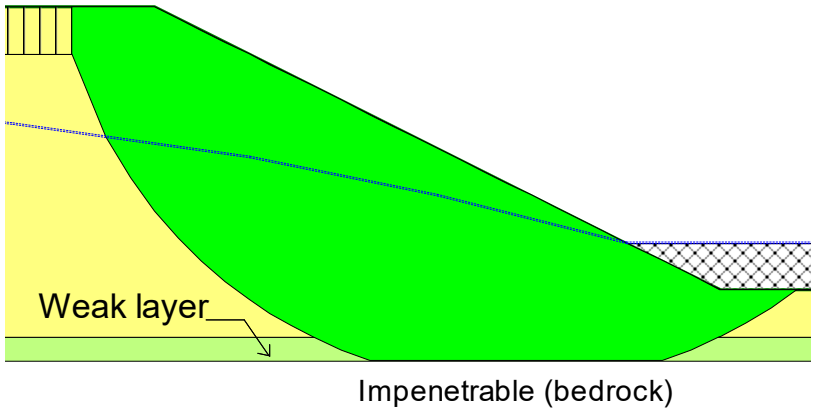

Figure 4-12 Impenetrable layer forces slip along weak layer

The impenetrable feature can also be used to analyze the sliding stability of cover material on a synthetic liner, as illustrated in Figure 4-13. The impenetrable layer causes the trial slip surface to follow the liner. A thin region just above the impenetrable material has properties representative of the frictional sliding resistance between the cover material and the liner. This is the shear strength along that portion of the slip surface that follows the impenetrable material.

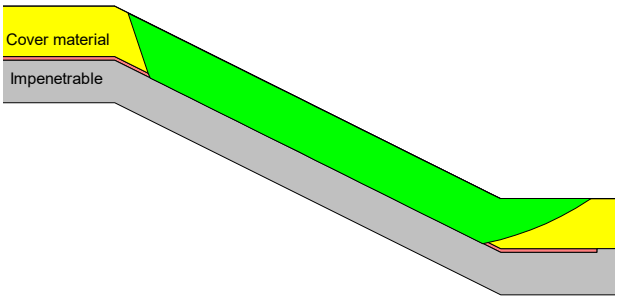

Figure 4-13 Sliding on a synthetic liner

Again this can be verified by graphing the strength along the slip surface. In this illustration the cover material has a friction angle of 30 degrees and the friction angle between the liner and the cover material is 15 degrees. This is confirmed by the SLOPE/W graph in Figure 4-14.

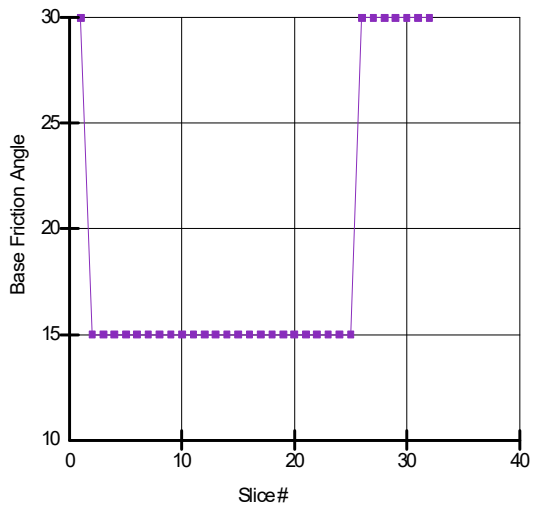

Figure 4-14 Variation of friction angle along slip surface

Note that the tensile capacity of the liner does not come into play in this cover sliding analysis. Considering the tensile strength would require a different setup and a different analysis.

In SLOPE/W, the concept of an impenetrable material is just a mechanism to control the shape of trial slip surfaces – it is not really a material.

4.4 Fully specified slip surfaces

A trial slip surface can be specified with a series of data points. This allows for complete flexibly in the position and shape of the slip surface. Figure 4-15 illustrates a fully-specified slip surface.

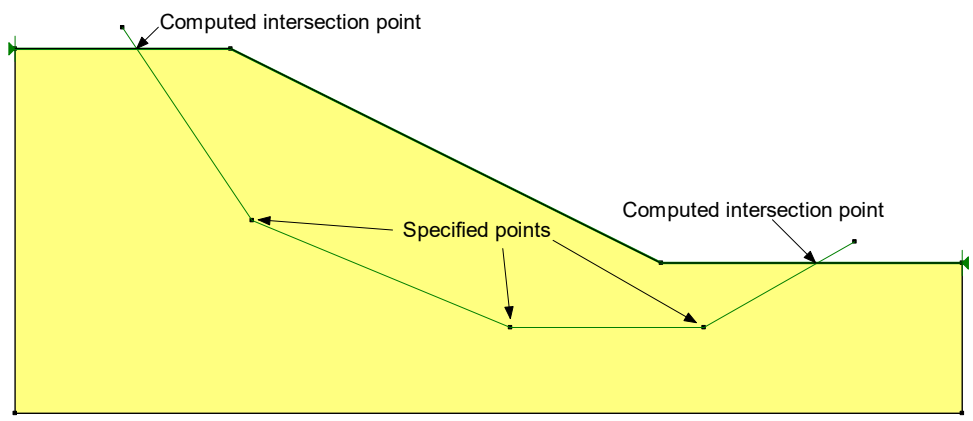

Figure 4-15 Fully specified slip surface

Note that the specified surface starts and ends outside the geometry. SLOPE/W can then compute the ground surface intersection points. Allowing SLOPE/W to compute these intersection points is better than trying to place a point on the ground surface, which can sometimes lead to some numerical confusion.

A point needs to be created about which to take moments. This is called the Axis Point (Figure 4-16). The Axis Point should be specified. In general, the Axis Point should be in a location close to the approximate center of rotation of all the specified slip surfaces. It is usually somewhere above the slope crest and between the extents of the potential sliding mass.

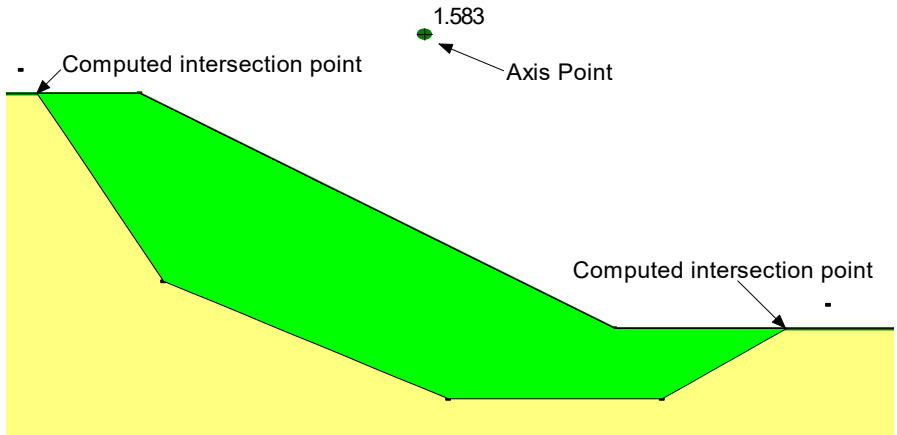

Figure 4-16 Axis point about which to compute moments

The factor of safety calculations are not sensitive to the position of the Axis point, for methods that satisfy both moment and force equilibrium (e.g., Spencer and Morgenstern-Price methods). However, for simplified methods (e.g., Ordinary and Simplified Bishop), the factor of safety calculations can be sensitive to the position of the Axis Point.

A common axis point for taking moment should be defined. The Axis Point should be in a location close to the approximate center of rotation of the fully specified slip surfaces. When missing, SLOPE/W estimates an axis point based on the geontry and the specified slip surfaces.

The Fully Specified method has a unique feature that any points on the slip surface can be specified as "Fixed". When a point is fixed, the point will not be allowed to move during the slip surface optimization process.

The Fully Specified method is useful when large portions of the slip surface position are known from slope inclinometer field measurements, geological stratigraphic controls and surface observations. The option may also be useful for other cases such as the sliding stability of a gravity retaining wall (Figure 4-17).

While the Fully Specified method is completely flexible with respect to trial slip surfaces shapes and position, it is limited in that each and every trial slip surface needs to be specified. The method is consequently not suitable for doing a large number of trials to find the critical slip surface.

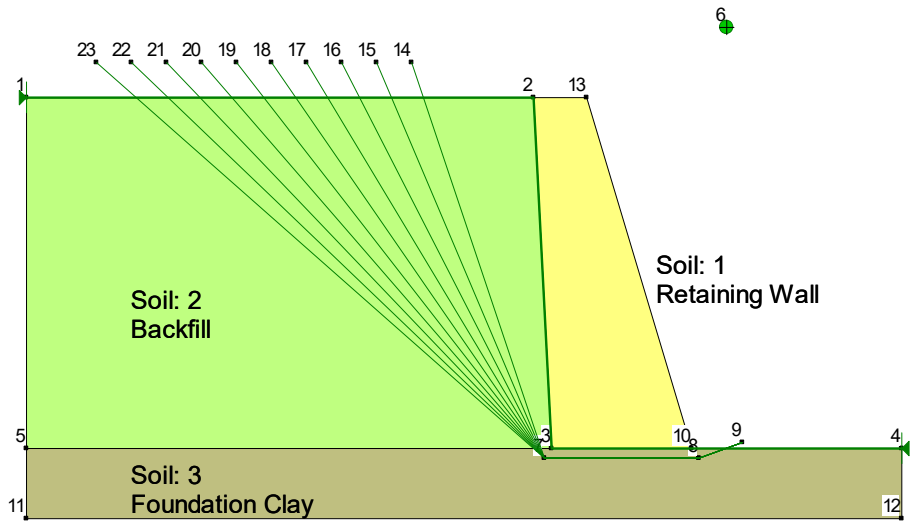

Figure 4-17 Sliding analysis of a gravity retaining wall

4.5 Block specified slip surface

General cross-over form

Block shaped analyses can be done by specifying two grids of points as shown in Figure 4-18. The grids are referred to as the left block and the right block. The grids are defined with an upper left point, a lower left point and a lower right point. In the example here the right block is defined by Points 11, 12 and 13.

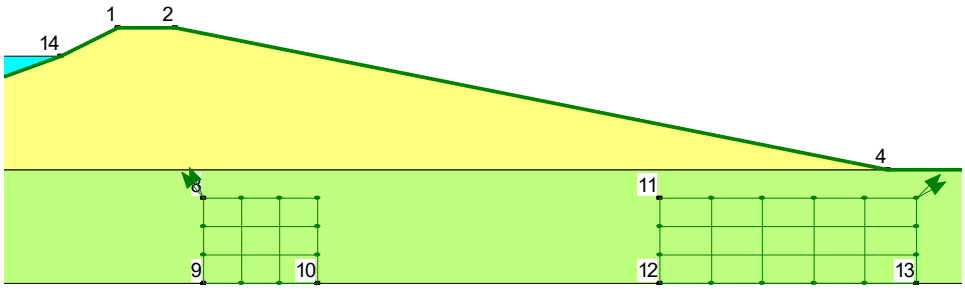

Figure 4-18 Grids in Block Specified method

The slip surface consists of three line segments. The middle segment goes from each grid point on the left to each grid point on the right. The other two segments are projections to the ground surface at a range of specified angles. Figure 4-19 presents the type of trial slip surface created.

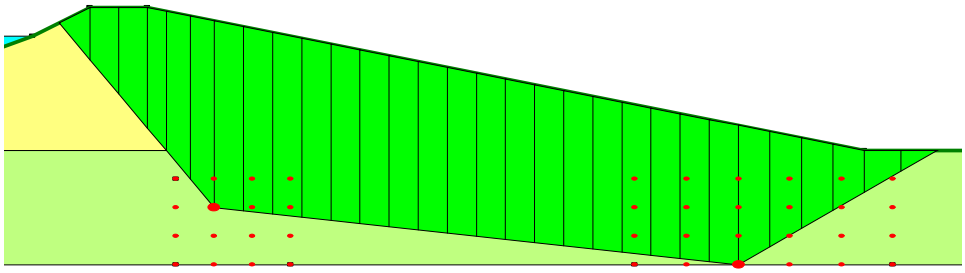

Figure 4-19 Slip surface shape in the Block method

By allowing the middle segments to go from each grid point on the left to each point on the right, the middle line segments cross over each other when multiple slips are viewed simultaneously, and hence the cross-over designation. An option where this is not allowed is also an option available within SLOPE/W that is discussed later in this chapter.

The end projections are varied, depending on the specified angles and the incremental variation in the angles. Arrows are drawn at the upper left and right corners as in Figure 4-20 to graphically portray the specified angles.

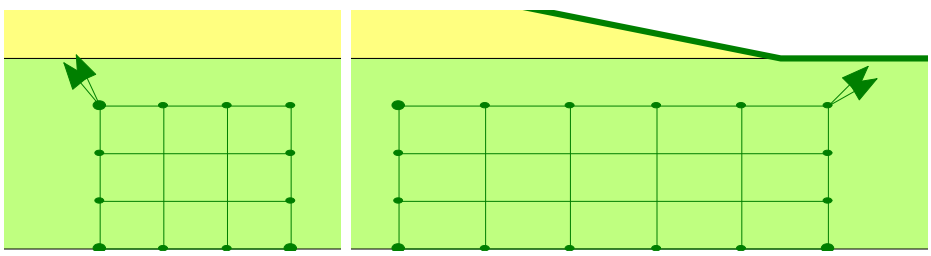

Figure 4-20 Projection angles in the Block method

The situation in the toe area is similar to a passive earth pressure condition where the sliding mass is being pushed outward and upward. In the crest area, the situation is analogous to active earth pressure conditions. From lateral earth pressure considerations, the passive (toe) slip surface rises at an angle equal to ($45 - \phi/2$) and the active slip line dips at an angle of ($45 + \phi/2$). These considerations can be used to guide the selection of the projection angles.

In SLOPE/W, geometric angles are defined in a counterclock-wise direction from the positive x-coordinate axis. An angle of zero means a horizontal direction to the right, an angle of 90 degrees means an upward vertical direction; an angle of 180 degrees means a horizontal direction in the negative x-coordinate direction, and so forth.

In the above example, the right toe (passive) projection angles vary between 30 and 45 degrees, and the left crest (active) projection angles vary between 115 and 130 degrees (between 65 and 50 degrees from the horizontal in the clock-wise direction).

Like the Fully Specified method, the Block method also needs a defined Axis about which to take moments. If the Axis point is not defined, SLOPE/W will compute an Axis location based on the geometry of the problem and the positions of the left and right blocks.

This method of creating trial slip surfaces can lead to a very large number of trials very quickly. For the illustrative example here the left block has 16 (4x4) grid points and the right block has 24 (4x6) grid points. At each end there are three different projection angles. The total number of trial slips is 16 x 24 x

3 x 3 which equals 3,456. Some caution is consequently advisable when specifying the size of the grid blocks and the number of projection angles.

The Block method is particularly useful in a case such as in Figure 4-19. Here an embankment with flat side slopes rests on a relatively thick stratum of soft foundation soil. The middle segment of the crucial slip surface tends to dip downward as in Figure 4-19 as opposed to being horizontal. Allowing the middle segments to vary between all the grid points makes it possible to find this critical potential mode of sliding.

A difficulty with the Block method is that it is not always possible find a converged solution when the corners along the slip surface become too sharp. A typical situation is shown in Figure 4-21. The break in the slip surface on the left is too sharp and this causes convergence problems.

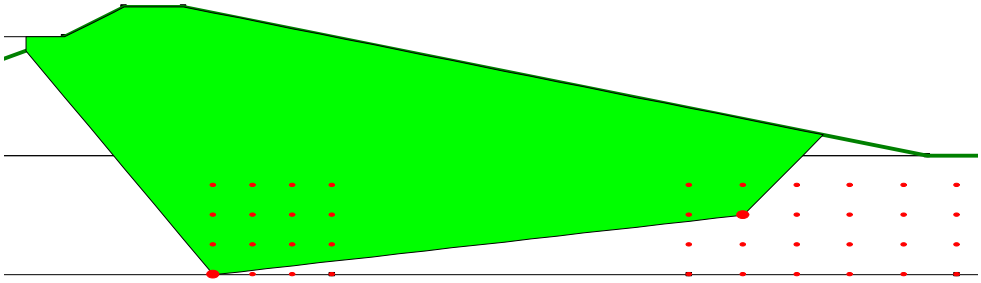

Figure 4-21 Trial slip surface with a sharp corner

The convergence difficulties with the Block method can result in a large number of trial slip surfaces with an undefined safety factor. This is particularly problematic when the grid blocks get close to each other. The Block method works the best and is the most suitable for cases where there is a significant distance between the two blocks. Stated another way, the middle segment line segment should be significantly longer than the two end projection segments.

Slip surfaces seldom, if ever, have sharp corners in reality, which is one of the assumptions made in the Block method. This reality points to another weakness of this method with respect to forming trial slip surfaces. This limitation can sometimes be overcome by the optimization technique discussed below.

Worth noting is that the two grid blocks can be collapsed to a line with points or to a single point. If the two left specified points in the grid block are the same, the block will collapse to a line. If all three points are the same, the grid block will collapse to a single point.

When generating slip surfaces with Block Search, it is quite easy to generate a lot of physically impossible slip surfaces.

Specific parallel form

There are situations where it is preferable to have all the middle line segments of the trial slip surface parallel. Take, for example, the case of a slope where the material is strongly bedded and the strength along the bedding is less than across the bedding. This is illustrated in Figure 4-22. The grid blocks are placed so that the bases are parallel to the bedding. By selecting the “No crossing” option, the middle segments of the trial slip surfaces will all be along the bedding.

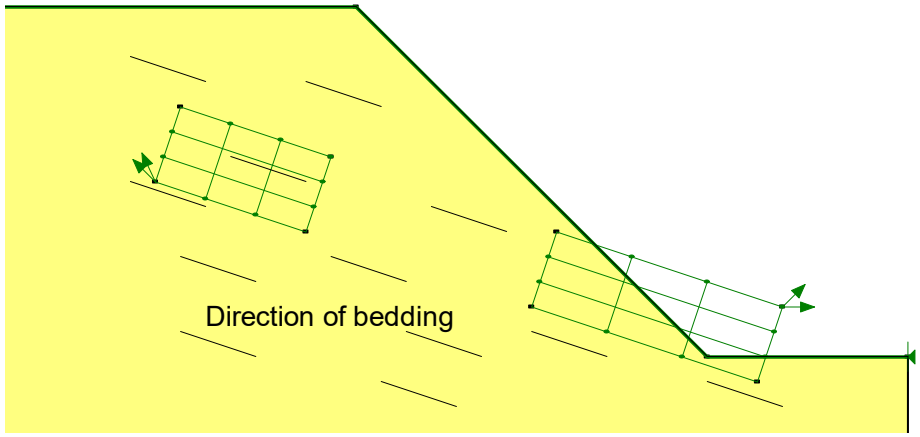

Figure 4-22 Slope with distinct bedding

A typical trial slip surface looks like the one in Figure 4-23.

A common axis point for taking moment should be defined. The Axis Point should be in a location close to the approximate center of rotation of the block slip surafces. When missing, SLOPE/W estimates an axis point based on the geontry and the positions of the left and right blocks.

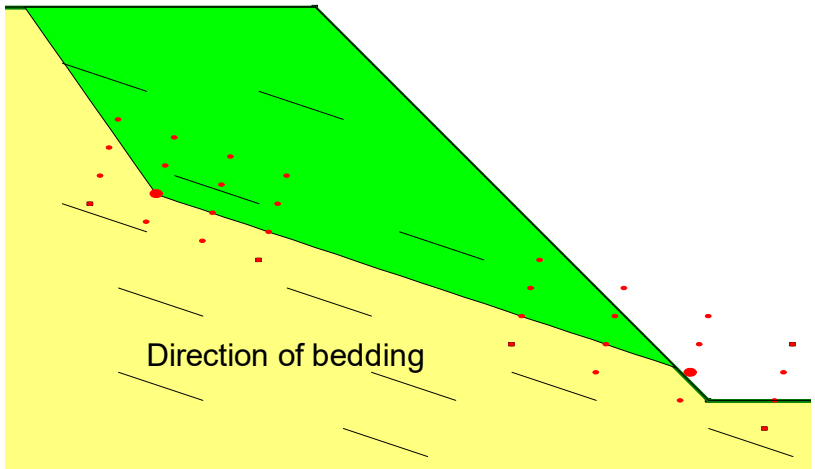

Figure 4-23 Trial slip surface follows the bedding

This approach can be combined with an anisotropic strength function to make the strength across bedding higher than along the bedding. The bedding is inclined at an angle of about 18 degrees. Let us specify the strength parameters along the bedding together with the anisotropic modifier function as in Figure 4-24. When the inclination of the slip surface is 18 degrees, the modifier is 1.0 and therefore the specified strength is used. Slip Surface inclinations other than 18 degrees will have a higher strength. The specified strength will be multiplied by a factor of 1.15, for example, if the slice base inclination is zero degrees (horizontal).

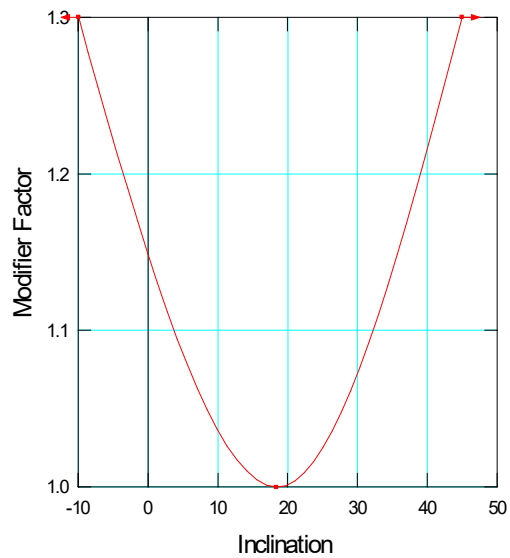

Figure 4-24 Anisotropic function

4.6 Entry and exit specification

One of the difficulties with the historic Grid and Radius method is that it is difficult to visualize the extents and/or range of trial slip surfaces. This limitation can be overcome by specifying the location where the trial slip surfaces will likely enter the ground surface and where they will exit. This technique is called the Entry and Exit method in SLOPE/W.

In Figure 4-25, there are two heavy (red) lines along the ground surface. These are the areas where the slip surfaces will enter and exit. The number of entries and exits can be specified as the number of increments along these two lines.

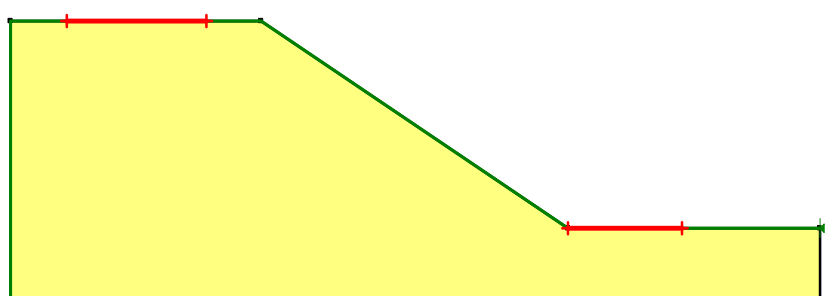

Figure 4-25 Entry and exit areas for forming trial slip surfaces

Behind the scenes, SLOPE/W connects a point along the entry area with a point along the exit area to form a line. At the mid-point of this connecting line, SLOPE/W creates a perpendicular line. Radius points along the perpendicular line are created to form the required third point of a circle (Figure 4-26). This radius point together with the entry and exit points are used to form the equation of a circle. SLOPE/W controls the locations of these radius points so that the circle will not be a straight line (infinite radius), and the entry angle of the slip circle on the crest will not be larger than 90 degrees (undercutting slip circle). The equation of a circle gives the center and radius of the circle, the trial slip surface is then handled in the same manner as the conventional Grid and Radius method and as a result, the Entry and Exit method is a variation of the Grid and Radius method. The number of radius increments is also a specified variable.

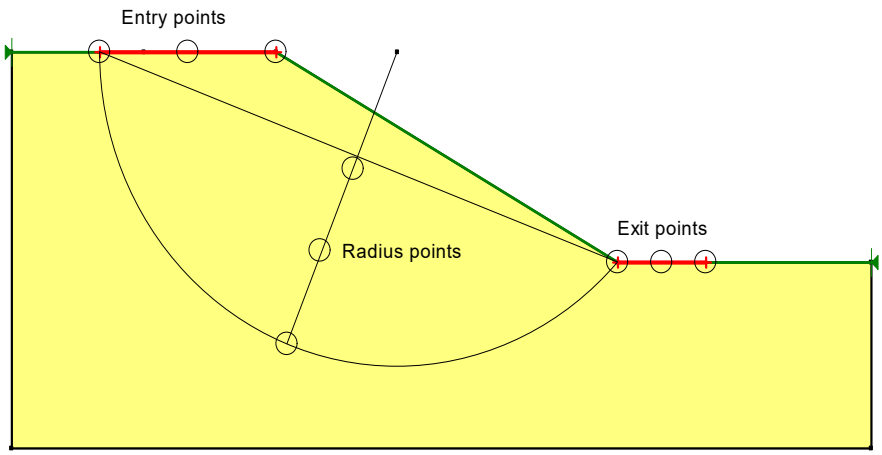

Figure 4-26 Schematic of the entry and exit slip surface

Figure 4-27 shows all the valid slip surfaces when the entry increments, the exit increments and the radius increments are set equal to 5. A total of 216 (6 x 6 x 6) slip surfaces are generated. The critical slip surface is the darker shaded area.

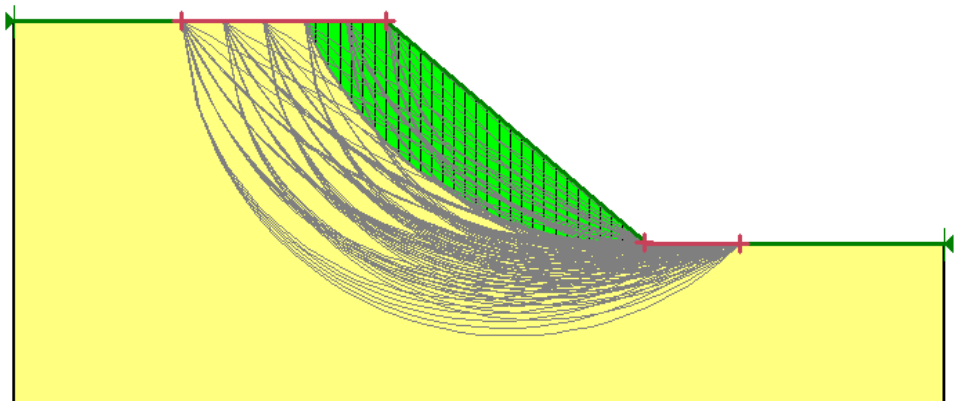

Figure 4-27 Display of all valid critical slip surfaces

In SLOPE/W, the generated slip surfaces from the Entry and Exit zones can be controlled with the 4 points radius specification in the same manner as the Gird and Radius method Figure 4-27 . The specified radius will force the generated slip surface to be tangent to the radius line Figure 4-27. In the case of a two point radius, all slip surfaces will pass through the specified radius zone. In the case of a

single point radius, all slip surfaces will be forced to pass through the radius point.

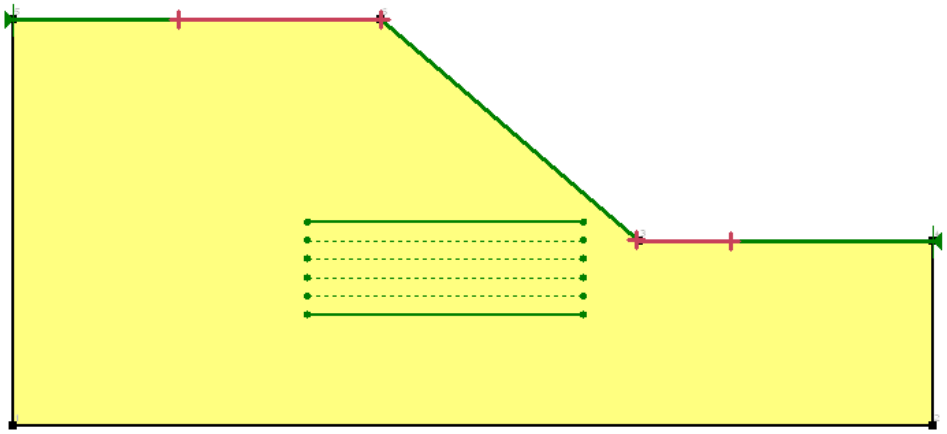

Figure 4-28 Entry and Exit slip surface with radius specification

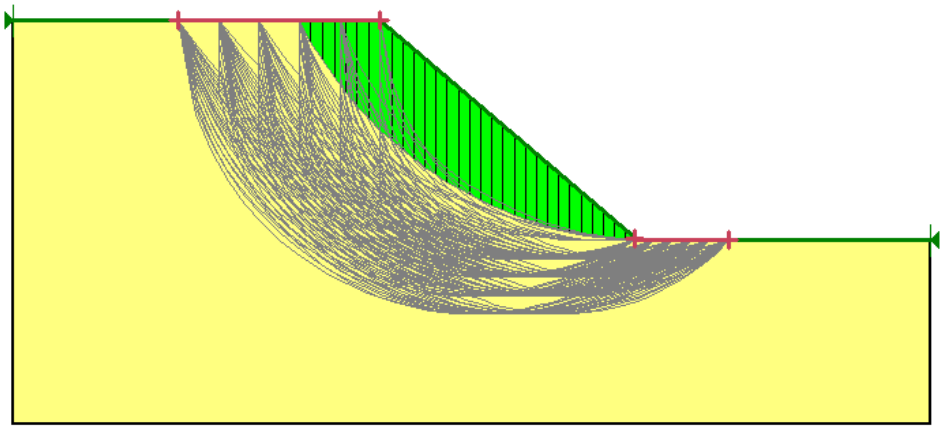

Figure 4-29 Display of all valid critical slip surfaces with radius specification

The radius specification in the Entry and Exit method can be useful in situations where the slip surfaces are controlled by beddings of weaker materials, or an impenetrable material layer (bedrock).

Note that although SLOPE/W posts no restriction to the location of the Entry and Exit zones, it is recommended that the Entry and Exit zones should be carefully defined on locations where the critical slip surface is expected to daylight. Defining a large Entry and Exit zones on the ground surface blindly may lead to many impossible slip surfaces and may miss the real critical slip surface.

4.7 Optimization

All the traditional methods of forming trial slip surfaces change the entire slip surface. Recent research has explored the possibility of incrementally altering only portions of the slip surface (Greco, 1996; Malkawi, Hassan and Sarma, 2001). A variation of the published techniques has been implemented in SLOPE/W. After finding the critical slip surface by one of the more traditional methods, the new segmental technique is applied to optimize the solution.

The first step in the optimization process is to divide the slip surface into a number of straight line segments. The slip surface in essence becomes just like a Fully Specified slip surface. Next, the end points of the line segments are moved to probe the possibility of a lower safety factor. The process starts with the point where the slip surface enters ground surface. This point is moved backward and forward randomly along the ground surface until the lowest safety factor is found. Next, adjustments are made to the next point along the slip surface until again the lowest safety factor is found. This process is repeated for all the points along the slip surface. Next, the longest slip surface line segment is subdivided into two parts and a new point is inserted into the middle. This process is repeated over and over until changes in the computed safety factor are within a specified tolerance or until the process reaches the specified limits (e.g., the maximum number of optimization trials).

Figure 4-30 presents an optimized slip surface relative to a traditional circular slip surface of a simple slope. The material above the toe is somewhat stronger than the underlying soil below the toe elevation in this example. The factor of safety for this circular slip surface is 1.280, while for the optimized case the factor of safety is 1.240. Of interest is the observation that there is another slip surface that leads to a lower factor of safety than the one obtained for an assumed circular slip surface.

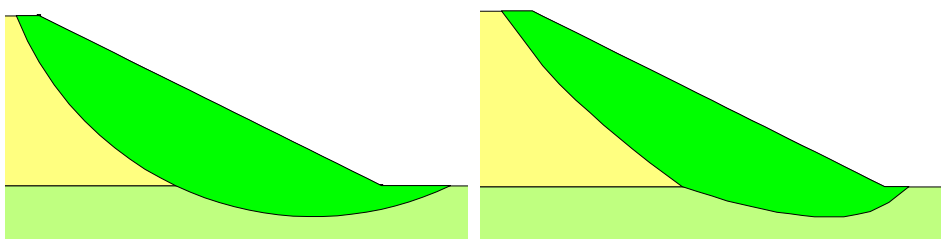

Figure 4-30 Traditional (Left) and Optimized (Right) slip surface

A key element in the optimization procedure is the technique used to move the end points of the line segments. SLOPE/W moves the points within an elliptical search area using a statistical random walk procedure based on the Monte Carlo method. This can be graphically illustrated in Figure 4-31.

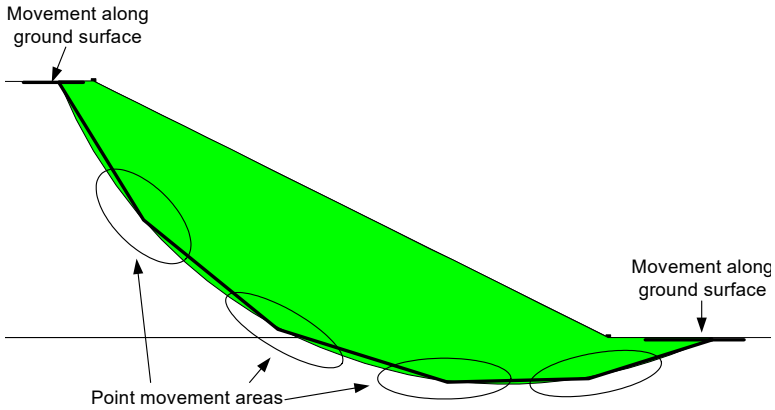

Figure 4-31 Movement areas of points in the optimization procedure

As is readily evident, the optimization is an iterative procedure and consequently some limits and controls are required. These controls include defining a tolerance when comparing safety factor, the maximum number of optimization trials and the number of line segments. These controlling parameters are explained in the online help.

The solution in Figure 4-32 was discussed in the section on the Block method. The optimized solution is presented in Figure 4-33. The Block factor of safety is 1.744 while the Optimized factor of safety is 1.609.

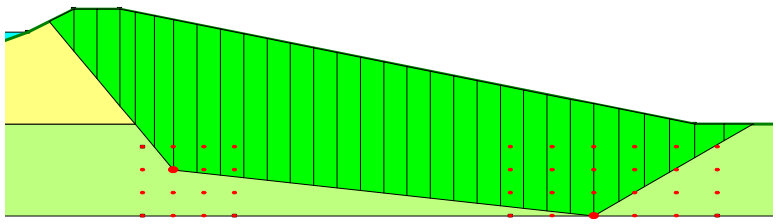

Figure 4-32 Slip surface when using the Block method

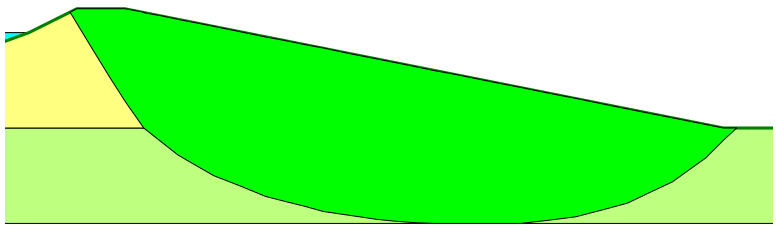

Figure 4-33 Slip surface when Block method optimized

The above two examples discussed here illustrate that slip surfaces do exist that have a lower safety factor than the trial slips that can be created by assumed geometric parameters. This is the attraction of optimization technique. Moreover, the optimized shape, without sharp corners, is intuitively more realistic.

Figure 4-34 shows the difference of a fully specified slip and the slip surface after optimization for geometry with a thin weak layer. The fully specified slip surface does not follow the weak layer and results in a factor of safety of 1.2, but the optimized process was able to locate the weak layer and found a smaller factor of safety 0.96. The Optimization process is appealing in that the trial slip surface is based on soil properties to some extent. The technique will be biased towards weak layers or weak directions for anisotropic strengths.

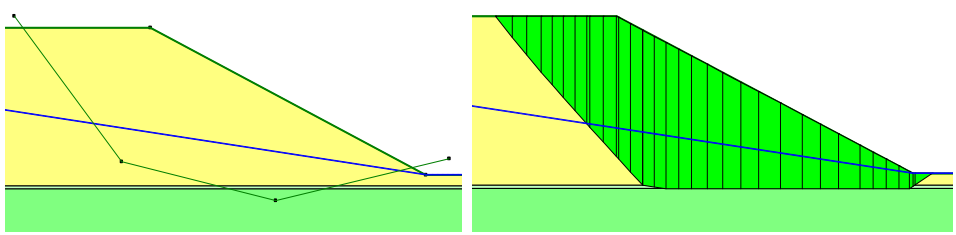

Figure 4-34 Fully specified slip surface (Left) after optimization (Right)

The Optimization procedure is somewhat dependent on the starting slip surface position. The main reason for this is the available elliptical search area during the random walk procedure. Since the elliptical search area is based on the starting slip surface, it is not difficult to understand that the final optimized slip surface can be limited by a poor selection of the starting slip surface.

In the example that had a thin weak layer, depending on the starting position of the slip surface, the optimization process may not be able to locate the critical slip surface along the weak layer (Figure 4-35).

In SLOPE/W, the critical slip surface from a regular search is always used as the starting slip surface in the optimization process. In most cases, a smaller factor of safety can be obtained after the optimization.

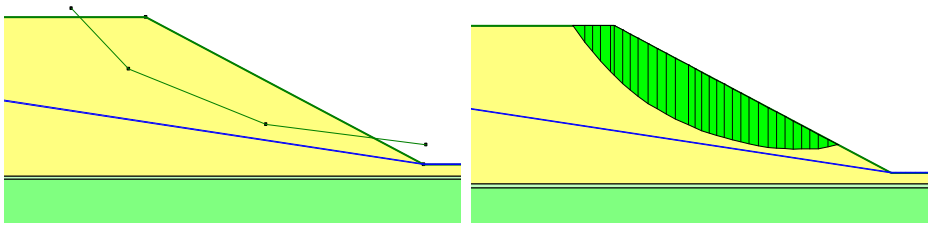

Figure 4-35 Fully specified slip surface (Left) after optimization (Right)

When a fully specified slip surface is used, any one of the points in the fully specified slip surface can be specified as "FIXED". The optimization process will not change the position of the "FIXED" point(s).

Please note that during the optimization stage, points within the elliptical search areas may move in all directions in an attempt to find a slip surface with lower factor of safety. Under normal conditions, the final optimized slip surface is "convex" in shape as shown in the preceeding figures. However, in some conditions with high external loads and large variations of material strength, the final optimzed slip surface may take a strange "concave" shape. The concave slip surface may give a lower factor of safety mathmatically, but the concave shape may not be physically admissible. In other words, you must judge the validity of an optimized solution not just based on the factor of safety but also based on the shape of the slip surface. SLOPE/W gives you the option to specify a maximum concave angles allowed for the upstream (driving side) and the downsteam (resisting side).

In a convex slip surface, the outside angle between two consecutive slices of the slip surface is larger than 180° . By the same token, in a concave slip surface, the outside angle between two consecutive slices of the slip surface is smaller than 180° .

4.8 Effect of soil strength

The fact that the position of the critical slip surface is dependent on the soil strength parameters is one of the most misunderstood and perplexing issues in slope stability analyzes. Coming to grips with this issue removes a lot of consternation associated with interpreting factor of safety calculations.

Purely frictional case

When the cohesion of a soil is specified as zero, the minimum factor of safety will always tend towards the infinite slope case where the factor of safety is,

$$F.S. = \frac{\tan\phi}{\tan\alpha}$$

where:

ϕ = the soil friction angle

α = the inclination of the slope.

Figure 4-36 shows a typical situation. The critical slip surface is parallel and immediately next to the slope face. The slope inclination is 26.57 degrees and the friction angle is 30 degrees. The computed factor of safety is 1.203, which is just over the infinite slope factor of safety of 1.15.

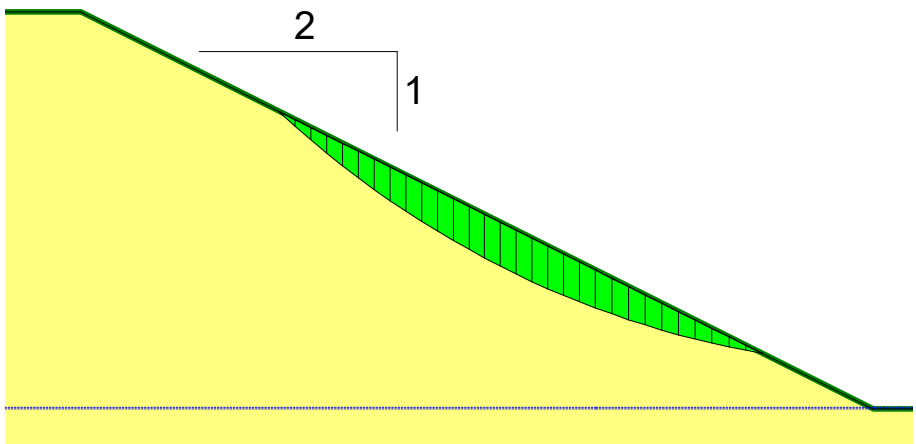

Figure 4-36 Shallow slip for purely frictional (c=0) case

The tendency to move towards the infinite slope case means the radius of the circle tends towards infinity. The minimum factor of safety is therefore usually on the edge of the grid of rotation centers. Figure 4-37 typifies this result. The minimum is right on the grid edge that represents the largest radius. Making the grid larger does not resolve the problem. The minimum occurs when the radius is at infinity, which cannot be geometrically specified. The Grid and Radius method appears to break down under these conditions, and the concept that the minimum factor of safety should be inside the grid is not achievable.

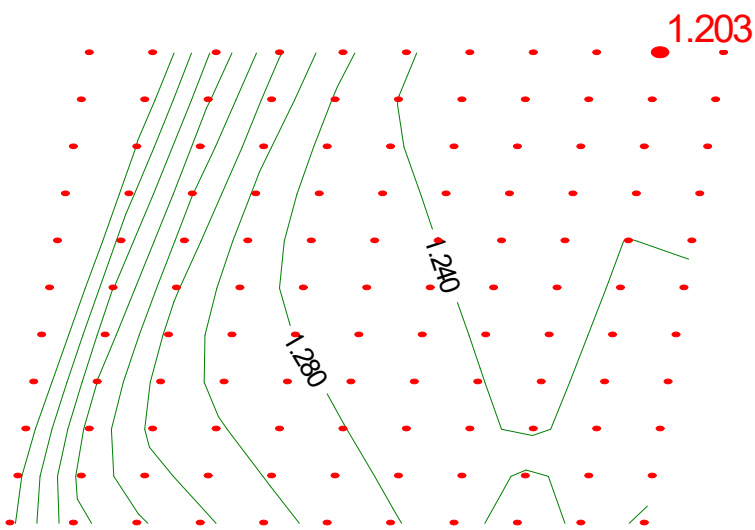

Figure 4-37 Minimum safety factor on edge of grid when c is zero

Undrained strength case

The opposite occurs when the soil strength is defined purely by a constant undrained strength; that is, ϕ is zero. In a case like this the critical slip surface will tend to go as deep as possible as shown in Figure 4-38. In this example the depth is controlled by the geometry. If the problem geometry was to be extended, the critical slip surface would go even deeper.

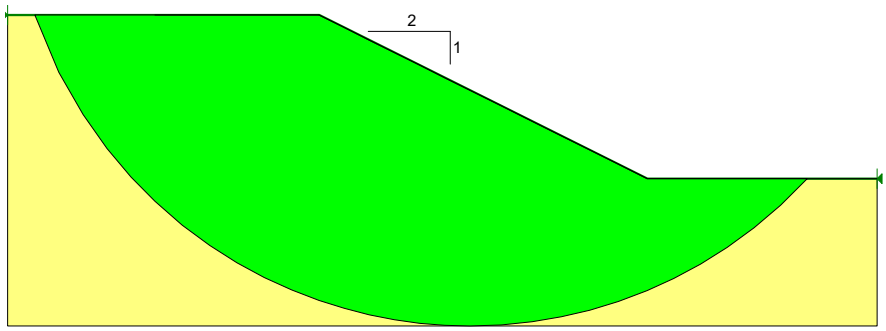

Figure 4-38 Deep slip surface for homogeneous undrained case

Figure 4-39 shows the factor of safety contour plot on the search grid. The minimum factor of safety is always on the lower edge of the search grid. Once again, for this homogenous undrained case it is not possible to define a minimum center inside the search grid.

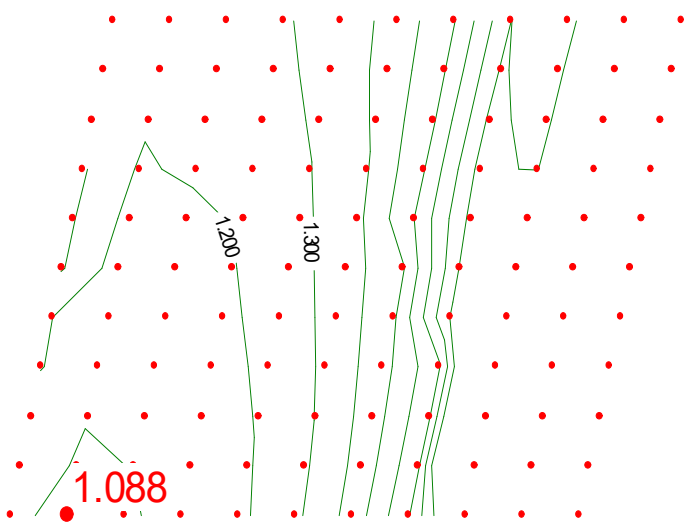

Figure 4-39 Minimum safety factor on edge of grid when ϕ is zero

Cause of unrealistic response

The reason for the unrealistic behavior in both the purely frictional case and the homogeneous undrained case is that the specified strengths are unrealistic. Seldom if ever, is the cohesion completely zero near the ground surface. Almost always there is a desiccated layer near the surface that has a higher strength or there a root-zone near the surface which manifests itself as an apparent cohesion. If the soil strength increases towards the ground surface, the critical slip surface will be at some depth in the slope.

The Shear Strength and Theory Chapter discuss how negative pore-water pressure (suction) increases the shear strength. This can be included in a SLOPE/W analysis by defining ϕ^b. If we make ϕ^b equal to 20

degrees, C equal to zero and ϕ equal to 30 degrees, then the position of the critical slip surface is as in Figure 4-40. Intuitively, this seems more realistic and is likely more consistent with field observations. Moreover, the minimum factor of safety is now inside the grid.

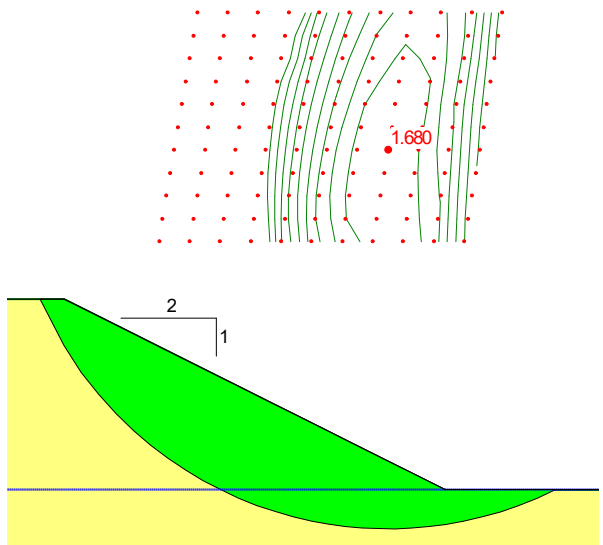

Figure 4-40 Critical slip surface when soil suction is considered

Figure 4-41 presents a plot of strength along the slip surface. Note the additional strength due to the suction and that the cohesion is zero everywhere.

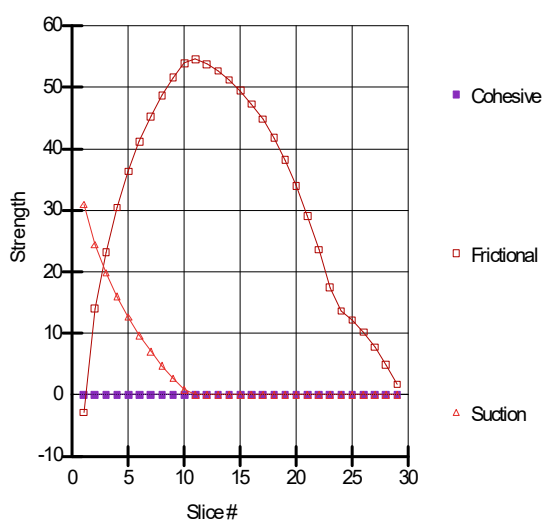

Figure 4-41 Strength components along the slip surface

The problem with the undrained case is that the undrained strength is the same everywhere. Once again, this is seldom, if ever, the case in the field. Usually there is some increase in strength with depth even for very soft soils. If the undrained strength is modeled more realistically with some increase with depth, the critical slip surface position no longer tends to go as deep as possible within the defined geometry. SLOPE/W has several soil models that can accommodate strength increase with depth.

Minimum depth

In SLOPE/W you can specify a minimum sliding mass depth. Say for example, that you specify a minimum depth of one meter. At least one slice within the potential sliding mass will then have a height greater or equal to the specified value. Any trial slips where all slice heights are less than the specified value are ignored.

The minimum depth parameter can be used to prevent SLOPE/W from analyzing very shallow slips. The slip surface with the minimum factor of safety will, however, still be the shallowest one analyzed and the lowest factor of safety will often still be on the edge of the rotation grid. As a result, this parameter does not really solve the underlying inherent problem. The minimum depth parameter should consequently only be used if the implications are fully understood.

Most realistic slip surface position

The most realistic position of the critical slip surface is computed when effective strength parameters are used and when the most realistic pore-water pressures are defined. This includes both positive and negative pore-water pressures.

Someone once said that the main issue in a stability analysis is shear strength, shear strength, shear strength. The main issue is actually more correctly pore-water pressure, pore-water pressure, pore-water pressure. Effective strength parameters can be fairly readily defined with considerable accuracy for most soils and rocks. This is, however, not always true for the pore-water pressure, particularly for the negative pore-water pressures. The difficulty with the negative pore-water pressures is that they vary with environmental conditions and consequentially vary with time. Therefore the stability can only be evaluated for a certain point in time.

The most likely position of the critical slip surface will be computed when effective strength parameters are used together with realistic pore-water pressures.

Shallow slips near the ground surface actually do happen if the cohesion indeed goes to zero. This is why shallow slips often occur during periods of heavy rain. The precipitation causes the suction near the surface to go to zero and in turn the cohesion goes to zero, and then indeed shallow slips occur as would be predicted by SLOPE/W. Another case is that of completely dry sand. Placing completely dry sand from a point source will result in conical shaped pile of sand and the pile will grow by shallow slips on the surface exactly as predicted by SLOPE/W for a material with no cohesion.

4.9 Tension cracks and exit projections

The steepness of the entrance and exit of the slip surface can have some negative numerical consequences. At the crest, the normal at the base of the first slice will point away from the slice, indicating the presence of tension instead of compression. Generally, this is considered unrealistic, particularly for materials with little or no cohesion. Physically, it may suggest the presence of a tension crack. In the exit area, steep slip surface angles can sometimes cause numerical problems with the result that it is not possible to obtain a converged solution. Both of these difficulties can be controlled with specified angles.

Tension crack angle

In SLOPE/W, it is possible to specify a tension crack angle. What it means is that if the base of a slice in a trial slip exceeds the specified angle, SLOPE/W removes the slice from the analysis. This has the effect

and appearance of a tension crack, as shown in Figure 4-42. In this case, the first slice on the left had a base inclination that exceeded the specified allowable; consequently the slice was ignored and replaced with a tension crack.

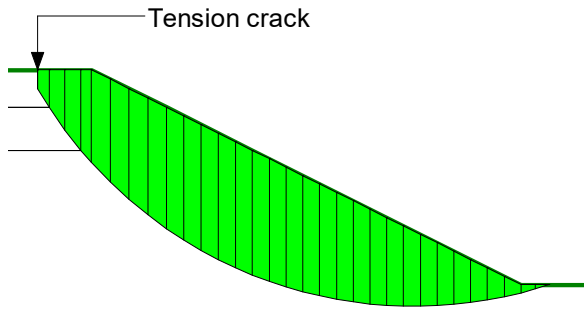

Figure 4-42 Tension crack based on specified inclination angle

Angles are specified in a counter-clockwise direction from the positive x-coordinate axis. In this example the tension crack angle was specified as 120 degrees. So any slice base inclination equal to or greater than 60 degrees from the horizontal is ignored.

The slip surface entrance point is analogous to an active earth pressure situation. Theoretically, the active earth pressure slip line is inclined at $(45 + \phi/2)$ degrees from the horizontal. While this is not strictly applicable, it is nonetheless a useful guide for specifying tension crack angles.

Constant tension crack depth

A constant tension crack depth can also be specified as part of the geometry, as discussed earlier.

Tension crack fluid pressures

Tension cracks can be assumed to be dry or filled with water. The extent to which the crack is full of water is expressed by a number between zero and 1.0. Zero means dry and 1.0 means completely full. If there is water in the tension crack, a hydrostatic force is applied to the side of the first element. The value of the lateral fluid force can always be verified by viewing the slice forces.

The idea of a significant fluid pressure in a tension crack is likely not very real. First of all, it is hard to imagine that a tension crack could hold water for any period of time. Secondly, the volume of water in a narrow tension crack is very small, so any slight lateral movement of the sliding mass would result in an immediately disappearance of the water and the associated lateral force. So considerable thought has to be given to whether a tension crack filled with water can actually exist and if it can exist, will the lateral hydraulic force remain when there is some as movement.

Toe projection

As noted earlier, steep exit angles can sometimes cause numerical difficulties. To overcome these difficulties, the steepness of the exit can be controlled with a specified angle, as illustrated in Figure 4-43. If the slice base has an inclination greater than the specified angle, SLOPE/W reforms the trial slip surface along a projection at the specified angle. Note how, in Figure 4-43, the curvature of the slip surface transforms into a straight line in the exit area.

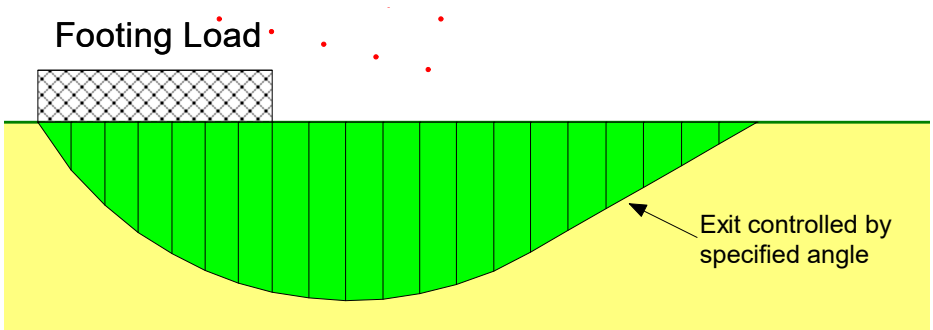

Figure 4-43 Exit angle controlled by specified angle

The toe area of a sliding mass is somewhat analogous to passive earth pressure conditions. In the example in Figure 4-43 the toe area is being pushed up and to the right just in a passive earth pressure case. Theoretically, the inclination of the passive slip line is at an angle of $(45 - \phi/2)$. This can be used as a guide when specifying this exit projection angle.

4.10 Physical admissibility

A consequence of the procedures used to generate trial slip surfaces, is that trial slip surfaces are sometimes formed that are not physically admissible; that is, they cannot exist in reality, or movement cannot possibly take place along the trial slip surface. Fortunately, in many cases it is not possible to obtain a solution for a physically inadmissible trial slip surface due to lack of convergence. Unfortunately, sometimes factors of safety are computed and displayed for cases where it is highly improbable that the potential sliding mass can slide or rotate as would be dictated by the trial slip surface.

This issue is complicated by the fact that there are no firm criteria to mathematically judge physical inadmissibility. SLOPE/W has some general rules that prevent some unreal cases like, for example, the inclination of the slip surface exit angle. If the slip surface exit is too steep, the results can become unrealistic and so the exit angle is arbitrarily limited to a maximum value. It is, however, not possible to develop similar rules for all potentially inadmissible cases. Consequently, it is necessary for the analyst to make this judgment. While performing limit equilibrium stability analyses, you should constantly mentally ask the question, can the critical trial slips actually exist in reality? If the answer is no, then the computed results should not be relied on in practice.

Some of the more common inadmissible situations are when the slip surface enters the ground at a steep angle and then exits at a steep angle with a relatively short lateral segment as illustrated in Figure 4-44. Described another way, the situation is problematic when the steep enter and exit segments are longer than the lateral segment of the slip surface. The problem is further complicated by very sharp breaks or corners on the trial slip surface. For the example in Figure 4-44 it is not possible to compute a Spencer or Morgenstern-Price factor of safety.

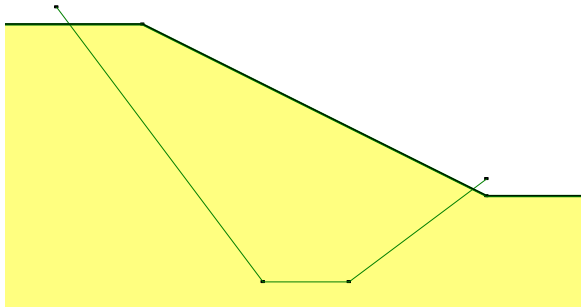

Figure 4-44 An example of a physically inadmissible slip surface

Another example of physical inadmissibility is when a very strong material overlies a very weak material. In the extreme case, if the weak material has essentially no strength, then the upper high strength material needs to sustain tensile stresses for the slope to remain stable. In reality, the soil cannot sustain tensile stresses. Mathematically, this manifests itself in lack of convergence. In other words, the model attempts to represent something that cannot exist in reality.

Sometimes it can be useful to assess the problem in a reverse direction. Instead of finding a factor of safety, the objective is to find the lowest strength of the weak material that will give a factor of safety equal to 1.0; that is, what is the lowest strength to maintain stability? Then the lowest strength required to maintain stability can be compared with the actual shear available. If the actual strength is less than what is required, then the slope will of course be unstable.

As a broad observation, convergence difficulties are often encountered when the model is beyond the point of limiting equilibrium or the sliding mode is physically inadmissible.

In the end, it is vital to remember that while SLOPE/W is a very powerful analytical tool, it is you who must provide the engineering judgment.

4.11 Invalid slip surfaces and factors of safety

A typical analysis may involve many trial slip surfaces; however, some of the slip surfaces may not have a valid solution. In such cases, a factor of safety with a value ranging from 983 - 999 is stored. It is important to realize that these values are not really factors of safety; they actually represent different error conditions of the particular trial slip surface.

The invalid slip surface may be due to convergence difficulties, in which a 999 is stored instead of the real factor of safety. Quite often, the invalid slip surface is also due to the position of the trial slip surface, the position of the grid center in a grid and radius, the pressure line definition, the direction of the sliding mass, the thickness of the sliding mass and overhanging ground surface etc. Although, the Verify feature in SLOPE/W attempts to identify these conditions before the actual computation, many of these conditions can only be detected during the computation inside the solver. In such cases, the solver outputs a factor of safety error code instead of the true factor of safety. SLOPE/W RESULT interprets the error conditions and displays a message concerning the error when you attempt to view the invalid slip surface using the Draw Slip Surfaces command.

The following summarizes the various error conditions:

983 – Slip Surface encounters missing stresses at the slice base center. This is not allowed in SLOPE/W. This happens when finite element stresses are used in the stability analysis and if the slip surface is sliding inside the interface elements defined with a “Slip surface” material model in SIGMA/W. The “Slip surface” material model does not compute any stresses. The work around is to limit the slip surface

from sliding inside the interface elements, or to use an “Elastic-Plastic” material model for the interface elements instead of the “Slip surface” material model.

984 – Slip Surface encounters an air gap or vertical / overhanging bedrock region (Figure 4-45). This happens when adjacent regions are not connected properly or when a slip surface goimg through a vertical or overhanging bedrock. This causes the slip surface to be discontinous which is not allowed in SLOPE/W.

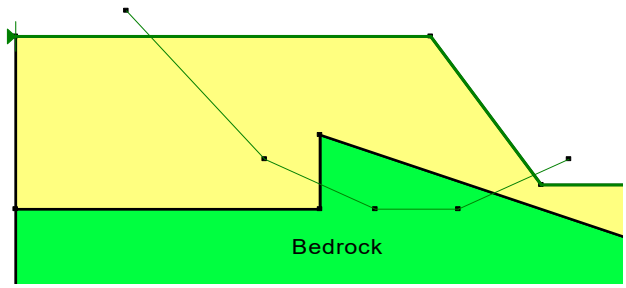

Figure 4-45 Slip surface intersecting an overhanging or vertical bedrock

985 – Overlapping Pressure lines exist. This happens when multiple pressure lines are defined at the same x-coordinate above the ground surface. This is not allowed in SLOPE/W.

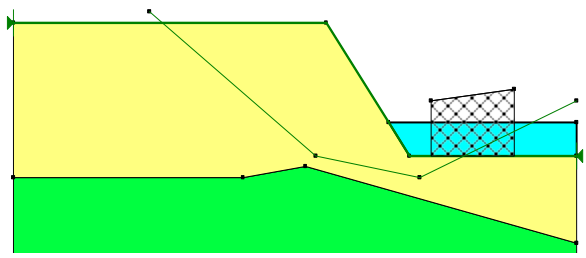

Figure 4-46 Slip surface intersecting a pressure line inside a zero strength material

987 - Slip surface inside a region with an internal pressure line (**Error! Reference source not found.**). This happens when a pressure line is defined below the ground surface. A pressure line must be defined above the ground surface to have the loading handled properly. A pressure line defined below the ground surface is intuitively impossible and is therefore not allowed in SLOPE/W.

988 - Slip surface does not contain any material with strength. This is not allowed in SLOPE/W. This happens when the entire slip surface is inside material region with no material strength model defined.

990 - Slip surface does not intersect the ground surface line. This happens when there is problem in the trial slip surface. For example if a fully specified slip surface does not cut through the ground surface line. No slip surface can be generated.

991 - Slip surface center defined below the slip surface exit points. This results in a slice with base angle larger than 90 degrees. This is not allowed in SLOPE/W.

992 - Slip surface cannot be generated (Figure 4-47). This happens whenever there is a problem in generating a trial slip surface. There may be problems in finding the ground surface line or finding the slip surface intersecting points with the ground surface. This also happens with an overhanging slip surface or when a slip surface is trying to undercut itself. No factor of safety can be computed when a slip surface cannot be generated.

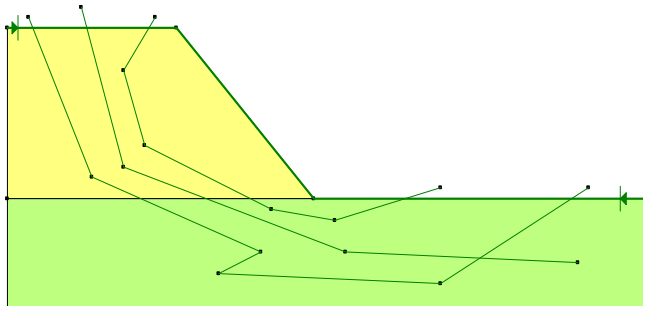

Figure 4-47 Slip surface cannot be generated

993 - Slip surface is too shallow (Figure 4-48). This happens when the thickness of all slices are smaller than the specified minimum slip surfaces thickness. In a purely frictional material, the critical slip surface tends to develop on the shallow ground surface where the normal force is small and the shear strength is low. Although this is theoretically correct and physically admissible, this shallow critical slip surface may not be of any interest to you. SLOPE/W allows you to set a minimum slip surface thickness so that any slip surface shallower than the specified limit will be considered invalid and will not included in the factor of safety calculation.

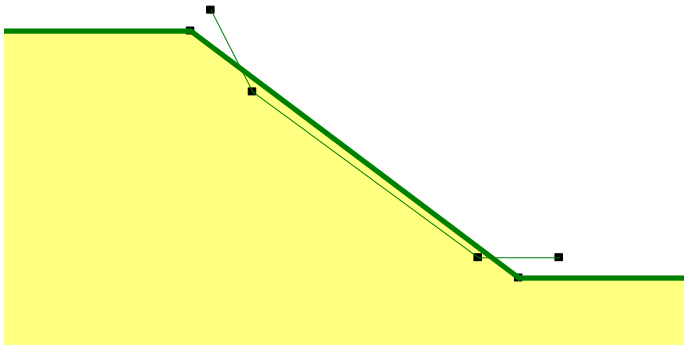

Figure 4-48 Slip surface with thickness less than specified minimum

994 - No intersecting point is obtained in the factor of safety versus lambda plot for the GLE formulation (Figure 4-49). This happens when there are convergence difficulties or when the specified lambda values are not sufficient for the factor of safety by moment and factor of safety by force to obtain an intersecting point on the factor of safety versus lambda plot.

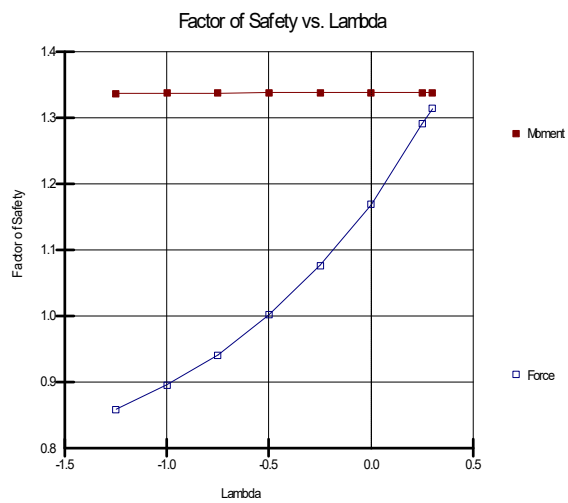

Figure 4-49 No intersecting point in a GLE formulation

995 - Slip surface could not be analyzed. This happens when all other conditions appear to be fine, but the solver encounters problems in the factor of safety computation. For example, the mobilized shear reistance is in the opposite direction due to a large negative normal force. This error message could also be related to extreme soil properties or large external forces relative to the sliding mass.

996 - Slip surface is not in the same direction as the specified direction of movement. This happens when the direction of movement is not set properly in SLOPE/W or in a complex geometry where a slip surface has an exit point higher than the entry point.

997 - Slip surface exit angle is too steep (M-alpha approaches zero). In limit equilibrium, the M-alpha value used in the computation of the normal force at the base of a slice is a function of the slice base angle and the material frictional angle. The normal force approaches infinity when M-alpha approaches zero. This is not allowed in SLOPE/W. This happens when a frictional mterial is used and when the exit angle of a slip surface is too steep (usually larger than 45°). Please refer to the "M-alpha value" discussion in the Theory chapter of the book for details.

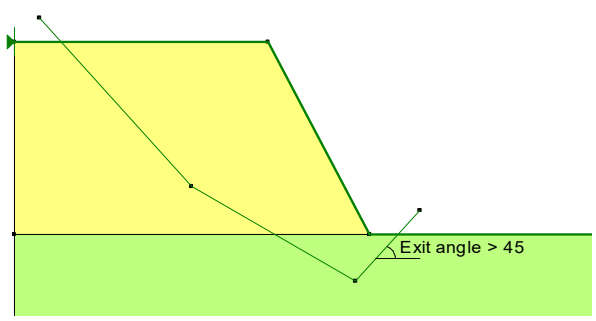

Figure 4-50 Slip surface with exit angle larger than 45 degrees

998 - Slip surface enter or exit beyond the slip surface limit. This happens when the slip surface extends beyond the specified slip surface limits (Figure 4-51). Both of the fully specified slip surfaces in the figure below have at least one exit or entry point beyond the slip surface limits.

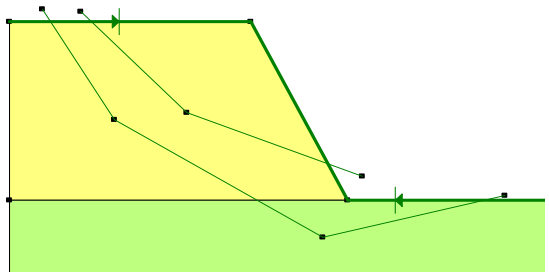

Figure 4-51 Slip surface enter and exit beyond the limits

999 - Slip surface does not have a converged solution. This happens when the solution for the slip surface does not converge. SLOPE/W uses an iterative procedure to solve the nonlinear factor of safety equation until the factor of safety converges within a specified tolerance. The convergence difficulties may be due to conditions with unreasonable soil strength properties, unreasonably large concentrated point loads or reinforcement loads, unreasonable seismic coefficient, unreasonable pore water pressure etc. By default, SLOPE/W uses a convergence tolerance of 0.01. While this tolerance is fine for most situations, you may like to relax this tolerance in order to obtain a solution when modeling extreme conditions.

For simplicity, the fully specified slip surface is used to illustrate the various problems with slip surfaces and geometry, however, the same situations would apply to other types of slip surface methods. In a slope stability analysis, it is quite common that some of the trial slip surfaces are invalid especially when using a grid and radius slip surface where the search grid is large and the search radius is long relative to the overall slope. It simply means that many trial slip surfaces are entering or exiting beyond the limits of the slope. Most likely, these invalid slip surfaces are of little interest to you and it is very unlikely that these invalid slip surfaces will be the most critical slip surfaces of the slope. You may choose to ignore these invalid slip surfaces, or you may like to better control the position of the search grid and radius to eliminate these invalid slip surfaces. The Entry and Exit slip surface method is much easier in controlling the position of the trial slip surfaces.

4.12 Concluding remarks

As noted in the introduction, finding the position of the critical slip surface requires considerable guidance from the analyst. SLOPE/W can compute the factors of safety for many trials very quickly, but in the end, it is up to the analyst to judge the results. Assuming that SLOPE/W can judge the results better than what you as the engineer can do is a perilous attitude. The SLOPE/W results must always be judged in context of what can exist in reality.

5 Geometry

5.1 Introduction

SLOPE/W uses the concept of regions to define the geometry. Basically this simply means drawing a line around a soil unit or stratigraphic layer to form a closed polygon, similar to what we would do when sketching a problem to schematically explain a particular situation to someone else. In this sense, it is a natural and intuitive approach.

Regions are a beneficial aid for finite element meshing. SLOPE/W by itself does not need a finite element mesh, but regions defined in SLOPE/W can also be used to create a mesh for an integrated finite element analysis. In GeoStudio the objective is to only define the geometry once for use in many different types of analyses. Using regions in SLOPE/W as well as in the finite element products makes this possible even though SLOPE/W uses slice discretization instead of finite element discretization. SLOPE/W can then use the results readily from other analyses, such as SEEP/W and SIGMA/W in a stability analysis.

This chapter describes the basics of regions and shows some examples of how they can be used to define various geometric conditions. Included as well are descriptions and discussions on how to define SLOPE/W specific features including point loads, surface surcharge pressures, tension crack and ponded water.

5.2 Regions

Regions are in essence n-sided polygons. Polygons with three sides are triangles and polygons with four sides are quadrilaterals. Figure 5-1 shows some representative basic regions.

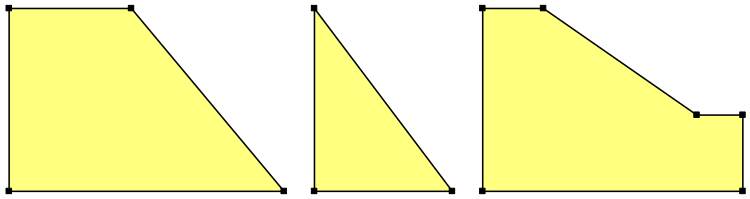

Figure 5-1 Representative basic regions

All regions need to be connected to form a continuum. This is done with the use of Points. The small black squares at the region corners in Figure 5-1 are the points. The regions are connected by sharing the points. In Figure 5-2, Points 6 and 7 are common to the two regions and the two regions consequently behave as a continuum.

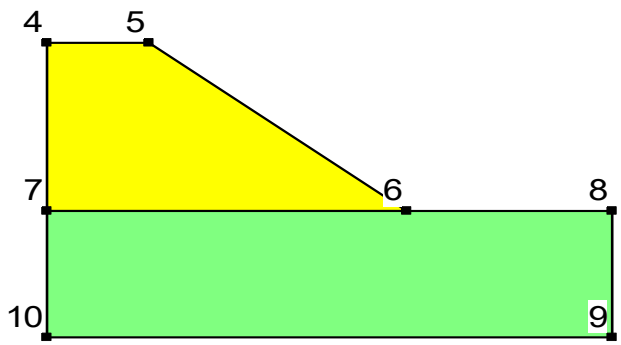

Figure 5-2 Region points

Figure 5-3 shows a typical slope stability case defined with regions. Here Points 2 and 8 are common to the top two regions. Points 3, 7 and 10 are common to the bottom two regions.

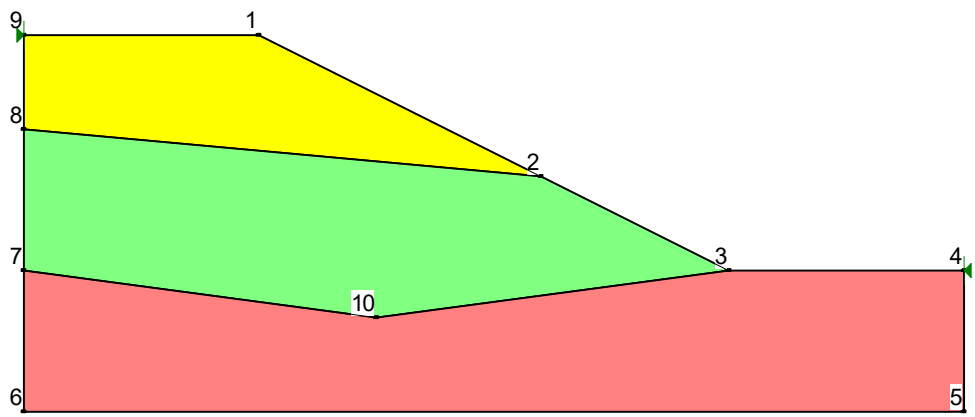

Figure 5-3 Typical regions for a slope stability analysis

Figure 5-4 shows a case where the triangular region on the left represents a soil layer that pinches out in the slope. Region 2-3-11-10 represents water impounded up against the slope.

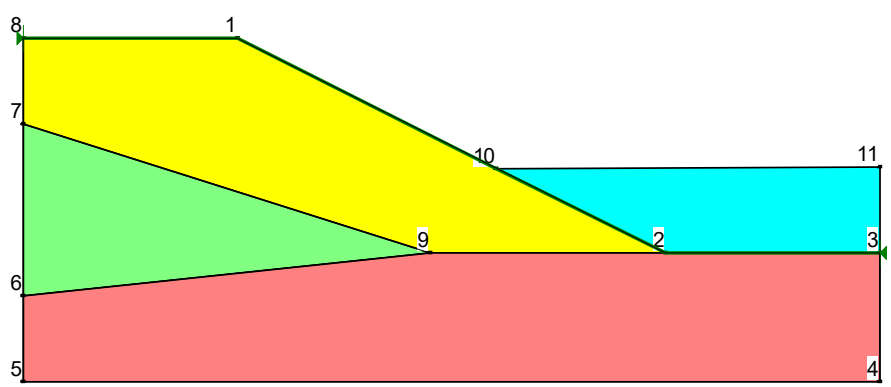

Figure 5-4 Example of pinching out region and water region

Figure 5-5 illustrates a typical tailings impoundment case. The quadrilateral regions on the left represent dykes, and the upper dyke sits on top of tailings; that is, the tailings under-cut the upper dyke.

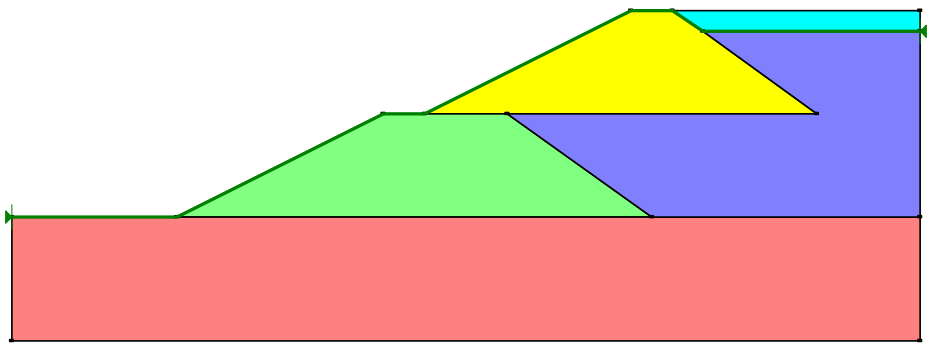

Figure 5-5 Example of an under-cutting region.

From these few examples, it is easy to see how almost any stratigraphic section can be easily and quickly defined with regions.

One of the attractions of regions is that the geometry can be so easily modified by moving the points. The regions do not necessarily have to be redrawn – only the points have to be moved make modification to the geometry.

Regions do have a couple of restrictions. They are:

- A region can have only one material (soil) type. The same soil type can be assigned to many different regions, but each region can only be assigned one soil type.
- Regions cannot overlap.

An island of a particular soil type can be defined by dividing the surrounding soil into more than one region. Figure 5-6 illustrates this. Two regions of the same soil type are drawn such that they encompass the isolated quadrilateral of a different soil type. There may be other ways of defining this particular situation, but at no time can regions overlap. In other words, the pinching out layer in Figure 5-6 cannot be drawn on top of the other soil.

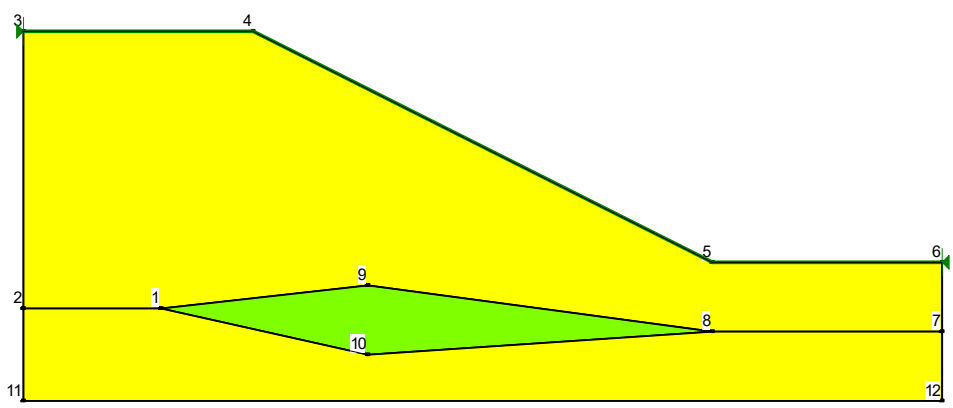

Figure 5-6 Section with an island of soil of a different type

5.3 Slice discretization

SLOPE/W uses a variable slice width approach in the sliding mass discretization. In other words, SLOPE/W will discretize the soil mass with slices of varying widths to ensure that only one soil type exists at the bottom of each slice. In also is used to prevent a ground surface break occurring along the top

of the slice and to prevent the phreatic line from cutting through the base of a slice. The objective is to have all the geometric and property changes occur at the slice edges.

Initially SLOPE/W divides the potential sliding mass into section as shown in Figure 5-7. The first section starts on the left where the slip surface enters the ground surface. Other sections occur where (1) the slip surface crosses the piezometric line, (2) the slip surface crosses a stratigraphic boundary, (3) wherever there is a region point, and (4) where the piezometric line crosses a soil boundary. The last section ends on the right where the slip surface exits the ground surface.

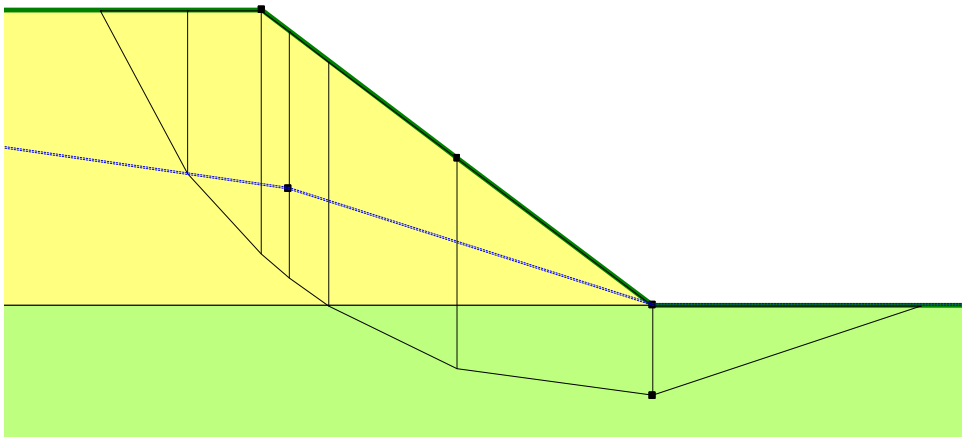

Figure 5-7 Sections in the slice discretization process

As a next step, SLOPE/W finds the horizontal distance from slip surface entrance to exit and divides this distance by the number of desired slices specified by the user (the default is 30). This gives an average slice width. The last step is to compute how many slices of equal width approximately equal to the average width can fit into each section. The end result is as shown in Figure 5-8 when the specified number of slices is 15.

Depending on the spacing of the sections, the variable slice approach will not always lead to the exact number of slices specified. The actual number of slices in the final discretization may be slightly higher or lower than the specified value. In this case, the total number of slices is 16.

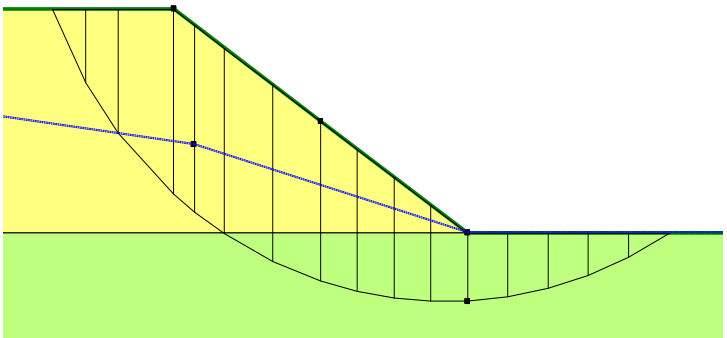

Figure 5-8 Discretization when the specified number is 15 slices

The variable slice width approach makes the resulting factor of safety relatively insensitive to the number of slices. Specifying the number of slices to be greater than the default number of 30 seldom alters the factor of safety significantly. Specifying the number of slices lower than the default value of 30 is not recommended unless you want to investigate a specific issue like, for example, comparing the SLOPE/W

results with hand calculations. Making the number of slices too high simply creates an excessive amount of unnecessary data without a significant improvement in safety factor accuracy. Figure 5-9 shows the discretization when the number of specified slices is 30.

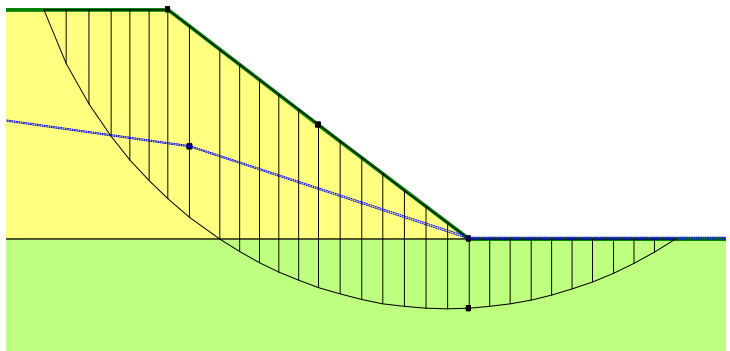

Figure 5-9 Discretization when specified number is 30 slices

5.4 Ground surface line

A special geometric object in GeoStudio is the ground surface line. It is a necessary feature for controlling what happens at the actual ground surface. Climate conditions, for example, can only act along the ground surface line.

In SLOPE/W, the ground surface line is used to control and filter trial slip surfaces. All trial slip surfaces must enter and exit along the ground surface. Trial slip surfaces that enter or exit along the perimeter of the problem outside of the designated ground surface are considered inadmissible. Triangular markers indicating the extents of ground surface line can be moved along the ground surface as illustrated on Figure 5-10.

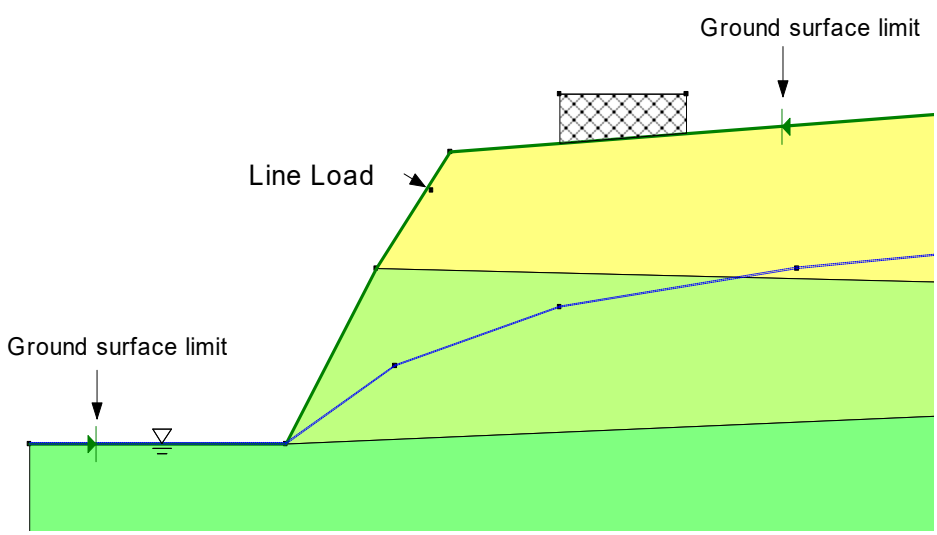

Figure 5-10 Example of a ground surface line and limit markers

SLOPE/W has a particular technique for specifying trial slip surfaces called “enter-exit”. Line segments can be specified which designate specific locations where all trial slip surfaces must enter and exit. These line segments are attached to the ground surface line. The specifics of this technique are discussed in more detail in the chapter on Slip Surface Shapes.

SLOPE/W computes the ground surface line and displays it as a heavy green line. Some care is required in the definition of the geometry to ensure that the computed line is the actual ground surface. For example, if the intended vertical extents of a problem are not truly vertical, the ground surface line may follow the near vertical ends of the problem. This can happen when there are small numerical differences in the x-coordinates in the points along the ends. The smallest and largest x-coordinates in the problem are used to identify the ends of the intended ground surface line.

5.5 Tension crack line

A tension crack can be specified with a tension crack line, as illustrated in Figure 5-11. When a tension crack line is specified, the slip surface is vertical in the tension crack zone. The tension crack can have water in it, which results in a lateral force being applied to the end slice. Procedural details on this feature are in the online help. The tension crack line option is discussed here because it is, in essence, a geometric definition.

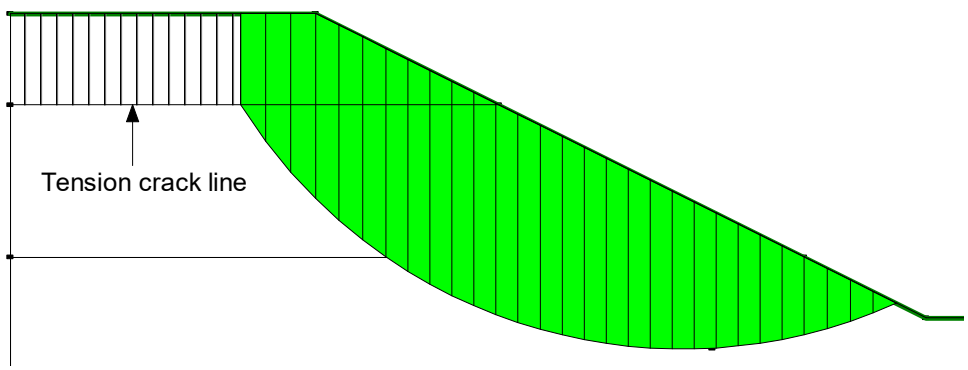

Figure 5-11 Tension crack line

There are other more advanced ways of including the possibility or presence of a tension crack in a stability analysis. A better way is to assume a tension crack exists if the slice base inclination becomes too steep. The angle at which this occurs needs to be specified.

The tension crack line concept is now somewhat outdated, but is still included for backward compatibility and for historic reasons. The other two options are more recent concepts, and offer more realistic behavior, particularly the angle specification method.

5.6 Concentrated point loads

Like the tension crack line, concentrated point loads are discussed here because they contain a geometric aspect.

Concentrated point loads must be applied inside the potential sliding mass. Intuitively, it would seem that the point loads should be applied on the surface. This is possible, but not necessary. Attempting to apply the point load on the surface is acceptable, provided it is done with care. Due to numerical round-off, a point load can sometimes be ignored if the computed application point is slightly outside the sliding mass.

The possibility of missing the point load in an analysis can be mitigated by ensuring the application of the pint load is inside the sliding mass (Figure 5-12). Remember that a point load is included in the force equilibrium of a particular slice. All that is required is to ensure the point load is inside a slice, and slight differences in precisely where the point loads are placed within the mass are negligible to the solution.

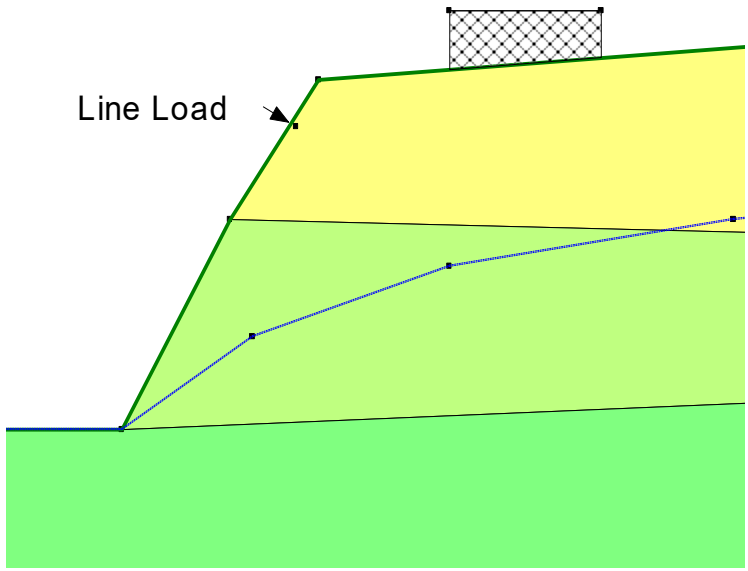

Figure 5-12 Example of a Point load on the slope surface

Alternatively, you may add an extra point to the surface of a region and have the point load specified on the same point. This will ensure that the point load will be added to the slice containing the point. However, since there are so many application forces, it is always wise and prudent to check that the point load has been applied as intended by viewing the computed slice forces. A point load is always displayed at the top of the slice at the applied direction. As illustrated on Figure 5-13, the applied point load is 100 lbs on slice 18.

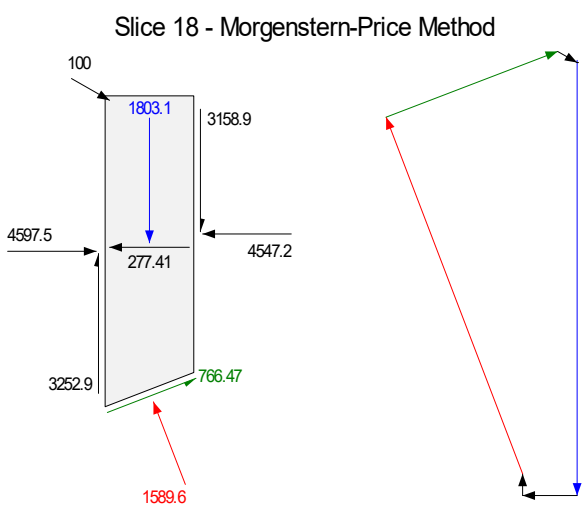

Figure 5-13 Example of a Point load force at top of slice

5.7 Ponded water

SLOPE/W identifies the existence of ponded water by means of positive pore water pressures on the ground surface. The same procedure is used regardless of the means by which the pore water pressure conditions were defined (e.g. from a piezometric line or finite element SEEP/W or SIGMA/W analysis). For example, a surcharge load representing the ponded water is automatically created if a piezometric line is defined above the ground surface (Figure 5-14). The corresponding elevation to which the ponded water rises is painted on the domain by default. Water loads are applied normal to the ground surface.

Note that since each material may have a different piezomeytric line, only the ground surface materials defined with a piezometric line above the ground surface will be considered as ponded water. In other words, if the piezometric line on the same figure is only assigned to the orange material but not the green material, the defined piezometric line will not be treated as a surface pond, and you will not see the water load or blue painting.

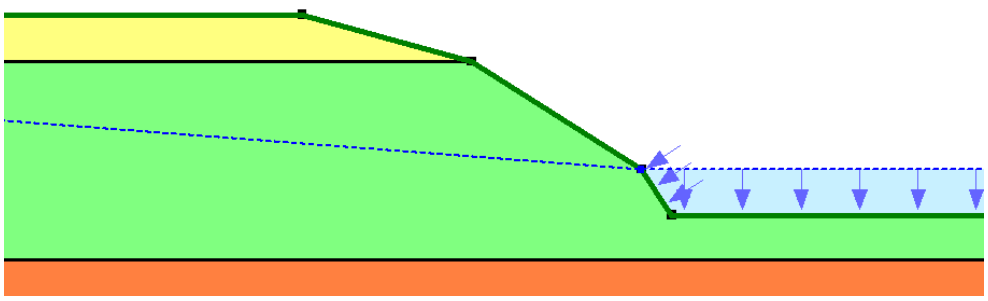

Figure 5-14 Ponded water created by SLOPE/W

A force representing the weight of the ponded water is added to the top of each slice as a point load. The force is equal to the vertical distance at mid-slice from the ground surface to the piezometric line times the slice width times the specified unit weight of water.

The computed surcharge forces on a slice should always be checked and verified by viewing the slice forces. The force is displayed at the top of the slice at the applied direction. The 45 force on top of the slice in Figure 5-15 is the applied force due to the weight of the ponded water.

SLOPE/W uses the pore water pressure condition on the ground surface line to determine if any ponded water exit. If a ponded water exits, the weight of the water is automatically applied as a point load in a direction normal to the groud surface. .

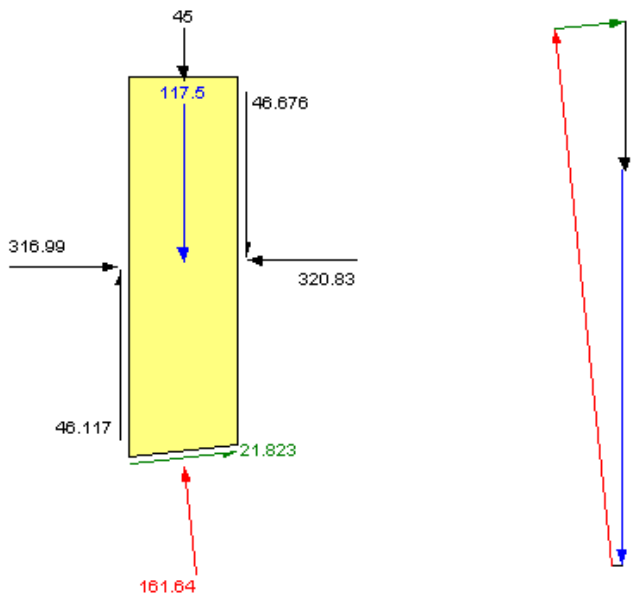

Figure 5-15 Example of a force due to ponded water at top of slice

The weight of the ponded water is always applied normal to the ground surface at the top of each slice. As a result, there will no longer be one large horizontal hydrostatic force acting on the first or last slices as in the older versions of SLOPE/W. In the situation of a vertical wall, the horizontal hydrostatic force is applied automatically to the vertical side of the slice.

The weight of the ponded is computed with the specified unit weight of water. In the case if the modeled water pond has a different unit weight, a surcharge load can be used to increase or decrease the unit weight of the pond water from the specified unit weight of water. Please refer to the surcharge load section for more details and example.

5.8 Surface surcharge loads

Surface surcharge pressures can be simulated with what is known as a surcharge load. Figure 5-16 shows two surcharge loads. The surcharge at the toe of the slope represents a berm. Beyond the slope crest the

surcharge could represent the weight of a building or perhaps some type of equipment.

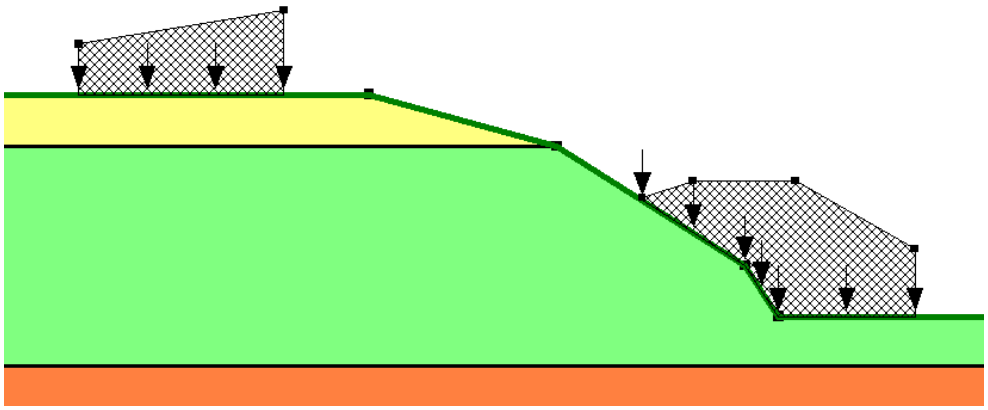

Figure 5-16 Ground surface surcharge loads

The surcharge load must be defined above or on the ground surface line. The loading can be applied in a vertical direction or in a direction normal to the ground surface line. As illustrated in the figure, the surcharge load regions are cross-hatched and the black arrows indicated the selected load direction.

SLOPE/W creates slices so that slice edges fall at the ends of the surcharge load. A force representing the surcharge is added to the top of each slice as a point load. The force is equal to the vertical distance at mid-slice from the ground surface to the top of the surcharge load times the slice width times the specified surcharge (or unit weight).

A useful trick for applying a uniform pressure is to make the distance from the ground surface to the surcharge load line unity (1.0). The specified surcharge (or unit weight) will then be the applied pressure. This can be useful when simulating situations such as a footing pressure.

The computed surcharge forces on a slice should always be checked and verified by viewing the slice forces. The surcharge force is displayed at the top of the slice at the applied direction. The 51.86 force on top of the slice in Figure 5-17 is a surcharge force.

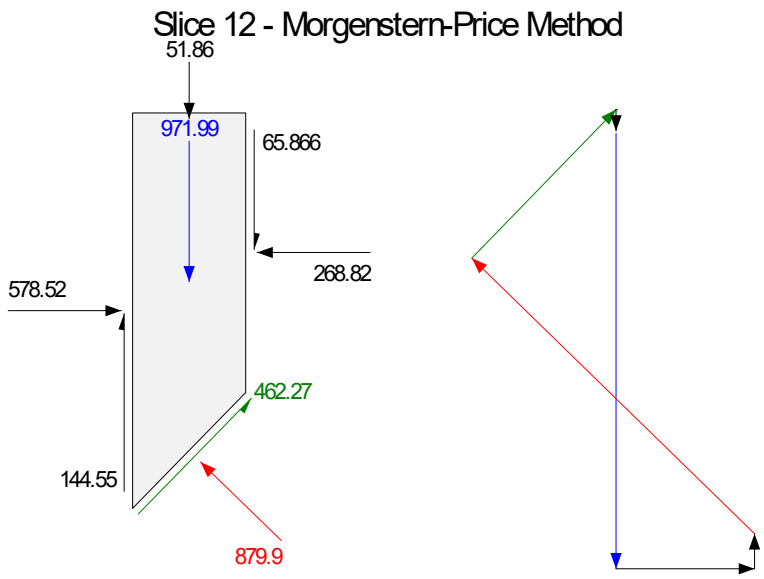

Figure 5-17 Example of a surcharge force at top of slice

The direction of the surface load can be vertical or normal to the ground surface. The vertical option is useful when modeling a berm or a surcharge load exerted from a building or equipment. The normal direction can be used when modeling water or other fluid type of material when the loading is hydrostatic.

Surcharge load can be specified as positive or negative and the surcharge load can be superimposed with the ponded water weight. Therefore, surcharge load can be used to increase or decrease the unit weight of the pond water. This is useful when modeling a pond of fluid material with different unit weight than water,

In the example shown in Figure 5-18, the unit weight of water is specified as 10 kN/m3, but the fluid material has a unit weight of 11 kN/m^3. To model the additional weight of the fluid material, a surcharge load of 1 kN/m^3 is added to the pond with the load direction selected as normal. Note the cross-hatching of the ponded water and the presence of both blue arrows and black arraow.

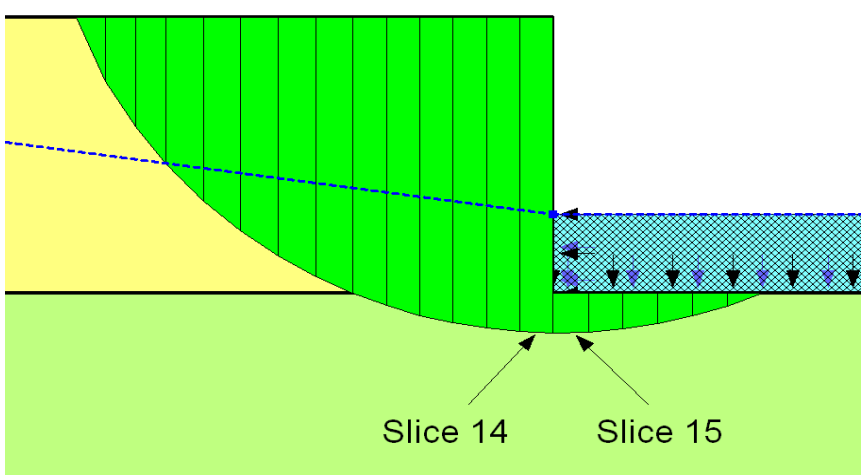

Figure 5-18 Superpositioning of ponded water and surcharge load

The detail slice force of the slice #15 is shown in Figure 5-19. The weight of the ponded fluid is shown as a point load on the top of the slice. The 17.916 kN is computed by the unit weight of the fluid (11 kN/m^3/m) times the depth of the pond (2m) times of width of the slice (0.81437m).

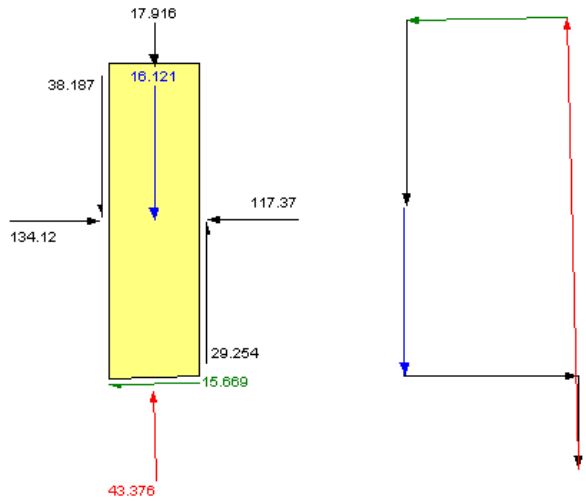

Figure 5-19 Example of a fluid surcharge force at top of slice

The detail slice force of the vertical slice (slice #14) is shown in Figure 5-20. The hydrostatic force of the ponded water is shown with a horizontal force shown on the top right corner of the free body diagram. The total is 22 kN which is equal to the total unit weight of the fluid (11 kN/m^3/m) times the square of the depth of the pond (4m^2) divided by 2.

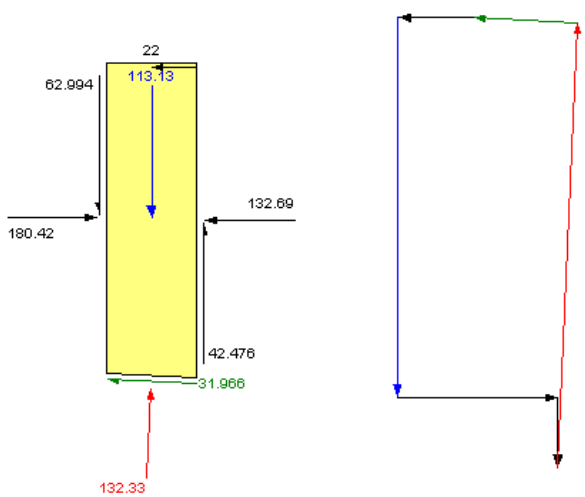

Figure 5-20 Example of a hydrostatic force on the side of slice

It is important to note that the "normal" direction of the surcharge load must be chosen in order to model the hydrostatic nature of ponded waters. When the normal direction is chosen, the surcharge load is

applied to the top of each slice in the direction normal to the ground surface. In the case of ponding next to a vertical wall, the hydrostatic force is applied horizontally (normal) to the side of the vertical slice.

Surcharge load can be defined as positive or negative. The surcahge load can be superimposed with the ponded water weight. This is useful when mdoling ponded with material heavier or lighter than water.

6 Functions in GeoStudio

User specified functions are used throughout GeoStudio to specify soil material properties, to specify modifier parameters for constants or other functions, or to specify boundary conditions that change over time. It is important to have an understanding of how the functions are specified and used by the solver and also to know what your options are for inputting these functions. A functional relationship between "x" and "y" data can be defined using:

- Natural and weighted splines between data points
- Linear lines between data points
- A step function between data points
- A closed form equation that is based on parameters and does not require data points
- A user written externally complied code (dll library) that connects with GeoStudio data or data from another process (eg, Excel)
- A spatial function that varies based on geometry x and y coordinate

New in GeoStudio 7.1 are spatial functions which return a different value based on both x and y coordinate within any given soil material. This option is available for strength parameters in SLOPE/W and for activation values in the other finite element codes. Activation values are starting pressures or temperatures, for example, that are present in the ground when the model first starts a transient process.

The type of function you choose to use will depend on what your needs are.

In many cases a function you need can be estimated from other data you have input. An example is the hydraulic conductivity function for soils that is based on a user input water content function. Several GeoStudio material models require functions that may be estimated if you do not already have a full set of data.

6.1 Spline functions

A spline function is a mathematical technique to fill in the gaps between adjacent data points with curved line segments. Unfortunately, all our data points do not always fit nicely along a path with a predictable curvature such as a logarithmic or exponential decay. Many of the functions in geo-technical engineering have double curvature with an inflection point between. Consider the water content function that is initially concave downwards, and then at higher suctions is concave upwards. Splining is an advantageous technique to fit lines through these data points because the spline settings can be altered to fit almost any set of data.

In GeoStudio you can control the look of a spline function by adjusting its degree of curvature and its level of fit with the input data points. Consider the two images below.

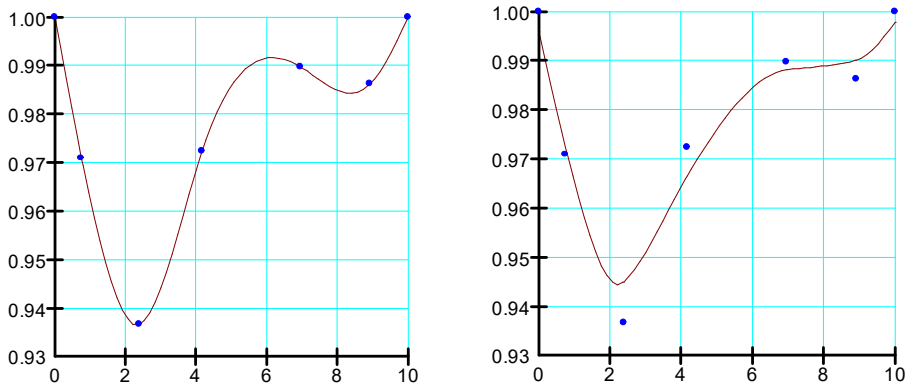

Figure 6-1 Spline functions with different settings

The left image has the spline fit almost exactly through the data points with fairly curved segments. The right image has more linear segments that only fit the data approximately. The range of fit and curvature is controlled by two "slider controls" and can range between values of zero and 100%. The important thing to note is that the solver will use the data represented by the splined fit. What you see in the function set up is EXACTLY what the solver will use when needed.

Slopes of spline functions

Sometimes, the solver does not require the "Y" value of a function at a given "X" value but the slope of the function at a given "X" value. This is the case for the water content function where the slope is used directly in the solution of the transient seepage and air flow equations. You must be careful when setting spline values because while a spline may look smooth, its slope may not be so.

The two images below are the slopes of the two functions shown above. You can see that the more natural curved function (left side images) with 100% curvature and exactness in the spline settings produces a much smoother slope function than the approximated function. While not usually critical, you should know if the function you are using is dependent on its slope being well behaved.

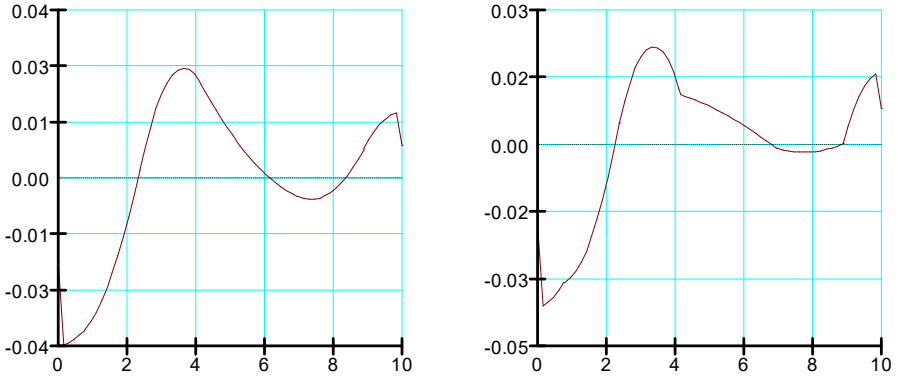

Figure 6-2 Slope of spline functions

6.2 Linear functions

A linear function is a spline function with the curvature setting to 0% and the fit set to 100% exact as shown below.

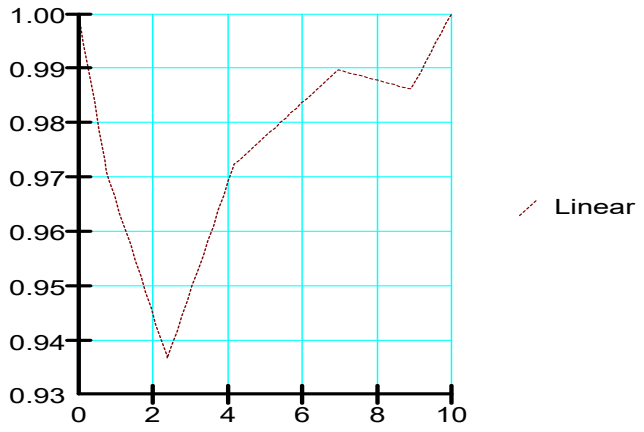

Figure 6-3 Linear fit spline

6.3 Step functions

GeoStudio 2007 has an option for functions that result in "steps" between data points. This can be useful if your data changes abruptly over time, for example, rainfall on different days. When you use a step function, you need to be careful of the location of the blue data point. You can see that the functions will assume the starting time of the step is at the data point and that its duration extends just up to but not reaching the next data point.

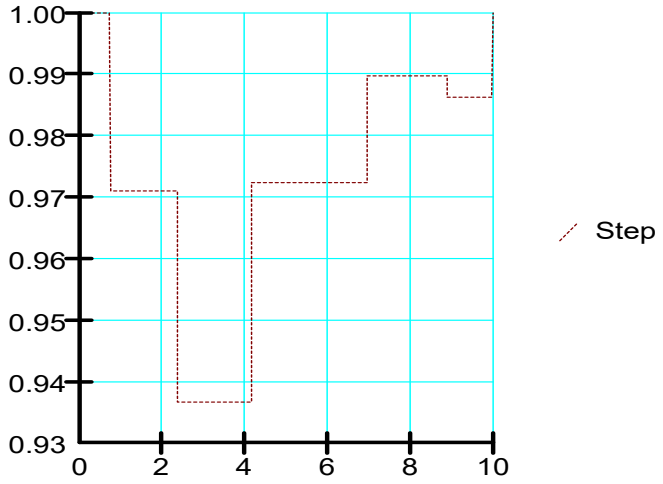

Figure 6-4 Step function

A comparison of all four data point functions is shown below on one image. When multiple functions are viewed simultaneously in GeoStudio, the data points are hidden and just the computed functions are displayed.

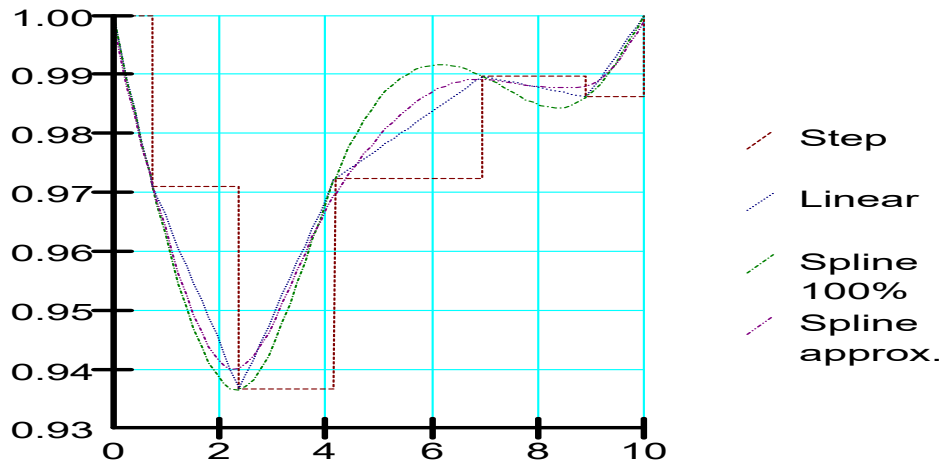

Figure 6-5 Comparison of all data point functions

6.4 Closed form curve fits for water content functions

The storage function is defaulted to be represented by a spline function; however, it is possible to have the function represented by a closed form equation that is fit to the data. Two common methods exist in the literature for water content functions: the Fredlund and Xing method, and the Van Genuchten method. Each of these curve fits require that you enter fitting parameters that are usually published or provided by soil laboratories. The only advantage to using these techniques in GeoStudio 2007 is that you do not have to enter a series of data points. If you know the fit parameters, you may enter them directly to obtain the function. More information about these two fit equations are provided in the chapter on Material Models and Soil Properties in this book.

6.5 Add-in functions

GeoStudio Add-Ins are supplemental programs run by the solver as part of a GeoStudio analysis. A Function Add-In is an object that takes the place of a function defined in GeoStudio, and offers the flexibility of computing function results that vary dynamically based on the current analysis state. For example, Add-Ins can be assigned to Slip Surface Slices (via strength functions), Mesh nodes (via boundary condition functions), and Mesh gauss points (via material property functions). Please consult the Add-In Developers Kit (SDK) available on the website (www.geo-slope.com/downloads) for full details.

6.6 Spatial functions

A spatial function is a material property value that is dependent on both x and y coordinates within any soil property. The functions are created over all x and y but are then confined to a geometry region by being linked with a soil property that is assigned to a region. Spatial functions can be created in

SLOPE/W strength parameters (Unit Weight, Cohesion and Phi) and for all activation values in the finite element products. Activation values include pressure, temperature, concentration, and air pressure.

When you first create a spatial function you will not see its contoured colors appear on the geometry. However, once you assign the function to a material model and then assign that model to a geometry region, you can return to the Key In Spatial Function command, make changes and edits to the function data, and see instantly what the new function will look like when applied to your model. An example of this is shown below for activation pore-water pressures.

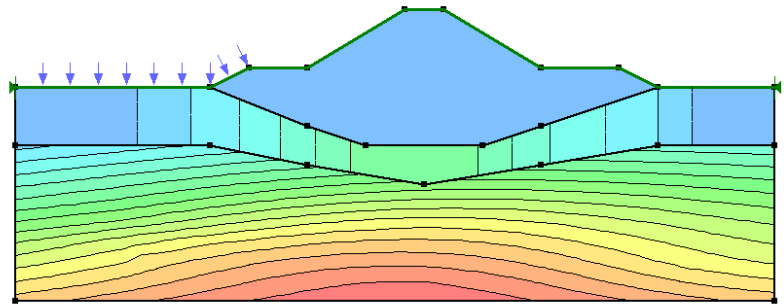

Figure 6-6 Example of spatial function assigned to bottom soil region material

From the spatial function which is defined with discrete value points, the solver generates a continuous value surface over the defined region using either the “Kriging interpolation” or the “Linear interpolation” techniques. Note that, for the same data set, the two interpolation techniques may yield a considerably different distribution especially when insufficient points are defined. To ensure that the solver is using the same value as what you have expected, it is important to view the resulting contours generated by the two techniques in DEFINE before doing the actual analysis.

7 Material Strength

7.1 Introduction

There are many different ways of describing the strength of the materials (soil or rock) in a stability analysis. This chapter describes and discusses all the various models available in SLOPE/W.

7.2 Mohr-Coulomb

The most common way of describing the shear strength of geotechnical materials is by Coulomb's equation which is:

$$\tau = c + \sigma_n \tan\phi$$

where:

τ	=	shear strength (i.e., shear at failure),
c	=	cohesion,
σ_n	=	normal stress on shear plane, and
ϕ	=	angle of internal friction (phi).

This equation represents a straight line on a shear strength versus normal stress plot (Figure 7-1). The intercept on the shear strength axis is the cohesion (c) and the slope of the line is the angle of internal friction (ϕ).

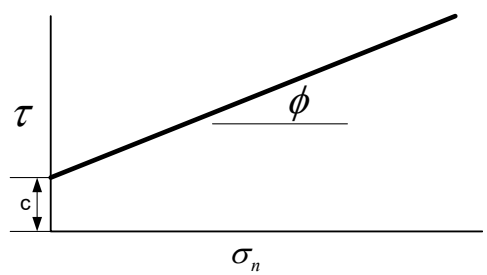

Figure 7-1 Graphical representation of Coulomb shear strength equation

The failure envelope is often determined from triaxial tests and the results are presented in terms of half-Mohr circles, as shown in Figure 7-2, hence the failure envelope is referred to as the Mohr-Coulomb failure envelope.

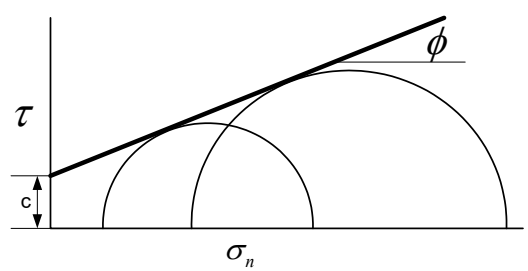

Figure 7-2 Mohr-Coulomb failure envelope

For undrained conditions when ϕ is zero, the failure envelope appears as shown in Figure 7-3. The soil strength then is simply described by c.

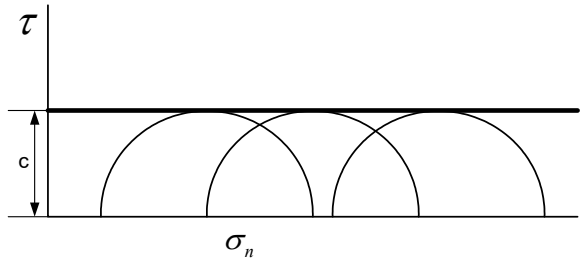

Figure 7-3 Undrained strength envelope

The strength parameters c and ϕ can be total strength parameters or effective strength parameters. SLOPE/W makes no distinction between these two sets of parameters. Which set is appropriate for a particular analysis is project-specific, and is something you as the software user, need to decide. The software cannot do this for you.

From a slope stability analysis point of view, effective strength parameters give the most realistic solution, particularly with respect to the position of the critical slip surface. The predicted critical slip surface position is the most realistic when you use effective strength parameters. When you use only undrained strengths in a slope stability analysis, the position of the slip surface with the lowest factor of safety is not necessarily close to the position of the actual slip surface if the slope should fail. This is particularly true for an assumed homogeneous section. This issue is discussed further in the Chapter on Slip Surface Shapes and Positions.

When you are doing a "Staged Rapid Drawdown" analysis or a "Staged Pseudo-Static" analysis using undrained strengths, you must use the Mohr-Coulomb strength model in SLOPE/W. In this case, c and ϕ are the effective strength parameters and you must enter the R-envelope strength values, c_R and ϕ_R, to represent the undrained strength of the soil. Setting the c_R and ϕ_R equal to zero signifies that the soil is a "free drained" material in a staged analysis.

Furthermore, if you have done a QUAKE/W dynamic analysis and when you want to use the QUAKE/W pore water pressure condition in your stability analysis, you may use the Mohr-Coulomb strength model to consider the reduced strength of the soil due to liquefaction. In this case, you may specify the "steady-state strength" of the soils due to liquefaction.

7.3 Spatial Mohr-Coulomb model

It is now possible to specify a spatial function for C, Phi, and unit weight as functions of both x and y geometry coordinates. Once a spatial function is defined, it can be applied to the Spatial Mohr-Coulomb model and then applied to any geometry region. The new Contour option in DEFINE can be used to view the actual applied values as they will be interpreted by the solver. An example of a spatial function for cohesion is shown in Figure 7-4.

The upper region has a constant cohesion applied, the middle region has a linear variation of cohesion as a function of x-coordinate, and the lower region has a previously defined spatial function for cohesion in terms of both x and y coordinate.

Once a function is defined and applied to a model and subsequently a soil region, it is possible to return to the Key In function command and change values while viewing a live update of the function on screen.

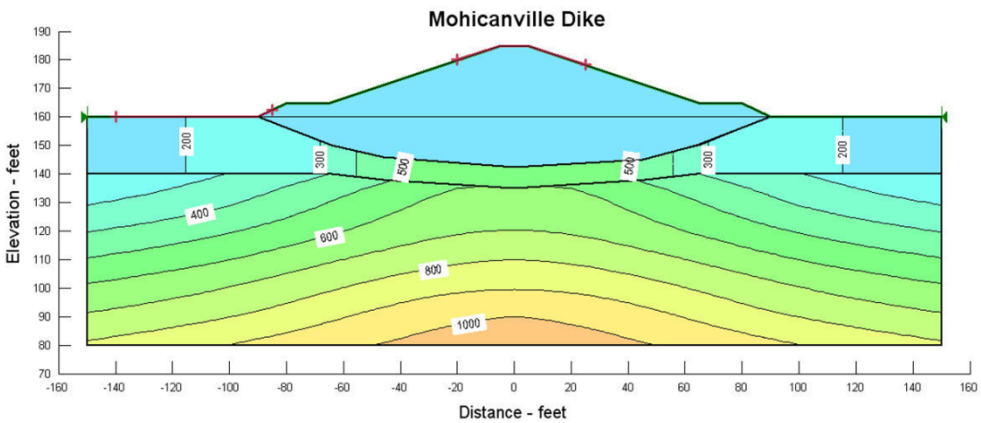

Figure 7-4 Example of spatial function assigned to bottom soil region material

7.4 Undrained strength

The Undrained strength option is a convenient way in SLOPE/W of setting ϕ to zero in the Mohr-Coulomb model (Figure 7-3). With this option, the shear strength of the material is only described by the *c* value and the pore-water pressure has no effect to the shear strength of the material.

7.5 High strength

A High strength material is an easy way to model materials with very high strength such as a concrete retaining wall. The strength is assumed to be infinity, therefore, any slip surfaces passing through the high strength material is considered very stable and consequently not consideied. You will be asked to specify the unit weight of the high strength material which will be used to compute the total overburden stress for the materials beneath the high strength material.

7.6 Impenetrable (Bedrock)

The Impenetrable strength option is really not a strength model, but a flag for the software to indicate that the slip surface cannot enter this material. It is an indirect mechanism for controlling the shape of trial slip surfaces. This soil model type is also sometimes referred to as bedrock. The Chapter on Slip Surface Shapes and Positions discusses this soil model option as to how it can be used to simulate certain field conditions.

7.7 Bilinear

Figure 7-5 shows the form of the Bilinear model. The failure envelope is described by two ϕ values, a cohesion value and a normal stress at which the break occurs.

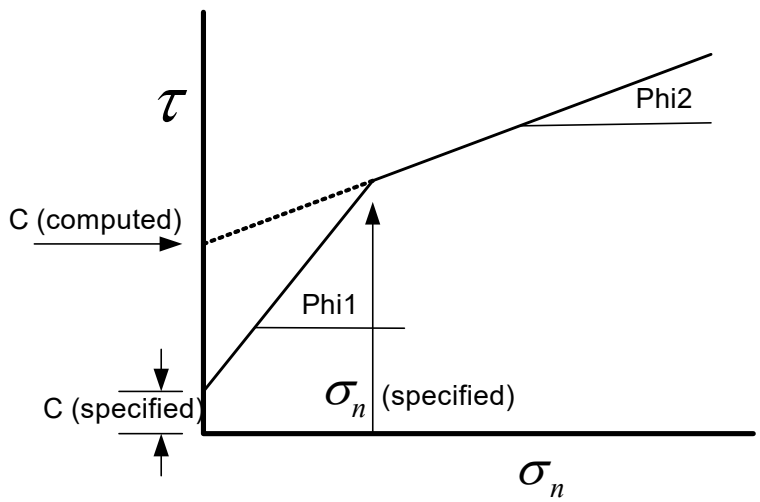

Figure 7-5 Bilinear shear strength envelope

For slice base normal stresses greater than the specified normal stress, SLOPE/W projects the Phi2 ($\phi 2$) line segment back to the shear strength axis and computes an equilivalent cohesion intercept. When you look at slice forces or plot strength along the slip surface you will see Phi2 ($\phi 2$) and the computed cohesion intercept. Internally, SLOPE/W treats the Bilinear model as two Mohr-Coulomb models.

The Bilinear strength model was the first attempt in SLOPE/W to accommodate a nonlinear strength envelope. Since then better options have been implemented for specifying nonlinear strength envelopes and the Bilinear model has lost some of its usefulness. The model is still included and available primarily for historic and backward compatibility reasons.

7.8 General data-point strength function

A completely general strength envelope can be defined using data points. A smooth spline curve is drawn through the specified points as shown in Figure 7-6.

For each slice, SLOPE/W first computes the normal stress at the slice base. Next SLOPE/W computes the slope of the spline curve at the slice base normal stress. The spline-curve slope (tangent) is taken to be ϕ for that particular slice. The tangent is projected to the origin axis to compute an intercept, which is taken to be c. Each slice consequently has a c and ϕ relative to the slice base normal stress.

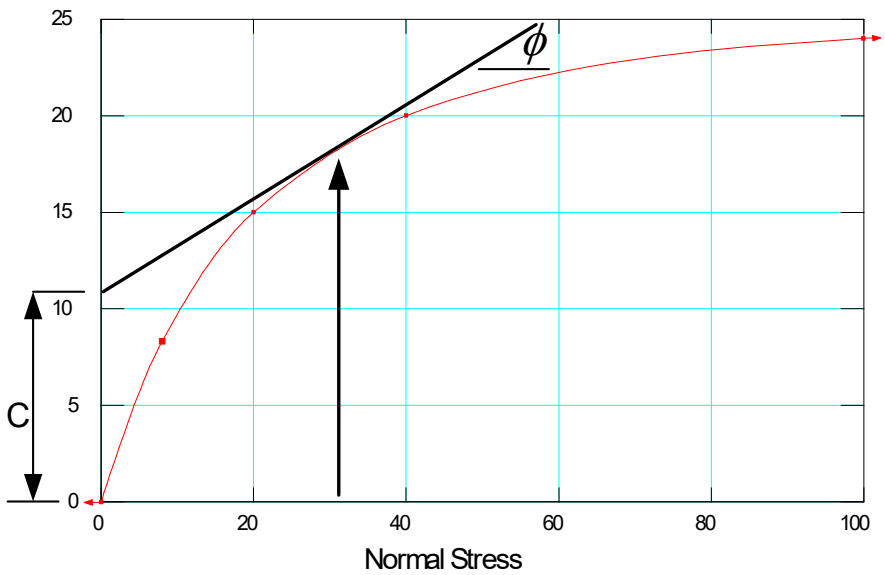

Figure 7-6 General data-point shear-normal function

The *c* value in this model should not be thought of as a true cohesive strength when the normal stress on the shear plane is zero. The *c* value in this case is simply an intercept on the shear strength axis. The intercept, together with the tangent, can be used to compute the shear strength at the base of the slice.

This data-point spline curve technique is a more recent development for dealing with curved strength envelopes and is consequently preferred over the Bilinear option.

Techniques for specifying the data and controlling the spline behavior are given in the online help.

The slope (tangent) at the end of the specified curve is used for normal stresses greater than the largest normal stress specified. The small arrow at the end of the curve is a graphical reminder of this behavior. Another point is that *c* is not allowed to drop below zero.

The normal stress defined in the function is the effective normal stress. It is computed by substracting the total normal stress by the pore water pressure at the slice base center.

With this option, an Add-in function can be developed to return any strength at the base of each slice. Some base slice informations (such as base lengthm base angle, normal stress, pore-water pressure) are also available for the development of Add-in function. Please refer to sections on Add-in Functions for implementation details.

7.9 Anisotropic strength

This strength model uses the following equation for dealing with anisotropy in the soil strength:

$$c = c_h \cos^2 \alpha + c_v \sin^2 \alpha$$

$$\phi = \phi_h \cos^2 \alpha + \phi_v \sin^2 \alpha$$

The subscripts stand for horizontal and vertical. The horizontal and vertical components are specified. Alpha (α) is the inclination of the slice base. In other words, you may enter the c and ϕ in both the

horizontal and vertical directions if they are different. This model provides a smooth transition of the c and ϕ based on the inclination angle of the slice base.

Say that the slice base inclination is 25 degrees, that c_h is 20, c_v is 30, ϕ_h.= 30° and ϕ_v.= 35°. The cohesion and friction angle for this slice then will be:

$$c = 20(\cos 25)^2 + 30(\sin 25)^2 = 21.8$$
$$\phi = 30(\cos 25)^2 + 35(\sin 25)^2 = 30.9^o$$

Each slice has a c and ϕ depending on the base inclination angle.

7.10 Strength using an anisotropic function

This is a general strength model for anisotropic soil. The variation of c and ϕ with respect to the base inclination angles is described by a general function. The input c and ϕ values are multiplied with the modifier factor obtained from the anisotropic function before use in the shear strength computation

Figure 7-7 shows a typical anisotropic function in which a modifier factor is defined as a function of the inclination angle of the slice base. Let us say the modifier function in Figure 7-7 has been applied to a particular specified undrained strength (c). When the slice base inclination is, for example, 20 degrees, c will be multiplied by 1.08, and if the inclination is -20 degrees, c will be multiplied by 1.1. The maximum modifying factor is 1.3 when the inclination angle is about 45 degrees. When the slice base is horizontal (zero degrees) the modifier factor is 1.0; in other words, the strength remains the same value as was specified.

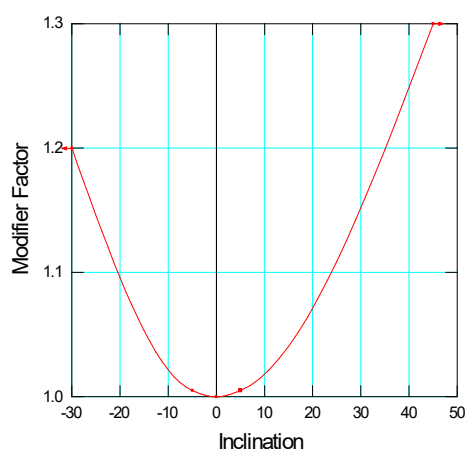

Figure 7-7 Typical anisotropic modifier function

The modifier function can be applied to any c or ϕ specified for a soil.

You can have as many functions as deemed necessary, and/or you can apply the same function to various strength parameters.

The first step in defining the modifier is to decide what strength parameter is known and at what inclination. The modifier factor at the known strength and known inclination is 1.0. The remainder of the function can then be specified relative to this known point.

Figure 7-8 shows the sign convention of the inclination angle used in SLOPE/W. Inclination angles measured from the positive x-axis are positive and negative when measured from the negative x-axis.

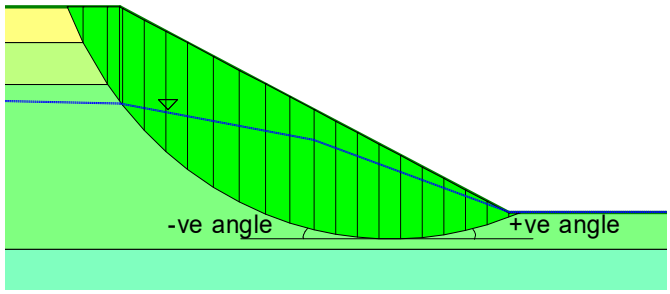

Figure 7-8 Sign convention of inclination angle used in SLOPE/W

7.11 Strength as a function of depth

Soft normally or slightly over-consolidated soil usually exhibits an increase in undrained strength with depth. SLOPE/W has two options for describing this type of strength profile. One is referenced to the top of the soil layer and the other is referenced to a specified datum. The two variations are illustrated below.

Relative to top of soil layer

With this option, it is necessary to specify the undrained strength (*c*) at the top of the layer and to specify the rate of increase with depth; that is, kPa per meter or psf per foot. In addition, a maximum cohesion can be specified. Figure 7-9 illustrates how this soil model could be used.

The top of the soil layer does not need to be a straight line. SLOPE/W finds the top of layer line for each slice.

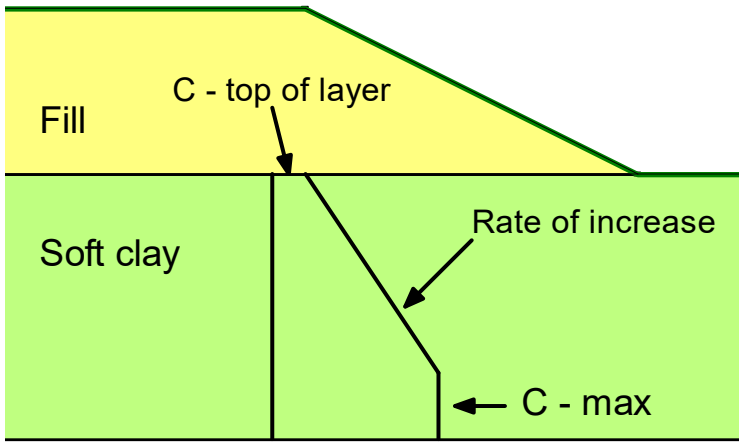

Figure 7-9 Shear strength as function of depth below top of layer

Relative to specified datum

A variation of specifying strength as function of depth is to define the strength parameters relative to a specified datum. This option is illustrated in Figure 7-10.

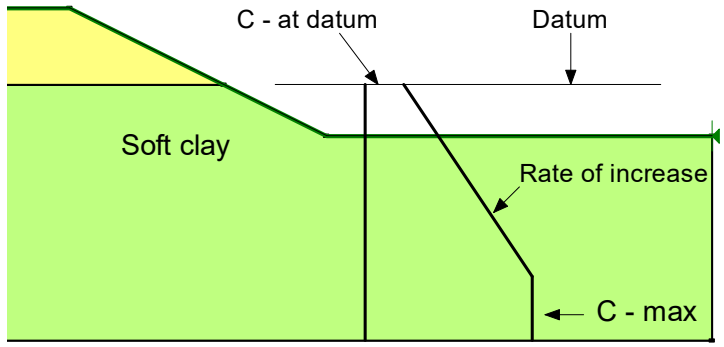

Figure 7-10 Shear strength as a function of depth below a datum

7.12 Frictional-undrained combined models

The frictional-undrained shear strength model was developed and is used in the Scandinavian countries where they have a lot of relatively soft marine clays. The clay is in essence treated as a c-ϕ soil, but with a maximum undrained strength as illustrated in Figure 7-11. The model has evolved from strength testing observations.

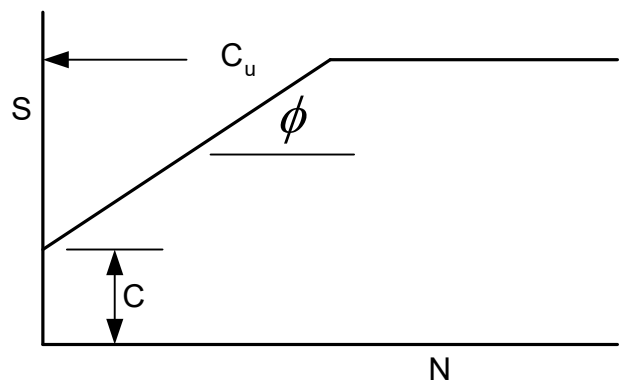

Figure 7-11 Combined frictional-undrained strength model

In addition, the cohesive components of the strength can vary with depth or relative to a specified datum. Either c or c_u can be specified at the top of a layer or at a certain datum together with a rate of increase with depth (kPa/m for example). The concept is similar to that in Figure 7-9 and Figure 7-10.

The c and c_u parameters can also be correlated by specifying a ratio. In SLOPE/W, c is computed from the c/c_u ratio if the ratio is non-zero. If the ratio is zero (undefined), the specified values for c and $c_{rate\ increase}$ are used.

The use of this combined frictional-undrained model is recommended only if you are intimately familiar with the background related to this model.

7.13 SHANSEP: Strength as a function of overburden stess

The SHANSEP (Stress History and Normalized Soil Engineering Properties; Ladd and Foott, 1974; Ladd, 1991) model varies the undrained shear strength with vertical effective stress. There are three options in SLOPE/W for parameterizing the model:

1. specify a ratio $S = s_u/\sigma_v^{'}$, where s_u is undrained strength and $\sigma_v^{'}$ vertical effective stress;
2. specify a functional relationship between undrained shear strength and vertical effective stress using a generalized spline function or an an add-in, and
3. By defining the paramaters of the closed-form equation:

$$s_u = \sigma_v^{'}(S_{NC})OCR^m$$

where OCR overconsolidation ratio, m an exponent controlling non-linearity, and S_{NC} the ratio of undrained strength to veritical effective stress for the normally compressed state. The overconsolidation ratio can vary with y-coordinate, which causes the ratio $s_u/\sigma_v^{'}$ to vary nonlinearly with depth if $m < 1$.

Consider the case of placing an embankment on soft ground as illustrated in Figure 7-12. The first 2m below the ground is a desiccated layer and the water table is at the contact between the desiccated layer and the underlying soft soil. The weight of the sand fill will increase the total overburden stress as well as the pore water pressure in the soft clay layer. Since the **effective** overburden stress is required in the SHANSEP model, special care is required to make sure that the pore-water pressure in the soft clay layer is modeled correctly.

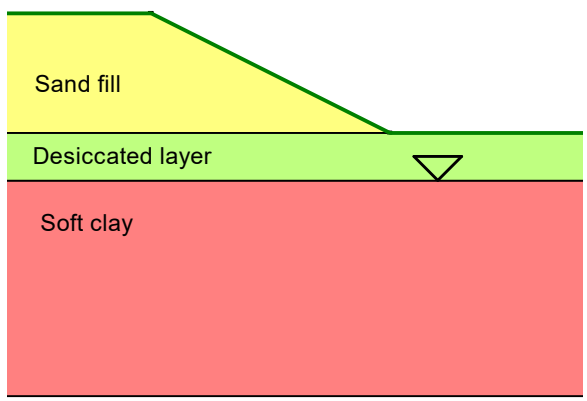

Figure 7-12 Case with SHANSEP model applied to soft clay

To get the correct pore water pressure and consequently the effective stress in the soft clay, it is necessary to do the following:

- The "piezomeric line with B-bar" pore water pressure should be chosen.
- The soft clay is assigned a B-bar value of 1.0.
- A piezometric line which represents the water table is assigned only to the soft clay.
- The sand fill is flagged as the material that the "weight will be added" in the B-bar pore water pressure calculation of the soft clay layer.
- The desiccated layer does not have a B-bar and does not have an assigned piezometric line.

B-bar is defined as:

$$\bar{B} = \frac{u}{\sigma_v}$$

When B-bar is 1.0, all the weight of the sand fill will increase the pore-water pressure in the soft clay layer. In other words, the additional vertical stress from the sand fill is added to the initial pore-water pressure represented by the specified piezometric line.

If all of the fill weight goes to increasing the pore-water pressure, then the vertical effective stress in the soft clay is not affected by the sand fill. This is the objective in the SHANSEP model so that the undrained shear strength is the same before and after the fill placement.

The pore-water pressures used in the stability calculations should be thoroughly checked and verified by plotting the pore pressure along the slip surface to make sure that appropriate shear strength is being used.

In some cases, the SHANSEP strength definition can be modeled with a "Strength as a function of depth" soil model as discussed in a previous section. It is perhaps easier to use and understand than the SHANSEP model. You can estimate the undrained strengths at the surface and at the bottom of the soft clay layer based on its effective overburden stress. You can then estimate the rate of increase of the undrained strength. When specified correctly, the two models should give the same solution.

Surcharge loads as well as surface load due to ponded water on the ground surface are used in the computation of the vertical stress and therefore are considered in the SHANSEP formulation. However, individual point loads are not considered, so how you model additional loads to the ground surface will determine whether they add to the vertical stress or not.

7.14 Hoek and Brown model

The Hoek and Brown model is a nonlinear shear strength model for rock. This model has evolved in stages over a couple of decades. The most recent version is known as the Generalized Hoek-Brown Criterion or the Hoek-Brown Failure Criterion-2002 Edition (Hoek, Carranza-Torres and Corkum, 2002).

Four input parameters are required to compute the shear strength versus normal stress curve. The four parameters are:

σ_{ci} = the uniaxial compressive strength of the intact rock

m_i = a property of the intact rock

GSI = Geological Strength Index (0-100)

D = rock mass disturbance factor (0-1)

The D, GSI and m_i properties are used to compute m_b as follows:

$$m_b = m_i \exp\frac{(GSI - 100)}{(28 - 14D)}$$

Two curve parameters a and s are computed from:

$$a = \frac{1}{2} + \frac{1}{6}\left(e^{-GSI/15} - e^{-20/3}\right)$$

$$s = \exp\left(\frac{GSI - 100}{9 - 3D}\right)$$

For intact rock GSI is 100 and so s is 1.0. In an earlier form of the failure criterion, the coefficient a was assumed to be a constant value of 0.5. It is now considered to be a variable dependent on GSI.

The relationship between the principal stresses at failure is:

$$\sigma_1 = \sigma_3 + \sigma_{ci}\left(m_b \frac{\sigma_3}{\sigma_{ci}} + s\right)^a$$

To establish the strength curve, SLOPE/W computes σ_1 for a range of σ_3 values.

The σ_3 default values range from the a negative value representing the rock tensile strength up to a value equal to half the uniaxial compressive strength where the tensile strength is computed as:

$$\sigma_t = -s\frac{\sigma_{ci}}{m_b}$$

Once the σ_1 - σ_3 pairs at failure are known, a series of τ - σ_n data points are computed as follows:

$$\sigma_{ratio} = \frac{\sigma_1}{\sigma_3} = 1 + a\, m_b\left(m_b \frac{\sigma_3}{\sigma_{ci}} + s\right)^{a-1}$$

$$\sigma_n = \left(\frac{\sigma_1 + \sigma_3}{2}\right) - \left(\frac{\sigma_1 - \sigma_3}{2}\right) \times \left(\frac{\sigma_{ratio} - 1}{\sigma_{ratio} + 1}\right)$$

$$\tau = (\sigma_1 - \sigma_3)\frac{\sqrt{\sigma_{ratio}}}{\sigma_{ratio} + 1}$$

From these data points, SLOPE/W computes a spline curve the same for the General Data Point function discussed above.

Figure 7-13 shows an example strength function when:

σ_{ci} = 20,000 kPa (20 MPa)

m_i = 10

GSI = 45

D = 1.0

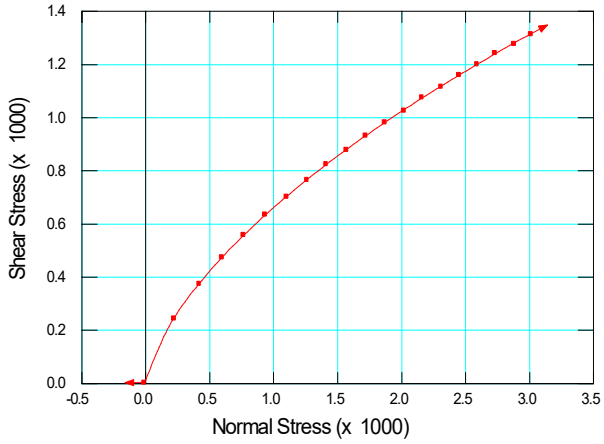

Figure 7-13 Strength function based on generalized Hoek – Brown strength criterion

SLOPE/W computes the normal stress at the base of each slice and the finds the slope of the splined curve, which is taken as the friction angle ϕ. A tangent line to the curve is projected to the τ axis and the intersection point on the τ axis is assumed to be equal to the cohesion. Each slice base consequently will have separate $c - \phi$ parameters depending on the slice base normal.

The following three tables provide some guidelines for selecting and specifying uniaxial compressive strengths, m_i constants and GSI values.

The following tables come from Evert Hoek's course notes entitled Practical Rock Engineering (2000 ed., Chapter 11), and reproduced here simply for convenience reference.

The D parameter is an indication of the amount of disturbance the rock may have undergone during excavation or blasting. A D value of zero means the rock has undergone very little disturbance, while a D value of 1.0 represents a condition where the rock has undergone significant disturbance due to heavy production blasting that may exist in situations such as an open pit mine (Hoek et al, 2002)

Table 7-1 Field estimates of uniaxial compressive strength (After Hoek, 2000)

Grade*	Term	Uniaxial Comp. Strength (MPa)	Point Load Index (MPa)	Field estimate of strength	Examples
R6	Extremely Strong	> 250	>10	Specimen can only be chipped with a geological hammer	Fresh basalt, chert, diabase, gneiss, granite, quartzite
R5	Very strong	100 - 250	4 - 10	Specimen requires many blows of a geological hammer to fracture it	Amphibolite, sandstone, basalt, gabbro, gneiss, granodiorite, limestone, marble, rhyolite, tuff
R4	Strong	50 - 100	2 - 4	Specimen requires more than one blow of a geological hammer to fracture it	Limestone, marble, phyllite, sandstone, schist, shale
R3	Medium strong	25 - 50	1 - 2	Cannot be scraped or peeled with a pocket knife, specimen can be fractured with a single blow from a geological hammer	Claystone, coal, concrete, schist, shale, siltstone
R2	Weak	5 - 25	**	Can be peeled with a pocket knife with difficulty, shallow indentation made by firm blow with point of a geological hammer	Chalk, rocksalt, potash
R1	Very weak	1 - 5	**	Crumbles under firm blows with point of a geological hammer, can be peeled by a pocket knife	Highly weathered or altered rock
R0	Extremely weak	0.25 - 1	**	Indented by thumbnail	Stiff fault gouge

* Grade according to Brown (1981).
** Point load tests on rocks with a uniaxial compressive strength below 25 MPa are likely to yield highly ambiguous results.

Table 7-2 Values of constant m_i for intact rock by rock group; values in parentheses are estimates (after Hoek, 2000)

Rock type	Class	Group	Texture			
			Coarse	Medium	Fine	Very fine
SEDIMENTARY	Clastic		Conglomerate (22)	Sandstone 19	Siltstone 9	Claystone 4
				Greywacke (18)		
	Non-Clastic	Organic		Chalk 7		
				Coal (8-21)		
		Carbonate	Breccia (20)	Sparitic Limestone (10)	Micritic Limestone 8	
		Chemical		Gypstone 16	Anhydrite 13	
METAMORPHIC	Non Foliated		Marble 9	Hornfels (19)	Quartzite 24	
	Slightly foliated		Migmatite (30)	Amphibolite 25 - 31	Mylonites (6)	
	Foliated*		Gneiss 33	Schists 4 - 8	Phyllites (10)	Slate 9
IGNEOUS	Light		Granite 33		Rhyolite (16)	Obsidian (19)
			Granodiorite (30)		Dacite (17)	
	Dark		Diorite (28)		Andesite 19	
			Gabbro 27	Dolerite (19)	Basalt (17)	
			Norite 22			
	Extrusive pyroclastic type		Agglomerate (20)	Breccia (18)	Tuff (15)	

* These values are for intact rock specimens tested normal to bedding or foliation. The value of m_i will be significantly different if failure occurs along a weakness plane.

Table 7-3 Estimates of Geological Strength Index (GSI) based on geological description (after Hoek, 2000)

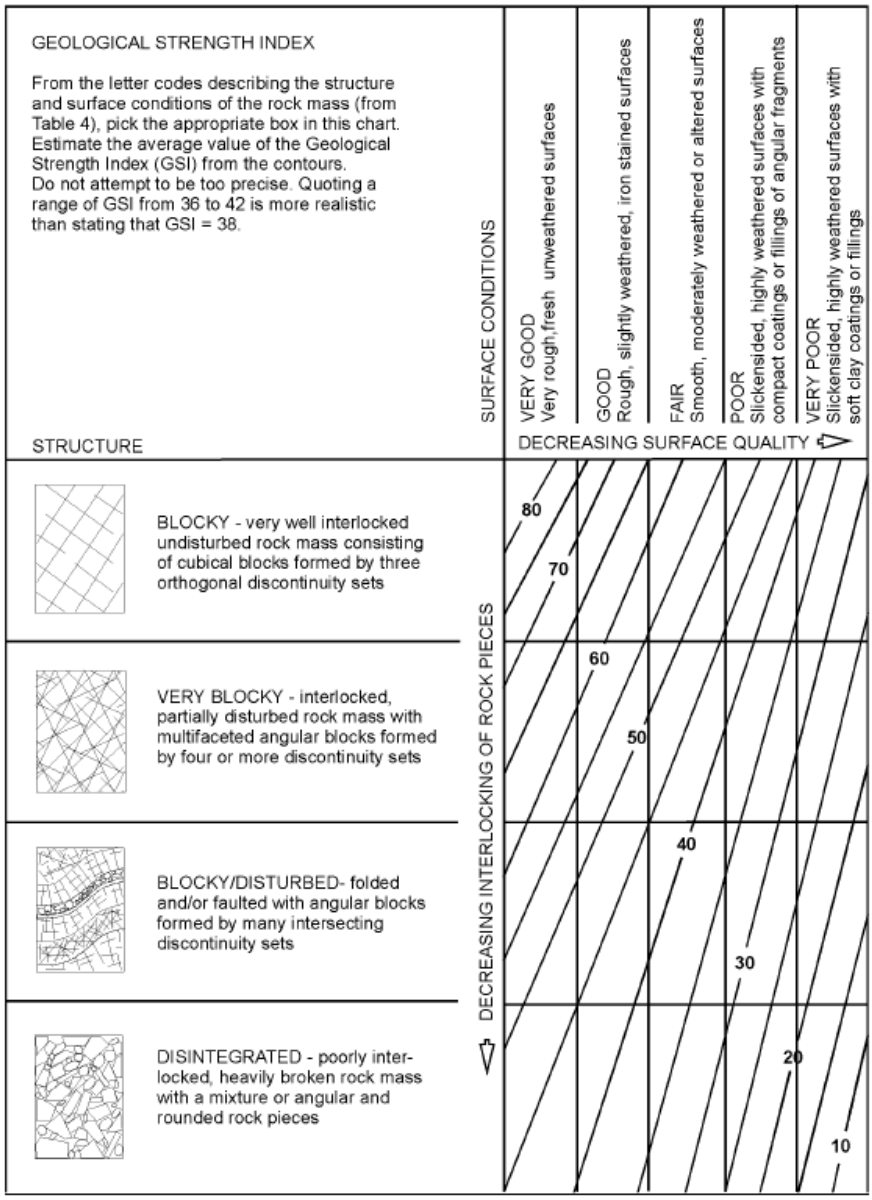

7.15 Unsaturated shear strength

Soil suction or negative water pressures have the effect of adding strength to a soil. In the same way that positive pore-water pressures decrease the effective stress and thereby decrease the strength, negative pore-water pressures increase the effective stress and in turn increase the strength.

The shear strength of unsaturated soil is:

$$s = c' + \sigma_n \tan\phi' + \left(u_a - u_w\right)\tan\phi^b$$

where:

u_a	=	the pore-air pressure,
u_w	=	the pore-water pressure, and
ϕ^b	=	an angle defining the increase in strength due to the negative pore-water pressure.

The term ($u_a - u_w$) is called suction when presented as a positive number. The angle ϕ^b is a material property. For practical purposes, ϕ^b can be taken to be about ½ ϕ'.

In SLOPE/W, ϕ^b is treated as a constant value, but in actual fact this parameter varies with the degree of saturation. In the capillary zone where the soil is saturated, but the pore-water pressure is under tension, ϕ^b is equal to the friction angle ϕ'. As the soil desaturates, ϕ^b decreases. The decrease in ϕ^b is a reflection of the fact that the negative pore-water pressure acts over a smaller area. More specifically, ϕ^b is related to the soil water characteristic curve which is also known as the volumetric water content function as discussed at length in the SEEP/W documentation.

Considerable research has been done to better quantify the unsaturated shear strength of a soil using the soil-water characteristic curve and the effective shear strength parameters (c' and ϕ'). As a better alternative to the use of ϕ^b to model the increase of shear strength due to soil suction, the following estimation equation proposed by Vanapalli et. al. (1996) is implemented in SLOPE/W:

$$s = c' + (\sigma_n - u_a)\tan\phi' + (u_a - u_w)\left[\left(\frac{\theta_w - \theta_r}{\theta_s - \theta_r}\right)\tan\phi'\right]$$

In the above equation, θ_w is the volumetric water content, θ_s is the saturated volumetric water content and θ_r is the residual volumetric water content. With SLOPE, you can specify a volumetric water content function to be used in the suction strength computation based on the above equation. Furthermore, you can also specify a residual volumetric water content at which the suction strength becomes zero (Θ_r) to be used in the unsaturated shear strength computation. Please refer to the unsaturated strength discussion section in the Theory Chapter for more details.

SLOPE/W offers two ways to model the increase of shear strength due to soil suction: 1 – use of a constant ϕ^b parameter, 2 – use of a volumetric water content function.

When you plot shear strength along the slip surface, you will notice the selection of three strength components: cohesive, frictional and suction. This type of plots should always be created when it is your intention to include the suction strength component in an analysis. From the plots, it is important to verify that specified unsaturated strength parameter has been used properly and to gain an appreciation as to how significant the suction strength is relative to the cohesive and frictional strength.

7.16 Soil unit weight

The sliding mass weight or gravitational force is applied by assigning the soil a unit weight. The slice cross sectional area times the specified unit weight determines the weight of the slice.

As discussed in the Limit Equilibrium Fundamentals Chapter, SLOPE/W is formulated on the basis of total forces. The unit weight consequently needs to be specified as the **total** unit weight.

SLOPE/W allows for a separate unit weight above the water table, but use of this parameter is seldom necessary.

The soil unit weight is:

$$\gamma = \gamma_w \frac{G + Se}{1 + e}$$

where:

γ_w	=	the unit weight of water,
G	=	specific gravity,
S	=	the degree of saturation, and
e	=	the void ratio.

For illustration purposes, assume that G = 2.7, γ_w = 10 kN/m^3, and e = 0.7. Below the water table where the soil is saturated (S = 1) and the unit weight is 20.0 kN/m^3. Above the water table where the soil is unsaturated, assume the degree of saturation is 80%, (i.e., S = 0.8) the unit weight of water would be19.2 kN/m^3, about a 4% difference.

From a stability analysis point of view, the 4% difference in the unit weight is insignificant. First of all there is the capillary zone where *S* is 100% and the unit weight therefore is the same above and below the water table in the capillary zone. Secondly, factor of safety calculations are not very sensitive to the unit weight. If the slice weight increases, the gravitational driving force increases, but the shear resistance also increases because of a higher normal at the slice base, and vise versa. Therefore, defining different unit weights above and below the water table usually has little effect on the resulting factor of safety.

The unit weight above the water table should certainly not be specified as the dry unit weight. In the field, the soil is seldom completely dry except for perhaps a relatively thin layer near the ground surface.

A situation where the difference in unit weight above and below the water table may be significant is when very coarse rock fill is placed in water to create a water break as illustrated in Figure 7-14.

For this type of situation, assume that *e* is 1.0, *G* is 2.7 and γ_w is 10 kN/m^3. Below the water line where *S* is 1.0 the unit weight is 18.5 kN/m^3. Above the water line where *S* is zero, the unit weight is 13.5 kN/m^3. This is a significant difference and consequently worth the effort to specify two different unit weights.

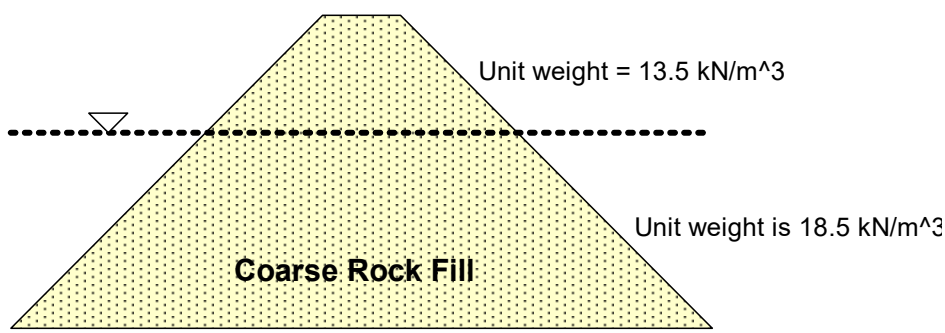

Figure 7-14 Different unit weight above and below the water in rock fill

In the end it is really up to the analyst whether a separate unit weight is specified for the soil above the water table. The option is available in SLOPE/W as an advanced parameter.

Like Cohesion and Phi, unit weight of the material can be model as a"Constant", a "Linear Function" or a "Spatial Function" using the Spatial Mohr-Coulomb strength model.

7.17 Other soil parameters

There are other soil property parameters, but they will be discussed in the context of their specific application. For example, all the material parameter variability or dispersion are discussed and explained in the Chapter on Probabilistic Analyses. In addition, the residual strength parameters are discussed in connection with Seismic and Dynamic Stability Analyses.

8 Pore-water

8.1 Introduction

In the previous chapter, it was noted that the most realistic position of the critical slip surface is obtained when effective strength parameters are used in the analysis. Effective strength parameters, however, are only meaningful when they are used in conjunction with pore-water pressures. In this sense, the pore-water pressures are as important in establishing the correct shear strength as the shear strength parameters themselves.

Due to the importance of pore-water pressures in a stability analysis, SLOPE/W has various ways of specifying the pore-water pressure conditions. This chapter gives an overview of the options available, and presents some comments on the applicability of the various methods.

8.2 Piezometric surfaces

The most common way of defining pore-water pressure conditions is with a piezometric line. With this option, SLOPE/W simply computes the vertical distance from the slice base mid-point up to the piezometric line, and multiplies this distance times the unit weight of water to get the pore-water pressure at the slice base. This is graphically illustrated in Figure 8-1.

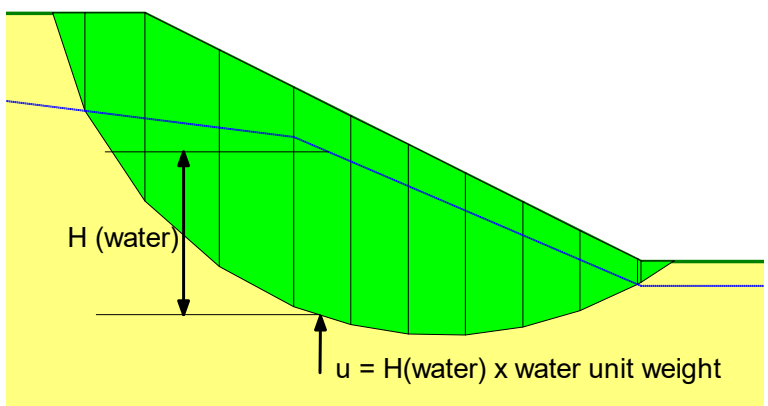

Figure 8-1 Pore pressure from a piezometric line

When thinking about pore-water pressures in SLOPE/W, it is vitally important to recognize that pore-water pressures only come into play in the calculation of the shear strength at the base of each slice – they do not enter into the interslice force calculations.

When the slice base mid-point is located above the piezometric line, the negative pore-water pressures are presented in SLOPE/W RESULT, but additional strength due to the matric suction is assumed to be zero unless ϕ^b (Phi B) or a volumetric water content function is also assigned to the material strength model. This is explained further in this chapter under the topic of negative pore-water pressures.

Single piezometric line

Usually a profile has only one piezometric line and it applies to all soils. However, sometimes more complex pore-water pressures exist and in SLOPE/W, it is possible to be more selective and precise, if necessary. For example, a piezometric line can be applied only to selected soil layers and not to the entire

profile. Consider the case of a sand embankment on soft clay soil as shown in Figure 8-2. Assume we want to make the pore-water pressures equal to zero in the sand, but we want to represent the pore-water pressure in the clay by a piezometric line that exists above the clay surface due to some excess pressure in the clay. A piezometric line can be drawn and assigned only to the clay layer. As a result, pore-water pressures will not exist in the sand layer. This option is useful when it is combined with a Ru or B-bar value.

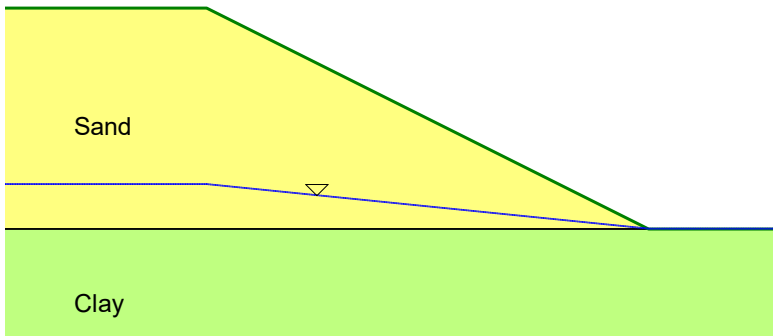

Figure 8-2 Piezometric assigned only to the clay

Multiple piezometric lines

In SLOPE/W, each soil type can have its own piezometric line making it possible to represent irregular non-hydrostatic pore-water pressure conditions. In practice this option is not all that applicable. Highly irregular pore-water pressure conditions are better specified by one of the other more advanced methods discussed below.

Phreatic correction

In a sloping profile, the flow of water is usually from the uplands towards the slope toe which results in the piezometric surface curving downwards. As we know from flow net design, under these conditions the equipotential lines are not vertical. The assumption in SLOPE/W of relating the pore-water pressure to the vertical distance from slice base to the piezometric line is consequently not strictly correct. A correction factor can be applied to more accurately represent the pore-water pressure, if this is deemed important.

Figure 8-3 illustrates how phreatic correction is applied. The equipotential lines are perpendicular to the piezometric line. The inclination of the phreatic surface is at an angle A. Without phreatic correction, H_w is the height used to compute the pore pressure at the base center of the slice. With phreatic correction, H_w is corrected and H_c is used to compute the pore pressure at the base center of the slice.

$$H_c = H_w \cos^2 A$$

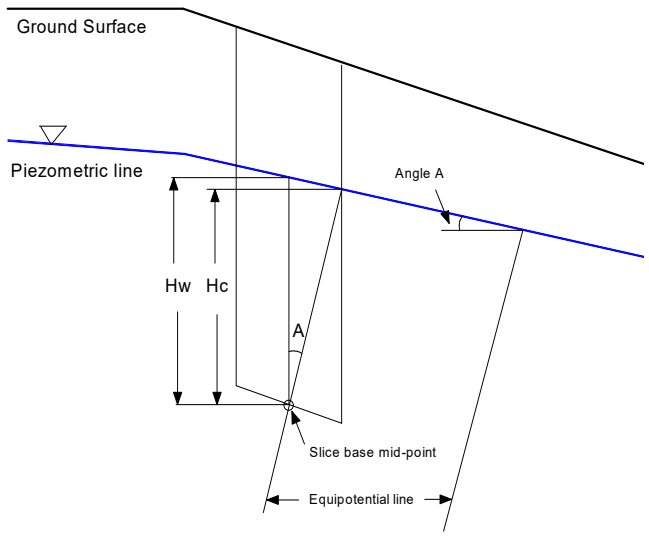

Figure 8-3 Phreatic surface correction

Note that when the piezometric line is horizontal (A=0), the phreatic correction factor (cos^2A) is 1 and H_c is equal to H_w. When the piezometric line is approaching a vertical line, the correction factor is approaching 0. Since the correction factor is always between 0 and 1, applying the phreatic correction always generates a pore water pressure smaller or equal to a non-corrected condition. In other words, the computed factor of safety is always the same or higher when the phreatic correction is applied.

8.3 R_u Coefficients

The pore-water pressure ratio R_u is a coefficient that relates the pore-water pressure to the vertical overburden stress. The coefficient is defined as:

$$R_u = \frac{u}{\gamma_t H_s}$$

where:

u = the pore-water pressure

γ_t = the total unit weight

H_s = the height of the soil column.

The denominator of the R_u equation includes external loads (Budhu, 2007). Accordingly, SLOPE/W includes the effect of ponded water or surcharge loads in the calculation of pore-water pressure at the base of a slice. By rearranging the variables, the pore-water pressure u becomes:

$$u = R_u \, \gamma_t H_s$$

The concept of R_u was developed primarily for use with stability charts (Bishop and Morgenstern, 1960) and is included in SLOPE/W mainly for historical reasons. Attempting to make use of the option is not recommended, except in simple cases that are consistent with the original intention of the method.

One of the difficulties with the R_u approach is that the coefficient varies throughout a slope if the phreatic surface is not parallel to the ground surface. It is therefore necessary to establish R_u at a number of points within the domain for this scenario. In a multi-layered stratigraphic section, R_u can be applied selectively to each of the soil units. Moreover, R_u is not intended to model the generation of excess pore-water pressures due to loading.

Pore-water pressures based on R_u calculations can be added to conditions represented by a piezometric line. This action is different than B-bar (discussed below) because R_u uses the the total overburden stress; B-bar uses only soil layers flagged as adding to the pore-water pressure.

Consider slice 10 shown in Figure 8-4. The piezometric line is located at the clay-sand contact and the clay has been assigned a R_u value of 0.2. The unit weight for both the sand and clay is 20 kN/m^3. The vertical distance from the ground surface to the bottom of sand layer is 7.22m. The vertical distance from the slice base center to the piezometric line is 2.14m. The R_u component of the water pressure is (7.22m + 2.14m) x 20.0 kN/m^3 x 0.2 = 37.44 kPa. The pore pressure from the piezometric line is 2.14m x 9.81 kN/m^3 = 20.99 kPa. Therefore, the total pore-water pressure at the base center when R_u is used together with the piezometric line is 58.43 kPa.

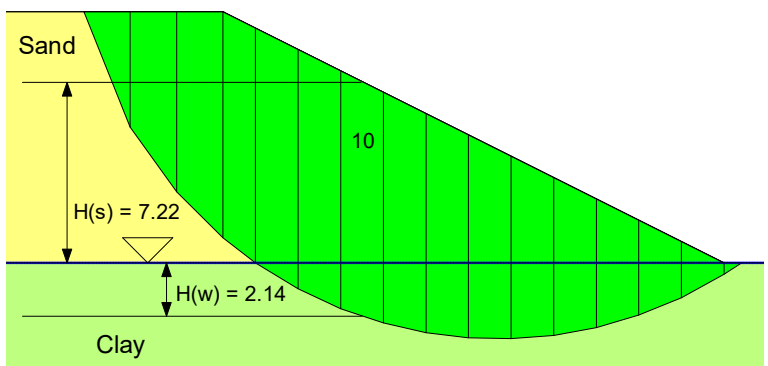

Figure 8-4 Combination of R_u/B-bar with piezometric pore-water pressures

Combining R_u computed pore-water pressures with piezometric pore-water pressures can be confusing and is incongruous with the original intention of the method. It is therefore highly recommended that the pore-water pressure distribution along the slip surface be verified using a graph.

8.4 B-bar coefficients

B-bar ($\overline{B}$) is a pore-water pressure coefficient related to the major principal stress. In equation form:

$$\overline{B} = \frac{\Delta u}{\Delta \sigma_1}$$

In many situations, the major principal stress is near vertical and, consequently, σ_1 can be approximated from the overburden stress. This approximation is used in the B-bar application in SLOPE/W.

The distinguishing feature about B-bar in SLOPE/W is that individual soil layers can be selected for computing the overburden stress. Consider the same case as shown in the previous section, but now instead of a R_u value, the clay is assigned a B-bar value of 0.2 (Figure 8-4). Only the sand has been flagged as adding to the pore-water pressure. The pore-water pressure from the sand weight is 7.22m x 20.0 kN/m^3 x 0.2 = 28.88 kPa. The pore-water pressure from the piezometric line is 2.14m x 9.81 kN/m^3

= 20.99 kPa. The total pore-water pressure at the base center when B-bar is used together with the piezometric line is 49.87 kPa.

Please note that in this case only the sand weight is added to the pore-water pressure calculations, but the B-bar is assigned to the clay layer.

Note that Ru and B-bar are only used in the computation of pore water pressure at the base center of each slice along the slip surface. Ru and B-bar do not contribute to the pore water pressure condition on the ground surface.

8.5 Pore-water pressures head with spatial function

A powerful and highly flexible option in SLOPE/W for defining pore-water pressure conditions is to specify the actual pressure at any discrete points. Figure 8-5 shows an example with pore-water pressure head specified using a spatial function as described in the chapter on Functions in GeoStudio.

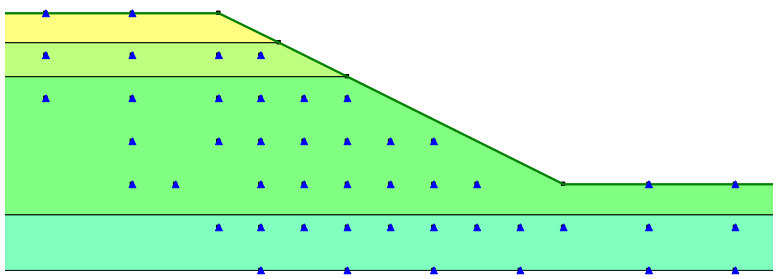

Figure 8-5 Grid of pore water pressure head

Using krigging techniques (see Theory Chapter for details), SLOPE/W constructs a smooth surface that passes through all the specified points. Once the surface has been constructed, the pore-water pressure can be determined at any other x-y coordinate point in the vicinity of the specified data points. For each slice, SLOPE/W knows the x-y coordinates at the slice base mid-point. These x-y coordinates together with the pore-water pressure surface are then used to establish the pore-water pressure at the base of each slice.

The pressure head with spatial function is useful when the pore-water pressures are fairly irregular or non-hydrostatic. Spatial function is also useful for directly including field piezometric measurements in an analysis.

When using the pressure head with spatial function option in SLOPE/W, it is necessary to give careful thought to all the locations the pore-water pressure is known. Say you have an unsaturated zone and you do not wish to consider the suction. Some data points would then be required in the unsaturated zone where the pressure head is zero. If there is ponded water, a pressure head equal to the depth of the water would need to be specified along the water-soil contact line. On a seepage face where the pore-water pressure is zero, the pressure head would need to be specified as zero. In summary, the pore-water pressure needs to be specified at all locations where the pore-water pressure condition is known with certainty.

The number of data points does not need to be excessively large. The data points can be fairly sparsely spaced except in areas where there are sudden large changes in the pore-water pressures. Also, remember pore-water pressures come into play only along the slip surfaces, and so the data points need to be concentrated in the zone of potential slip surfaces.

You can use the Contouring feature in DEFINE to now view the applied grid of pressures prior to solving the analysis. You no longer need to view pore-pressure data along the base of the slices as the only means of checking the input grid of pressures.

Note that when positive pressure is computed on the ground surface, ponding is assumed and the weight of the pond will be added automatically to the slice. SLOPE/W gives a graphical presentation of the pond when that happens.

8.6 Negative pore-water pressures

SLOPE/W can accommodate negative pore-water pressures just as well as positive pressures. Soil suction (negative pore-water pressure) has the effect of increasing the soil strength,as previously discussed. The additional suction related strength is included if the ϕ^b parameter is specified.

When a piezometric line is used to define pore-water pressures, SLOPE/W computes the negative pressure in the same way as the positive pressures. Where the slice base is above the piezometric line, the vertical distance between the slice base center and the piezometric line is a negative value (y-coordinate of piezometric line minus y-coordinate of slice base center). The pore-water pressure is consequently negative.

If you do not want the suction value (negative pore-water pressure) to extend indefinitely above the piezometric line, SLOPE/W gives you the ability to cap the maximum suction value of a piezometric line.

8.7 Finite element computed pressures

SLOPE/W is fully integrated with the finite element products available in GeoStudio. This makes it possible to use finite element computed pore-water pressures in a stability analysis. For example, the pore-water pressures can come from a:

- SEEP/W steady-state seepage analysis
- SEEP/W transient analysis at any particular time step
- SIGMA/W analysis where there are excess pore-water pressures due to some kind of loading
- SIGMA/W transient consolidation analysis
- QUAKE/W dynamic earthquake analysis at any time during the shaking or at the end of shaking
- VADOSE/W ground surface evaporative flux analysis.

In general, the pore-water pressures can come from any finite element analysis that creates a head or pore-water pressure file. For all the nodes on the ground surface line, when the pore water pressure is positive (i.e., surface ponding condition), SLOPE/W automatically computes the equivalent weight of the water above the ground surface.

To use the finite element computed pore-water pressures, SLOPE/W first finds the element that encompasses the slice base center. Next, the local element coordinates (r,s) are determined at the slice base. The pore-water pressures are known at the element nodes either directly from the finite element results or by mapping the Gauss point values to the nodes. The nodal pore-water pressures and local r-s coordinates together with the inherent finite element interpolating functions are then used to compute the pore-water pressure at the slice base center. The power of this approach is that the pore-water pressures can have any irregular distribution and represent conditions at various times.

An example of using irregular finite element computed pore-water pressures in SLOPE/W is presented in Figure 8-6 and Figure 8-7 . A less permeable layer mid-height in the slope has caused a perched water table to form due to the infiltration. This type of pore-water pressure distribution can be modeled in SEEP/W and then integrated with SLOPE/W.

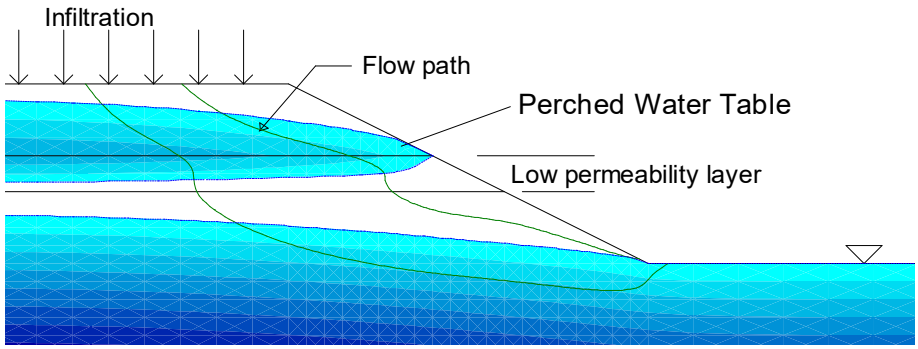

Figure 8-6 SEEP/W computed pore-water pressures

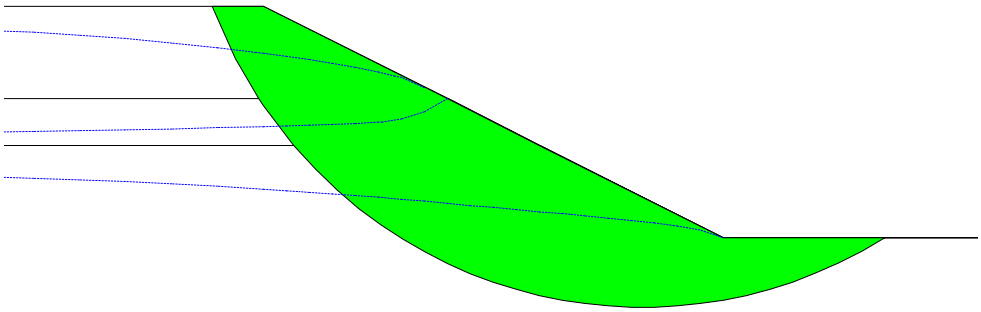

Figure 8-7 SEEP/W pore-water pressures in SLOPE/W

Figure 8-8 shows the distribution of pore-water pressure along the slip surface. The pore-water pressure starts out negative at the crest, then becomes positive in the perched water zone, becomes negative again in the unsaturated zone and then is positive through the base saturated zone.

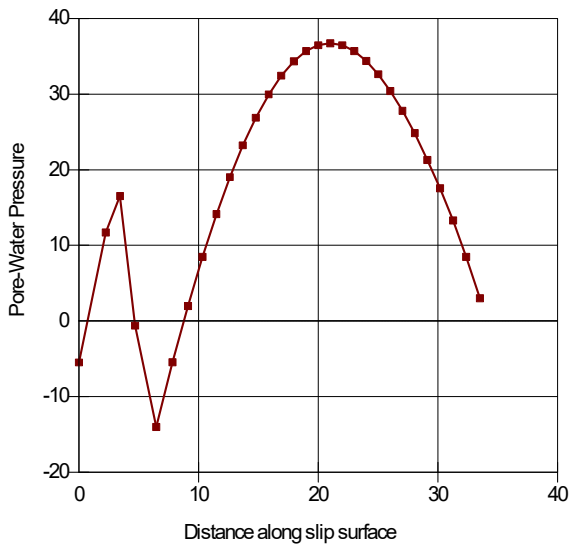

Figure 8-8 Pore-water pressure distribution along slip surface

There are few restrictions on using finite element computed pore-water pressures in SLOPE/W. The one thing to be careful about is that all trial slip surfaces must fall within the finite element mesh. No portion of a slip surface can exist outside the mesh.

Note: Whenever the pore water pressure on the ground surface is positive, a ponding condition is assumed and the weight and hydrostatic force of the water is automatically computed in SLOPE/W.

When the finite element pore-water pressure analysis has multiple time steps, you may select the pore-water pressure of a certain time step to be used in the analysis. Alternatively, SLOPE/W allows you to select all the time steps to be included automatically in the stability analysis. For example, in the case of transient SEEP/W analysis of a drawdown or filling of an earth dam, this feature will be very useful in assessing the factor of safety versus time as shown in Figure 8-9.

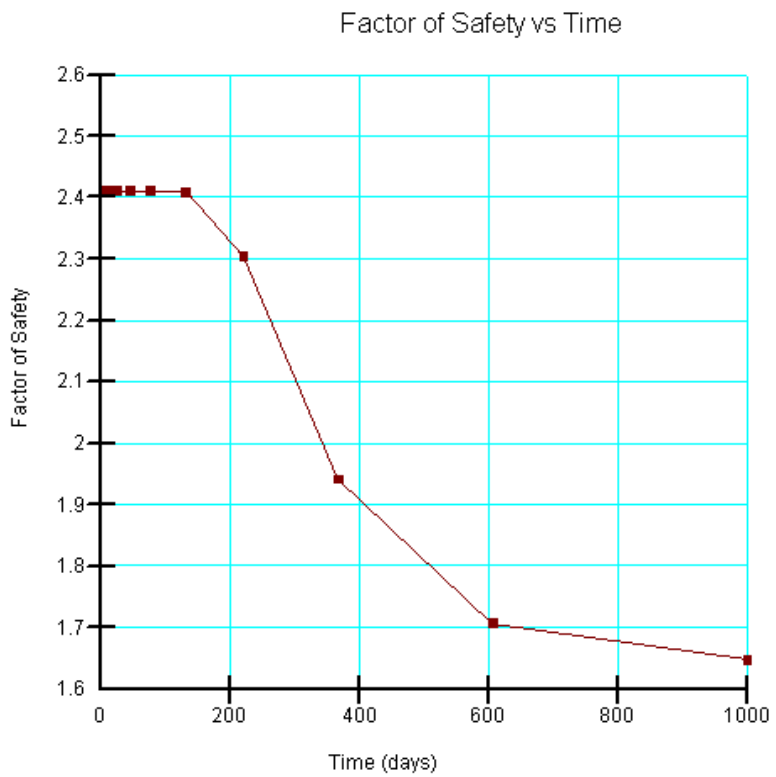

Figure 8-9 Factor of safety versus time

8.8 Recommended practice

As has been noted several times already, we highly recommend that you graph the pore-water pressure acting along the slip surface, to check that the pore-water pressures used by SLOPE/W are as you expect and are reasonable (Figure 8-8). This should be done periodically throughout a stability analysis.

9 Reinforcement and Structural Components

9.1 Introduction

The limit equilibrium method of slices was initially developed for conventional slope stability analyses. The early developers of the method recognized some of the inherent potential difficulties of determining realistic stress distributions. For example, Lambe & Whitman (1969), in their textbook *Soil Mechanics* note that the normal stress at a point acting on the slip surface should be mainly influenced by the weight of the soil lying above that point. It seems like the authors were concerned that other factors could influence the base normal stress and that this may not be appropriate.

In spite of the early developers' concerns, over the years concentrated loads were incorporated into the method mainly to simulate equipment or other surcharge loading on the slope crest. Later, thoughts on the subject migrated to the idea that if concentrated point loads can be included in the method, then other lateral concentrated point loads to represent reinforcement could be included. Conceptually, there seemed to be no reason for not doing this, and consequently the simulation of reinforcement with lateral concentrated loads has become common in limit equilibrium stability analyses.

Unfortunately, including lateral concentrated loads in a limit equilibrium analysis has some undesirable side effects. The resulting stress distributions, for example, throughout the potential sliding mass may be totally unrealistic, the critical slip surface may be in an unrealistic position, and the results may be difficult to interpret due to convergence difficulties. In spite of these negative side effects, the concepts can be successfully used in practice provided the procedures are fully understood and applied with considerable care.

This chapter starts with a discussion on some fundamentals related to applying lateral concentrated loads to simulate reinforcement in a limit equilibrium analysis. The numerical issues are the same regardless whether the reinforcement is an anchor, a nail or a fabric. The details of the specified parameters are, however, somewhat different for each of the various types of reinforcement and separate discussions are therefore devoted to each type of reinforcement.

The later part of this chapter deals with using finite element computed stress in the stability analysis of reinforced earth structures.

9.2 Fundamentals related to concentrated lateral loads

All reinforcement in a limit equilibrium analysis is represented using a concentrated point load. The concentrated point loads act on the free body, which is the potential sliding mass, and must therefore be included in the moment and force equilibrium equations. Although there are many convenient ways of specifying the properties of the reinforcement, the specified parameters are ultimately used to create a concentrated point load in the factor of safety calculations.

Mobilization of reinforcement forces

The effect of reinforcement can conceptually act immediately or develop with some strain. A pre-stressed anchor, for example, acts immediately. The force is induced by the pre-stressing. The force in a geosynthetic, on the other hand, may develop over time during construction and during stress re-distribution upon completion of the construction (Hoek and Bray, 1974). In other words, the reinforcement forces are mobilized in response to straining in the same way that the soil strength is mobilized as the soil strains.

Another way of looking at the reinforcement is that the reinforcement reduces the activating forces; that is, the reinforcement forces reduce the destabilizing forces. The reinforcement reduces the gravitational driving force. Alternatively, the reinforcement increases the shearing resistance and thereby increases the safety factor.

The SLOPE/W equilibrium equations are based on the shear mobilized at the base of each slice, and the mobilized shear is the shear strength divided by the factor of safety. In equation form, the mobilized shear S_m is:

$$S_m = \frac{S_{soil}}{F\ of\ S}$$

If the reinforcement is to be included to increase the shear resistance, then the reinforcement forces must also be divided by the factor of safety. S_m then is:

$$S_m = \frac{S_{soil}}{F\ of\ S} + \frac{S_{\text{reinforcement}}}{F\ of\ S}$$

A point of significance is that the soil strength and the shear resistance arising from the reinforcement are both divided by the same overall global factor of safety. The implication is that the soil shear resistance and reinforcement shear resistance are developed and mobilized at the same rate. This is likely not entirely correct in reality, but that is the assumption with this approach.

When the reinforcement is considered as contributing to reducing the destabilizing force, then it is assumed that the reinforcement is fully mobilized immediately and the reinforcement forces consequently are not divided by the overall global factor of safety. Reduction factors may be specified to limit the allowable loads in the reinforcement, but they do not directly come into the SLOPE/W factor of safety calculations. The specified or the allowable reinforcement forces are directly used in the SLOPE/W calculations.

SLOPE/W allows for both these approaches to include reinforcement in the stability calculations. The option is selected by flagging the reinforcement as “F of S dependent”, Yes or No. The Yes option increases the shear resistance and the reinforcement forces are divided by the global factor of safety to obtain the mobilized reinforcement forces. The No option uses the specified allowable reinforcement forces directly in the analysis.

The “F of S Dependent” Yes option is considered appropriate for ductile reinforcement such as some polymeric geosynthetics. The No option is considered appropriate for pre-stressed anchors or nails that are rigid relative to soil stiffness. By default, SLOPE/W uses the Yes option for fabrics and the No option for anchors and nails. The defaults can, however, be changed and defined as deemed appropriate for each particular design.

The “F of S Dependent” Yes option divides the specified reinforcement forces by the overall global factor of safety. The “F of S Dependent” No option uses the allowable specified reinforcement forces directly, and the reinforcement is not altered by the global factor of safety.

The two approaches are quite different in that with the “F of S Dependent” No option the specified anchor force is treated as the full mobilized force without consideration of the SLOPE/W computed factor of safety. With the “F of S Dependent” Yes option the computed factor of safety is applied to the reinforcement in the same way as to the soil strength. As shown in the Theory Chapter, it is the mobilized

shear at the base of the slice (S_m) that is used in the equilibrium equations, and S_m is the shear strength divided by the factor of safety (*S/F of S*). In the same way, it is only the mobilized reinforcement forces that can be included in the summation of the resisting forces, not the specified reinforcement forces. The specified reinforcement force is divided by the SLOPE/W factor of safety to obtain the mobilized reinforcement forces.

The Yes and No approaches will give similar results when the factor of safety is 1.0 or when the reinforcement forces are only a small fraction of the weight of the entire potential sliding mass.

The reduction factors in the reinforcement definition, discussed subsequently, should generally be set to 1.0 so that only the global factor of safety is used to factor the pullout resistance and tensile capacity of the reinforcement.

Slice forces and stress distributions

In SLOPE/W a reinforcement load is applied to the slice that has its base intersected with the line of action of the reinforcement. The reinforcement load is treated as a concentrated point load acting at the intersecting point at the base of a slice.

Another important point is that concentrated point loads must become part of the force resolution of one particular slice. The following is the equation for summation of moments about a point as explained in the Theory Chapter. The concentrated load is represented by *D*.

$$\sum Wx - \sum S_m R - \sum Nf + \sum kWe \pm \sum Dd \pm \sum Aa = 0$$

Now let us look at an example that was introduced earlier in the Limit Equilibrium Fundamentals chapter. The example is a tie-back wall with two rows of pre-stressed anchors (Figure 9-1). Each anchor can apply 150 kN of force

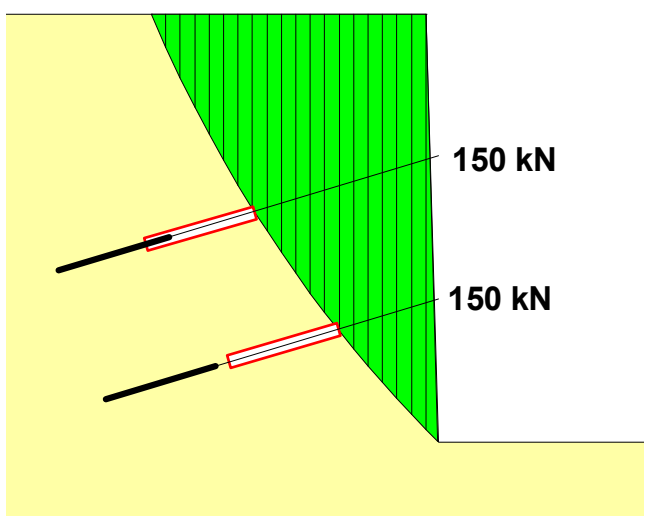

Figure 9-1 Illustration of a tie-back wall

The free body diagrams and force polygons for the two slices that included the reinforcement loads are presented in Figure 9-2 and Figure 9-3.

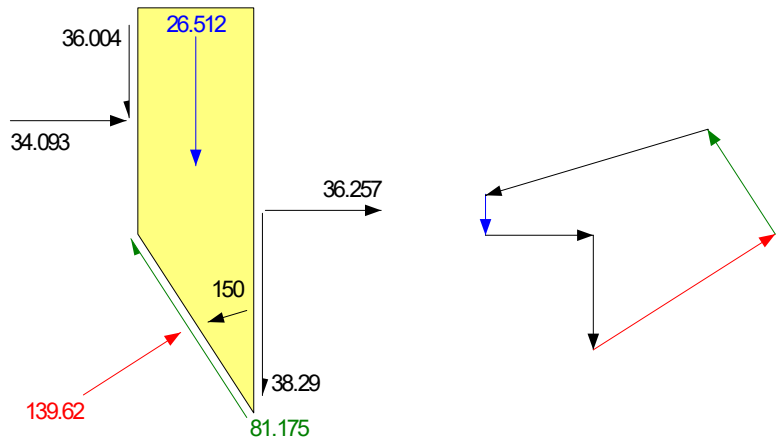

Figure 9-2 Free body and force polygon for upper anchor

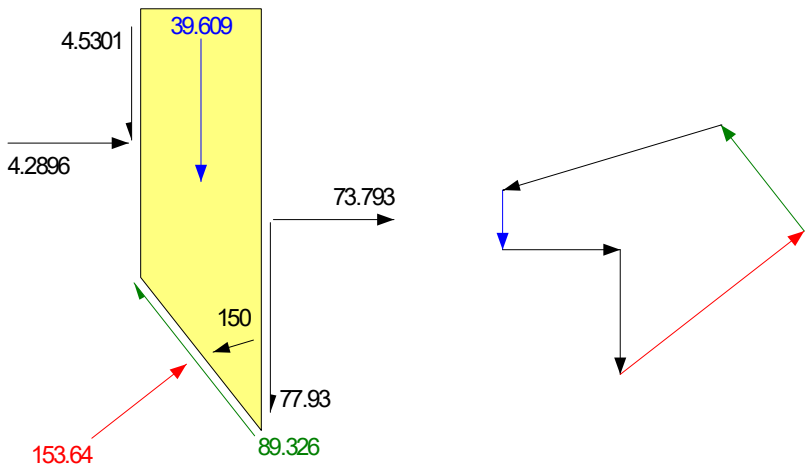

Figure 9-3 Free body and force polygon for lower anchor

The first point to note is that the interslice normal forces point away from the slice on the right side. This indicates tension between the slides, which is obviously not the case in the field. Plotting the interslice forces as in Figure 9-4 further highlights this difficulty. At each of the anchor locations, the interslice normals become negative and the interslice shear forces reverse direction. Of significance, however, is the fact that the force polygons close, signifying that the slices are in equilibrium. The forces may not be realistic, but they are the forces that provide force equilibrium for the slices, which is the fundamental objective of the method.

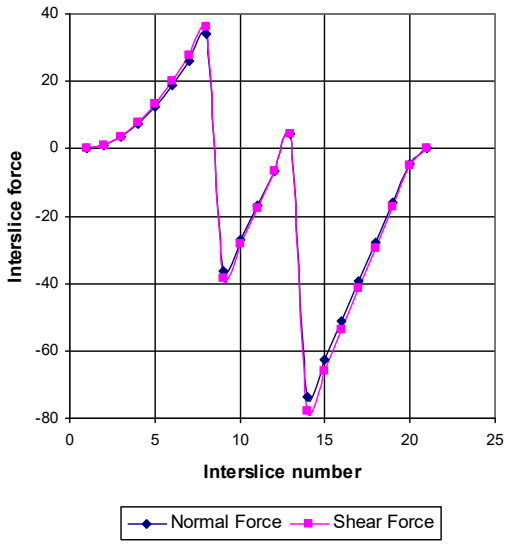

Figure 9-4 Interslice shear and normal forces with anchor loads applied at the slip surface

Now we will model the effect of the anchors by applying equivalent point loads on the wall face. The anchor loads are now included in the equilibrium of the slice on the right side. The interslice forces are now completely different. Figure 9-5 again shows the interslice shear and normal forces. The normal force increases evenly and gradually except for the last two slices. Of interest is the interslice shear force. The direction is now the reverse of that which usually occurs when only the self weight of the slices is included (simple gravity loading). The shear stress reversal is a reflection of a negative lambda (λ).

The large differences in the interslice forces also lead to significantly different normal stress distributions along the slip surface, as shown in Figure 9-6. It is noted in the Theory chapter that the equation for the normal at the base of the slices includes terms for the interslice shear forces. This example vividly illustrates this effect.

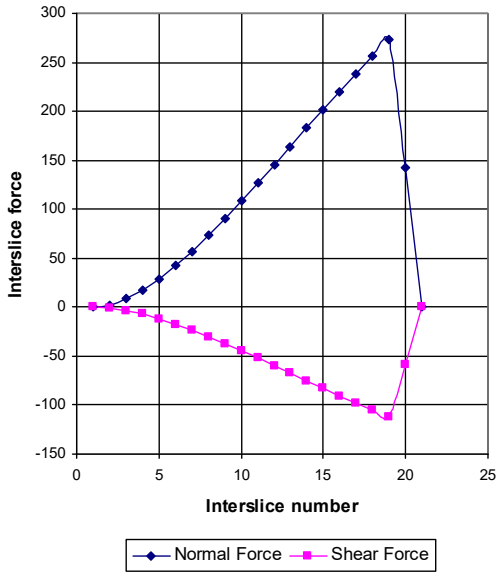

Figure 9-5 Interslice shear and normal forces with anchor loads applied at the face of wall

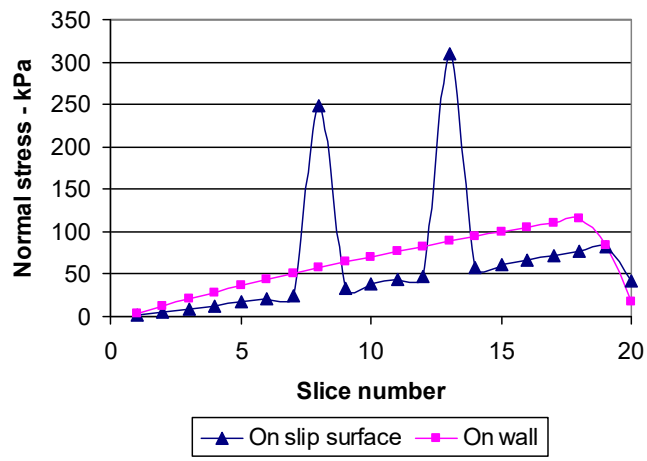

Figure 9-6 Comparison of normal stress distributions

Interestingly, in spite of the vastly different stresses between the slices and along the slip surface, the factors of safety are nearly identical for these two treatments of the concentrated point loads. With the anchors applied at the slip surface location, the factor of safety is 1.075 while when they are applied at the wall, the factor of safety is 1.076. For all practical purposes they are the same. The following table highlights this important and significant result.

Anchor Force Location	Factor of Safety
On slip surface	1.075
On the wall	1.076

The question arises, why do such vastly different stress distributions end up with essentially the same factor of safety? The answer is discussed in detail in the Limit Equilibrium Fundamentals chapter. In summary, there are two main characteristics that lead to this situation which are:

- The forces on each slice are the forces that ensure force equilibrium of each slice.
- They may not be realistic forces, but they do provide for force equilibrium.

The forces on each slice are such that the factor of safety is the same for each slice. Again, this does not represent reality, but it is a symptom of the formulation. The redeeming characteristic of the formulation is that the potential sliding mass (the free body as a whole) is in force and moment equilibrium. The internal stresses may not represent reality, but the sliding mass as a whole is nonetheless in equilibrium. It is for this reason that the method is useful, in spite of its idiosyncrasies.

SLOPE/W has the option to distribute the reinforcement load amongst all the slices intersected by the reinforcement. The option is called Distributed. Selecting this option gives a more realistic stress distribution for the case being discussed here as illustrated in Figure 9-7. It removes the sharp spikes in the normal stress distribution at exist when the reinforcement load is applied only at the slip surface. Distributing the reinforcement load also overcomes the problem of negative normal forces between slices discussed earlier. Moreover, the more realistic stress distribution resulting from distributing the reinforcement load aids in overcoming convergence problems.

The disadvantage of disturbing the reinforcement load is that the results are somewhat more difficult to interpret. Say the total reinforcement load is 150 kN and the reinforcement intersects 13 slices. The force

per slice is 11.54 kN. This is further complicated when a slice intersects more than one reinforcement. The contributing forces from each reinforcement load are summed and presented as a single force for presentation in the slice free body diagram and related force polygon.

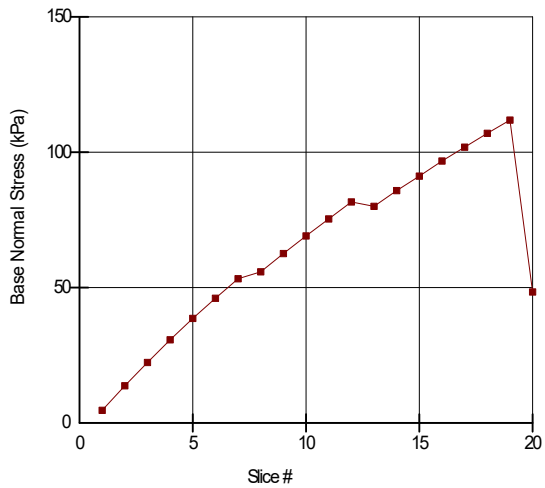

Figure 9-7 Stress distribution along slip surface when reinforcement load is distributed

As discussed earlier, in spite of the seeming more realistic stress distributions associated with distributing the reinforcement loads, the factor of safety essentially remains the same when all else is the same. The factor of safety for the case when the reinforcement load is distributed is 1.077, which is the same as the 1.075 and 1.076 values discussed earlier.

As with so many other options, there are no firm rules on which option is best for a particular situation. The best approach is to try both Concentrated and Distributed reinforcement loads and then make a selection based on your particular problem.

Reinforcement Anchorage

Four types of reinforcement can be modeled with SLOPE/W including anchors, nails, geosynthetics, and piles. With the exception of piles, reinforcement requires an estimation of the pullout resistance available to the reinforcement. This available pullout resistance depends on the amount of bonded length behind the slip surface (in the passive zone) or in front of the slip surface (in the active zone).

Ideally, reforcement such as anchors and nails use proper anchorage to the slope face through nuts and bearing plates or other measures. However, SLOPE/W provides an option to model the reinforcement with or without anchorage. The renforcement is treated as an integral part of the sliding mass when anchorage is selected. The available pullout resistance is therefore governed by the amount of bonded length behind the slip surface and the tensile capacity of the reinforcement.

The available pullout resistance depends on the amount of bonded length behind the slip surface and within the sliding mass if the anchorage option is not selected. SLOPE/W calculates the pullout resistance in both the active and passive zones and uses the smaller of the two values (Figure 9-7).

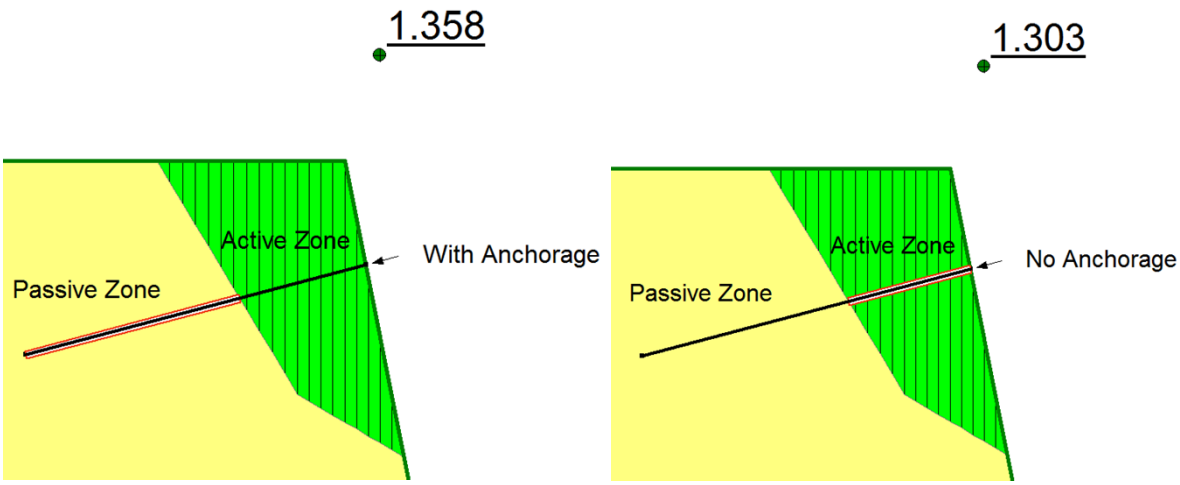

Figure 9-8 The effect of Anchorge showing the governing bond length in the passive and active zones.

In SLOPE/W, reinforcement anchorage is defaulted to 'yes'. The Anchorage option is not applicable to piles.

Convergence

Applying lateral concentrated loads can create considerable convergence difficulties. Reinforcement is required due to the steepness of the slope or wall. This means that portions of the critical slip surface are fairly steep. A steep slip surface, together with the lateral concentrated loads, often makes it difficult to obtain a converged solution.

Not being able to compute a factor of safety is bad enough, but the minimum factor of safety is often located immediately next to the area where non-convergence becomes a problem. Sometimes the minimum factor of safety is among non-converged slip surfaces. The critical slip surface is often in the proximity of the active wedge line inclined at $45+\phi/2$, which is also the inclination at which the convergence difficulties frequently start. The difficulty is that the critical factor of safety can be somewhat suspect when its neighbors represent a non-converged case.

A typical situation is portrayed in Figure 9-9. In this example a converged solution could not be obtained for most of the grid rotation centers in the lower right hand triangular area. The grid rotation centers without a factor of safety beside them are the ones where it was not possible to get a converged solution. These non-converged grid centers mostly represent steep slip surfaces. The critical grid rotation centre is represented by the point with the larger dot, and is surrounded by points for which it was not possible to obtain a converged solution.

Furthermore, convergence is a problematic issue when very large lateral concentrated loads are applied; loads that are larger than what would reasonably be mobilized in reality. Convergence becomes particularly troublesome when large lateral point loads are applied near to top of a slope. Care and thought is consequently required when specifying these types of loads. Blindly specifying these lateral loads can lead to unreasonable results.

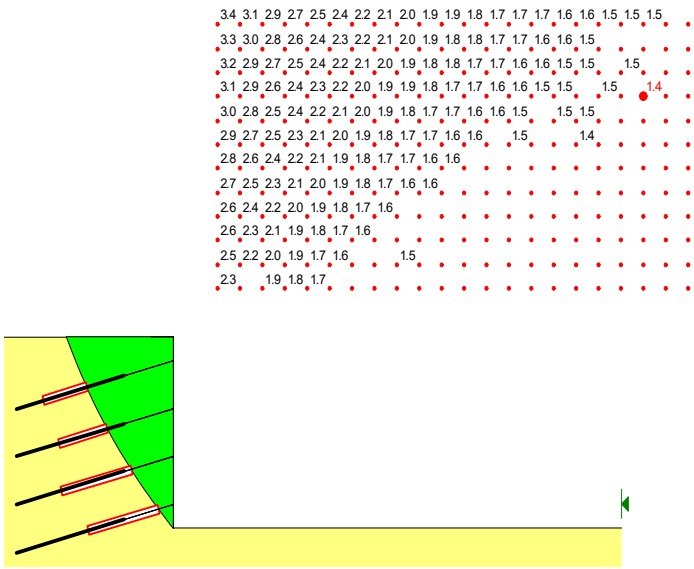

Figure 9-9 Rotation grid with convergence problems in lower right corner

Safety factors of the various components

With the “F of S Dependent” No option, SLOPE/W can only provide the factor of safety against sliding of the potential sliding mass. SLOPE/W cannot directly account for a margin of safety with respect to the reinforcement material or with respect to the pullout resistance between the soil and the material. Reduction factors associated with these aspects have to be considered separately. It is vitally important to recognize these safety factors are not directly involved in the SLOPE/W factor of safety calculation. This will become clearer as we discuss the details of the various types of reinforcement.

With the “F of S Dependent” Yes option, the SLOPE/W computed factor of safety is used to determine the mobilized reinforcement force. As explained earlier, the computed factor of safety is applied to the reinforcement force as well as to the soil strength.

Recommended analysis approach

In consideration of the limit equilibrium responses when lateral concentrated loads are included, it is often useful to apply some reverse logic. The first step should be to find the force required from the reinforcement that will provide an adequate factor of safety against sliding of the retained soil wedge. Then, once the required reinforcement force is known, the appropriate reinforcement can be selected and sufficient embedment can be computed. This is somewhat opposite of the usual design procedure. The usual procedure is to select the possible materials and create a possible design, and then check the stability. The downside of this approach is that the material strength may be too high, for example, and if the applied lateral concentrated loads are unnecessarily too high, it may not be possible to obtain a converged solution or it may lead to the wrong position of the critical slip surface. To obtain the best SLOPE/W solution, the applied lateral concentrated loads should not be greater than the required mobilized force. The specified reinforcement loads should not necessarily be the capacity of the reinforcement; it should be the portion of the capacity that will be mobilized or needs to be mobilized. You will note that this approach is reflected in the details discussed below on how to use and interpret the results associated with the various types of reinforcement.

Summary

When analyzing problems with reinforcement, it is useful to remember and consider the following:

- Lateral concentrated loads can lead to unrealistic internal stress distribution.
- The overall potential sliding mass can be in equilibrium in spite of poor internal stress distributions.
- The applied lateral loads representing reinforcement should be no greater than the associated expected mobilized force to mitigate convergence problems; it should not necessarily be the reinforcement capacity.
- With the "F of S Dependent" Yes option, the SLOPE/W computed factor of safety is applied to the reinforcement forces in the same way as to the soil strength. The mobilized reinforcement forces are the specified forces divided by the factor of safety.
- The best analysis approach often is to first find the forces required from the reinforcement and then detail and dimension the reinforcement, as opposed to detailing and dimensioning the reinforcement and then checking the stability.

9.3 Anchors and nails

The effects of soil reinforcement by anchors and nails can be incorporated into SLOPE/W (Figure 9-10 and Figure 9-11, respectively). The calculation of the pullout force that is applied to the free body diagram is identical for both reinforcement types; however, the differentiating input is the specification of bond length for the anchor (Figure 9-10). The bond length is the grouted length. In contrast, a soil nail is assumed to have the potential to mobilize pullout resistance over its entire length (and therefore the specification of bond length is not required).

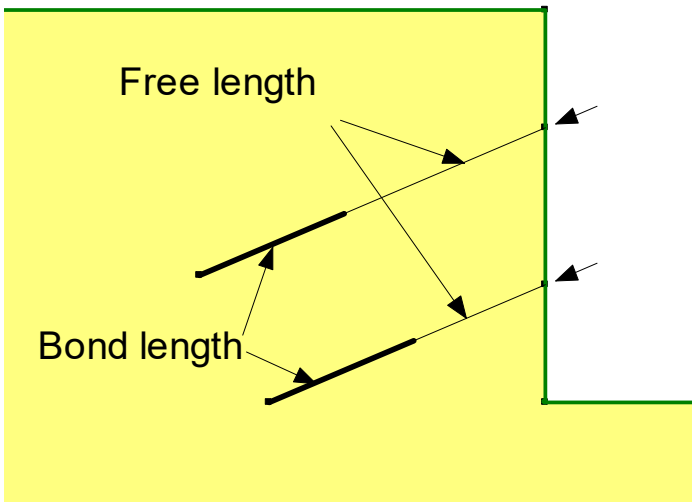

Figure 9-10 Reinforcement using anchors

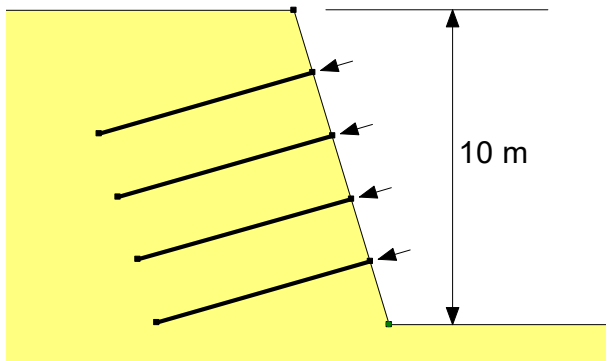

Figure 9-11 Soil slope reinforced using nails

The pullout resistance is specified with the units of force per area of grouted section and reinforcement in contact with the soil (note: soil nails can also be grouted). The following additional inputs are required for both the nail and anchor reinforcement types:

- Bond diameter (D): the diameter of the grouted section in contact with the soil.
- Resistance reduction factor (RRF): can be used as a "scale effect correction factor" to account for nonlinear stress reduction over the embedded length.
- Spacing (S): the distance in the out-of-plane dimension between the anchors or nails.
- Tensile capacity (TC): tensile strength of the reinforcement.
- Reduction factor (RF): accounts for the reduction of the ultimately tensile capacity due to physical processes such as installation damage, creep, and durability.
- Shear force: to incorporate a force that represents the shear stress mobilized within the reinforcement.
- Shear reduction factor: a factor to reduce the input shear force.
- Apply shear: a value ranging between 0 and 1 to control the orientation of the shear force on the free body. A value of zero 0 applies the force parallel to the orientation of the reinforcement; a value of 1 applies the force parallel to the slice base (Figure 9-12).

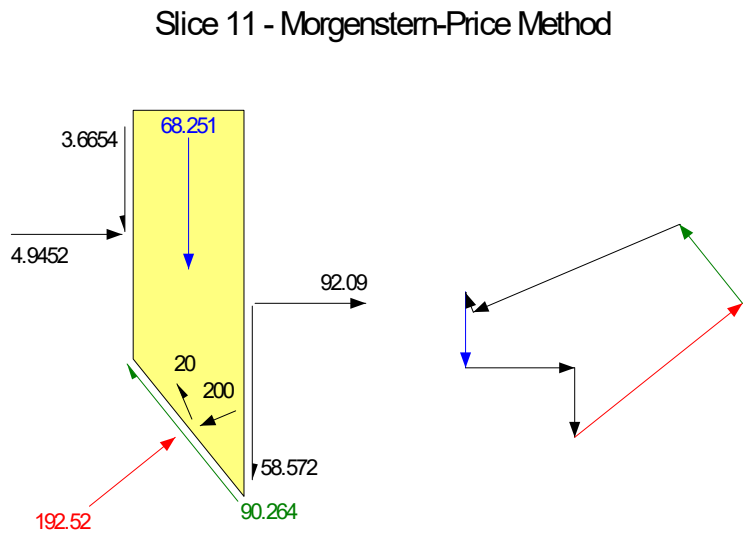

Figure 9-12 Slice free body with a shear force

The factored pullout resistance FPR per length of grouted section or nail behind the slip surface is calculated from the specified pullout resistance PR as:

$$FPR = \frac{PR(\pi D)}{RRF(S)FS}$$

The pullout force (PF) that could be applied to the free body is calculated as:

$$PF = FPR(l)$$

where l is the length of the grouted section or nail behind the slip surface. The maximum pullout force must not exceed the factored tensile capacity FTC:

$$FTC = \frac{TC}{RF(S)FS}$$

where the factor of safety FS is only included if the "F of S Dependent" option is selected to be "Yes". The pullout force that is applied to the free body is the lesser of PF or FTC. These equations make it apparent that the reduction factors should generally be specified as 1.0 if the "F of S Dependent" option is selected to be "Yes".

The detailed example files should be consulted for further insights into the functionality of anchor and nail reinforcement and the graphical features available to assist with interpretation of the results. Specifically, visual features are available to indicate (a) if the pullout force applied to the free body was governed by the factored pullout resistance or factored tensile capacity; and (b) the length over which pullout resistance was mobilized (compare Figure 9-13 and Figure 9-14). In addition, the View | Object information can be used to explore both the reinforcement inputs and values used in the factor of safety calculations.

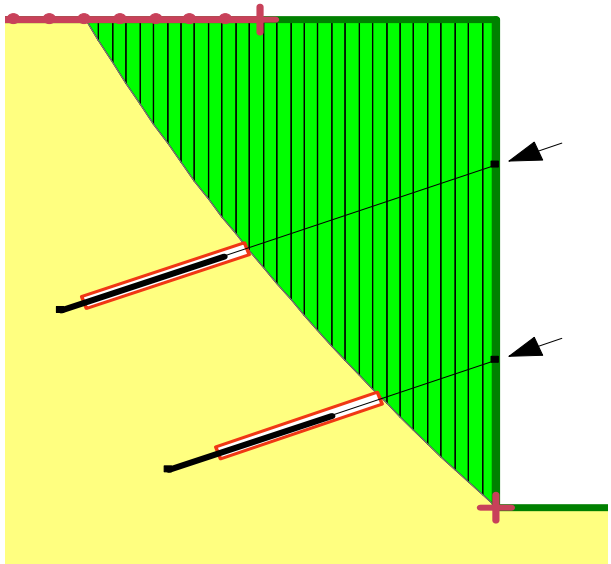

Figure 9-13 Visual effects to indicate that the factored pullout resistance governed the pullout force (solid lines) and that the full length of grouted section mobilized resistance (anchors extend outside the boxes that sit against the slip surface).

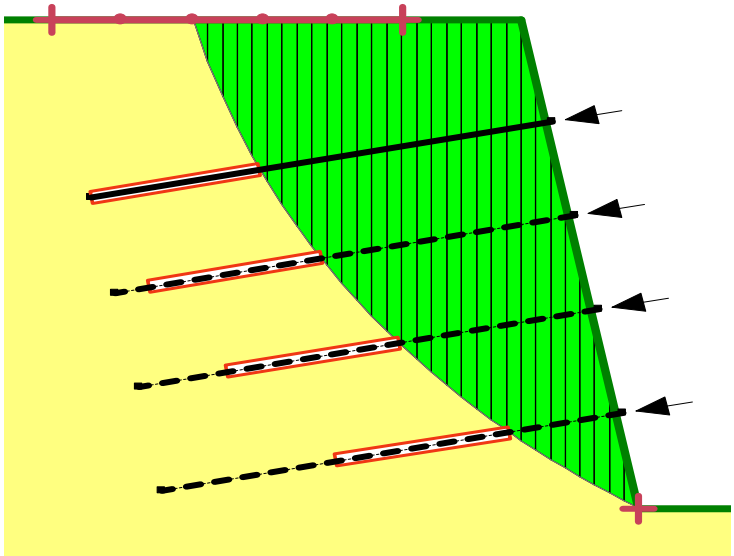

Figure 9-14 Visual effects to indicate that the factored tensile capacity governed the pullout force (dotted lines) on the bottom three anchors.

9.4 Geosynthetic reinforcement

Geosynthetic reinforcement such as geotextiles and geogrids can be incorporated into SLOPE/W (Figure 9-15). Two methods of obtaining the pullout resistance are available. The selection is dependent on the stress transfer mechanism of the reinforcement. The pullout resistance can be specified if passive resistance is the dominant stress transfer mechanism. Passive resistance refers to the development of bearing type stresses on relatively stiff members of the reinforcement that are situated normal to the

direction of pullout (e.g. geogrid). Alternatively, the pullout resistance can be calculated from the overburden stress if frictional resistance dominates the stress transfer mechanism (e.g. sheet geotextiles).

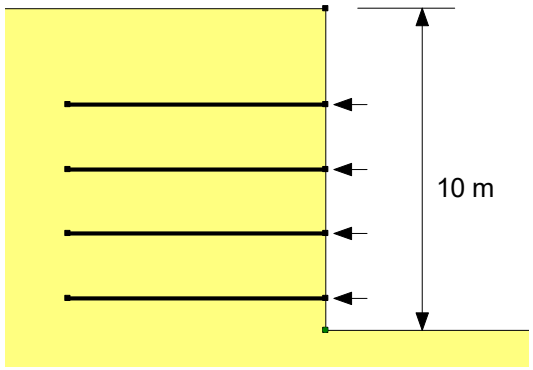

Figure 9-15 Slope reinforced with geosynthetic

The pullout resistance is specified with the units of force per unit length of geosynthetic per unit width in the out-of-plane direction. The calculated pullout resistance option requires the specification of:

- Interface adhesion (S_{IA}): apparent cohesion (adhesion) if effective drained soil strengths are being considered. Alternatively, the parameter can be used to specify the undrained strength at the interface between the geosynthetic and soil.
- Interface shear angle (δ): angle of interface shearing resistance if effective drained soil strengths are being assumed.
- Surface area factor (SAF): used to account for mobilized pullout resistance on the top and bottom of the geosynthetic. The default parameter is 2 for resistance on both sides of the geosynthetic; however, this input could be used to account for different soils on the top and bottom of the geosynthetic.

The calculated pullout resistance PR is given by:

$$PR = \left(S_{IA} + \sigma_v^{'} \tan \delta\right) SAF$$

where $\sigma_v^{'}$ is the effective overburden stress. The effective overburden stress is calculated based on the height of soil above the intersection point with the base of the slice and includes the effects of surcharge loads. Point loads are not included in the calculation. Regardless of the selected approach, the following inputs are required:

- Resistance reduction factor (RRF): can be used as a "scale effect correction factor" to account for nonlinear stress reduction over the embedded length of highly extensible reinforcement.
- Tensile capacity (TC): tensile strength of the reinforcement.
- Reduction factor: accounts for the reduction in the ultimately tensile capacity of the reinforcement due to physical processes such as installation damage, creep, and durability.
- Load orientation: a value ranging between 0 and 1 to control the orientation of the pullout force on the free body. A value of zero 0 applies the load parallel to orientation of the geosynthetic; a value of 1 applies the force parallel to the slice base (Figure 9-16).

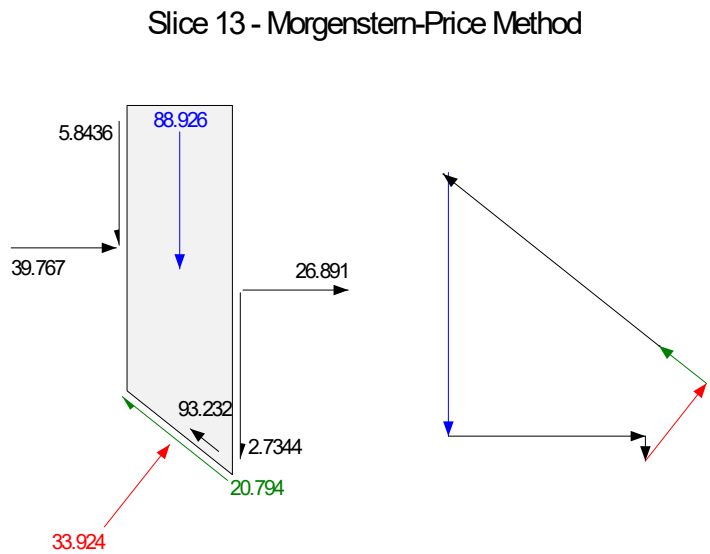

Figure 9-16 Pullout force parallel to slice base

The factored pullout resistance FPR per unit length of geosynthetic behind the slip surface is calculated from the pullout resistance PR as:

$$FPR = \frac{PR}{RRF(FS)}$$

The pullout force that could be applied to the free body is calculated as:

$$PF = FPR(l)$$

where l is the length of the geosynthetic behind the slip surface. The maximum pullout force must not exceed the factored tensile capacity FTC:

$$FTC = \frac{TC}{RF(FS)}$$

where the factor of safety FS is only included if the "F of S Dependent" option is selected to be "Yes". The pullout force that is applied to the free body is the lesser of PF or FTC. These equations make it apparent that the reduction factors should generally be specified as 1.0 if the "F of S Dependent" option is selected to be "Yes".

The detailed example files should be consulted for further insights into the functionality of geosynthetic reinforcement and the graphical features available to assist with interpretation of the results. Specifically, visual features are available to indicate if the pullout force applied to the free body was governed by the factored pullout resistance or factored tensile capacity (Figure 9-17). In addition, the View | Object information can be used to explore both the reinforcement inputs and values used in the factor of safety calculations.

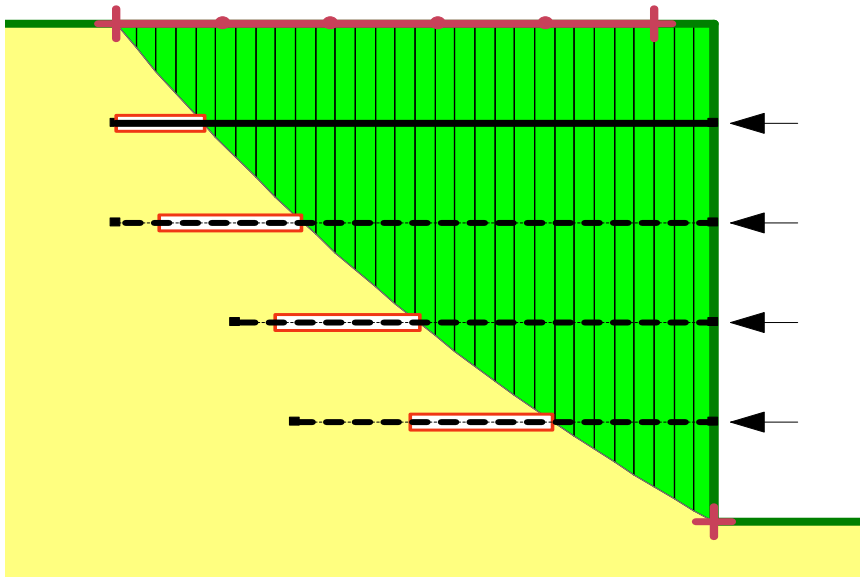

Figure 9-17 Visual effects to indicate required or available length (boxes) and if factored pullout resistance or factored tensile capacity governed the pullout force (solid versus dotted line).

Surcharge loads are included in the computation of overburden stress to determine bond resistance. However individual Point load is not included in the overburden stress.

9.5 Piles

A pile in SLOPE/W is reinforcement that only provides shear resistance. An example is presented in Figure 9-18. The specified parameters for this type of reinforcement are:

- Spacing
- Shear force
- Shear reduction factor
- Direction of application - parallel to slip surface or perpendicular to reinforcement

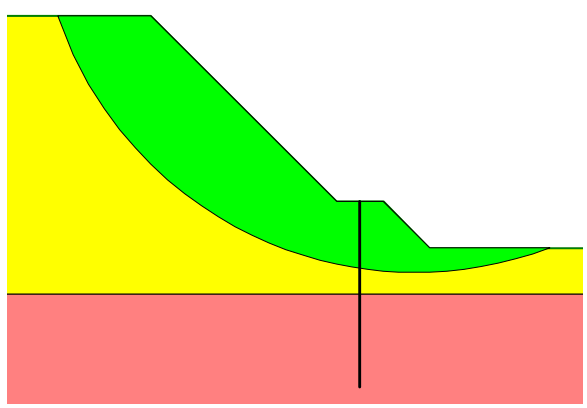

Figure 9-18 Slope reinforced with a pile or dowel

Figure 9-19 shows the slice free body and force polygon for the slice that includes the pile. In this case, the shear force was specified as being parallel to the slice base. The 100 kN force in Figure 9-19 confirms this.

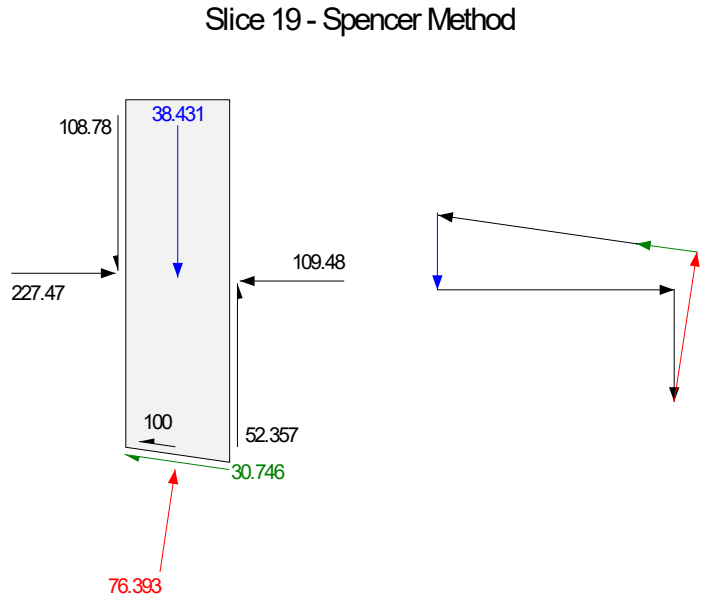

Figure 9-19 Shear force of pile on slice free body

9.6 User defined reinforcement

Reinforcement load can be incorporated into stability calculations based on a user defined reinforcement force versus distance function. The reinforcement force can either be a pullout or a shear force. The distance in the function is the length from the starting point of the reinforcement to the intersecting point with the slip surface. Other input parameters are:

- Spacing
- Reduction factor
- Force orientation - relative to the slice base (0 to 1: 0 is Axial, 1 is parallel to slice base) or perpendicular to the reinforcement

The user defined reinforcement allows for consideration of various modes of failure such as pullout, tensile capacity (of the reinforcement), plate capacity (or connector failure) and so on. The user defined reinforcement can also be used model variations in the mobilized shear force over the length of a pile. The application of the user defined reinforcement for simulating a pile requires that the force be applied perpendicular to the reinforcement. The determination of a shear force function is relatively straightforward. Only the pullout force along the reinforcement is discussed.

Consider the following reinforcement load components:

- T_f – reinforcement-facing connection strength (F)
- T_t – reinforcement tensile strength (F)
- T_e – embedded end strength (F)

- T_s – pullout resistance (F/L), $T_s = \tau * L_a$, here τ is the reinforcement-soil interface shear strength (F/L^2) and L_a is the effective anchorage length of reinforcement

Relative to various potential failure modes (**Figure 9-20**), the maximum reinforcement forces at the intersecting point can be determined as follows:

a) Stripping (F_1) - stripping occurs if the pullout force exceeds the combined capacity from facing connection and soil-reinforcement adhesive/frictional shear resistance in the sliding mass.
b) Pullout (F_2) - reinforcement pullout from behind the slip surface when the pullout force exeeds the combined capacity from embedded end bearing and soil-reinforcement adhesive/frictional shear resistance in retaining zone.
c) Overstressing (F_3) – the pullout force cannot exceed the reinforcement tensile capacity.

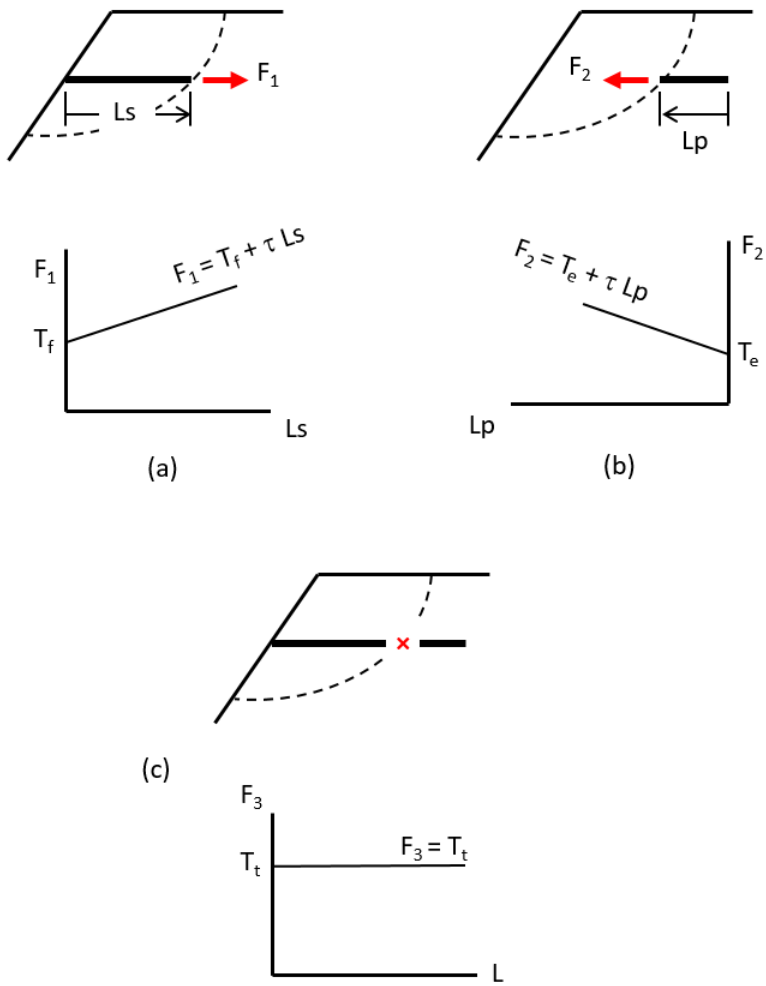

Figure 9-20 Reinforcement forces considering (a) stripping, (b) pullout, and (c) overstressing

The reinforcement force versus distance function can be determined by

$F = min(F_1, F_2, F_3)$

Figure 9-21 illustrates an example reinforcement function that simulates a 23 m long user defined reinforcement with plate capacity of 40 kN, end bearing capcity of 100 kN, reinforcement tensile capcity of 200 kN, and soil-reinforcement interface shear force of 20 kN/m.

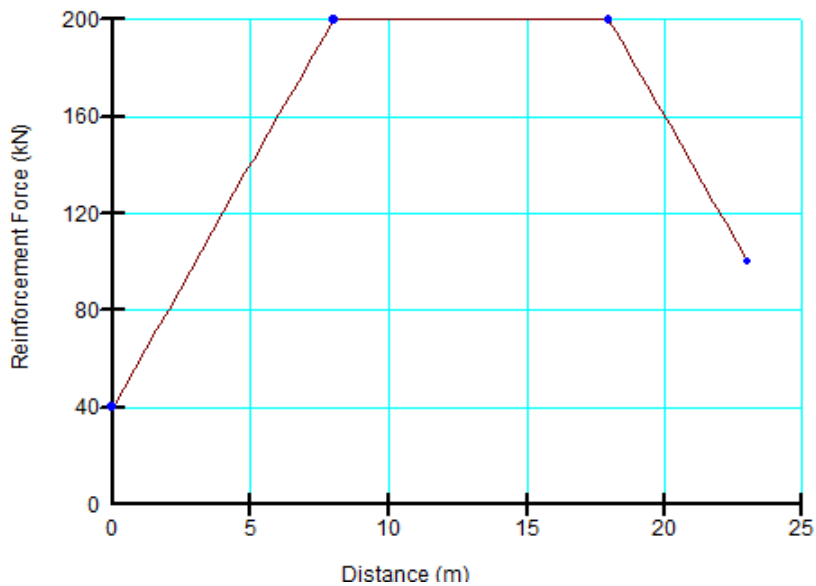

Figure 9-21 An example reinforcement function

Note that the reinforcement partial factor that is linked to the user defined type is the pullout resistance factor regardless the force orientation.

9.7 Manufacturer Reinforcement

Several manufacturer geosynthetic reinforcements are incorporated into SLOPE/W. The reinforcement parameters are automatically calculated based on installation and site specific conditions that influence the overall reduction factor on the tensile capacity. The pullout resistance (PR) for all manufacturer reinforcements is calculated similar to the geosynthetic reinforcements as:

$$PR = \left(S_{IA} + \sigma_v^{'} \tan \delta\right) SAF$$

where:

S_{IA} is the interface adhesion, which is assumed to be 0 for manufacturer reinforcements,

δ is the interface shear angle, and

SAF is the surface area factor, which is assumed to be 2 for manufacturer reinforcements.

For manufacturer reinforcement, the interface shear angle is calculated as:

$$\delta = \cot^{-1}\left(a^{'} \tan \varphi^{'}\right)$$

where $a^{'}$ is the pull-out coefficient. The pullout coefficient is either prescribed by the manufacturer based on the backfill material or it is a user-input value.

The inputs for each manufacturer reinforcement are dependent on the product type selected. The inputs are used to calculate the overall reduction factor (RF_O) for calculation of the factored tensile capacity (FTC) as:

$$FTC = \frac{TC}{RF_O(FS)} = \frac{TC}{RF_{ID} \times RF_{CR} \times RF_{CH} \times RF_W \times RF_D(FS)}$$

where:

FTC is the factored tensile capacity, or the long-term tensile strength,

TC is the tensile capacity, or the short-term tensile strength,

RF_O is the overall reduction factor, which is calculated in SLOPE/W based on the other reduction factors,

(FS) is the optional inclusion of the factor of safety in the calculation of the factored tensile capacity, if the "F of S Dependent" option is set to "True",

RF_{ID} is the reduction factor for installation damage,

RF_{CR} is the reduction factor for creep,

RF_{CH} is the reduction factor for chemical/environmental effects,

RF_W is the reduction factor for weathering, and

RF_D is the reduction factor for the extrapolation of data.

Each of the reduction factors are influenced by site-specific and environmental conditions. Required inputs that determine the individual reduction factors may include soil type or particle size, fill material, temperature, design life, and/or soil pH levels.

9.8 Sheet pile walls

The embedment of sheet piling below the base of an excavation offers lateral resistance to a potential toe failure, as illustrated in Figure 9-22. The question is how to represent this lateral resistance. The strength of the piling cannot be included directly in the geometric definition; that is, the piling cannot be represented by a material with a very high strength. Also, forces outside the free body representing the potential sliding mass cannot be included in the equations of statics – only forces acting on the free body can be included in the statics equations.

One way of including the embedment lateral resistance is with a concentrated point load that acts on the potential sliding mass. The concentrated point load arises either from the shear strength of the sheet piling or the passive toe resistance offered by the embedment. The magnitude of the passive toe resistance is:

$$P_p = \frac{\gamma H^2}{2} K_p$$

where:

K_p is the passive earth pressure coefficient.

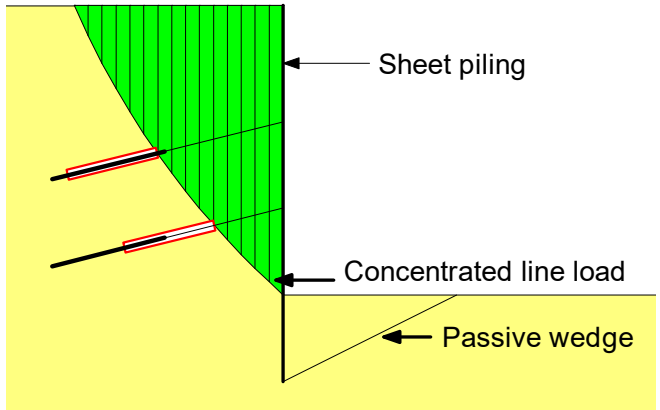

Figure 9-22 Embedded sheet pile

The passive earth pressure K_p coefficient is highly dependent on the friction between the sheet piling and the soil. K_p can vary from approximately 3 to 12, which makes it difficult to make an accurate prediction of the lateral passive resistance. Furthermore, significant displacements are generally required to mobilize the full passive resistance – at least more than what is tolerable for a retaining structure like this. Consequently, it is likely necessary to use a fairly conservative safety factor on the passive resistance – something around 3.0, particularly if there is a heavy reliance on the friction between the piling and the soil.

The impact of the embedment can be considered in a much more realistic way by doing a finite element soil structure interaction analysis and then using the resulting stresses in the stability assessment as discussed in detail below in this chapter. Unfortunately, in a limit equilibrium analysis, the soil interaction component has to be represented by a concentrated point load, even though intuitively it is not a totally satisfactory procedure.

9.9 Deep-seated instability

Deep-seated stability is usually not the most critical potential mode of failure, but it is an issue that needs to be addressed, particularly before the decision is made to shorten the lower reinforcement. Often the lower level reinforcement appears too long for a toe failure, but the deep-seated potential failure needs to be checked as part of the decision to dimension the lower level reinforcement.

Figure 9-23 illustrates a deep-seated analysis. The slip surface passes behind the anchors and underneath the base tip of the sheet piling. All the structural components consequently do not come into the SLOPE/W stability analysis. The structural components simply go along for the ride, so to speak.

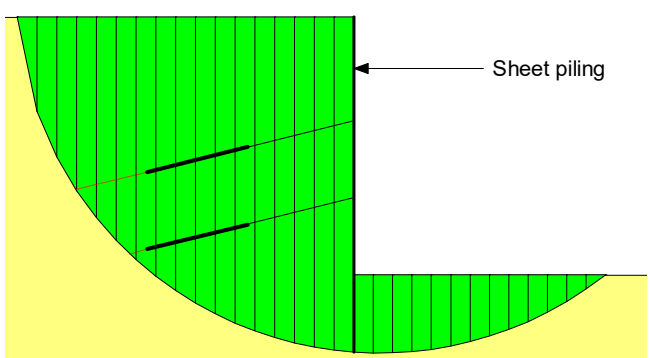

Figure 9-23 Deep seated failure

9.10 Mitigation of numerical problems

Several times in the above discussion, it has been noted that lateral concentrated loads representing reinforcement can cause difficulty with convergence and finding the position of the critical slip surface. A procedure that can be used to mitigate the numerical difficulties is to work with reinforcement forces that give a factor of safety around unity. In other words, what are the forces that represent the point of limiting equilibrium? This tends to give the best numerical behavior. Later when the response of the analysis is better understood, the reinforcement loads can be increased to be more representative of actual conditions.

A point to remember is that the numerical behavior tends to deteriorate as the lateral forces increase relative to the gravitational mobilized shear. Care is also required to make sure that the lateral forces are not so high as to pull (push) the potential sliding mass uphill. This is another reason to start the analysis with low lateral forces and then increase the magnitude in small stages.

High lateral loads are particularly troublesome when they are applied near the top of a wall. So another trick that can be used to reduce numerical problems is to specify the higher loads near the bottom of the wall and the lighter loads closer to the top of the wall. The total specified for all the reinforcement remainds the same, but the specific forces for each reinforcement can be redistributed sometimes to help out with numerical problems, at least until the wall response is fairly clear.

The convergence tolerance in SLOPE/W can also sometimes be relaxed to obtain more converged solutions. Also, sometimes more converged solutions are available when only moment or only force equilibrium is satisfied, as in the Bishop Simplified and Janbu Simplified methods. Using these simpler methods can sometimes help increase one's confidence as to the position of the critical slip surface.

The concentrated point loads representing reinforcement should always be verified and checked using the View Slice Information tool in SLOPE/W RESULT.

The slice free body diagrams and force polygons have been used extensively in the above discussion to illustrate the magnitude and behavior of the concentrated loads. We highly recommend that you use the View Slice Information tool extensively when reinforcement is included in an analysis. It is vitally important to always check the exact concentrated point loads used by SLOPE/W to make sure that the applied concentrated point loads match your expectations and understanding. The importance of this cannot be overemphasized.

9.11 Finite element stress-based approach

An alternate approach to analyzing the stability of reinforced structures is to use the stresses from a finite element analysis. The interaction between the reinforcement and the soil alters the stress state such that the resulting shear resistance is greater than the mobilized shear force.

Wall with nails

Figure 9-24 shows a vertical wall reinforced with four rows of nails. The nails are modeled as structural elements in SIGMA/W.

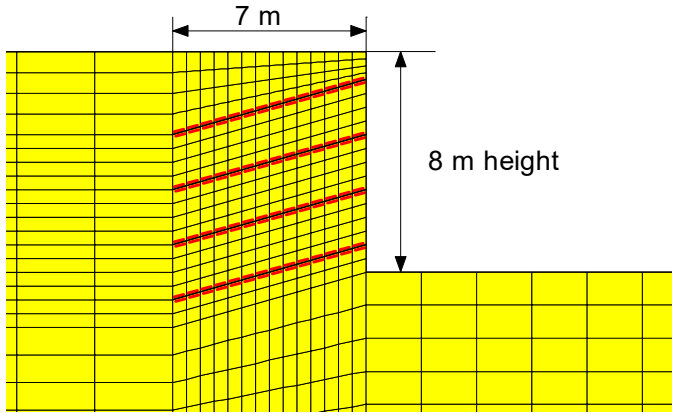

Figure 9-24 A vertical wall retained with nails

One of the possible procedures for computing the stresses in the ground is to do a gravity "turn-on" analysis. Basically, this means that we have constructed the structure and then we turn on gravity to check the performance of the structure. In reality, this is of course not possible, but this is possible with numerical models. The thinking here is that the modeling does not exactly follow the construction procedure, but after the construction is complete the stresses will adjust themselves to something close to that obtained from a gravity turn-on analysis.

The structural elements representing the nails can have both flexural (bending) stiffness and axial stiffness. Any shear in the nails is consequently included in the stress analysis. The flexural stiffness is related to the specified moment of inertia, and the axial stiffness is related to the *E*, (Young's Modulus) and the effective cross sectional area.

The finite element stresses computed from SIGMA/W or QUAKE/W can be used in SLOPE/W to compute a safety factor. One key point here to remember is that you should model the pore water pressure condition in SIGMA or QUAKE/W and use both the finite element computed stresses and pore water pressure in SLOPE/W. Failure to do may lead to erroneous factor of safety. The safety factors are computed as explained in the Theory Chapter.

The SLOPE/W results are presented in Figure 9-25. There are several significant features in the results. The first is that there is no issue with convergence in a limit equilibrium analysis as discussed earlier in this chapter. A safety factor can be obtained for all trial slip surfaces regardless of how steep the trial slip surfaces become. This confirms that there is a ligitimate minimum. The lowest safety factor is nicely encompassed within safety factor contours. Visual inspection of the diagram in Figure 9-25 shows that the position of the critical slip surface is close to the active wedge angle (i.e., $45^o+\phi/2$).

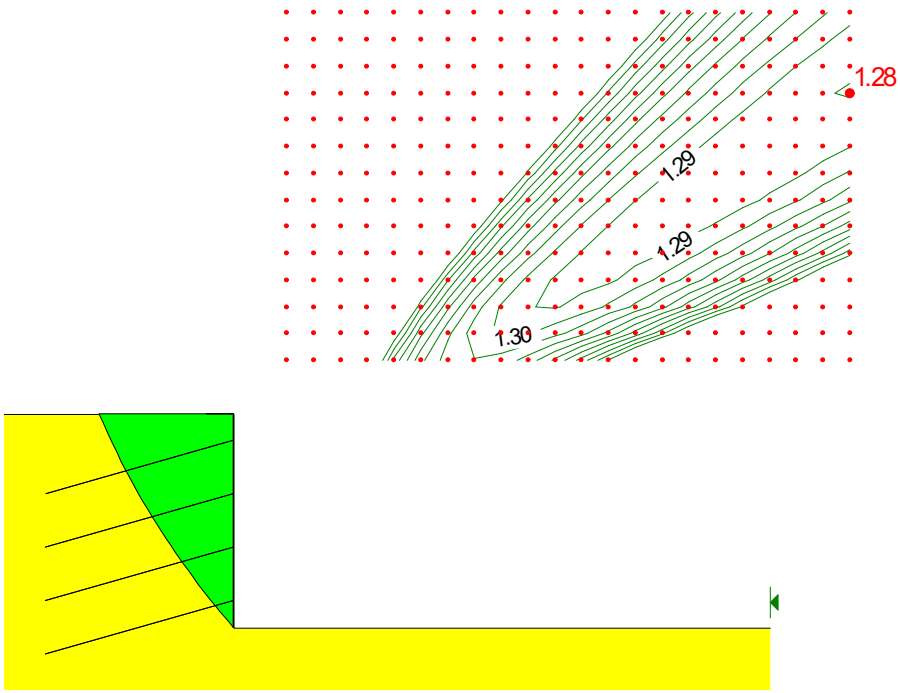

Figure 9-25 SLOPE/W stability analysis results based on SIGMA/W stresses

The nails are not included in the SLOPE/W analysis as concentrated point loads. The effect of the nails is in the SIGMA/W stress distribution and it is the SIGMA/W stresses that give an indication of the safety factor.

Another significant observation is that there are many trial slip surfaces with very similar safety factors. Note all the trial slip surface centres encompassed by the 1.29 safety factor contour. This indicates that there is not one critical slip surface, but a potential failure zone where the safety factors are all very similar.

The integrated approach has the attraction that we can actually look at the stress distributions in the nails. In a limit equilibrium analysis we can only deal with concentrated point loads with the assumption that the nail can somehow provide the load. In a stress analysis we can actually examine the axial, moment and shear distributions in the nails. Figure 9-26 and Figure 9-27 show the axial, moment and shear distributions in the nail third from the top.

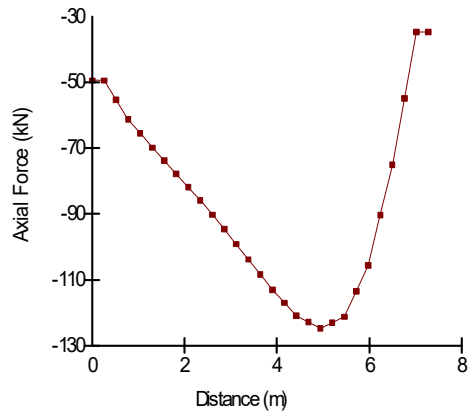

Figure 9-26 Axial force in nail

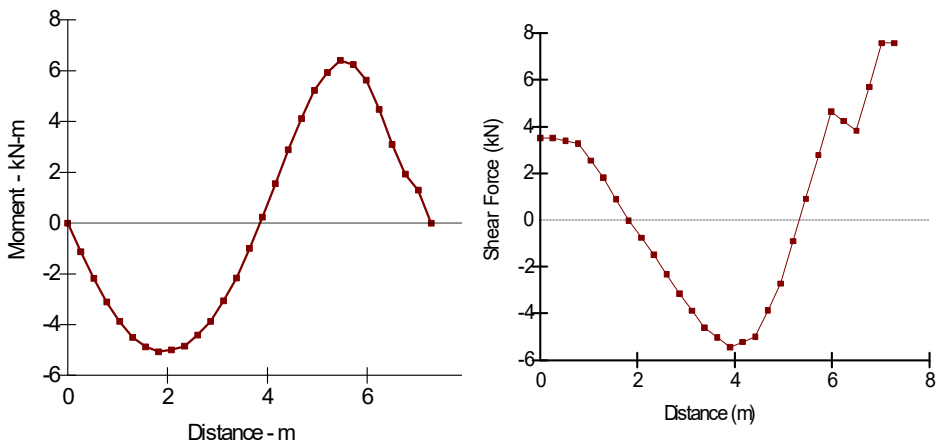

Figure 9-27 Moment and shear distribution in the nail

The acting nail stresses can be compared with the structural capacity of the nails to ensure that they do not exceed safe limits. This assessment needs to be done independently of the SIGMA/W and SLOPE/W analyses.

Examination of the SIGMA/W stresses shows that there is no horizontal tension in the reinforced zone as indicated by a limit equilibrium analysis. Earlier in this chapter it was pointed out that in a limit equilibrium analysis with lateral concentrated loads, tension is required between slices in order to achieve slice force equilibrium. In reality that is not the case, as we can see in Figure 9-28 which shows the horizontal stress along the slip surface. There is a small amount of tension near the ground surface, but this is as one would expect.

The more realistic stress distribution is possible because the local safety factor is now not limited to be a constant value across the slip surface, as it is in a limit equilibrium analysis. The local safety factor now varies as illustrated in Figure 9-29. Locally the factor of safety varies a lot, but globally the overall the factor of safety is 1.28.

Near the toe there two slices that have a safety factor less than 1.0. This is the result of a linear-elastic analysis, which does not re-distribute stresses in overstressed zones. For stability analyses, the consequence of small overstressed zones is discussed in detail in the Limit Equilibrium Fundamentals Chapter.

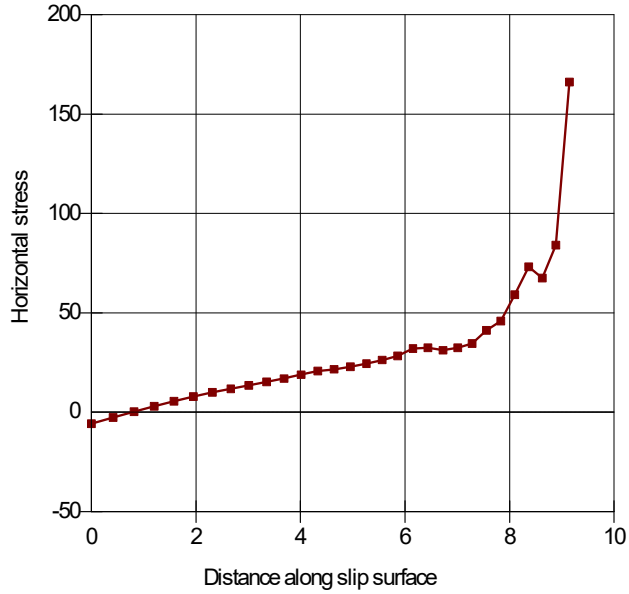

Figure 9-28 Horizontal stress along slip surface

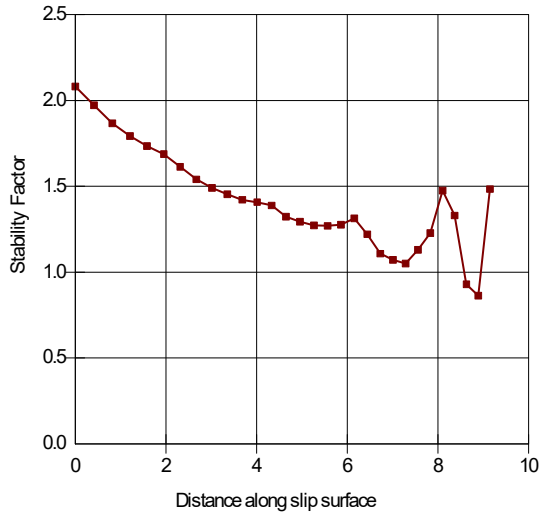

Figure 9-29 Local safety factors along the slip surface

Wall facing has been ignored in the SIGMA/W analysis the same as in a LE analysis. In reality, some form of structural facing is clearly required to prevent spalling and squeezing of the soil past the nails. Structural elements representing the facing could be included in a SIGMA/W analysis, but such added detail is not always necessary for a global stability analysis.

Tie-back wall

Figure 9-30 shows the case of a tie-back retaining structure. The wall is sheet piling and the anchors are pre-stressed at the time of installation. The wall was created in five steps by first excavating to a level below the top anchor. The top anchor was then installed and pre-stressed. Next, the excavation proceeded

to a level below the lower anchor, and then the lower anchor was installed and pre-stressed. Finally, the last of the excavation material was removed.

This example is different than the wall with nails discussed above in that the insitu stresses were first established and then the excavation process was simulated by removing elements from the SIGMA/W analysis. The details of this case are included with SIGMA/W as one of the examples.

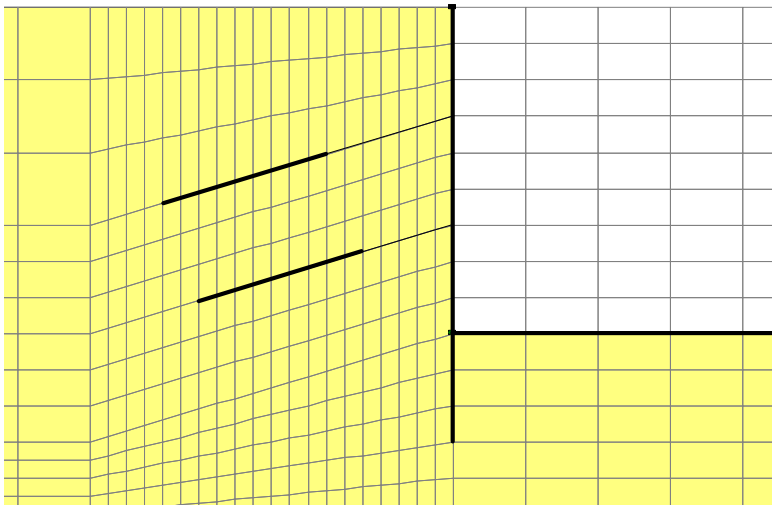

Figure 9-30 A sheet pile wall with pre-stressed tie-back anchors

When using the stresses computed at the end of construction in a stability analysis, the results are as in Figure 9-31. As with the nailed wall discussed earlier, there is no difficulty with convergence and consequently a true minimum safety factor exists within the grid. The minimum value is nicely encompassed by the 1.5 contour. Also, again there are many trial slip surfaces that have very similar safety factors. Figure 9-32 shows the 20 most critical slip surfaces, and they all fall within a relatively narrow band.

An interesting observation is the position of the critical slip surface. It is well behind the traditional active wedge line as shown graphically in Figure 9-33. The anchors have altered the stresses in the ground such that the critical slip surface is further back from the wall than one would expect from simple earth pressure considerations.

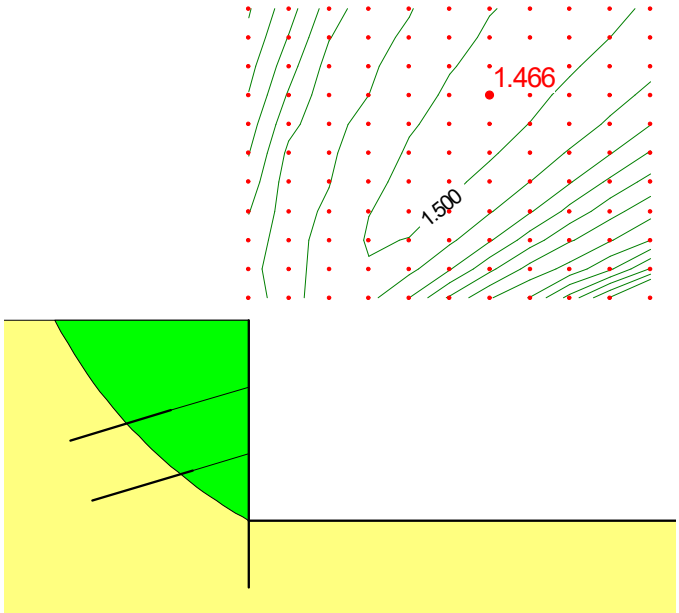

Figure 9-31 Stability analysis based on finite element stresses

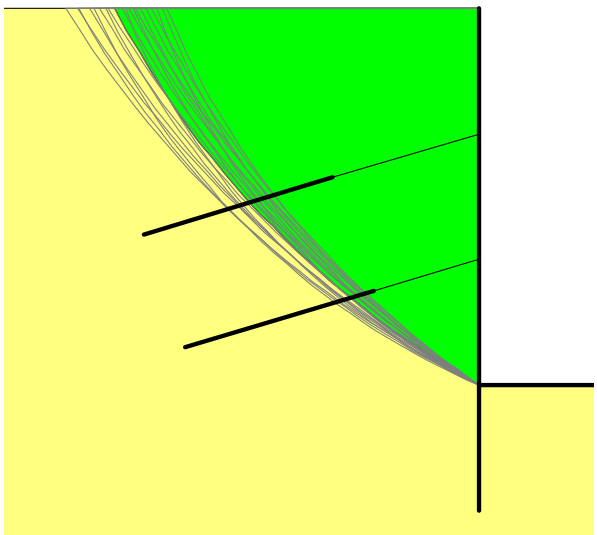

Figure 9-32 Twenty most critical slip surfaces

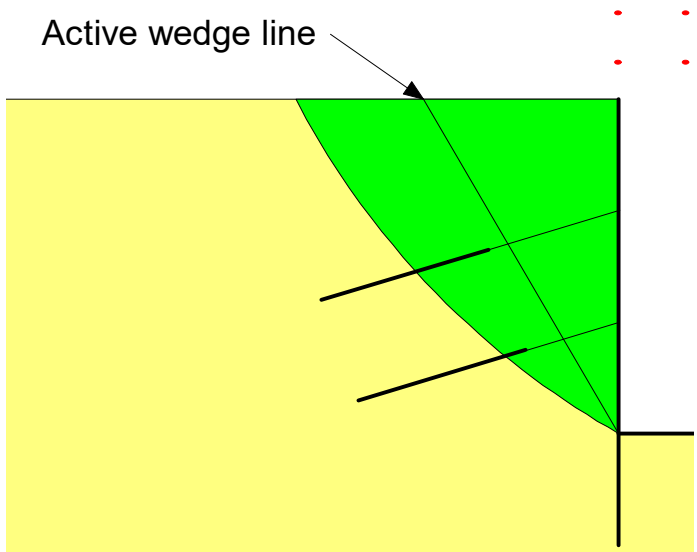

Figure 9-33 Position of critical slip surface relative to active wedge

Now we not only get the stresses in the anchors, but we can also get the stresses in the sheet piling. Figure 9-34 shows, for example, the moment distribution in the wall at the end of construction.

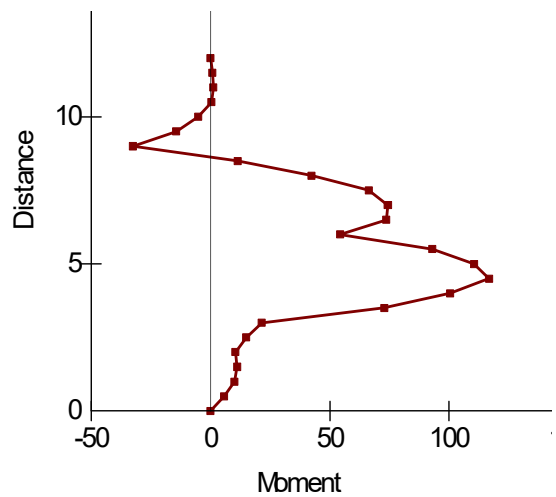

Figure 9-34 Moment distribution in sheet piling

Soil-structure interaction safety factors

Care is required when interpreting safety factors based on finite element computed stresses, particularly if structural components are included.

To start with, let us look at a simple active earth pressure situation (Figure 9-35). The lateral earth pressure is represented by a resultant P_a at the lower third-point on the wall.

The coefficient of active earth pressure is:

$$K_a = \tan^2(45 - \phi/2)$$

So when ϕ is 30 degrees, K_a is 0.33.

Assume that the wall height is 10m and the soil unit weight is 20 kN/m^3. The theoretical lateral earth pressure resultant then is:

$$P_a = \frac{\gamma H^2}{2} K_a = \frac{20 \times 10^2}{2} \times 0.33 = 330$$

If a line P(a) of 330 kN is applied in SLOPE/W, the resulting factor of safety is very close to 1.0. A factor of safety of unity (1.0) therefore represents the active earth pressure case.

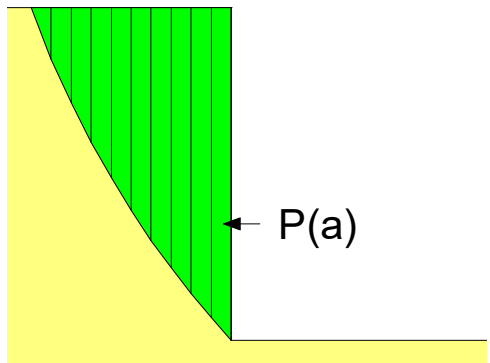

Figure 9-35 Active earth pressure calculation

In both the nailed wall and tie-back wall discussed above the safety factor is greater than 1.0. This means that the structural components are retaining forces that are greater than those represented by the active case. In the case of the tie-back wall, the sheet piling together with the anchors is stiff enough and strong enough to retain equivalent forces that are greater than those represented by the active case.

The main point here is that the SLOPE/W factor of safety has to be viewed differently than in a conventional slope stability analysis. In the case of the tie-back wall, a factor of safety of 1.0 or less does not mean the structure will necessarily collapse. The structure will maintain its integrity provided the structural components are not overstressed and more resisting capacity can be mobilized from the structural components. In an extreme case like a strutted wall, the material behind the wall could conceptually be a weak fluid-like mass, but if the structural components are intact, the wall and the material would remain stable even though the SLOPE/W factor of safety would be near zero.

Assessing the stability of retaining structures such as those discussed here requires more than just looking at the SLOPE/W factor of safety. SLOPE/W only provides the margin of safety against the potential sliding of the soil wedge that is retained. The structural components need to be assessed separately to check that they are not overstressed.

Perhaps the objective is to design for pressures greater than the active case. Then the SLOPE/W factor of safety would need to be greater than 1.0. That would be a legitimate design objective. In the end, it is vitally important to fully comprehend the significance and meaning of the SLOPE/W factor of safety when the computations are based on finite element soil-structure interaction analyses.

Care is required in interpreting the SLOPE/W safety factors when finite element stresses from a soil-structure interaction analysis are used in the stability assessment.

Shear wall

SIGMA/W computed stresses can also be useful when assessing the effectiveness of a shear wall to improve the stability of a slope. Figure 9-36 shows a slope with a slip surface where the Safety Factor is 1.17. The objective is to attempt to improve the margin of safety by driving piles from the bench through the upper weaker material into the underlying more competent material.

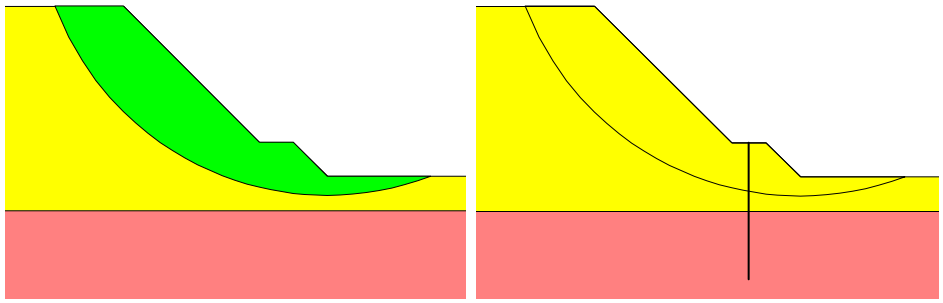

Figure 9-36 Finite element analysis with a shear wall

A SIGMA/W analysis can be done with and without the pile. The pile is modeled as a structural element. If the structural element is assigned a flexural (bending) stiffness, but no axial stiffness, then the stresses can be determined using a gravity "turn-on" approach. If the pile is assigned an axial stiffness, then the surrounding soil hangs-up on the pile when the gravity is turned on. This results in unreasonable stresses around the pile. A more realistic stress distribution can be obtained if the pile axial stiffness is ignored by making $E = 0$ or a small number.

The bending stiffness (moment of inertia) alters the stress distribution and in turn improves the margin of safety. When the SIGMA/W stresses with the pile in place are used in SLOPE/W, the Safety Factor is 1.52, as demonstrated in Figure 9-37.

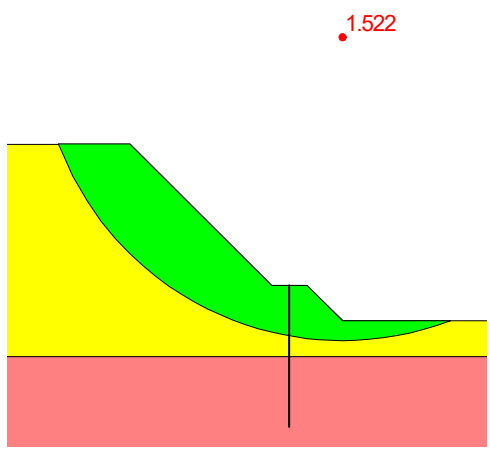

Figure 9-37 Factor of safety with the shear wall in place

Figure 9-38 shows the horizontal stress distributions along the slip surface without and with the pile in place. Note that with the pile in place (right diagram) the horizontal stress peaks at about 90 kPa and then suddenly drops to 40 kPa. In other words, up-slope of the pile, the horizontal stresses are higher and down-slope of the pile, the stresses are lower than when the pile is not present.

In a conventional limit equilibrium analysis, the effect of the pile has to be included as a specified shear value as discussed earlier in this chapter. The difficulty is in knowing the magnitude of the shear.

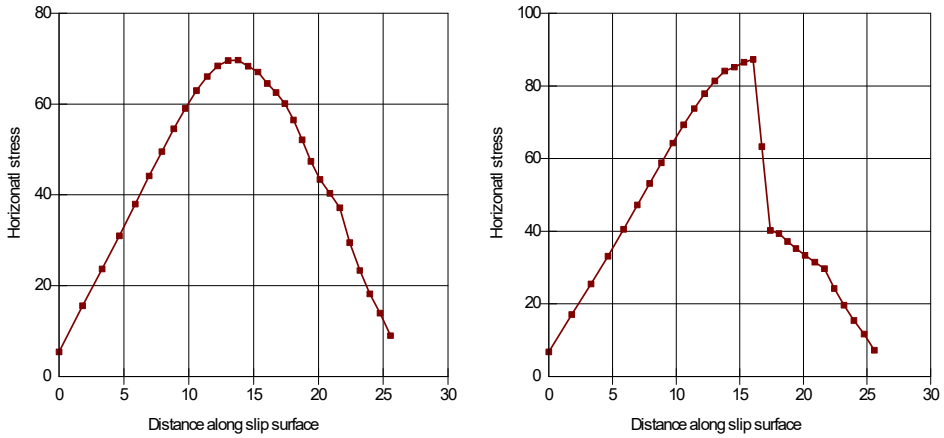

Figure 9-38 Horizontal stresses along slip surface without and with pile

As with any of these soil-structure interaction problems, the structural integrity has to be checked independently. SIGMA/W can provide the moment and shear distributions, as illustrated in Figure 9-39. These data can be used to check that the pile has not been overstressed.

As with the retaining structures discussed above, the factors of safety obtained from as shear-wall analysis need to be interpreted with considerable care. Once again, a factor of safety of less than unity does not necessarily mean the structure will collapse. If the structural components are not overstressed, then the structure may very well be stable even though the SLOPE/W factor of safety is less than 1.0. This is something that needs to be judged in the context of the project requirements and the site-specific design. The important point here is to highlight the need for careful evaluation of the meaning of the SLOPE/W computed factor of safety.

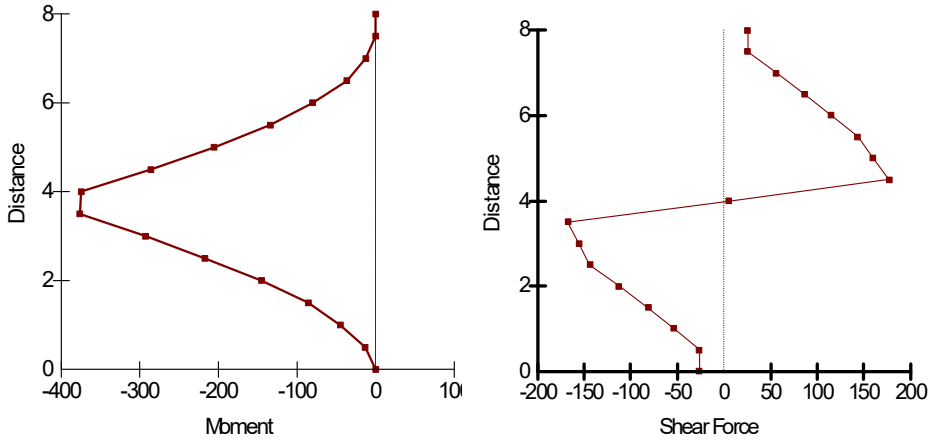

Figure 9-39 Moment and shear distribution in wall

A shear-wall concept can be effective if the structure is founded in competent underlying soil. The underlying soil needs to be able to resist the lateral thrust of the unstable upper soil and the pile needs to transfer this thrust to the competent soil. Without a competent underlying stratum, the shear wall concept is generally not very effective in improving stability.

Key issues

Assessing the stability of geotechnical structures using finite element computed stresses has many attractions and advantages over conventional limit equilibrium types of analyses. It overcomes many of the numerical difficulties associated with limit equilibrium formulations. Unfortunately, establishing the finite element stresses is not all that straightforward. The analyst needs to be intimately familiar with finite element stress-strain types of analyses. Correctly modeling the interaction between the soil and the structural components is a fairly advanced task and needs to be done with considerable care.

Remember, the stress-based approach for assessing the stability of retained structures is only as good as the computed finite element stresses.

Also, it is vitally important to recognize that the actual stresses in the field will be highly dependent on the construction details and procedures. Any stress-based stability analysis needs to be judged and evaluated in light of the actual installation.

Moreover, it is important to remember that using finite element computed stresses in a stability analysis is a fairly new technique. Software tools such as SIGMA/W and its integration with SLOPE/W now makes it possible to do these types of analyses, but the method has as yet not been used extensively in practice, at least not in routine practice as have limit equilibrium types of analyses. Until the industry has more experience with the stress-based approach, it is perhaps prudent to use both the older limit equilibrium methods and the newer stress-based approach to judge and assess the stability of retained earth structures.

One key point here to remember is that you should model the pore water pressure condition in SIGMA or QUAKE/Wand use both the finite element computed stresses and pore water pressure in SLOPE/W..

10 Seismic and Dynamic Stability

10.1 Introduction

This chapter deals with seismic or dynamic forces and how they can be considered in a stability analysis. These types of forces are usually oscillatory, multi-directional, and act only for moments in time. In spite of this complex response, static forces are sometimes used to represent the effect of the dynamic loading. The second concern is that the slope may not completely collapse during the shaking, but there may be some unacceptable permanent deformation.

In SLOPE/W, dynamic effects can be considered in several ways. The simplest is a pseudostatic type of analysis. A more complex way is to use QUAKE/W finite element dynamic stresses and pore-water pressures together with SLOPE/W.

10.2 Rapid loading strength

Under certain conditions, it can be argued that the dynamic loading is so rapid that the soil strength behaves in an undrained manner. This may be the case for saturated clayey soils, for example, but not for unsaturated gravels or rock fill.

As discussed in the Limit Equilibrium Fundamentals chapter, a limit equilibrium formulation finds those forces acting on a slice so that the slice is in force equilibrium and so that the factor of safety is the same for every slice. If a dynamic force is applied to a slice, the slice forces will be re-adjusted, which will include a re-adjustment of the base shear strength. SLOPE/W has an option to keep the slice base shear strength unaltered even when the dynamic force is applied.

Consider the simple slope in Figure 10-1. For illustrative and explanation purposes here, only one slip surface is considered. The strength parameters are c equal to zero and ϕ equal to 30 degrees.

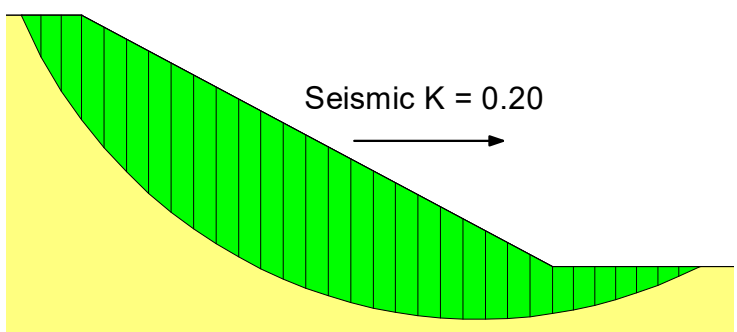

Figure 10-1 Illustrative example with seismic forces

Figure 10-2 compares the shear strength along the slip surface with and without any seismic forces. Applying the seismic forces alters the shear strength profile. This is primarily due to a change in normal stress distribution along the slip surface.

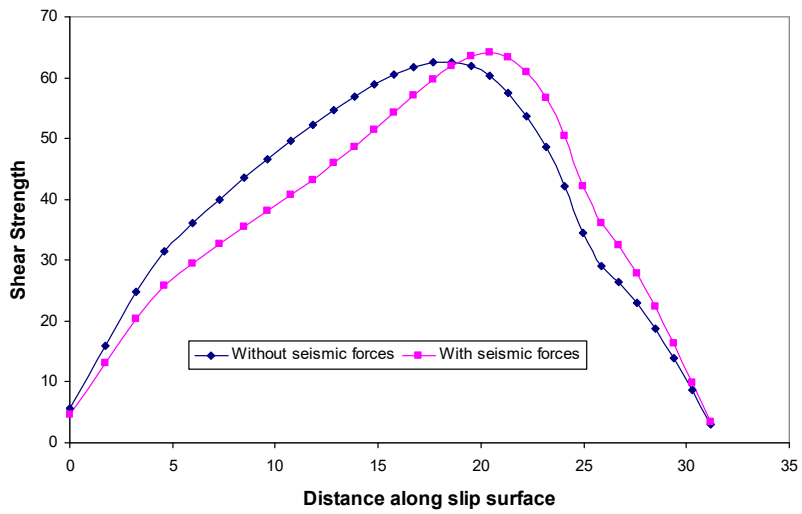

Figure 10-2 Effect of seismic forces on altering the shear strength

If the option to keep the shear strength unaltered due to seismic forces is selected, SLOPE/W first does an analysis without any seismic forces, to establish the strength along the slip surface. The shear strength at the base of each slice is then converted into an equivalent undrained (cohesive) strength. The analysis is then repeated with the seismic loading. The undrained shear strength is not a function of the normal stress and, consequently, the seismic loads do not alter the shear strength. This is illustrated in Figure 10-3. The graph on the left shows the frictional strength before the seismic forces are applied. The graph on the right shows that the strength was converted into an equivalent cohesive strength. Note that the strengths are the same in both graphs.

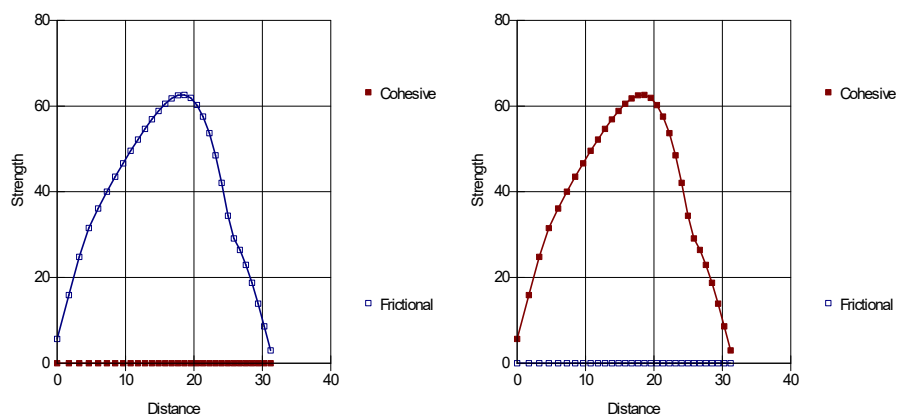

Figure 10-3 Conversion of frictional strength to cohesive strength

Selecting the option to convert to an undrained strength while the seismic forces are applied tends to increase the factor of safety slightly. In this simple illustrative case, the factor of safety increases from 1.102 to 1.150. This suggests that allowing the shear strength to change in response to the seismic forces errs on the safe side.

In the end, the decision to use this option needs to be made in the context of the particulars of each specific project. It is always advisable to do an analysis with and without selecting this option and then make a decision in light of the difference.

10.3 Pseudostatic analysis

A pseudostatic analysis represents the effects of earthquake shaking by accelerations that create inertial forces. These forces act in the horizontal and vertical directions at the centroid of each slice. The forces are defined as:

$$F_h = \frac{a_h W}{g} = k_h W$$

$$F_v = \frac{a_v W}{g} = k_v W$$

where:

a_h and a_v	=	horizontal and vertical pseudostatic accelerations,
g	=	the gravitational acceleration constant, and
W	=	the slice weight.

The ratio of *a/g* is a dimensionless coefficient *k*. In SLOPE/W, the inertial effect is specified as k_h and k_v coefficients. These coefficients can be considered as a percentage of *g*. A k_h coefficient of 0.2, for example, means the horizontal pseudostatic acceleration is 0.2g.

In SLOPE/W, the horizontal inertial forces are applied as a horizontal force on each slice as shown in Figure 10-4. For example, if k_h is 0.2 then the magnitude of the force is 0.2 times the slice weight which equals 22.697.

Vertical inertial forces in SLOPE/W are added to the slice weight. Say that k_v is 0.1. The weight for the same slice as in Figure 10-4 is then 113.48 plus (0.1 x 113.48) which equals 124.83. The diagram in Figure 10-5 confirms this. Note that the horizontal force is based on the actual gravitational weight of the slice and not on the altered weight.

Vertical coefficients can be positive or negative. A positive coefficient means downward in the direction of gravity; a negative coefficient means upward against gravity.

The application of vertical seismic coefficients often has little impact on the safety factor. The reason for this is that the vertical inertial forces alter the slice weight. This alters the slice base normal, which in turn alters the base shear resistance. If, for example, the inertial force has the effect of increasing the slice weight, the base normal increases and then the base shear resistance increases. The added mobilized shear arising from the added weight tends to be offset by the increase in shear strength. Of course this is only true for frictional strength components and not for cohesive strength components.

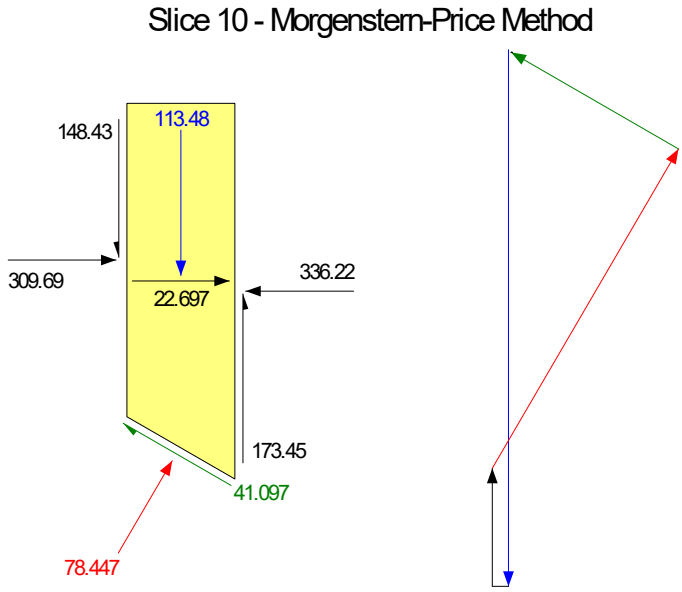

Figure 10-4 Horizontal seismic inertial force at slice centroid

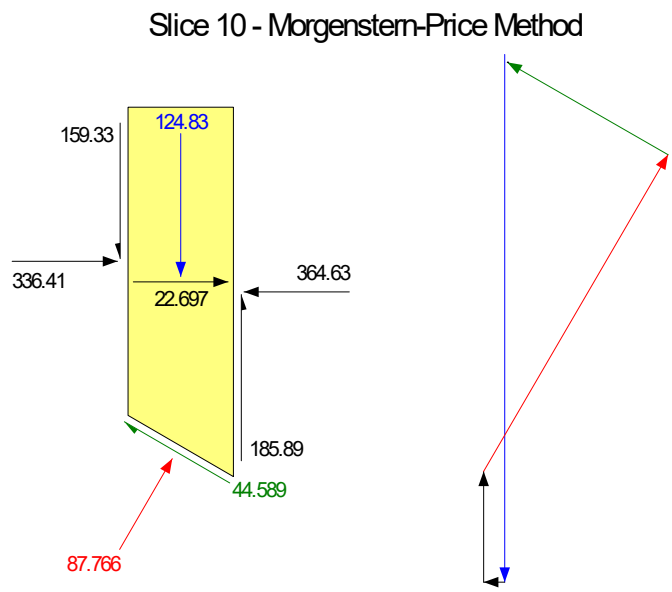

Figure 10-5 Slice forces with a k_v specified

The weight arising from ponded water up against a slope is not included in the calculation of the inertial forces. The thinking is that water (zero strength material) has no shear strength and therefore inertial forces acting on the water do not contribute to destabilizing the slope. Figure 10-6 illustrates a slope with a submerged toe. The inertial forces are now not directly equal to kW, as demonstrated in Figure 10-7. $K_h W$ is 0.2 times 76.474 = 15.29 for Slice 25 which is more than the actual 6.134 applied. The seismic coefficient is only applied to the total slice weight minus the surcharge water weight.

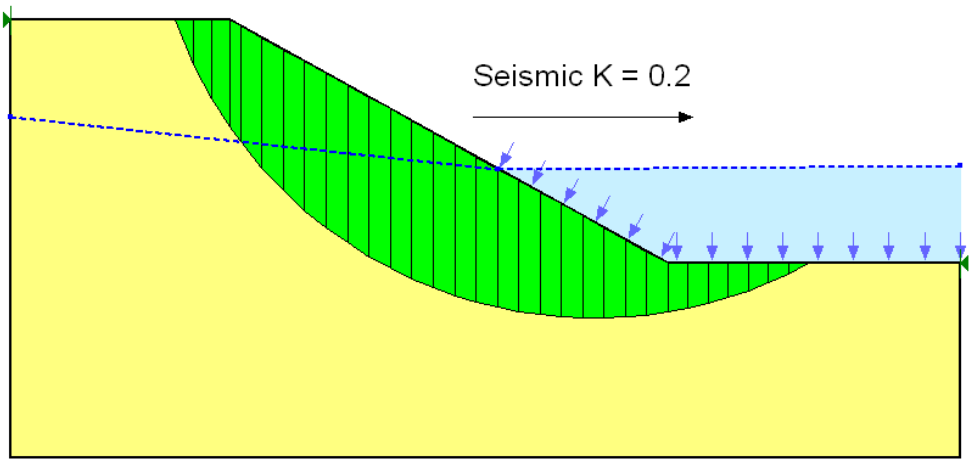

Figure 10-6 Example of slope with a submerged toe

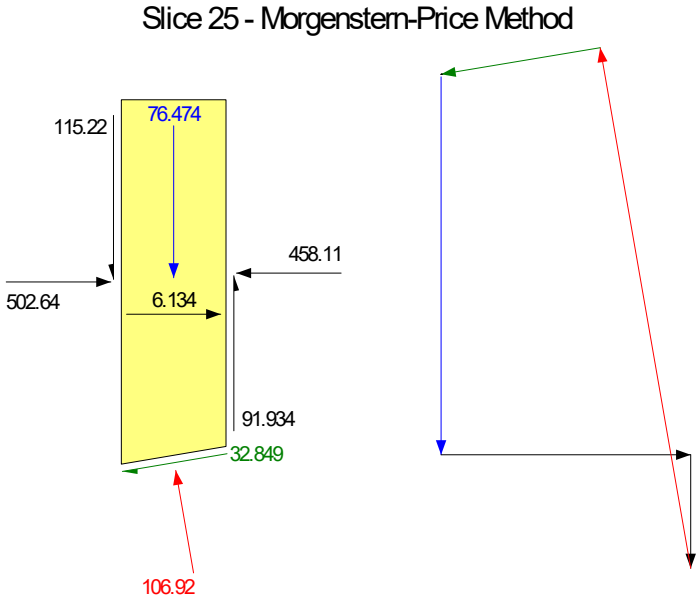

Figure 10-7 Inertial force for slice under water

Horizontal inertial seismic forces can have a dramatic effect on the stability of a slope. Even relatively small seismic coefficients can lower the factor of safety greatly, and if the coefficients are too large, it becomes impossible to obtain a converged solution. It is consequently always good practice to apply the seismic forces incrementally to gain an understanding of the sensitivity of the factor of safety to this parameter. It is often useful to create a graph such as in Figure 10-8. As the seismic coefficient increases, there should be smooth gradual decrease in the safety factor.

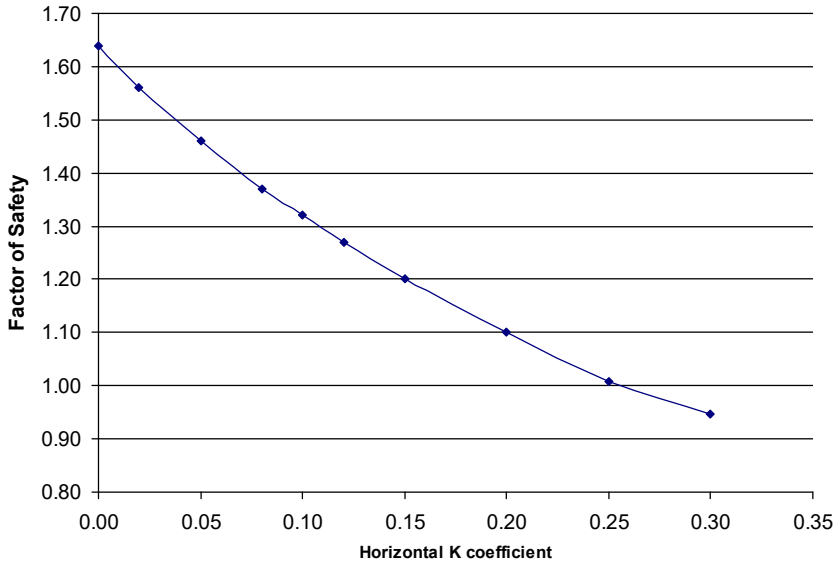

Figure 10-8 Factor of safety as function of k_h

The difficulty with the pseudostatic approach is that the seismic acceleration only acts for a very short moment in time during the earthquake shaking. As we will see in the next section, the factor of safety in reality varies dramatically both above and below static factor of safety. The factor of safety may even momentarily fall below 1.0, but this does not mean the slope will necessarily totally collapse. Looking at this issue more realistically requires knowing something about the shear stress variation during the earthquake shaking. This can be done with a QUAKE/W dynamic finite element analysis.

Staged Pseudostatic analysis

SLOPE/W has the option to perform a multi-staged pseudo-static analysis that ignores the seismic forces on the first stage of the analaysis in order to compute the shear strength at the base of each slice (KeyIn | Analyses | Staged Pseudo-static analysis). The seismic forces are included in the second stage of the analysis. The shear strength at the base of each slice is calculated using one of two options:

Option 1: Effective Stress Strengths

The effective stress shear strength at the base of each slice is calculated by the Mohr-Coulomb failure law using the effective base normal stress and the cohesion and friction angle in the material model definition.

Option 2: Undained Strengths (Duncan, Wright and Wong (1990)

The undrained strength is calculated by the equations proposed by Duncan et al. (1990), which make use of the R-envelop strength properties in the material model definition (Refer to the Section on Rapid Drawdown Analysis using the Staged Approach). The effective stress strengths are computed during the second stage of the analysis when the seismic forces are applied. The smaller of the undrained or effective stress strength at the base of a slice is used to calculate the factor of safety.

10.4 Dynamic analysis

Figure 10-9 presents an example of a 10-meter high slope. The slope is subjected to the 10 seconds of shaking arising from the earthquake record in Figure 10-10.

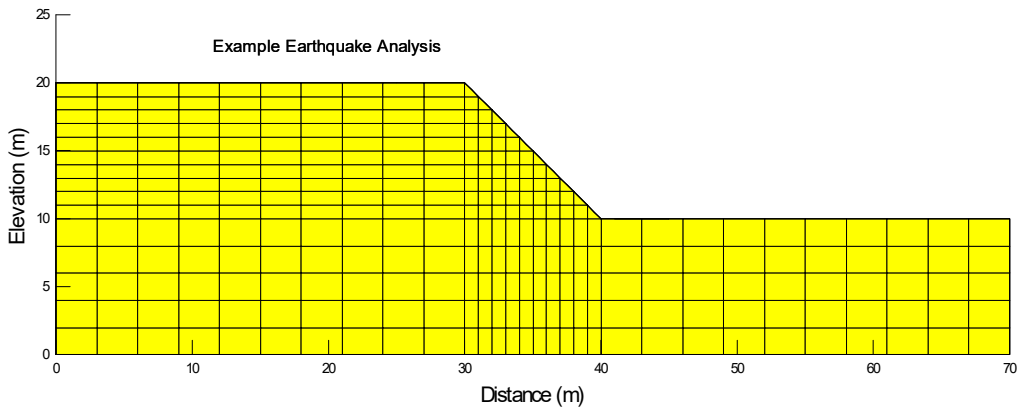

Figure 10-9 Slope subjected to earthquake shaking

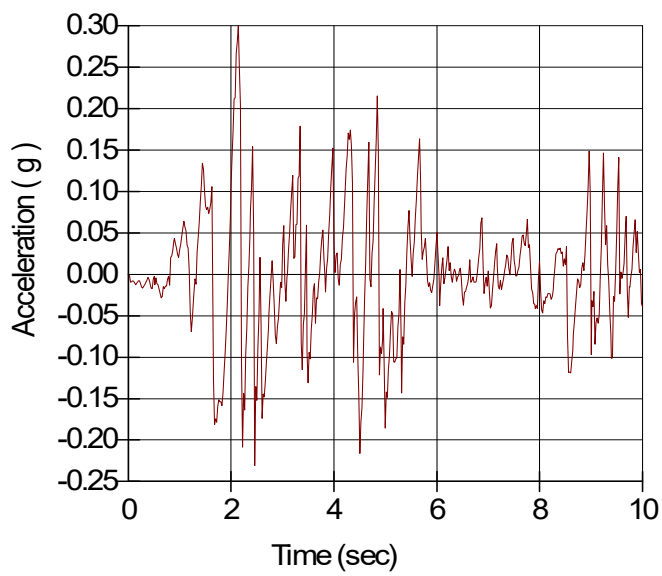

Figure 10-10 Example earthquake record

QUAKE/W can animate the motion of the slope during the entire 10 seconds. The diagrams in Figure 10-11 and Figure 10-12 are two snapshots during the shaking and as is readily evident, the dynamic stresses oscillate dramatically. The condition in Figure 10-11 may cause the factor of safety to decrease while the situation Figure 10-12 may cause the factor of safety to increase. This type of information is available for each time step the results are saved to a file during analysis. In this example, the integration along the earthquake record occurred at an interval of 0.02 seconds. The total of 500 integration steps is consequently required for the 10 seconds of shaking. The results were saved for every 10th time step resulting in 50 sets of output files.

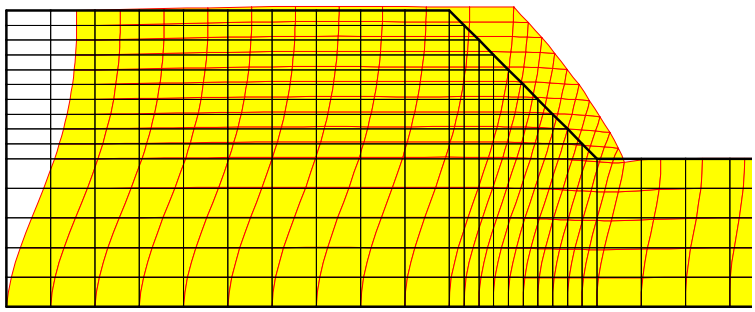

Figure 10-11 A snapshot of the deformation during an earthquake

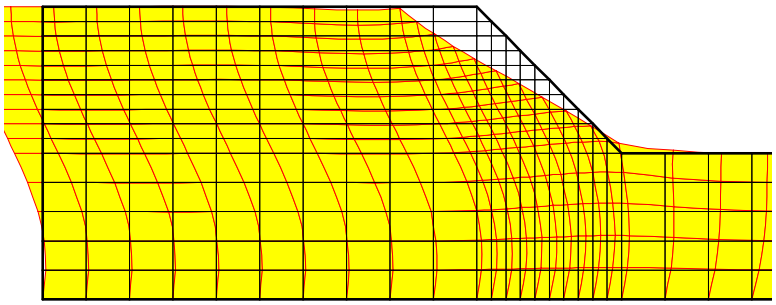

Figure 10-12 A snapshot of the deformation during an earthquake

The earlier chapter on Factor of Safety Methods describes how SLOPE/W can use finite element computed stresses to assess the stability of earth structures. The details will not be repeated here.

SLOPE/W computes a factor of safety for each time step the data is saved to a file. For this example, SLOPE/W computes 50 safety factors. These safety factors can then be plotted versus time as shown in Figure 10-13. The graph vividly illustrates the oscillation in the factor of safety as noted earlier. Note that the factor of safety momentarily falls below 1.0 several times during the shaking.

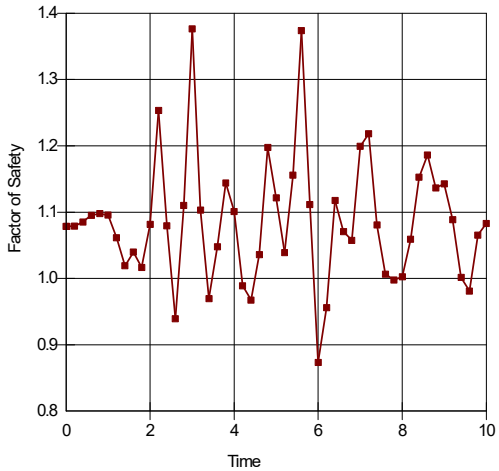

Figure 10-13 Factor of safety versus time

For the factor of safety calculations, the shear strength available along the slip surface is computed based on the initial insitu static stresses and then held constant during the shaking. This has the effect of treating the soil as behaving in an undrained manner during the shaking.

With such a wide variation in factors of safety during the earthquake shaking, it is difficult to say anything meaningful about the slope stability. The issue is more how much movement will take place during the shaking than the total collapse of the slope. An estimate of the resulting deformation can be made from this data, as described in the next section.

10.5 Permanent deformation

The stresses from QUAKE/W are the sum of the static plus dynamic stresses. The static stresses are known from the specified initial insitu stresses. Subtracting the initial static stresses from the QUAKE/W stresses therefore gives the dynamic stresses. In equation form:

$$\sigma_{dynamic} = \sigma_{QUAKE} - \sigma_{static}$$

The dynamic stress can be computed at the base of each slice. Integrating along the entire slip surface then gives the total dynamic mobilized shear. This is the additional shear created by the earthquake shaking.

Dividing the total mobilized dynamic shear by the potential sliding mass provides an average acceleration value. This value is obtained for each time integration step during the shaking and can be plotted against the corresponding factor of safety to produce a plot such as in Figure 10-14. The average acceleration corresponding to a factor of safety of 1.0 is called the yield acceleration, a_y. It is by definition the overall average acceleration that will cause the sliding mass to fail or move. In this example, a_y is 0.048.

The average acceleration obtained at each integration step can also be plotted with time as in Figure 10-15. Where the average acceleration exceeds a_y, the slope will move.

The average acceleration is representative of the resultant of both horizontal and vertical applied accelerations in the QUAKE/W analysis.

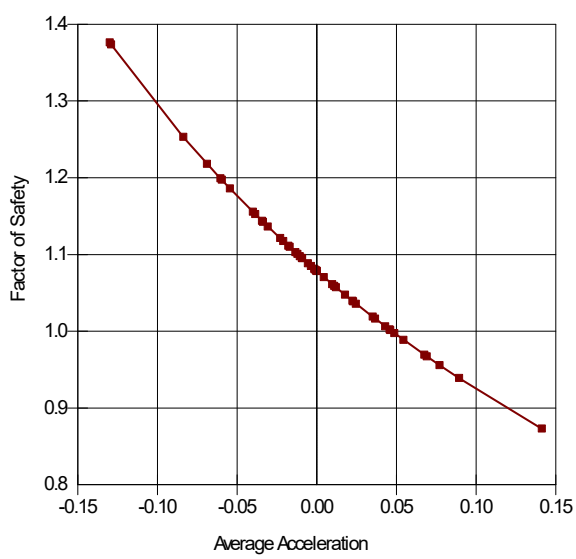

Figure 10-14 Average acceleration versus safety factors

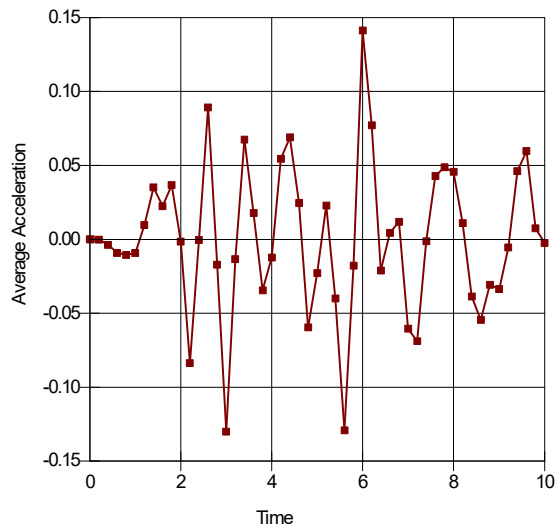

Figure 10-15 Average accelerations versus time during the shaking

Integrating the area under the average acceleration versus time curve where the acceleration exceeds a_y, gives the velocity of the sliding mass during the movement as in Figure 10-16.

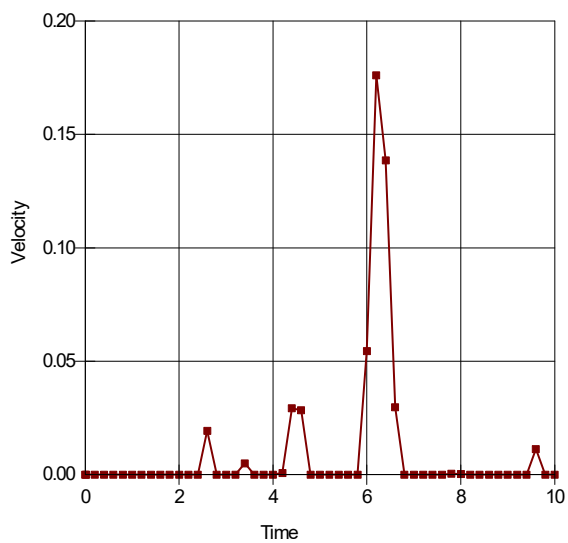

Figure 10-16 Velocity versus time

Integrating the area under the velocity versus time curve gives the cumulative movement during the shaking as in Figure 10-17.

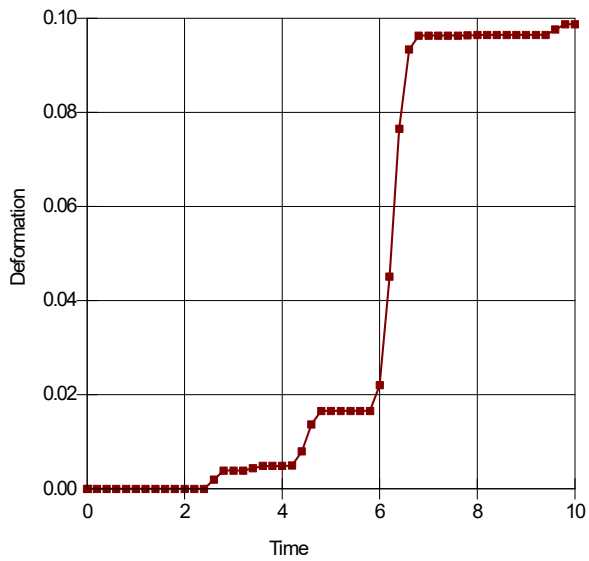

Figure 10-17 Cumulative movement during the shaking

The direction of the movement is parallel to the slip surface. The movement may therefore be both rotational and translational.

You will note that there are negative average accelerations that exceed the yield acceleration. This implies that there is also some up-slope movement, but as is common in these types of analyses, the potential up-slope movement is simply ignored.

SLOPE/W makes this type of calculation for each and every trial slip surface, and this makes it possible to find the trial slip surface with the largest potential movement. For convenience, the trial slip surfaces can be sorted by deformation rather than by factor of safety, to identify the one with the largest movement.

The procedure described here to estimate the permanent deformation is based on the concepts inherent in a Newmark Sliding Block analysis. A Newmark type of analysis is applicable only in certain specific circumstances. The procedure is ideal for cases where there is little or no degradation in the soil shear strength during the dynamic shaking. This may be the case for the rock-fill shells of an earth embankment, steep natural rock slopes or unsaturated, heavily over-consolidated clayey slopes. This procedure is not applicable to cases where there is a significant potential for a large loss in shear strength due to either the generation of excess pore-water pressures or the collapse of the soil grain structure as may be the case for loose silty and sandy soils. Kramer (1996, p. 437) points out that these types of analyses can be unreliable for situations where there is a large build up of excess pore-water pressures or where there is more than about a 15% degradation in the shear strength during the earthquake shaking.

A useful distinguishing characteristic that can help in deciding whether the Newmark procedure is or is not applicable is to decide if the major destabilizing factor is the inertial forces or the weakening of the soil. The Newmark approach is suitable for cases governed by the inertial forces; it is not applicable if soil weakening is the controlling issue.

10.6 Liquefaction stability

In earthquake engineering, there a line of thinking that says that even under the worst possible conditions the factor of safety should not fall below 1.0. That is to say, even if large pore-water pressures have been generated and the soil strength has fallen to its steady state strength, the factor of safety should not be

below 1.0 for design purposes. If the factor of safety is below 1.0 under these severe conditions, the thought is that the risk is unacceptably high for a possible catastrophic liquefaction flow failure.

Two pieces of information are available from a QUAKE/W analysis which can be used to assess the possibility of a flow liquefaction failure. One is the pore-water pressure conditions at the end of shaking and the second is the identification of elements where the soil may have liquefied. The elements that have liquefied can then be assigned the steady-state strength of the material to reflect the weakening associated with the liquefaction.

Figure 10-18 shows an example included with the QUAKE/W software. The shaded elements are ones that have liquefied. Steady-state strength can be used along portions of trial slip surfaces that pass through the liquefied elements.

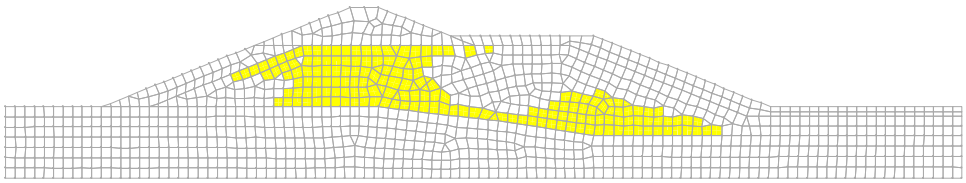

Figure 10-18 Example QUAKE/W analysis showing some liquefied elements

Figure 10-19 shows a trial slip surface. The peak c and ϕ parameters of the red soil are 5 psf and 34 degrees. The peak c and ϕ parameters of the green soil are 0 psf and 34 degrees. The steady-state strength for the green soil is 40 psf. Figure 10-20 shows how the strength parameters fall from peak to steady-state strength along the slip surface. The steady state strength is represented in the cohesion plot. Note that when the slip surface is in the liquefied elements, the steady state strength is used and the friction angle of zero is used.

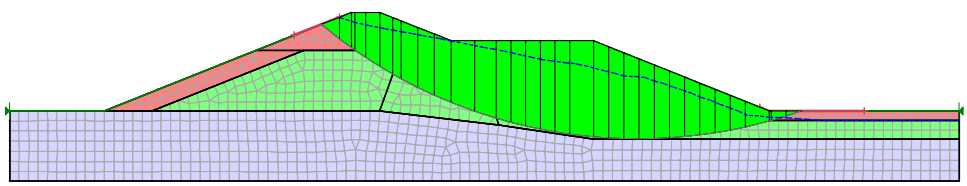

Figure 10-19 A slip surface passing some liquefied elements

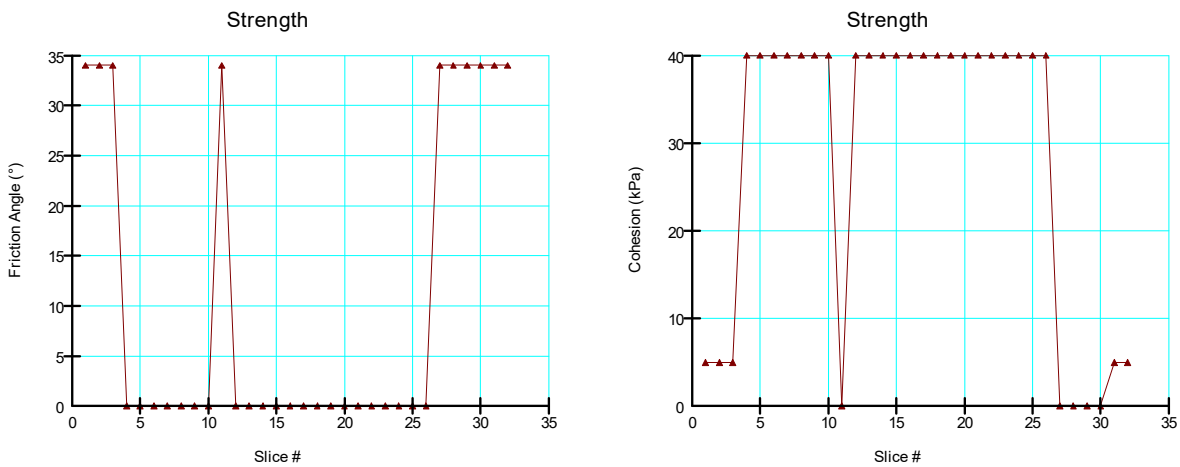

Figure 10-20 Strength parameters (c and ϕ) used along the slip surface

Generally, this analysis is done for stress and pore-water pressure conditions at the end of the shaking. The analysis can, however, technically be done for any time step for which QUAKE/W saved the data.

Using the QUAKE/W liquefaction flags makes the stability analysis relatively straight forward. The downside is that liquefied elements are not necessarily always in a nice cluster. There can be scattered and isolated elements that indicate liquefaction. Numerically this causes the strength parameters to jump back and forth between peak and residual values which may not be all that realistic (Figure 10-20). Furthermore, the system does not provide for any transition between the liquefied and non-liquefied zones. If these undesirable effects are deemed unacceptable in the analysis, then it may be better to use the QUAKE/W results indirectly. Based on interpretation and judgment, a separate stability analysis could perhaps be done by manually including a region in the stability section that is liquefied and assigning the region with the steady state strength. The QUAKE/W results are then only used to indirectly identify the region of possible liquefaction.

11 Probabilistic and Sensitivity Analyses

11.1 Introduction

There is an ever-increasing interest in looking at stability from a probabilistic point of view. University research into the area is increasing, as indicated by a recent Ph.D. study at the University of Alberta, Alberta, Canada (El-Ramly, Morgenstern and Cruden, 2002).

SLOPE/W includes a general comprehensive algorithm for probabilistic analyses. Almost all input parameters can be assigned a probability distribution, and a Monte Carlo scheme is then used to compute a probability distribution of the resulting safety factors. Once the probability distribution of the safety factors are known, other quantifying parameters, such as the probability of failure can be determined.

With a uniform probability distribution, the probabilistic scheme in SLOPE/W can also be used to conduct a sensitivity analysis.

This chapter explains the probabilistic capabilities and features available in SLOPE/W and briefly explains the underlying techniques and procedures used in the formulation. More details of the method can be found in the Theory chapter.

11.2 Probability density functions

Although most natural material parameters may vary statistically in a normal distribution manner, for general purposes, SLOPE/W includes the following probability density functions (PDF):

- Normal
- Lognormal
- Uniform
- Triangular
- Generalized Spline function

Normal function

As is well known, many natural data sets follow a bell-shaped distribution and measurements of many random variables appear to come from population frequency distributions that are closely approximated by a normal probability density function. This is also true for many geotechnical engineering material properties. In equation form, the normal probability density function is:

$$f(x) = \frac{e^{-(x-u)^2/2\sigma^2}}{\sigma\sqrt{2\pi}}$$

where:

x	=	the variable of interest,
u	=	the mean, and
σ	=	the standard deviation.

Figure 11-1 shows a typical Normal distribution for the soil property ϕ when the mean is 30 degrees and the standard deviation is 2 degrees.

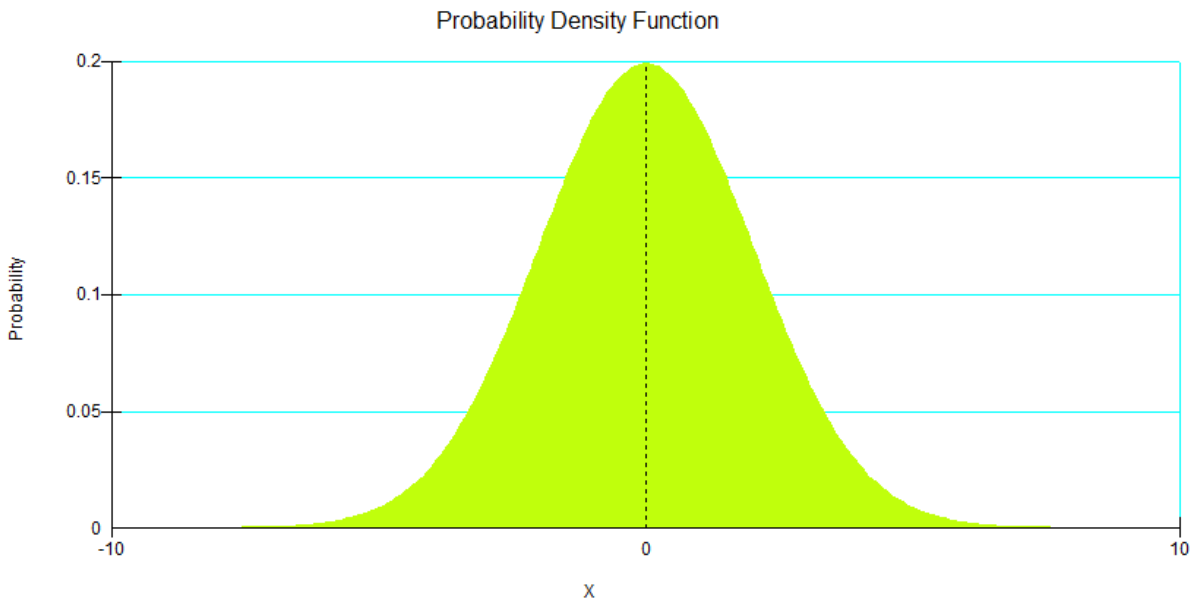

Figure 11-1 Normal probability density function

By default, SLOPE/W uses a range of ± 5 standard deviations. As a result, you will see an offset from the specified value of -10 and +10. That is the ϕ angle obtained from the sampling function during the Monte Carlo trials may vary form 20 degrees to 40 degrees. However, SLOPE/W allows you to specify your own minimum and maximum values. Figure 11-2 shows the same probability density function when clipped with a minimum off set of -5 degrees and a maximum offset of +5 degrees.

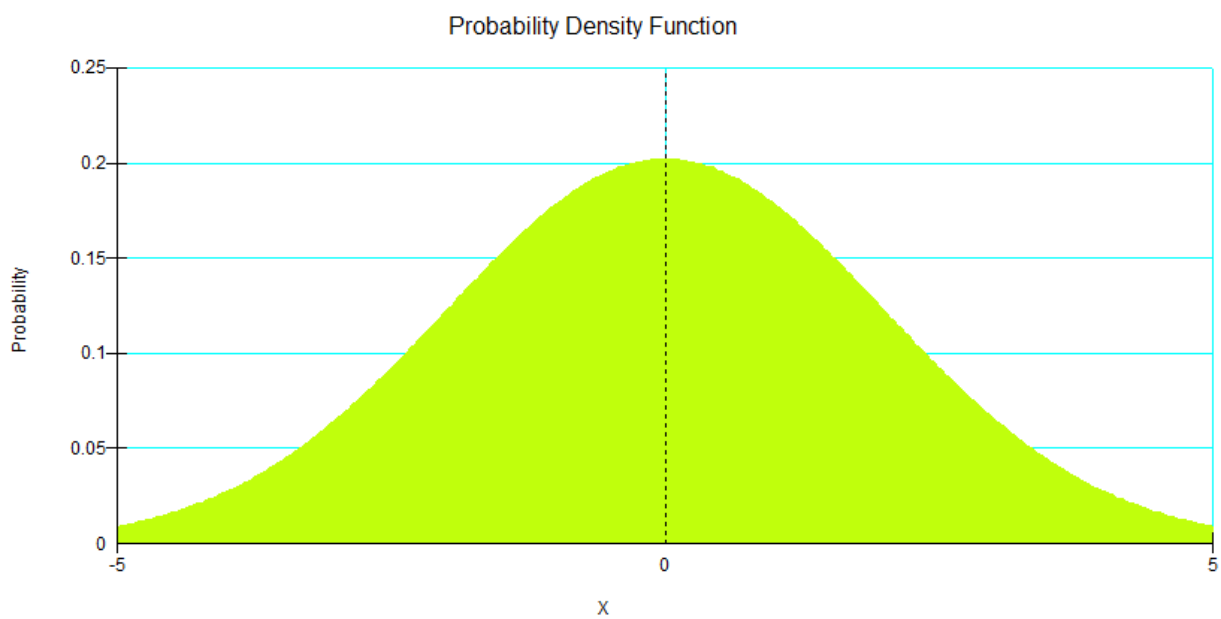

Figure 11-2 A clipped normal probability density function

From the probability density function, SLOPE/W integrates the area under the function to establish a cumulative distribution function and the cumulative distribution function is inverted to form an inverse distribution function or a percent point function.

In SLOPE/W, the inverse distribution function is called a sampling function, since it is this function that is at the heart of sampling the various statistical parameters. The x-axis covers the range of possible random numbers. So, each time a random number is obtained, the parameter is "sampled" using this function. Figure 11-3 presents the resulting sampling function of the clipped normal probability density function.

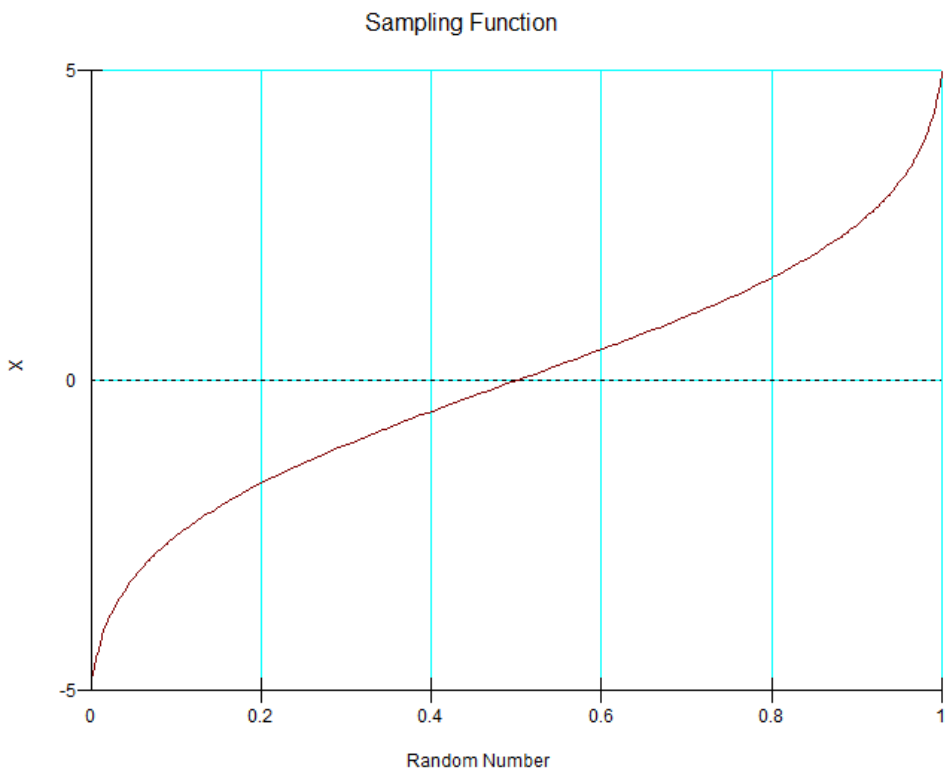

Figure 11-3 A normal sampling function

For the case of a normal probability function, the sampling function has a relatively straight segment in the middle. The implication of this is that parameters around the mean will be sampled more often than values at the extremities of the sampling function.

The normal curve has a convenient property that the area under the normal curve between the mean and any point depends only on the number of standard deviations away from the mean. For example, the area or probability of a value, x, lying between $\pm 1\sigma$ is 68.26%, between $\pm 2\sigma$ is 95.44%, between $\pm 3\sigma$ is 99.72%, between $\pm 4\sigma$ is 99.99% and between $\pm 5\sigma$ is approximately 100.00%.

For example, in SLOPE/W, the mean cohesion of a soil may be specified as 30 kPa with a standard deviation of 5 kPa. This means that for 100 samples, 68.26% of the samples will have a value between 25 and 35 kPa, and 95.44% of the samples will have a value between 20 and 40 kPa.

Lognormal function

With a lognormal function, a variable x is lognormally distributed if the natural log of x (i.e., $ln\ x$) is normally distributed. The general formula for a lognormal probability density function is:

$$f(x) = \frac{e^{-(ln(x-\theta)-m)^2/(2\sigma^2)}}{(x-\theta)\sigma\sqrt{2\pi}}$$

where:

σ	=	the lognormal standard deviation (or shape parameters),
m	=	the lognormal mean (or scale parameter), and
θ	=	the offset the lognormal mean (or the location parameter).

The lognormal distribution parameters σ and m are related to the mean and standard deviation (s.d.) of x by the following:

$$\sigma = \sqrt{ln\left(\left(\frac{s.d.}{mean}\right)^2 + 1\right)}$$

$$m = ln(mean) - \frac{1}{2}\sigma^2$$

The standard lognormal probability density function is the special case when there is no offset (i.e, $\theta = 0$) and a unit lognormal mean (i.e., $m = 1$). Figure 11-4 shows a lognormal probability density function when $\sigma = 1$, $m = 1$ and $\theta = 0$. The function is the same as the standard lognormal probability density function when $\sigma = 1$. Since a negative value cannot be supported in log mathematically, the standard lognormal function always has the distribution starting from zero and heavily skewed to the low x range

This special characteristic of the standard lognormal function posts a limitation to the use of the probability density function in modeling actual engineering parameters with a mean value (m) much larger than 1. SLOPE/W uses the general lognormal formula, where an offset value (θ) can be applied to shift the density function to better represent a probability density function. For example, if the actual mean value of the soil parameters is 18, we can apply an offset or location parameter of 17 (i.e., 18-1) to the general density function. Figure 11-5 shows the density function with the applied offset.

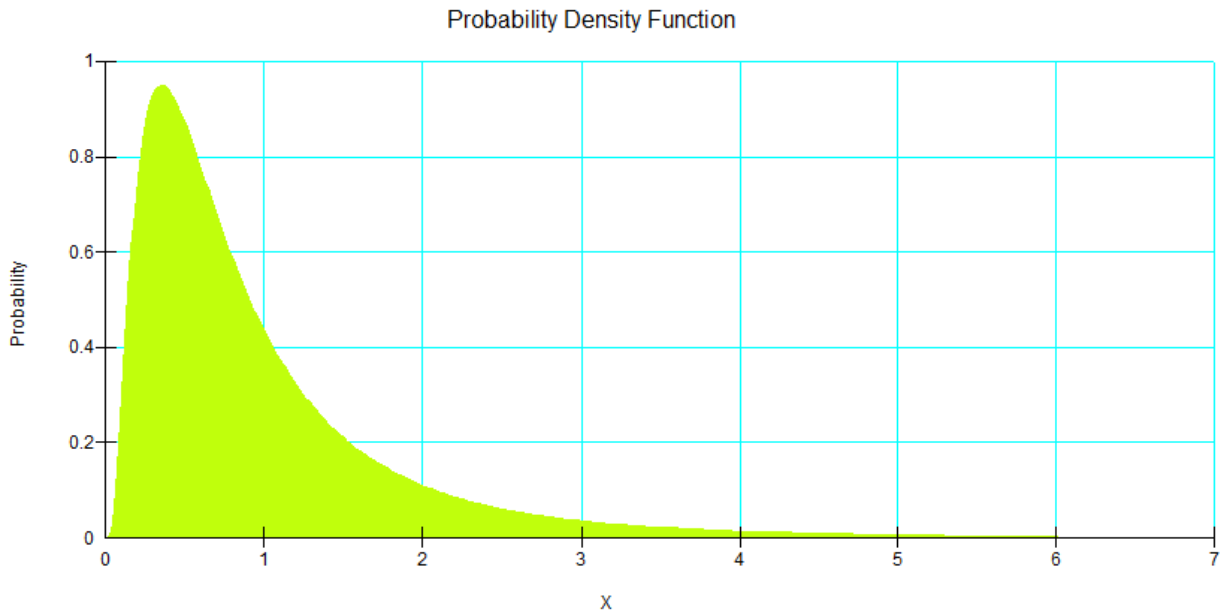

Figure 11-4 Lognormal probability density function

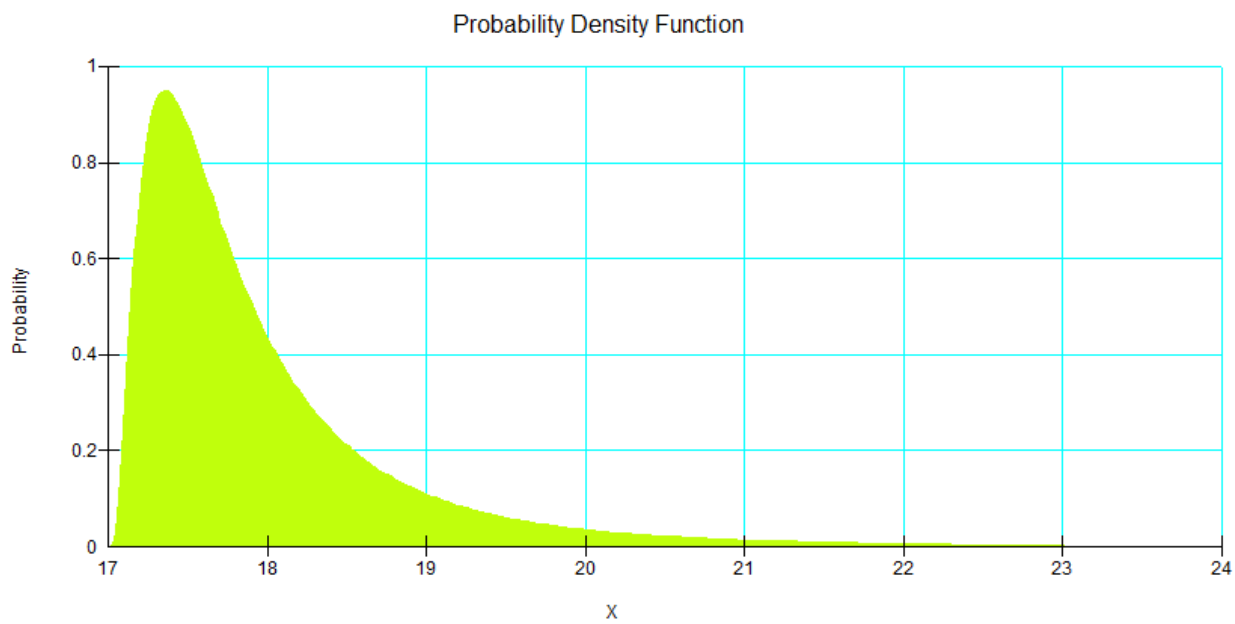

Figure 11-5 Lognormal probability density function with offset

The corresponding sampling function is shown in Figure 11-6. The sampling function indicates that when a random number is generated, there is an increased chance of obtaining a value between 17 and 19. This is consistent with the lognormal density function.

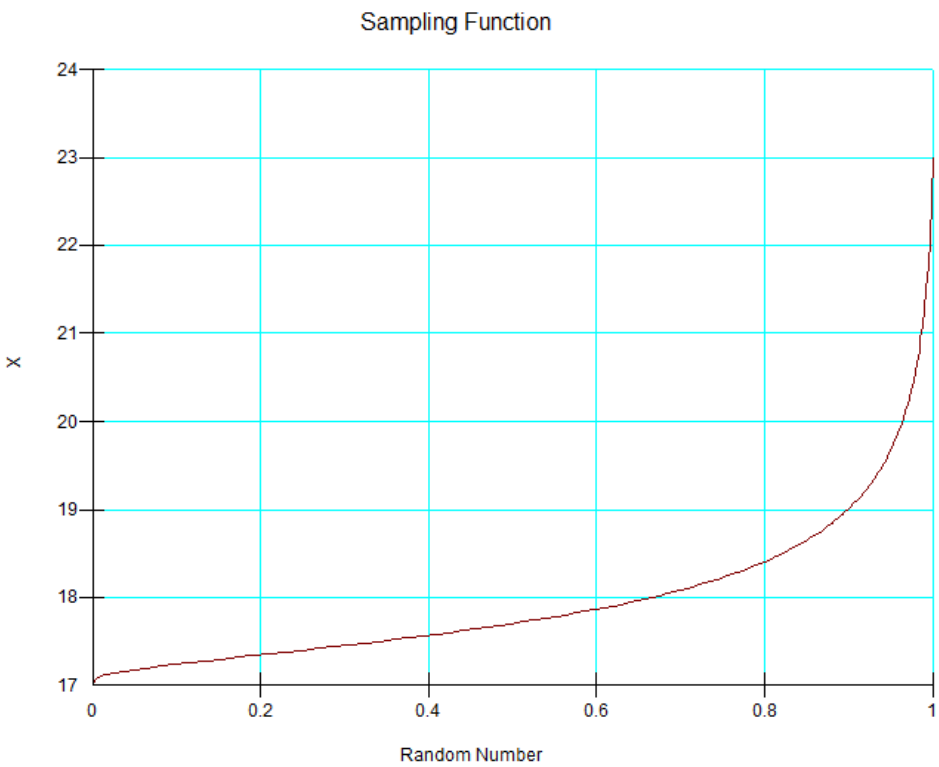

Figure 11-6 A log normal sampling function

Uniform function

A uniform function simply describes a range of values as illustrated in Figure 11-7. The characteristic of a uniform distribution is that all values have an equal probability of occurrence. This is further illustrated by the fact that the sampling function is a straight line as in Figure 11-8.

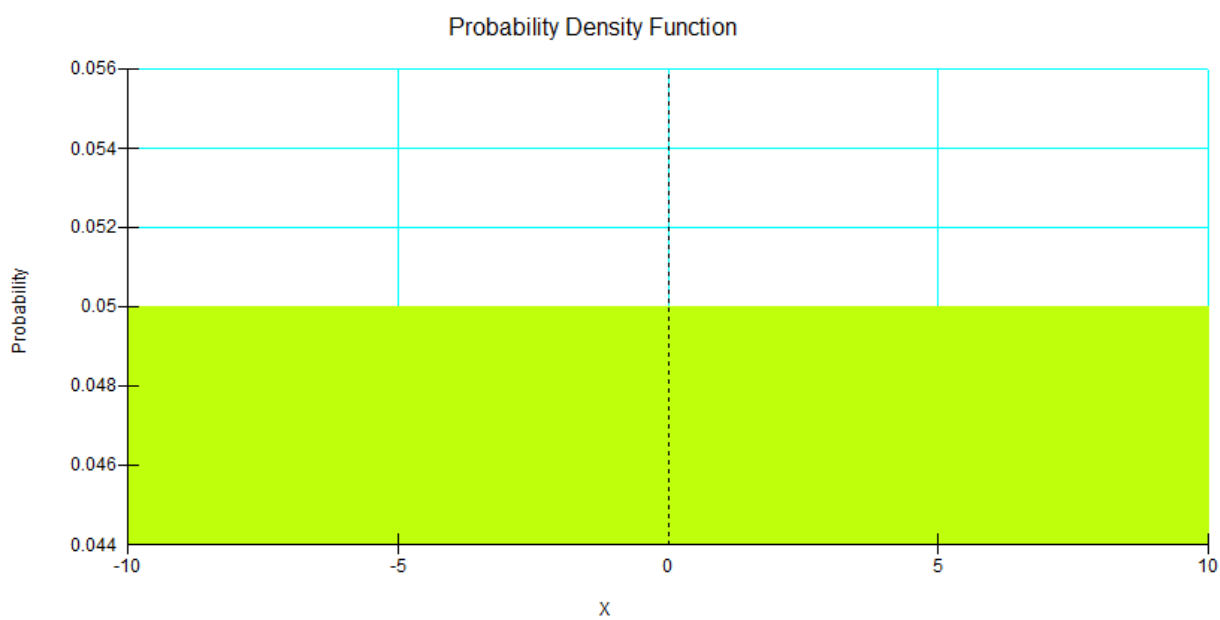

Figure 11-7 A uniform probability density function

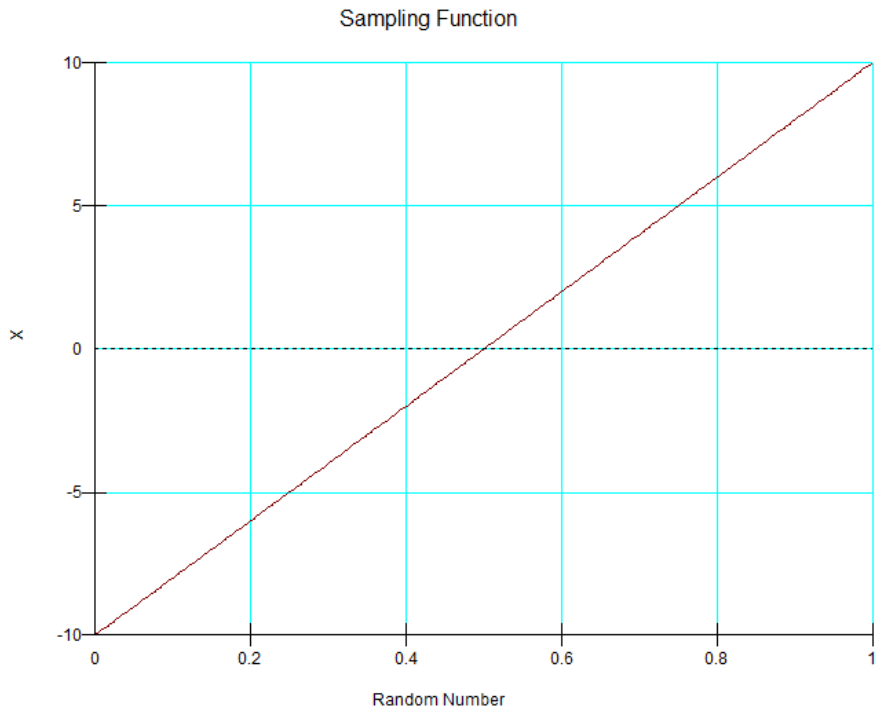

Figure 11-8 A uniform sampling function

11.3 Triangular probability function

A triangular probability density function can be specified with three points; the min and max values together with the apex value. Figure 11-9 shows a typical triangular probability density function when the apex value is 20, the minimum value is 15 and the maximum value is 45. To define this triangular distribution in SLOPE/W, you can enter the Mode to be zero, and the min as -5 (i.e., 15-20) and the max as 25 (i.e., 45-20). The associated sampling function of this triangular probability function is shown in Figure 11-10.

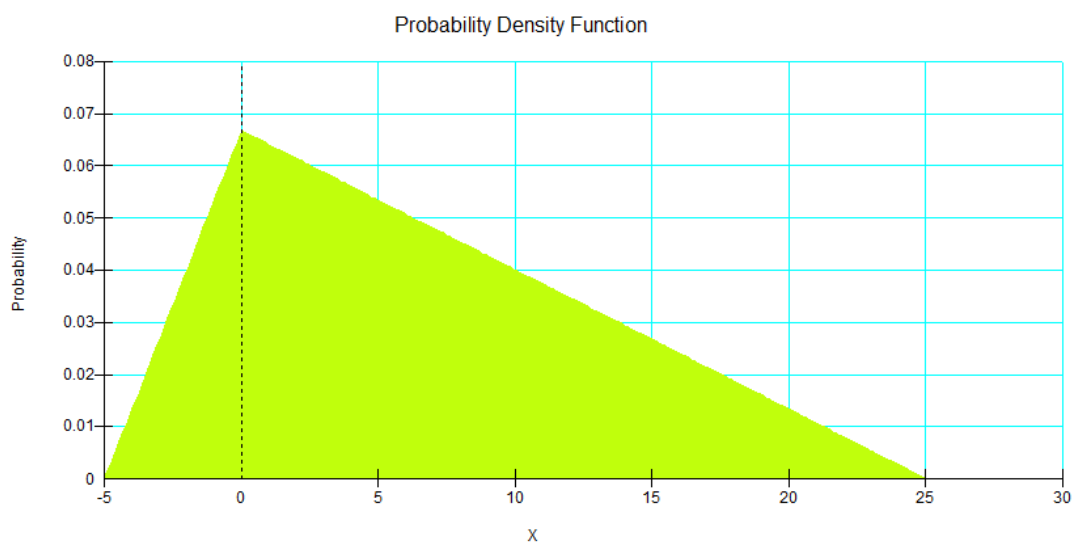

Figure 11-9 A triangular probability density function

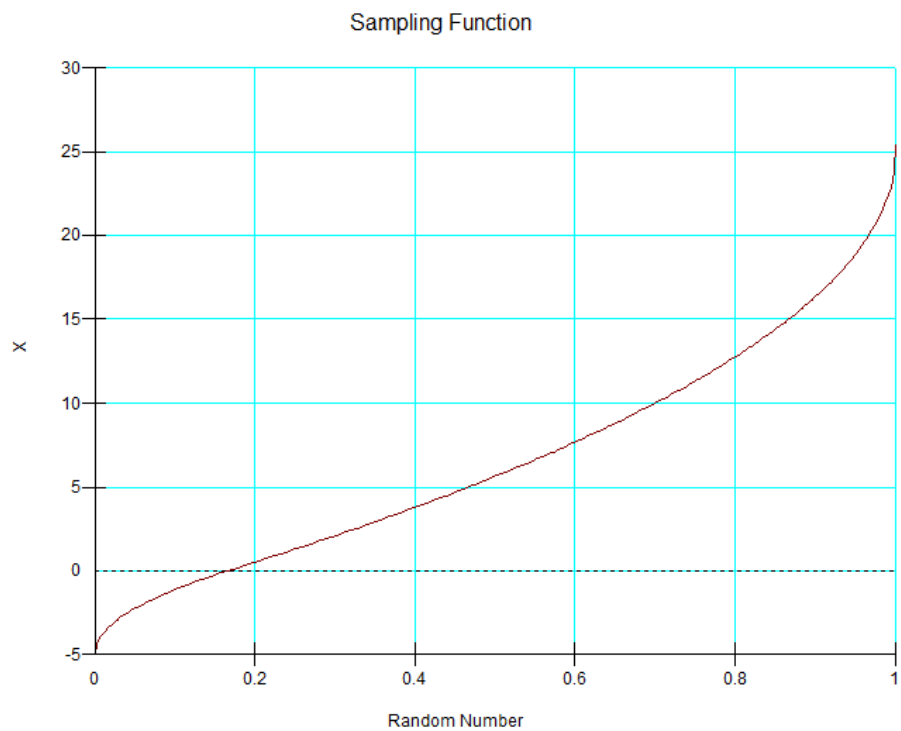

Figure 11-10 A triangular sampling function

11.4 General probability function

Any generalized spline shape function such as the bimodal function shown in Figure 11-11 can be defined in SLOPE/W as in Figure 11-11. This shape function can then be attached to any variable.

Assume that we apply this shape function to a cohesion value that ranges between 10 and 25. The resulting probability density function then is as shown in Figure 11-12 and the associated sampling function is as shown in Figure 11-13. The probability density function is created from the shape function and the minimum and maximum values, so that the area under the function is always 1.0.

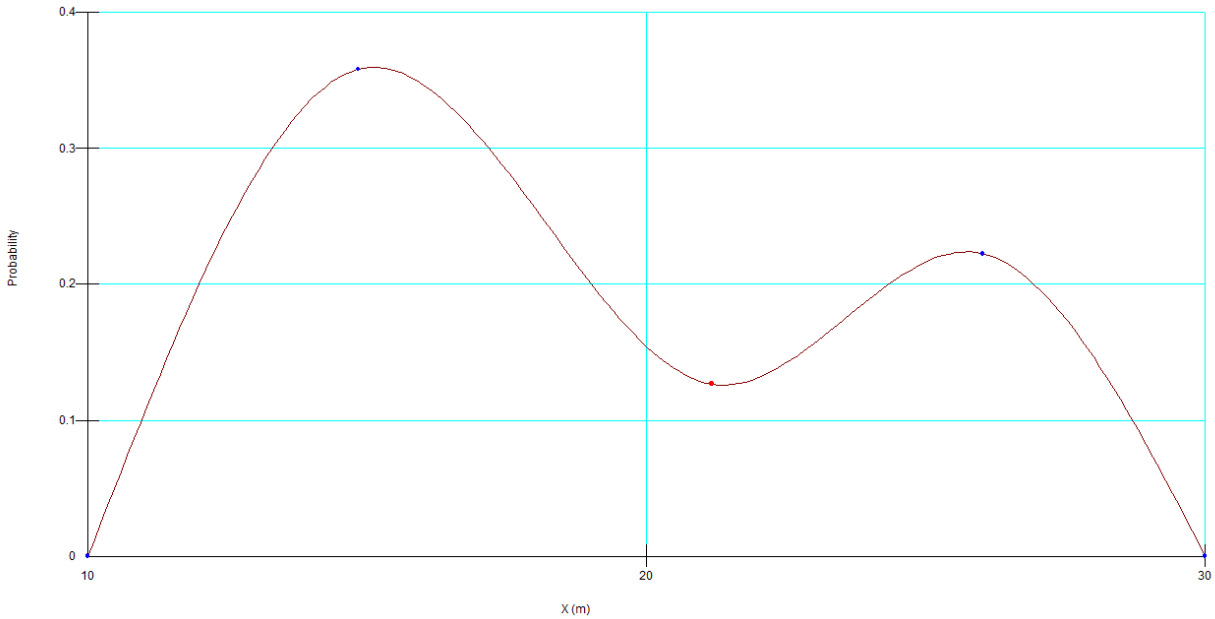

Figure 11-11 A generalized spline shape function

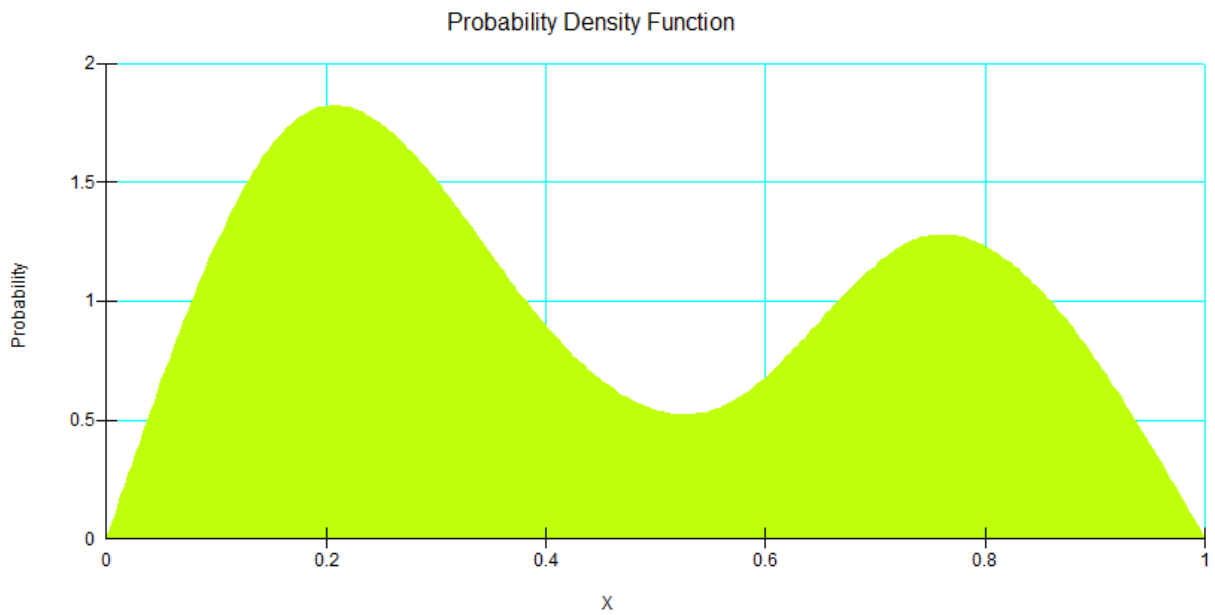

Figure 11-12 A generalized spline probability density function

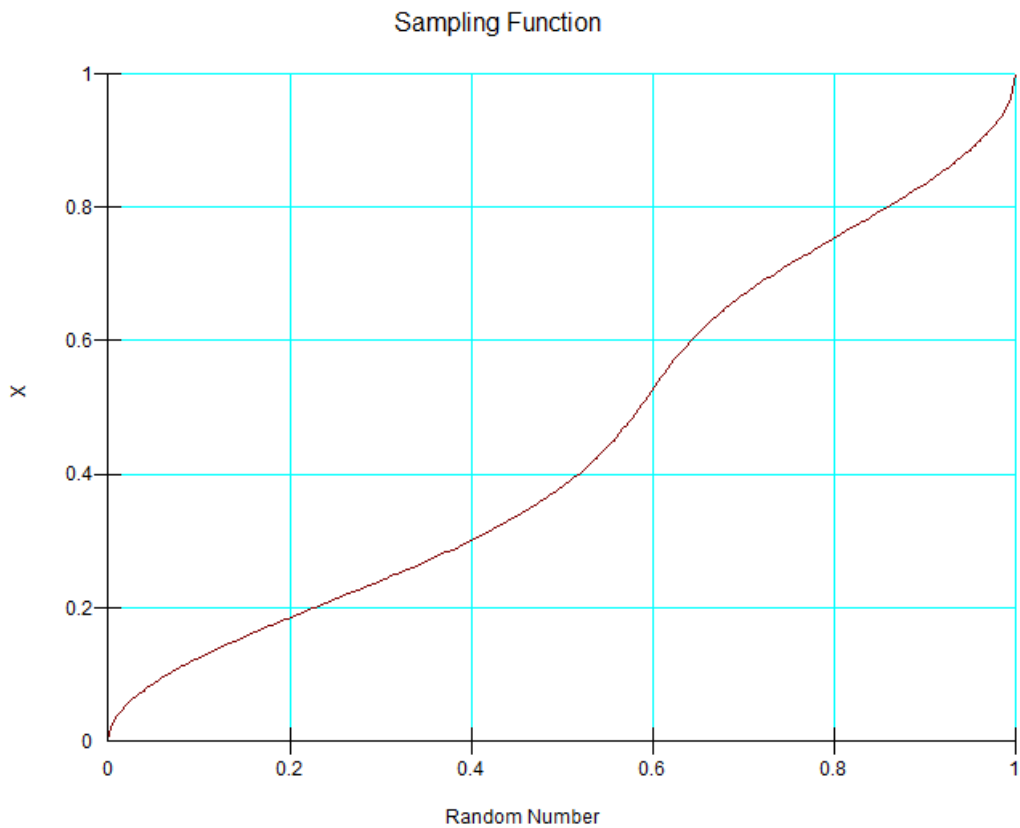

Figure 11-13 A generalized spline sampling function

The generalized spline probability distribution function makes it possible to consider any distribution function. This technique is particularly useful for any irregular distribution of actual measurements.

11.5 C – ϕ correlation

A correlation coefficient expresses the relative strength of the association between two parameters. Laboratory tests on a wide variety of soils (Lumb, 1970; Grivas, 1981 and Wolff, 1985) show that the shear strength parameters c and ϕ are often negatively correlated with correlation coefficient ranges from -0.72 to 0.35. Correlation between strength parameters may affect the probability distribution of a slope. SLOPE/W allows the specification of c and ϕ correlation coefficients for all soil models using c and ϕ parameters. Furthermore, in the case of a bilinear soil model, SLOPE/W allows the specification of correlation coefficient for ϕ and ϕ_2.

Correlation coefficients will always fall between -1 and 1. When the correlation coefficient is positive, c and ϕ are positively correlated, implying that larger values of c are more likely to occur with larger values of ϕ. Similarly, when the correlation coefficient is negative, c and ϕ are negatively correlated which reflects the tendency of a larger value of c to occur with a smaller value of ϕ. A zero correlation coefficient implies that c and ϕ are independent parameters.

11.6 Probability of failure and reliability index

A factor of safety is really an index indicating the relative stability of a slope. It does not imply the actual risk level of the slope, due to the variability of input parameters. With a probabilistic analysis, two useful

indices are available to quantify the stability or the risk level of a slope. These two indices are known as the probability of failure and the reliability index.

As illustrated in Figure 11-14, the probability of failure is the probability of obtaining a factor of safety less than 1.0. The probability of failure is determined by counting the number of safety factors below 1.0 and then taking this number as a percentage of the total number of converged Monte Carlo trials. For example, if there are 1000 Monte Carlo trials with 980 converged safety factors and 98 of them are below 1.0. Then the probabilistic of failure is 10%.

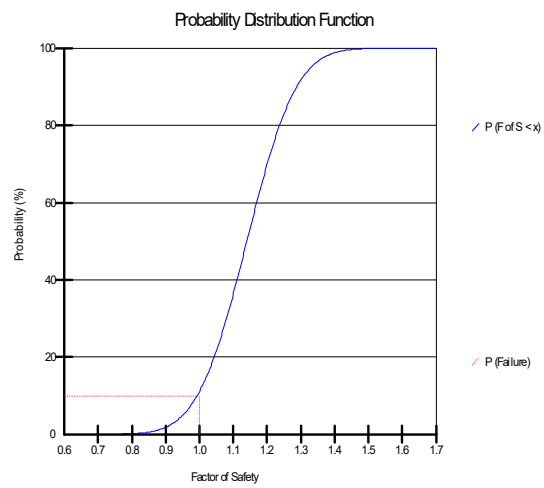

Figure 11-14 Factor of safety probability of failure

The probability of failure can be interpreted in two ways:

- If a slope were to be constructed many times, what percentage of such slopes would fail, or
- The level of confidence that can be placed in a design.

The first interpretation may be relevant in projects where the same slope is constructed many times, while the second interpretation is more relevant in projects where a given design is only constructed once and it either fails or it does not. Nevertheless, the probability of failure is a good index showing the level of risk of instability.

There is no direct relationship between the deterministic factor of safety and probability of failure. In other words, a slope with a higher factor of safety may not be more stable than a slope with a lower factor of safety. For example, a slope with factor of safety of 1.5 and a standard deviation of 0.5 may have a much higher probability of failure than a slope with factor of safety of 1.2 and a standard deviation of 0.1.

Another way of looking at the risk of instability is with what is known as a reliability index. The reliability index (β) is defined in terms of the mean (μ) and the standard deviation (σ) of the trial factors of safety as shown in the following equation:

$$\beta = \frac{(\mu - 1.0)}{\sigma}$$

The reliability index describes the stability by the number of standard deviations separating the mean factor of safety from its defined failure value of 1.0. It can also be considered as a way of normalizing the factor of safety with respect to its uncertainty.

When the shape of the probability distribution is known, the reliability index can be related directly to the probability of failure. Figure 11-15 illustrates the relationship of the reliability index to the probability of failure for a normally distributed factor of safety.

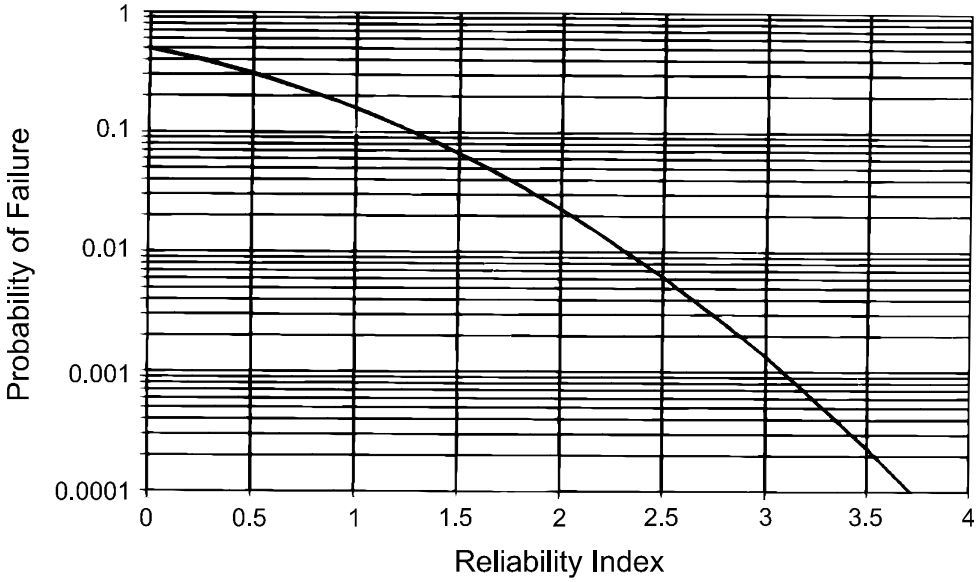

Figure 11-15 Relationship between reliability index and the probability of failure

SLOPE/W computes the reliability index for any and all probability distributions, but the concept is really only meaningful and applicable in SLOPE/W for normal distributions.

11.7 Spatial variability

Spatial variability can be an important issue if a potential slip surface has a significant length within one material. Consider the case in Figure 11-16. A significant portion of the slip surface is in the clay and consequentially it is reasonable to assume that there is some statistical variability in the clay along the slip surface. The length of the potential slip surface in the clay is around 25 m. The horizontal distance is 24 m.

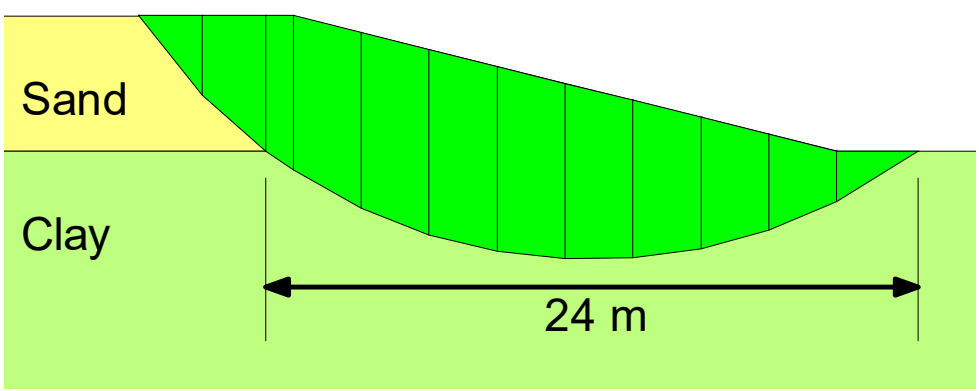

Figure 11-16 Case with statistical variability in the clay

The clay has a mean undrained strength (*c*) of 15 kPa with a standard deviation of ± 3. A clipped normal distribution varying between 5 and 25 kPa (i.e., an offset of -10 kPa and +10kPa) is assumed as shown in Figure 11-17.

SLOPE/W has 3 options for considering the spatial variability along the slip surface. The options deal with the number of times the soil properties are sampled along the slip surface. The options are:

- Sample the properties only once for each soil for the entire slip surface
- Sample the properties for each slice along the slip surface
- Sample the properties at a specified distance along the slip surface

If the clay strength is sampled only once for each Monte Carlo trial, the strength is constant along the slip surface, as illustrated in Figure 11-18. The graph shows possible strengths for four different Monte Carlo trials.

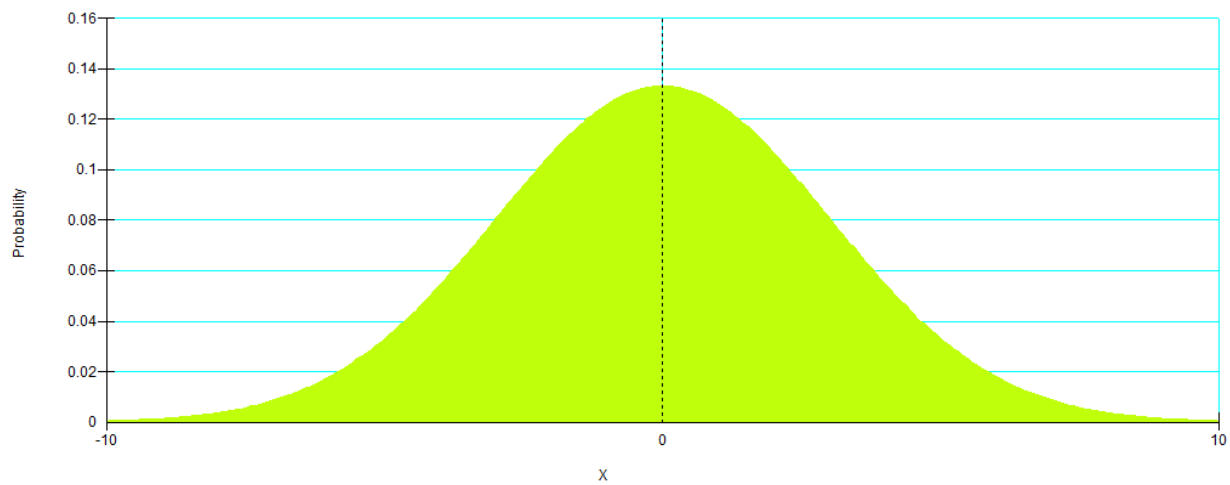

Figure 11-17 Probability density distribution for the clay

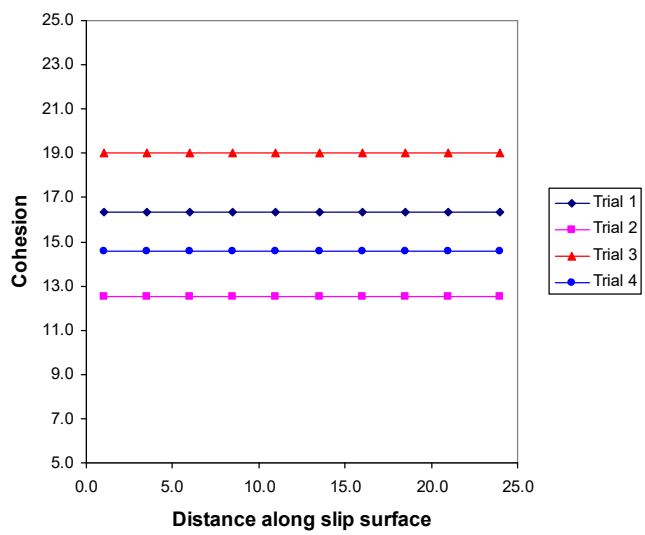

Figure 11-18 Strength variations in the clay when sampled once for each trial run

Statistically, the strength in the clay could be as low as 5 kPa or as high as 25 kPa. Intuitively, it seems unlikely that the strength along the entire slip surface could be at these outer limits, particularly if the slip surface has a significant length. Sampling more than once is likely more appropriate.

Another option is to sample the soil strength for each slice. The variation along the slip surface then could be as illustrated in Figure 11-19 for two trial runs. There are 10 slices in the clay and, consequently, there are 10 different strengths along the slip surface.

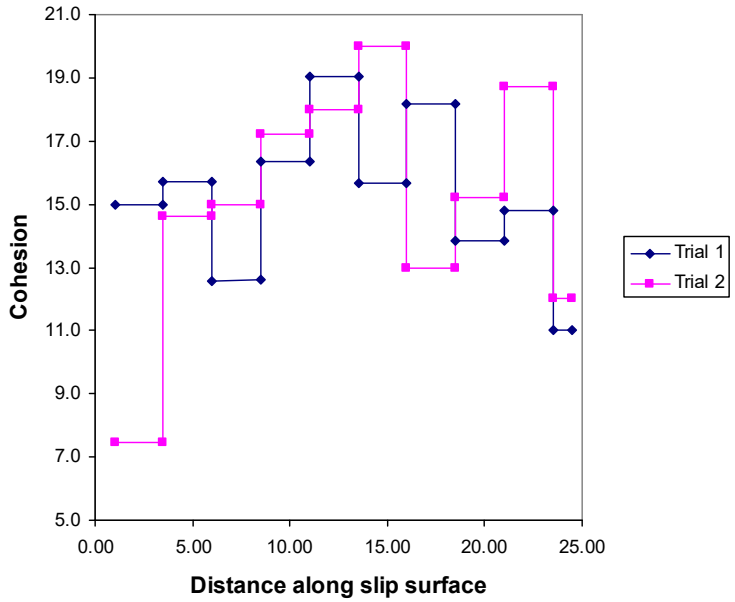

Figure 11-19 Strength variation along the slip surface when soil is sampled for every slice

As indicated on Figure 11-19, to sample the soil strength for each slice in every Monte Carlo trial may result in significant fluctuation of soil strength along the slip surface even within the same material. Although this is statistically possible, it seems quite unlikely in the field.

The third option in SLOPE/W is to sample the soil at a specified distance. For example, if the sampling distance is 10m, then the strength variation along the slip surface for two different Monte Carlo runs could be as shown in Figure 11-20.

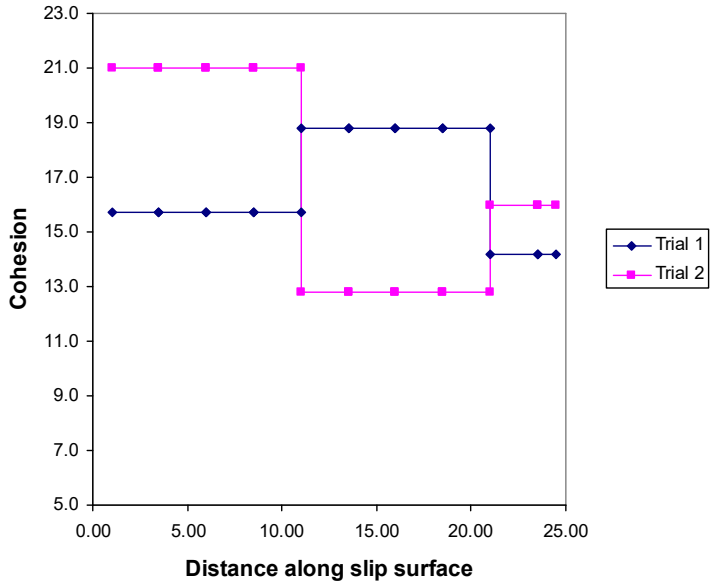

Figure 11-20 Strength variation along the slip surface with a sampling distance of 10 m

At this sampling distance, there are three different strengths along the slip surface.

There are two complete 10-m sampling distances and a third partial sampling distance. A partial sampling distance is considered to be correlated with the immediate preceding sampling distance. The coefficient of correlation between two soil sections can be computed with the equation as proposed by Vanmarcke (1983):

$$\rho(\Delta Z, \Delta Z') = \frac{Z_0^2\Gamma(Z_0) - Z_1^2\Gamma(Z_1) + Z_2^2\Gamma(Z_2) - Z_3^2\Gamma(Z_3)}{2\Delta Z \Delta Z' \left[\Gamma(\Delta Z)\Gamma(\Delta Z')\right]^{0.5}}$$

where:

ΔZ, $\Delta Z'$	=	the length between two sections,
Z_0	=	the distance between the two sections,
Z1	=	$\Delta Z + Z_0$,
Z2	=	$\Delta Z + Z_0 + \Delta Z'$,
Z3	=	$\Delta Z' + Z_0$. , and
Γ	=	a dimensionless variance function.

Γ is a dimensionless variance function, which Vanmarcke (1983) showed can be approximated by:

$\Gamma(Z)$	=	1.0 when $Z \leq \delta$, and
$\Gamma(Z)$	=	δ/Z when $Z > \delta$.

The symbol δ is called the scale of fluctuation. It is about twice the autocorrelation distance. In SLOPE/W, when spatial variation is considered, the value of δ is related to the desired sampling distance along the slip surface.

As is evident from the above equations, the correlation is strong when the partial distance is short relative to the specified sampling distance, and the correlation is weak when the partial distance approaches the specified sampling distance.

The probability of failure is related to the sampling distance, especially if there are only a few statistical parameters. The probability of failure is the highest when the soil is sampled only once for each trial run and is the lowest when the soil is sampled for each slice. For the simple case under discussion here, the probabilities of failure for various sampling frequencies are as listed in the following table.

Sampling Frequency	Probability of Failure (%)
Only once	19
Every 15 m	10
Every 10 m	6
Every slice	<1

When the strength is sampled only once there are more trial runs with a factor of safety less than 1.0 and therefore a high probability of failure. Sampling the soil for every slice tends towards an average mean strength and therefore a low probability of failure.

Selecting an appropriate sampling distance is not trivial. Generally, a thorough understanding of the statistical characteristics of the soil stratum is required, and spatial variability is a factor that can only be assessed in light of the details at each project and the amount of data available.

The two options in SLOPE/W of sampling the soil only once, and sampling the soil strength for each slice are perhaps both unrealistic for some situations, these two options are nonetheless useful. They provide a convenient means of bracketing the possible range of probabilities of failure. Knowing the limits can then help with selecting and evaluating a proper sampling distance.

If sufficient data is available, a variogram can be created as discussed by Soulié et al. (1990). The form of a variogram is illustrated in Figure 11-21. The differences in strength, for example, increase with distance between sampling points up to a certain distance after which the difference remains relatively constant. The point at which the variogram becomes horizontal is called the range, and it is the distance beyond which there is no correlation between strength measurements. The range from a variogram would be an appropriate sampling distance for a SLOPE/W probabilistic analysis.

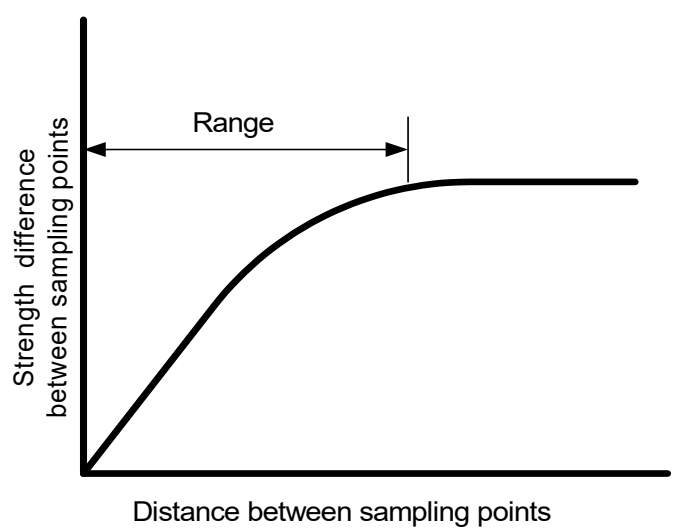

Figure 11-21 The form of a typical variogram

11.8 Multiple statistical parameters

In SLOPE/W, a wide range of parameters can be assigned a statistical dispersion and included in a Monte Carlo simulation. This includes soil strength parameters, concentrated loads, pore-water pressures, pseudostatic seismic coefficients and so forth. Each of the parameters is sampled for each Monte Carlo run. Using too many statistical parameters together in the same run tends to reduce the distribution of the computed safety factors. That is, the combination of multiple statistical parameters tends to smooth out the extreme of the variability and the probability of failure diminishes. Perhaps this is an appropriate response. The main point here is that it is important to be cognizant of this and to evaluate the results carefully when many parameters are included in a probability analysis.

11.9 Sensitivity analyses

A sensitivity analysis is somewhat analogous to a probabilistic analysis. Instead of selecting the variable parameters randomly, the parameters are selected in an ordered fashion using a Uniform Probability Distribution function.

Consider the simple example in Figure 11-22. A question may be: "Is the stability of the slope more sensitive to the frictional strength of the sand or the undrained strength of the clay?"

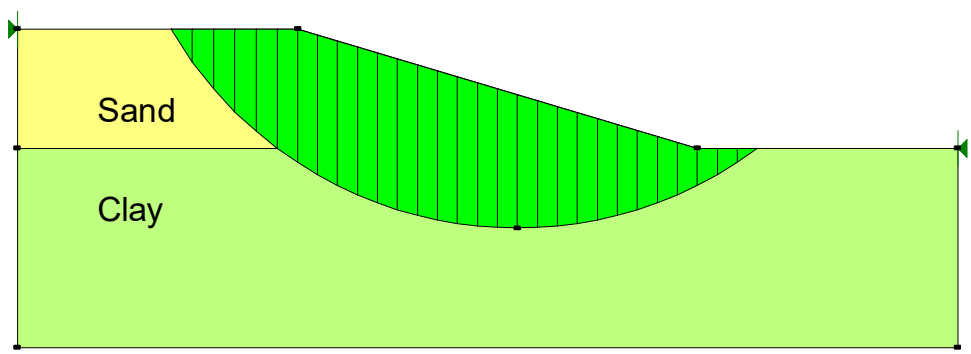

Figure 11-22 Illustrative case for a sensitivity analysis

Let us look at the case where ϕ for the sand is 30 degrees and the variation in ϕ will range from 25 to 35 degrees (11 different ϕ values). The undrained strength of the clay is 20 kPa and the range will be from 15 to 25 kPa.

First SLOPE/W holds the strength of the clay at 20 kPa and computes a factor of safety for each of the 11 trial ϕ values. Next the strength of the sand is kept constant at 30 degrees, and factors of safety are computed for of the 11 different cohesion values.

For presentation purposes, all the strengths are normalized to a value ranging between 0.0 and 1.0. Zero means the lowest value and 1.0 means the highest value. For the example here, zero means a ϕ of 25 degrees and a c of 15 kPa. A value of 1.0 means a ϕ of 35 degrees and a c of 25 kPa.

The results are presented as a sensitivity plot, such as in Figure 11-23. For this case, the stability is much more sensitive to changes in the undrained strength (c) than to changes in the sand friction angle ϕ. This is intuitively correct, since a major portion of the slip surface is in the clay layer.

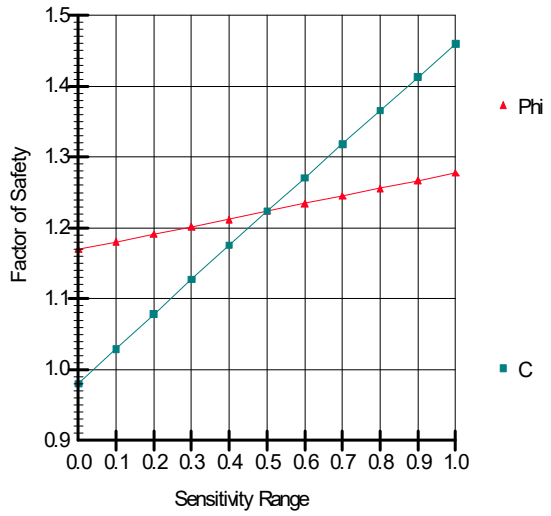

Figure 11-23 Illustration of a sensitivity plot

The point where the two sensitivity curves cross is the deterministic factor of safety or the factor of safety at the mid-point of the ranges for each of the strength parameters.

12 Partial Factors

Partial factors can be applied to characteristic material strength properties, actions, or resistances in accordance with a limit state design approach such as Eurocode 7, Norwegian Standard NS 3480, and British Standard 8006. The factored values are in turn used in the stability analysis to check if an ultimate limit state has been reached. The ultimate limit state is defined as a state associated with complete collapse or failure. The calculated factor of safety is interpreted as an over-design factor when partial factors are applied.

Material strength properties include effective stress or undrained strength properties. Actions refer to gravity forces, seismic forces, and point and surcharge loads. Gravity forces are factored via the unit weight of the soil and seismic forces via the seisimic coefficients. Point and surcharge loads must be declared by the user to be permanent or variable. The software determines if an action is favorable or unfavorable as discussed subsequently. Resistances include soil strengths, as opposed to material strength properties, and reinforcement resistances.

12.1 Favorable or unfavorable actions

An action is deemed to be favorable or unfavorable by considering the angle of the action relative to the angle of the slice base and relative to the direction of movement of the sliding mass. Figure 12-1 illustrates an action on an individual slice. Actions that resist and promote movement of the slice are considered favorable and unfavorable, respectively. The action shown in Figure 1 would be deemed favorable for a right-facing slope and unfavorable for a left-facing slope. Actions oriented at $\delta \pm 90°$ are deemed favorable if acting to increase the base normal force and unfavorable if otherwise.

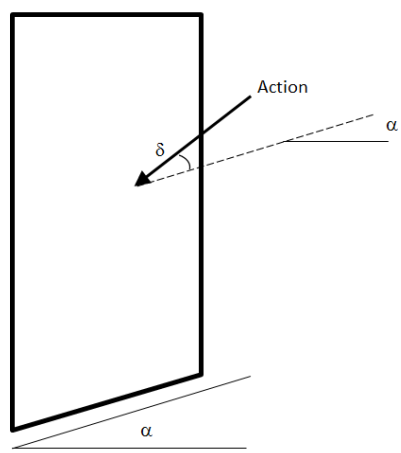

Figure 12-1 Favorable/Unfavorable Action Applied to a Slice

Gravity forces are vertical and are therefore always deemed unfavorable for slices in the active zone. Figure 12-2 compares the results of an analysis completed using a) characteristic values of unit weight; and b) derived values of unit weight calculated by multiplying the unit weight of unfavorable slices by a partial factor of 1.25. Slices 11 to 25 were deemed unfavorable, with the transition occurring between Slice 10 and 11 where the slice base angle changed sign. The increased slice weights in the active zone resulted in an over-design factor of 1.29 as opposed to the overall factor of safety of 1.44. Incidentally, the increased gravity forces in the active zone cause an increase in the base normal force, which in turn

increases the frictional shear resistance if effective stress strengths are being used. It is therefore possible for the over-design factor to exceed the overall factor of safety for some cases.

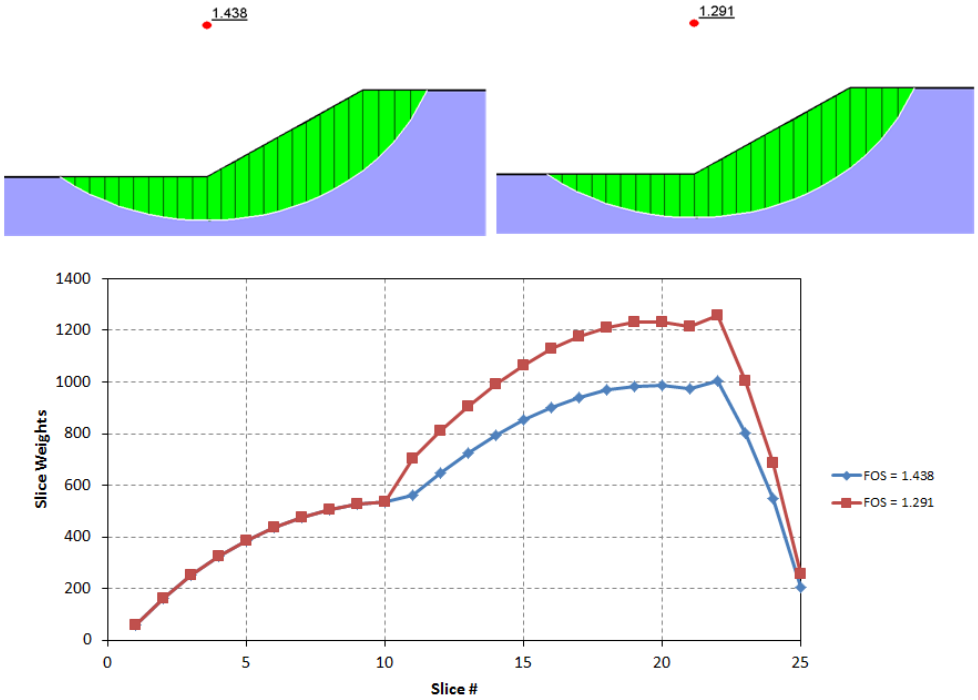

Figure 12-2 Result of applying a partial factor to the unit weight of unfavorable slices

12.2 Pore-water pressures and ponded water

Limit state design approaches sometimes allow for calculation of derived pore-water pressures and water loads by application of partial factors. SLOPE/W, however, does not apply partial factors to pore-water pressures or to water loads because of the possibility for illogical force distributions. Design values of pore-water pressures and water loads should be derived by applying a safety factor to the piezometric line(s) or to the boundary conditions that control the pore-water pressures in a finite element analysis. Consideration should be given to the permanent and variable components of the hydraulic regime when applying the safety factor.

Pore-water pressures are influenced by partial factors if calculated using the Ru or B-bar methods because of the implicit relationship to the unit weight of the soil (See Sections 8.3 and 8.4). Figure 3 compares the results of an analysis using a piezometric line with B-bar and completed using a) characteristic values of unit weight; and b) derived values of unit weight calculated by multiplying the unit weight of unfavorable slices by a partial factor of 1.25. The upper soil layer adds the weight and the lower soil layer has a B-bar of 1.0. Slices 4 through 14 are in the active zone and were therefore deemed unfavorable. Factoring the slice weights in the active zone by 1.25 resulted in the excess pore-water pressures being 1.25 greater than those produced using characteristic values. The pore-water pressures calculated by the Ru and B-bar methods can be thought of as being factored in the same manner as the unit weights.

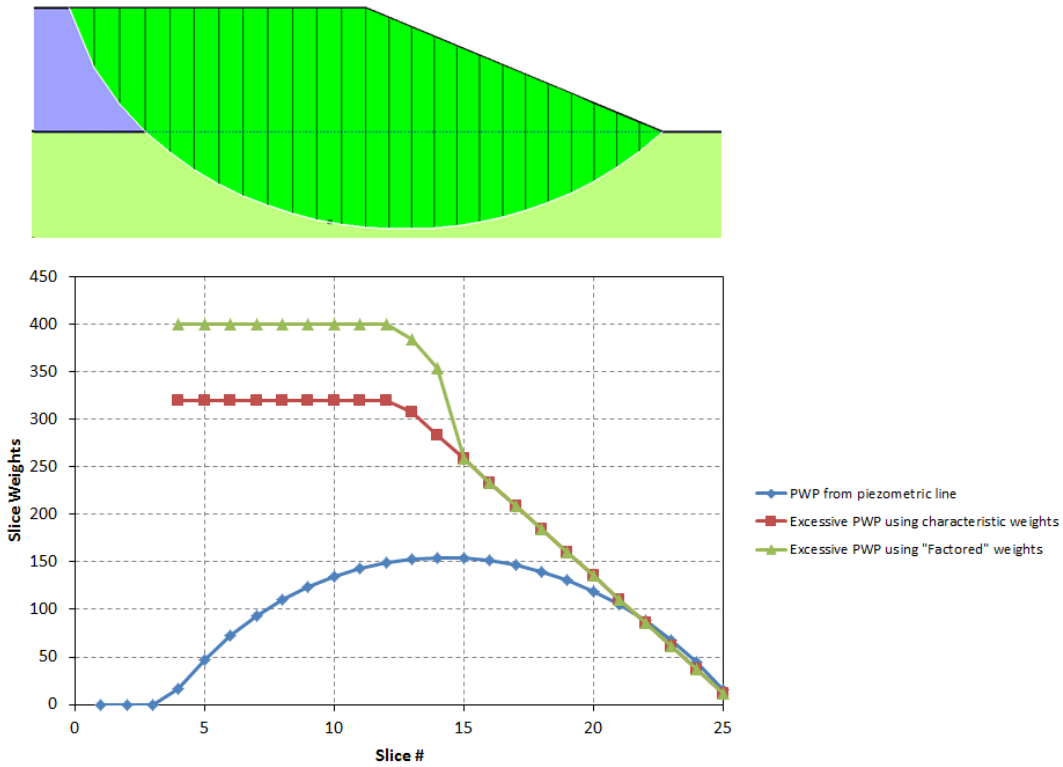

Figure 12-3 Excess pore-water pressures resulting applying a partial factor to the unit weight of unfavorable slices

12.3 Shear strength

Table 12-1 summarizes how the partial factors are applied to the material strength properties or shear strength of each relevant material model including: (1) effective cohesion c'; (2) effective coefficient of friction $\tan \emptyset'$; (3) undrained strength S_u; and, (4) soil strength. The effective stress strength models shown in Table 12-1 also comprise an optional suction strength component (See Section 7.15). The suction strength is calculated as a function of a coefficient of friction value; conseqeuntly, suction strength is implicitly part of category (2). An Earth Resistance partial factor can also be specified separately of the 4 material parameter factors, resulting in division of the entire numerator of the force and moment factor of safety equations by a single value. An equivalent result could be obtained by multiplying the factors in categories 1 through 4 by the required resistance factor while leaving the Earth Resistance factor specified as 1.0.

Table 12-1 Material model categorization for application of partial factors

Material Model	Category
Mohr-Coulomb	1,2
Undrained	3
S=f(depth)	3
S=f(datum)	3

High strength	N.A.
Bedrock	N.A.
Bilinear	4
Anisotropic strength	1,2
Anisotropic function	1,2
Shear-Normal function	4
Combined, S=f(depth)	1,2,3
Combined, S=f(datum)	1,2,3
S=f(overburden)	3
Spatial M-C	1,2
Generalized Hoek-Brown	4

Staged rapid drawdown and staged pseudo-static analyses involve the calculation of both drained effective stress strengths and undrained strengths (See Sections 3.15 and 10.3). Partial factors are applied to the effective stress strength properties and undrained shear strengthes in all stages of the analysis and in a manner consistent with material models in categories 1 and 2.

12.4 Reinforcement loads

Partial factors are applied to the reinforcement resistance parameters: pullout resistance, shear force, and tensile capacity. The partial factor is applied to the pullout resistance even if it is calculated from overburden stress and interface strength properties as can be done for geosynthetics.

13 Illustrative Examples

A variety of verification and illustrative examples has been developed and are shipped with the software. These examples can be useful in learning how to model various slope stability problems.

Each example comes with a PDF document which provides explanations on the problem setup, comments on modeling techniques and commentary on interpreting the results.

The GeoStudio example files include the solutions. This makes it possible to examine the input, definition and results using the **free** GeoStudio Viewer license.

The examples are also available on GEO-SLOPE's web site (www.geo-slope.com) .

It is possible to search for a particular type of analysis on the GeoStudio desktop. Clicking on the Examples title brings up the following search dialog window.

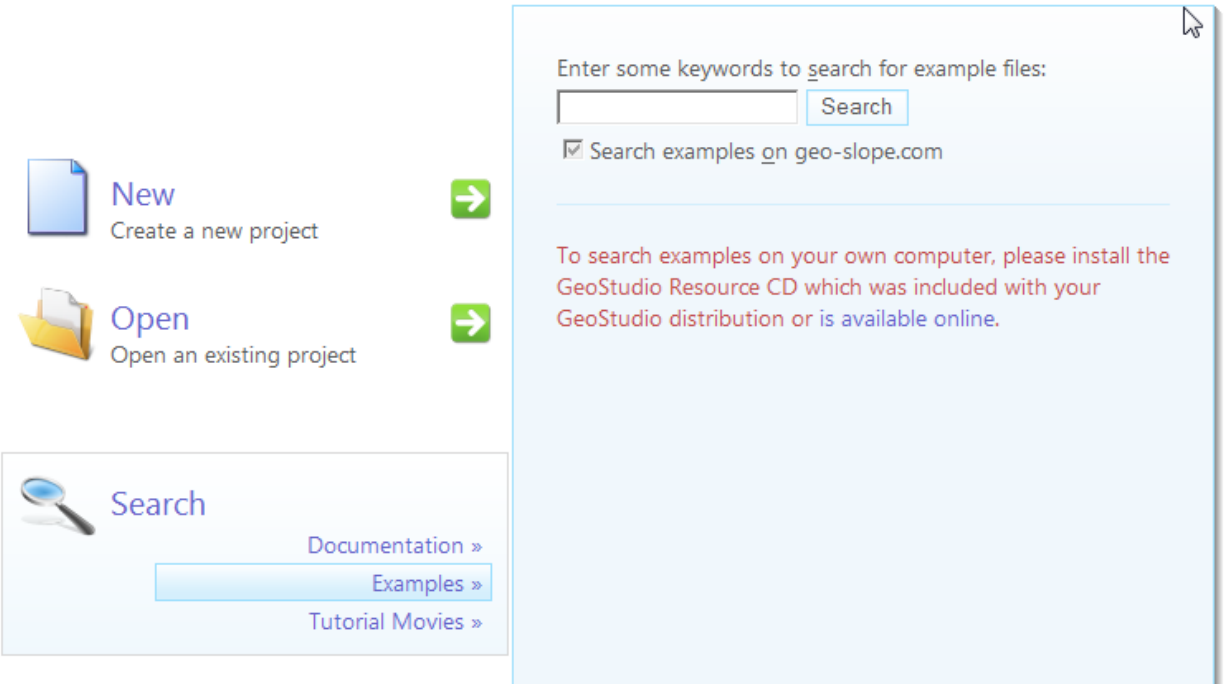

Some of these examples are verification of the software theoretical and numerical formulation; some illustrate application of unique SLOPE/W features and options in the modelings of pore water pressure, soil strength, slip surfaces and slope reinforcements; and some illustrate the power of integrating different types of analyses within GeoStudio.

Analysis integration

GeoStudio is a unique geotechnical engineering tool that has been designed to allow seamless integration between various types of geotechnical engineering analyses. Some examples of integration between analyses include:

- SEEP/W generated pore pressures in SLOPE/W stability analysis
- VADOSE/W generated pore pressures in SLOPE/W stability analysis
- SIGMA/W generated pore pressures in SLOPE/W stability analysis
- SIGMA/W generated static stresses in SLOPE/W stability analysis
- QUAKE/W generated pore pressures in SLOPE/W stability analysis
- QUAKE/W generated static stresses in SLOPE/W stability analysis
- QUAKE/W generated dynamic stresses in SLOPE/W stability analysis

14 Theory

14.1 Introduction

This chapter explains the theory used in the development of SLOPE/W. The variables used are first defined, followed by a brief description of the General Limit Equilibrium Solution Scheme (GLE). The relevant equations are derived, including the base normal force equation and the factor of safety equations. This is followed by a section describing the iterative procedure adopted in solving the nonlinear factor of safety equations. Attention is then given to aspects of the theory related to soils with negative pore-water pressures.

SLOPE/W solves two factor of safety equations; one equation satisfies force equilibrium and the other satisfies moment equilibrium. All the commonly used methods of slices can be visualized as special cases of the General Limit Equilibrium (GLE) solution.

The theory of the Finite Element Stress method is presented as an alternative to the limit equilibrium stability analysis. This method computes the stability factor of a slope based on the stress state in the soil obtained from a finite element stress analysis. Finally, the theory of probabilistic slope stability using the Monte Carlo method is also presented.

14.2 Definition of variables

SLOPE/W uses the theory of limit equilibrium of forces and moments to compute the factor of safety against failure. The General Limit Equilibrium (GLE) theory is presented and used as the context for relating the factors of safety for all commonly used methods of slices.

A factor of safety is defined as that factor by which the shear strength of the soil must be reduced in order to bring the mass of soil into a state of limiting equilibrium along a selected slip surface.

For an effective stress analysis, the shear strength is defined as:

$$s = c' + (\sigma_n - u)\tan\phi'$$

where:

s	=	shear strength,
c'	=	effective cohesion,
ϕ'	=	effective angle of internal friction,
σ_n	=	total normal stress, and
u	=	pore-water pressure.

For a total stress analysis, the strength parameters are defined in terms of total stresses and pore-water pressures are not required.

The stability analysis involves passing a slip surface through the earth mass and dividing the inscribed portion into vertical slices. The slip surface may be circular, composite (i.e., combination of circular and linear portions) or consist of any shape defined by a series of straight lines (i.e., fully specified slip surface).

The limit equilibrium formulation assumes that:

The factor of safety of the cohesive component of strength and the frictional component of strength are equal for all soils involved.

The factor of safety is the same for all slices.

Figure 14-1 and Figure 14-2 show all the forces acting on a circular and a composite slip surface. The variables are defined as follows:

W	=	the total weight of a slice of width b and height h
N	=	the total normal force on the base of the slice
S_m	=	the shear force mobilized on the base of each slice.
E	=	the horizontal interslice normal forces. Subscripts L and R designate the left and right sides of the slice, respectively.
X	=	the vertical interslice shear forces. Subscripts L and R define the left and right sides of the slice, respectively.
D	=	an external point load.
kW	=	the horizontal seismic load applied through the centroid of each slice.
R	=	the radius for a circular slip surface or the moment arm associated with the mobilized shear force, S_m for any shape of slip surface.
f	=	the perpendicular offset of the normal force from the center of rotation or from the center of moments. It is assumed that f distances on the right side of the center of rotation of a negative slope (i.e., a right-facing slope) are negative and those on the left side of the center of rotation are positive. For positive slopes, the sign convention is reversed.
x	=	the horizontal distance from the centerline of each slice to the center of rotation or to the center of moments.
e	=	the vertical distance from the centroid of each slice to the center of rotation or to the center of moments.
d	=	the perpendicular distance from a point load to the center of rotation or to the center of moments.
h	=	the vertical distance from the center of the base of each slice to the uppermost line in the geometry (i.e., generally ground surface).
a	=	the perpendicular distance from the resultant external water force to the center of rotation or to the center of moments. The L and R subscripts designate the left and right sides of the slope, respectively.
A	=	the resultant external water forces. The L and R subscripts designate the left and right sides of the slope, respectively.
ω	=	the angle of the point load from the horizontal. This angle is measured counter-clockwise from the positive x-axis.
α	=	the angle between the tangent to the center of the base of each slice and the horizontal. The sign convention is as follows. When the angle slopes in the same direction as the overall slope of the geometry, α is positive, and vice versa.

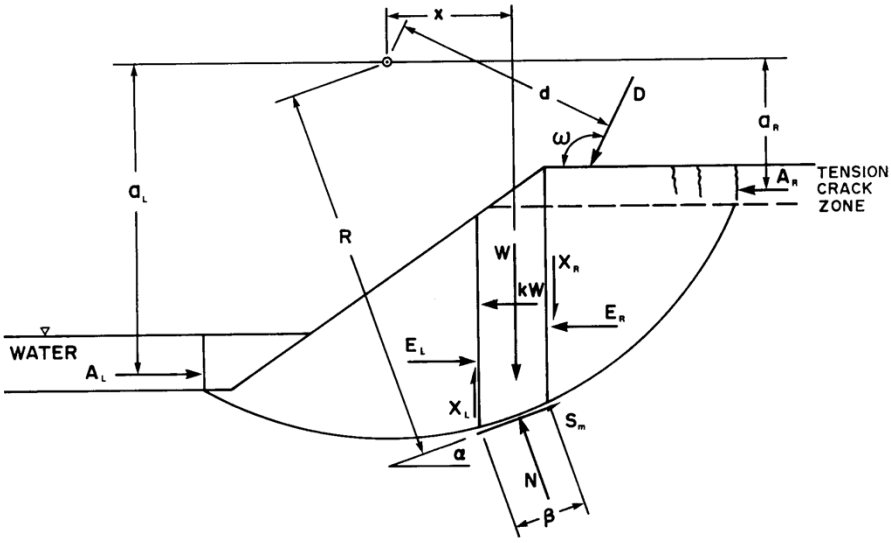

Figure 14-1 Forces acting on a slice through a sliding mass with a circular slip surface

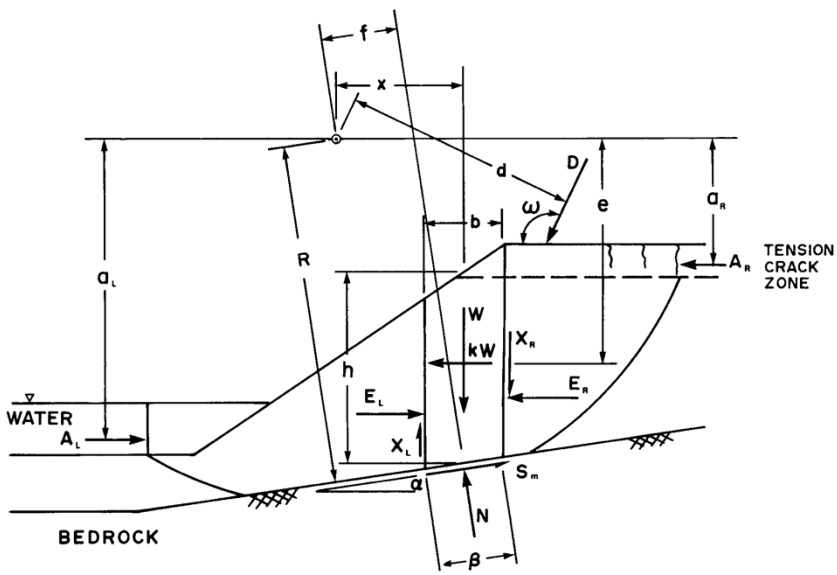

Figure 14-2 Forces acting on a slice through a sliding mass with a composite slip surface

Figure 14-3 shows the forces acting on a slip surface defined by a series of straight lines. This is the case when a fully specified or block specified slip surface is selected. The center for moment equilibrium (i.e., the axis point) is immaterial when both moment equilibrium and force equilibrium are satisfied. However, for simplified methods of analysis which do not satisfy both moment equilibrium and force equilibrium, the computed factor of safety can be quite sensitive to the center for moment equilibrium, therefore, it is important to select a reasonable axis point.

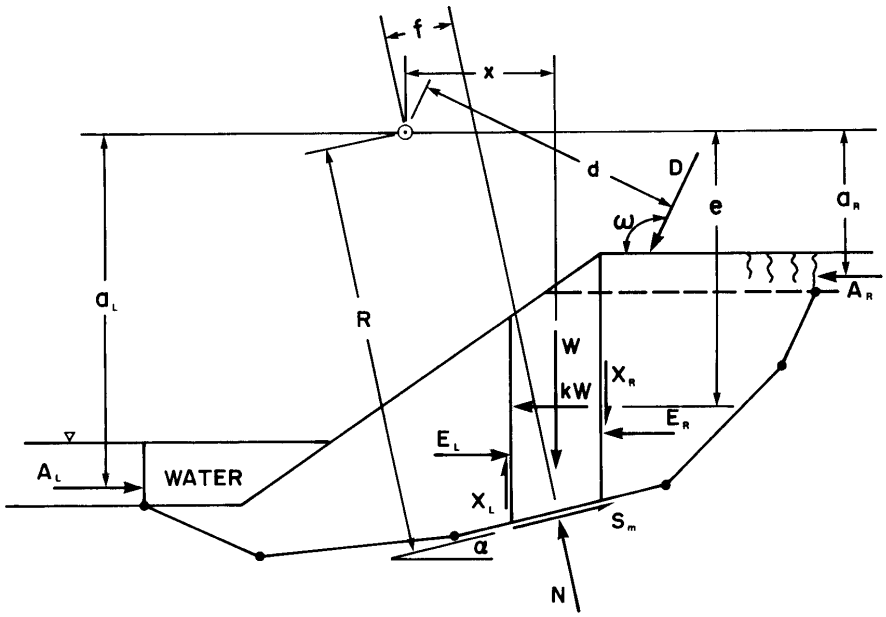

Figure 14-3 Forces acting on a slice through a sliding mass defined by a fully specified slip surface

The magnitude of the shear force mobilized to satisfy conditions of limiting equilibrium is:

$$S_m = \frac{s\,\beta}{F} = \frac{\beta\left(c' + \left(\sigma_n - u\right)\tan\phi'\right)}{F}$$

where:

$\sigma_n = \frac{N}{\beta}$	=	average normal stress at the base of each slice,
F	=	the factor of safety, and
β	=	the base length of each slice.

The elements of statics that can be used to derive the factor of safety are the summations of forces in two directions and the summation of moments. These, along with failure criteria, are insufficient to make the problem determinate. More information must be known about either the normal force distribution at the base of the slices or the interslice force distribution. Table 14-1 and Table 14-2 summarize the known and unknown quantities associated with a slope stability analysis.

Table 14-1 Summary of known quantities in solving for a safety factor

Number of Known Quantities	Description
n	Summation of forces in the horizontal direction
n	Summation of forces in the vertical direction
n	Summation of moments

n	Material Shear Failure Criterion
4n	Total number of equations

Table 14-2 Summary of unknown quantities in solving for a safety factor

Number of Unknown Quantities	Description
n	Magnitude of the normal force at the base of a slice, N
n	Point of application of the normal force at the base of each slice
n - 1	Magnitude of the interslice normal forces, E
n - 1	Magnitude of the interslice shear force, X
n - 1	Point of application of the interslice forces
n	Shear force on the base of each slice, Sm
1	Factor of safety, F
1	Value of Lambda, λ
6n - 1	Total number of unknowns

Since the number of unknown quantities exceeds the number of known quantities, the problem is indeterminate. Assumptions regarding the directions, magnitude, and/or point of application of some of the forces must be made to render the analysis determinate. Most methods first assume that the point of application of the normal force at the base of a slice acts through the centerline of the slice. Then an assumption is most commonly made concerning the magnitude, direction, or point of application of the interslice forces.

In general, the various methods of slices can be classified in terms of:

- the statics used in deriving the factor of safety equation, and
- the interslice force assumption used to render the problem determinate.

14.3 General limit equilibrium Solution Scheme

The General Limit Equilibrium Solution Scheme (GLE) uses the following equations of statics in solving for the factor of safety:

- The summation of forces in a vertical direction for each slice is used to compute the normal force at the base of the slice, *N*.
- The summation of forces in a horizontal direction for each slice is used to compute the interslice normal force, *E*. This equation is applied in an integration manner across the sliding mass (i.e., from left to right).
- The summation of moments about a common point for all slices. The equation can be rearranged and solved for the moment equilibrium factor of safety, F_m.
- The summation of forces in a horizontal direction for all slices, giving rise to a force equilibrium factor of safety, F_f.

The analysis is still indeterminate, and a further assumption is made regarding the direction of the resultant interslice forces. The direction is assumed to be described by a interslice force function. The direction together with the interslice normal force is used to compute the interslice shear force. The factors of safety can now be computed based on moment equilibrium (F_m) and force equilibrium (F_f).

These factors of safety may vary depending on the percentage (λ) of the force function used in the computation. The factor of safety satisfying both moment and force equilibrium is considered to be the converged factor of safety of the GLE formulation.

Using the same GLE approach, it is also possible to specify a variety of interslice force conditions and satisfy only the moment or force equilibrium conditions. The assumptions made to the interslice forces and the selection of overall force or moment equilibrium in the factor of safety equations, give rise to the various methods of analysis.

14.4 Moment equilibrium factor of safety

Reference can be made to Figure 14-1, Figure 14-2 and Figure 14-3 for deriving the moment equilibrium factor of safety equation. In each case, the summation of moments for all slices about an axis point can be written as follows:

$$\sum Wx - \sum S_m R - \sum Nf + \sum kWe \pm \sum Dd \pm \sum Aa = 0$$

After substituting for S_m and rearranging the terms, the factor of safety with respect to moment equilibrium is:

$$F_m = \frac{\sum \left(c'\beta R + \left(N - u\beta\right) R \tan \phi'\right)}{\sum Wx - \sum Nf + \sum kWe \pm \sum Dd \pm \sum Aa}$$

This equation is a nonlinear equation since the normal force, N, is also a function of the factor of safety. The procedure for solving the equation is described below in this chapter.

14.5 Force equilibrium factor of safety

Again, reference can be made to Figure 14-1, Figure 14-2 and Figure 14-3 for deriving the force equilibrium factor of safety equation. The summation of forces in the horizontal direction for all slices is:

$$\sum\left(E_L - E_R\right) - \sum \left(N \sin \alpha\right) + \sum \left(S_m \cos \alpha\right)$$
$$- \sum\left(kW\right) + \sum D \cos\omega \pm \sum A = 0$$

The term $\Sigma(E_L\text{-}E_R)$ presents the interslice normal forces and must be zero when summed over the entire sliding mass. After substituting for S_m and rearranging the terms, the factor of safety with respect to horizontal force equilibrium is:

$$F_f = \frac{\sum \left(c'\beta \cos \alpha + \left(N - u\beta\right) \tan \phi' \cos \alpha\right)}{\sum N \sin \alpha + \sum kW - \sum D \cos \omega \pm \sum A}$$

14.6 Slice normal force at the base

The normal force at the base of a slice is derived from the summation of forces in a vertical direction on each slice.

$$\left(X_L - X_R\right) - W + N\cos\alpha + S_m \sin\alpha - D\sin\omega = 0$$

Once again, after substituting for S_m the equation for the normal at the base of each slice is:

$$N = \frac{W + (X_R - X_L) - \left[\frac{c'\beta \sin\alpha - u\beta \tan\phi' \sin\alpha}{F}\right]}{\cos\alpha + \frac{\sin\alpha \tan\phi'}{F}}$$

The normal equation is nonlinear, with the value dependent on the factor of safety, F. The factor of safety is equal to the moment equilibrium factor of safety, F_m, when solving for moment equilibrium, and equal to the force factor of safety, F_f, when solving for force equilibrium.

The base normal equation cannot be solved directly, since the factor of safety (F) and the interslice shear forces, (i.e., X_L and X_R) are unknown. Consequently, N needs to be determined using an interactive scheme.

To commence the solution for the factor of safety, the interslice shear and normal forces are neglected and the normal force on each slice can be computed directly by summing forces in the same direction as the normal force.

$$N = W\cos\alpha - kW\sin\alpha + \left[D\cos\left(\omega + \alpha - 90\right)\right]$$

We can use this simplified normal equation to obtain starting values for the factor of safety computations. The factors of safety obtained using this simplified equation is the Fellenius or Ordinary method factor of safety.

If we ignore the interslice shear forces, but retain the interslice normal forces, then the slice base normal force equation is:

$$N = \frac{W - \frac{(c'\beta \sin\alpha + u\beta \sin\alpha \tan\phi')}{F} + \left[D \sin\omega\right]}{\cos\alpha + \frac{\sin\alpha \tan\phi'}{F}}$$

When we use this equation for the base normal, the factor of safety with respect to moment equilibrium is the Bishop Simplified factor of safety, and the factor of safety with respect to force equilibrium is the Janbu Simplified factor of safety.

14.7 M-alpha values

The denominator in the base normal equation is commonly given the variable name, m_α. This term can become problematic when the slice base inclination is too steep. As we can see from the above base normal equation and the diagram in Figure 14-4, the variable m_α is a function of inclination of the base of a slice, α, and $\tan\phi'/F$. Computational difficulties occur when m_α approaches zero. This situation can occur when α is negative and $\tan\phi'/F$ is large or when α is large and $\tan\phi'/F$ is small. Specifically, the m_α value will become zero when the base inclination of any slice, α, bears the following relationship to the mobilized friction angle, $\tan\phi'/F$:

$$\frac{\cos\alpha}{\sin\alpha} = \frac{1}{\tan\alpha} = -\frac{\tan\phi'}{F}$$

When the m_α value approaches zero, the computed normal force, N, on the slice becomes excessively large. As a result, the mobilized shearing resistance, S_m, becomes very large and exerts a disproportionately large influence on the computation of the factor of safety.

The factor of safety calculation can take on another extreme when m_α is negative. The m_α term can be negative when the base angle of the slice, α, is more negative than the limiting angle, α_1. In this case, the computed normal force is negative. Consequently, the computed factor of safety may be under-estimated, since the total mobilized shearing resistance is reduced. When a slice has a small, but negative mα value, its normal force becomes large and negative when compared with other slices. The large, negative value then dominates the stability calculations, and the computed factor of safety can go less than zero, which of course is meaningless.

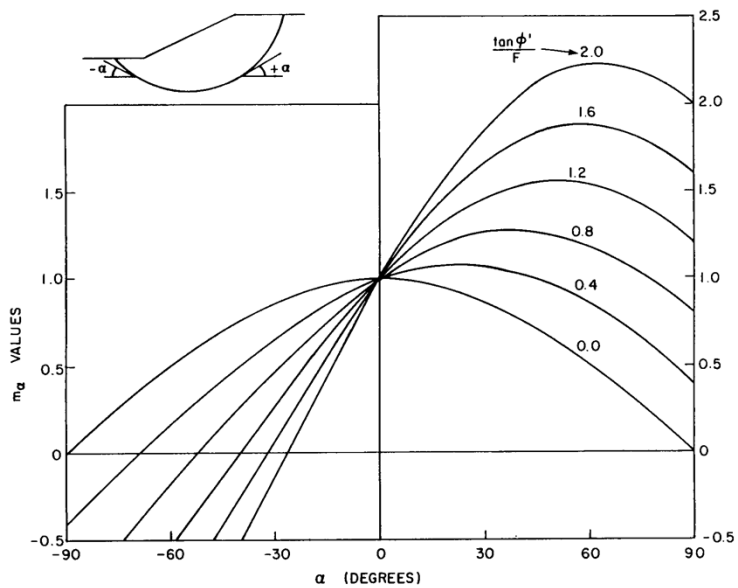

Figure 14-4 Magnitude of mα for various α, ϕ, and F values

Problems associated with the magnitude of m_α are mainly the result of an inappropriately assumed shape for the slip surface. Ideally, the classic earth pressure theory should be used to establish the limiting conditions for the shape of the slip surface. In applying the earth pressure theory, the soil is divided into two regions, namely an active earth pressure zone and a passive earth pressure zone. The inclination of the slip surface in the passive (toe) zone of the sliding mass should be limited to the maximum obliquity for the passive state. That is:

$$\alpha_1 < 45^0 - \frac{\phi'}{2}$$

Likewise, the inclination of the slip surface in the active (crest) zone should not exceed the value obtained from the following equation:

$$\alpha_1 < 45^0 + \frac{\phi'}{2}$$

These solutions will generally resolve the m_α problems. The active zone also may be combined with a vertical tension crack zone to alleviate m_α problems.

It is the responsibility of the user to ensure that the limiting angles with respect to the active and passive zones are not violated. However, if the conditions are violated, there is a check in SLOPE/W to prevent the absolute value of m_α from going too close to zero.

14.8 Interslice forces

The interslice forces are the normal and shear forces acting in the vertical faces between slices. The interslice normal forces are solved using an integration procedure commencing at the left end of each slip surface.

The summation of forces in a horizontal direction can be written for each slice as:

$$\left(E_L - E_R\right) - N\sin\alpha + S_m\cos\alpha - kW + D\cos\omega = 0$$

Substituting S_m in this and then solving for the interslice normal on the right side of each slice gives:

$$E_R = E_L + \frac{\left(c'\beta - u\beta\ \tan\ \phi'\right)\ \cos\ \alpha}{F} + N\left(\frac{\tan\ \phi'\ \cos\ \alpha}{F} - \sin\ \alpha\right)$$
$$- kW + D\cos\omega$$

Since the left interslice normal force of the first slice is zero (i.e., $E_L=0$), integrating from the left end of all slices, the interslice normal force of all slices can be computed. Note that the equation for computing the interslice normal force is depending on the factor of safety and it is updated during the iteration process.

Once the interslice normal force is known, the interslice shear force is computed as a percentage of the interslice normal force according to the following empirical equation proposed by Morgenstern and Price (1965):

$$X = E\,\lambda\,f\left(x\right)$$

where:

λ	=	the percentage (in decimal form) of the function used, and
$f(x)$	=	interslice force function representing the relative direction of the resultant interslice force.

Figure 14-5 shows some typical function shapes. The type of force function used in calculating the factor of safety is the prerogative of the user.

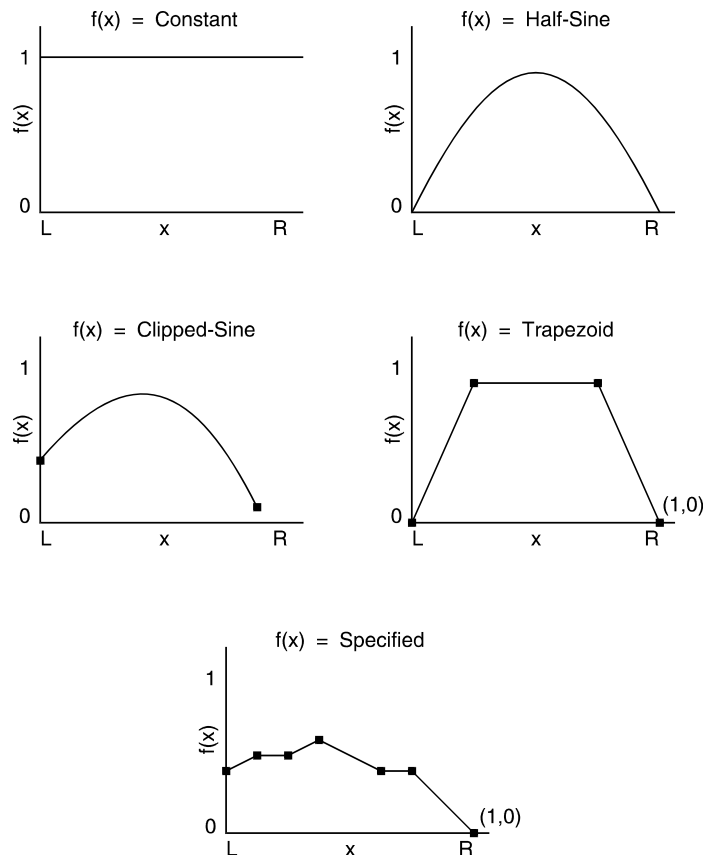

Figure 14-5 Example interslice force functions

The slices' interslice shear forces are required to calculate the normal force at the base of each slice. Figure 14-6 illustrates how the interslice force function $f(x)$ is used to compute the interslice shear force. Assume the use of a half-sine force function. Assume that the normal force E between Slice 1 and 2 is 100 kN, the applied Lambda value λ is 0.5 and a half-sine interslice force function is used. The $f(x)$ value at the location between Slice 1 and 2 is 0.45. The shear force X then is:

$f(x) = 0.45$

$\lambda = 0.5$

$E = 100$ kN

$X = 100 \times 0.5 \times 0.45 = 22.5$ kN

For this example, the ratio of shear to normal varies from 0.0 at the crest and at the toe, to a maximum of 0.5 at the midpoint along the slip surface.

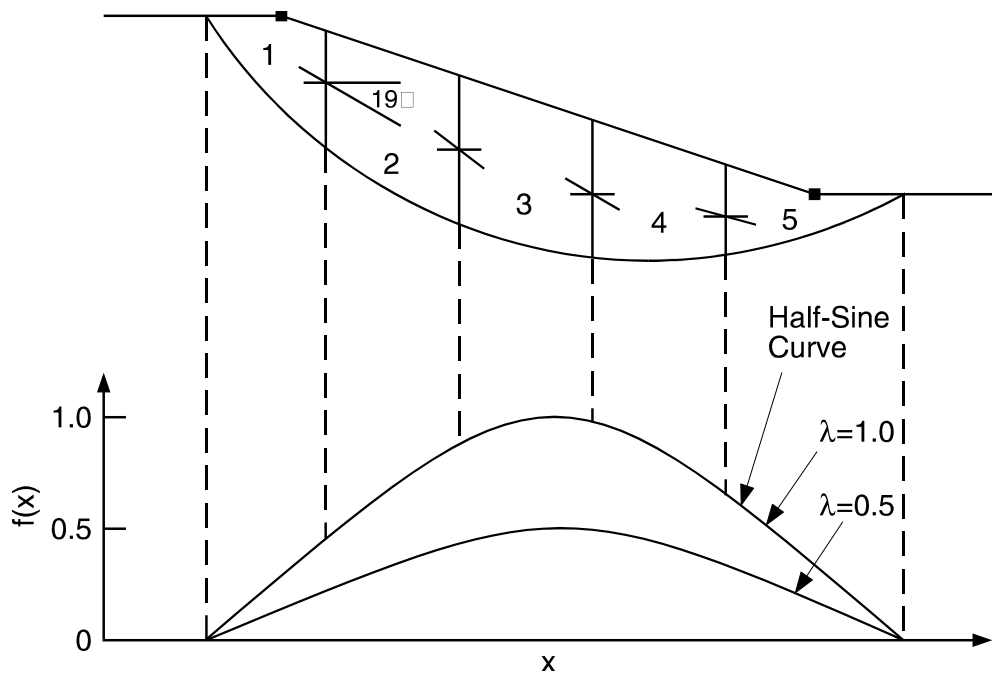

Figure 14-6 Example use of half-sine interslice force function

14.9 Effect of negative pore-water pressures

In locations above the groundwater table, the pore-water pressure in a soil is negative relative to the pore-air pressure. This negative pore-water pressure is commonly referred to as the matric suction of the soil. Under negative pore-water pressure conditions the shear strength may not change at the same rate as for total and positive pore-water pressure changes. Therefore, a modified form of the Mohr-Coulomb equation must be used to describe the shear strength of an unsaturated soil (i.e., a soil with negative pore-water pressures). The shear strength equation is:

$$s = c' + (\sigma_n - u_a)\tan\phi' + (u_a - u_w)\tan\phi^b$$

where:

u_a	=	pore-air pressure,
u_w	=	pore-water pressure, and
ϕ^b	=	an angle defining the increase in shear strength for an increase in suction.

This equation indicates that the shear strength of a soil can be considered as having three components: the cohesive strength due to c', the frictional strength due to ϕ and the suction strength due to ϕ^b.

14.10 Factor of safety for unsaturated soil

The mobilized shear can also be written for unsaturated soil conditions. In equation form:

$$S_m = \frac{\beta}{F}\left(c' + (\sigma_n - u_a)\tan\phi' + (u_a - u_w)\tan\phi^b\right)$$

The normal at the slice base is:

$$N = \frac{W + \left(X_R - X_L\right) - \dfrac{\left[c'\beta \sin\alpha + u_a \beta \sin\alpha \left(\tan\phi' - \tan\phi^b\right) + u_w \beta \sin\alpha \tan\phi^b\right]}{F} + D\sin\omega}{\cos\alpha + \dfrac{\sin\alpha \tan\phi'}{F}}$$

The above equation can be used for both saturated and unsaturated soils. For most analyzes the pore-air pressure can be set to zero. SLOPE/W uses ϕ^b whenever the pore-water pressure is negative and ϕ' whenever the pore-water pressure is positive.

SLOPE/W uses two independent factor of safety equations; one with respect to moment equilibrium and the other with respect to horizontal force equilibrium. When only moment equilibrium is satisfied, the factor of safety equation is:

$$F_m = \frac{\sum\left(c'\beta R + \left[N - u_w \beta \dfrac{\tan\phi^b}{\tan\phi'} - u_a \beta \left(1 - \dfrac{\tan\phi^b}{\tan\phi'}\right)\right] R \tan\phi'\right)}{\sum Wx - \sum Nf + \sum kWe \pm \sum Dd \pm \sum Aa}$$

The factor of safety equation with respect to horizontal force equilibrium is:

$$F_f = \frac{\sum\left(c'\beta \cos\alpha + \left[N - u_w \beta \dfrac{\tan\phi^b}{\tan\phi'} - u_a \beta \left(1 - \dfrac{\tan\phi^b}{\tan\phi'}\right)\right] \tan\phi' \cos\alpha\right)}{\sum N \sin_\alpha + \alpha \sum kW - \sum D \cos\omega \pm \sum A}$$

14.11 Use of unsaturated shear strength parameters

SLOPE/W only considers unsaturated shear strength conditions when the pore-water pressures are negative. Under these conditions the angle, ϕ^b, is used to compute the mobilized shear strength force at the base of a slice.

The following types of input data help in understanding how SLOPE/W accommodates unsaturated soil conditions:

When ϕ^b is left blank or set to 0.0, there will be no increase in the shear strength due to the negative pore-water pressures (suction). Often the engineer does not want to rely upon any shear strength due to the negative pore-water pressures. In this case, the ϕ^b angles should be set to 0.0.

The upper limit of ϕ^b is ϕ'. The input of a value of this magnitude states that negative pore-water pressures will be as effective in increasing the shear strength of a soil as positive pore-water pressures are in reducing the shear strength. This may be reasonable for the saturated capillary zone immediately above the groundwater table. However, the engineer must make the decision whether these negative pore-water pressures are likely to remain near the same magnitudes over the time span of interest.

Usually ϕ^b is greater than zero, but less than ϕ'. All published research literature has shown this to be the case in laboratory testing programs. Most common values range from 15 to 20 degrees. The use of ϕ^b is simple and gives a rough estimation as the increase of shear strength as a function of soil suction. The drawback of the use of ϕ^b is that the unsaturated strength envelop is assumed to be linearly increasing with soil suction which tends to overestimate the unsaturated shear strength particularly when the soil suction is very high.

Considerable research has been done to better quantify the unsaturated shear strength of a soil using the soil-water characteristic curve and the saturated shear strength parameters. In particular, Fredlund et. al.(1996) and Vanapalli et. al. (1996) developed simple equations to predict the shear strength of unsaturated soils. In their study, the predicted unsaturated strength of several soils compared reasonably well with laboratory and field measured data.

As a better alternative to the use of ϕ^b, SLOPE/W implemented the following equation proposed by Vanapalli et. al. (1996)

$$s = c' + (\sigma_n - u_a)\tan\phi' + (u_a - u_w)\left[\left(\frac{\theta_w - \theta_r}{\theta_s - \theta_r}\right)\tan\phi'\right]$$

In the above equation, θ_w is the volumetric water content, θ_s is the saturated volumetric water content and θ_r is the residual volumetric water content. This θ_r is the water cointent that soil suction strength becomes zero. In other words, the soil has drained so much that there is not sufficicent water phase available in the soil to generate any significant suction strength. SLOPE./W defaults this θ_r value to be 0.5 (50%) of the saturated volumetric water content, but depending on the material, you can enter any different value. Note that ϕ^b is not used in the above equation.

The unsaturated shear strength (s) of a soil can be estimated based on the soil-water characteristic curve and the saturated shear strength parameters of a soil.

14.12 Solving for the factors of safety

Four different stages are involved in computing the various factors of safety. The following section describes these stages.

Stage 1 solution

For the first iteration, both the interslice normal and shear forces are set to zero. The resulting moment equilibrium factor of safety is the Ordinary or Fellenius factor of safety. The force equilibrium factor of safety has received little mention in the literature and is of little significance. The first iteration factors of safety are used as approximations for starting the second stage.

Stage 2 solution

Stage 2 starts the solution of the nonlinear factor of safety equations. Lambda (λ) is set to zero and therefore, the interslice shear forces are set to zero. Usually 4 to 6 iterations are required to ensure convergence of the moment and force equilibrium factor of safety equations. The answer from the moment equation corresponds to Bishop's Simplified method. The answer from the force equilibrium equation corresponds to Janbu's Simplified method without any empirical correction.

Stage 3 solution

Stage 3 solution is required for all methods that consider interslice forces. In this stage, a series of lambda values are selected and the moment and/or force equilibrium factors of safety are solved. The factors of safety for various lambda values can be plotted as shown in Figure 14-7. The factor of safety satisfying both moment and force equilibrium is selected from the plot.

Stage 3 provides a complete understanding of the relationship between the moment and force equilibrium factors of safety for a specific interslice force function. It can be used to simulate essentially all slope stability methods that consider the interslice force function.

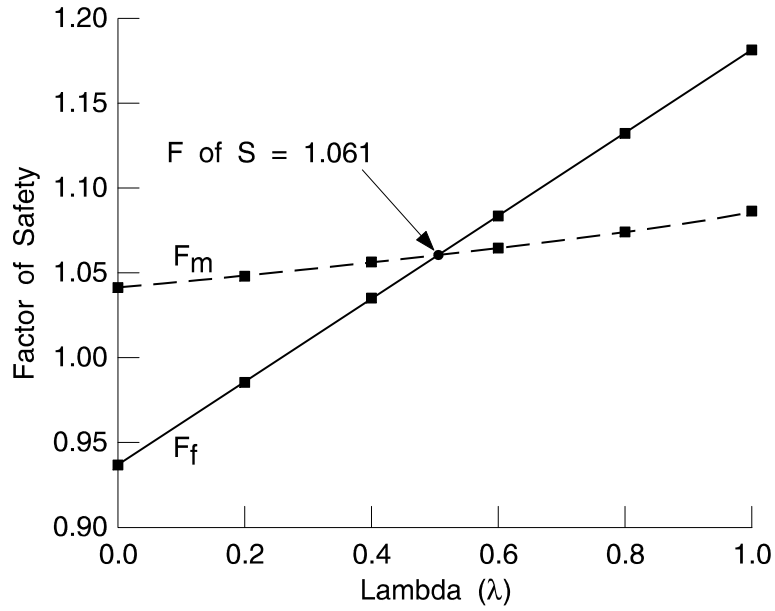

Figure 14-7 Example factor of safety versus lambda plot

14.13 Simulation of the various methods

The General Limit Equilibrium (GLE) formulation and solution can be used to simulate most of the commonly used methods of slices. From a theoretical standpoint, the various methods of slices can be categorized in terms of the conditions of static equilibrium satisfied and the assumption regarding the interslice forces. Table 14-3 summarizes the conditions of static equilibrium satisfied by many of the commonly used methods of slices. Table 14-4 summarizes the assumption used in each of the methods of slices to render the analysis determinate.

Table 14-3 Conditions of static equilibrium satisfied by various limit equilibrium methods

Method	Force Equilibrium		Moment Equilibrium
	1st Direction (e.g., Vertical)	2nd Direction (e.g., Horizontal)	
Ordinary or Fellenius	Yes	No	Yes
Bishop's Simplified	Yes	No	Yes
Janbu's Simplified	Yes	Yes	No
Spencer	Yes	Yes	Yes
Morgenstern-Price	Yes	Yes	Yes**
Corps of Engineers	Yes	Yes	No
Lowe-Karafiath	Yes	Yes	No
Janbu Generalized	Yes	Yes	No
Sarma	Yes	Yes	Yes
** Moment equilibrium on individual slice is used to calculate interslice shear forces			

Table 14-4 Assumptions used in various limit equilibrium methods

Method	Assumption
Ordinary or Fellenius	Interslice forces are neglected.
Bishop's Simplified	Resultant interslice forces are horizontal (i.e., there are no interslice shear forces).
Janbu's Simplified	Resultant interslice forces are horizontal. An empirical correction factor, f_o, can be used to account for interslice shear forces.
Spencer	Resultant interslice forces are of constant slope throughout the sliding mass.
Morgenstern-Price	Direction of the resultant interslice forces is determined using an arbitrary function. The percentage of the function, λ, required to satisfy moment and force equilibrium is computed with a rapid solver.
Corps of Engineers	Direction of the resultant interslice force is: i) equal to the average slope from the beginning to the end of the slip surface or ii) parallel to the ground surface.
Lowe-Karafiath	Direction of the resultant interslice force is equal to the average of the ground surface and the slope at the base of each slice.
Janbu Generalized	Location of the interslice normal force is defined by an assumed line of thrust.
Sarma	Direction of the resultant interslice force is calculated based on the interslice normal force and the user-specified cohesion and frictional angle between the interslice surface.

14.14 Spline interpolation

A spline interpolation technique is used to determine the pore-water pressure at the base of a slice when the pore-water pressures are defined at discrete points.

The technique involves the fitting of a spline function to a series of spatially distributed points. The fitting of the function to the points results in the calculation of weighting coefficients. The weighting coefficients can then be used to compute values for any other point in the region. Although the solving of a large problem using this technique requires considerable computer storage, it has been found that a small number of designated points can provide reasonably accurate results.

To illustrate the spline interpolation technique, consider the following two-dimensional problem. Suppose we know a set of values, u_i, at N given points (x_i,y_i *with* $i=1,N$), and we want to estimate the value of u at some other points, $M(x,y)$.

Let:

$$u(x,y) = P(x,y) + \sum_{i=1}^{N} \lambda_i K\left(h_m - h_i\right)$$

where:

$P(x,y)$	=	the chosen trend,
$K(h)$	=	the chosen interpolation function,
h	=	the distance between two points, (e.g., $h=h_m-h_i$)), where:

$$\left(h_m - h_i\right) = \left(x_m - x_i\right)^2 + \left(y_m - y_i\right)^2$$

λi	=	the computed weighting coefficients referred to as Kriging coefficients.

In the SLOPE/W formulation:

$$P\left(x, y\right) = a + bx + cy$$

and:

$$K\left(h\right) = \delta\left(0\right) + h^2 \log h$$

where $\delta(0)$ is the nugget effect. This will be explained later; for the present it is assumed to be zero.

The weighting coefficients ($a,b,c,\lambda_1, ,\lambda_2, \ldots.\lambda_N$) are the solution of the following set of linear equations:

$$\begin{bmatrix} K(0) \ldots & K(h_1\text{-}h_n) & 1 & x_1 & y_1 \\ & . & . & . & . \\ & & 1 & x_N & y_N \\ & & 0 & 0 & 0 \\ & & & 0 & 0 \\ & & & & 0 \end{bmatrix} \begin{bmatrix} \lambda_1 \\ . \\ . \\ a \\ b \\ c \end{bmatrix} = \begin{bmatrix} u_1 \\ . \\ u_N \\ 0 \\ 0 \\ 0 \end{bmatrix}$$

This system of linear equations is solved for the weighting coefficients. The value of $u(x,y)$ can now be computed at any point, x,y using the equation:

$$u\left(x, y\right) = a + bx + cy + \sum_{i-1}^{N} \left(\lambda_i \left(h_m - h_i\right)^2 \log\left(h_m - h_i\right)\right)$$

The following properties can be derived from this equation: At a point x_1,y_1, if a(0) = 0 and $K(0) = 0$), then $u(x_1,y_1) = u_1$. If for the point $x_1,y_1,K(0) = a_1$ *and* $u(x_1,y_1) \neq u_1$, then, $\delta(0) = \delta(1) \neq 0$.

Therefore, by selecting different nugget values for the initial points, it is possible to help the estimated values coincide with the initial values. At its limit, if $\delta(0)$ is the same for all points and its value becomes large:

$$u(x,y)=P(x,y)=a+bx+cy$$

This is equivalent to the least square solution of fitting.

With a function, $K(h) = h^2 \log h$, the solution of this spline problem can be visualized as a thin plate deforming in such a way as to pass through the deflection, u_i, at all points, x_i, y_i.

14.15 Moment axis

When the grid and radius method is used by default the moment factor of safety is computed by summing moments about each grid point. However, it is possible to use one single point at which to sum moments for all slip surfaces. This point is known as the axis. The grid point is used to define the shape of the slip surface, and the axis point is used for summing moments.

The position of the moment center has a negligible effect on factors of safety computed by methods that satisfy both force and moment equilibrium (e.g., the GLE, the Morgenstern-Price and the Spencer methods). The factor of safety can be slightly affected by the position of the moment axis when the slip surface is non-circular and the method satisfies only force or only moment equilibrium.

As a general rule, the axis point should be located approximately at the center of rotation of the slip surfaces.

14.16 Finite element stress method

In addition to the limit equilibrium methods of analysis, SLOPE/W also provides an alternative method of analysis using the stress state obtained from SIGMA/W, a GEO-SLOPE program for stress and deformation analysis. The following sections outline the theoretical basis and the solution procedures used by the SLOPE/W Finite Element Stress method.

Stability factor

As mentioned earlier in the Chapter, the factor of safety obtained using a limit equilibrium method is defined as that factor by which the shear strength of the soil must be reduced in order to bring the mass of soil into a state of limiting equilibrium along a selected slip surface. Furthermore, due to the nature of the method, the following two assumptions are made with respect to the factor of safety:

The factor of safety of the cohesive component of strength and the frictional component of strength are equal for all soils involved.

The factor of safety is the same for all slices.

The above assumptions are no longer necessary in the finite element stress method. In other words, the computed “factor of safety” using the finite element stress approach is not the same factor of safety as in the limit equilibrium approach. To preserve the original meaning of the factor of safety, the “factor of safety” computed using the Finite Element Stress method is referred to as the *stability factor* in SLOPE/W.

The stability factor (S.F.) of a slope by the finite element stress method is defined as the ratio of the summation of the available resisting shear force S_r along a slip surface to the summation of the mobilized shear force S_m along a slip surface In equation form, the stability factor (S.F.) is expressed as:

$$S.F. = \frac{\Sigma S_r}{\Sigma S_m}$$

The available resisting force of each slice is calculated by multiplying the shear strength of the soil at the base center of the slice with the base length. Therefore, from the modified form of the Mohr-Coulomb equation for an unsaturated soil the available resisting force is:

$$S_r = s\beta = \left(c' + (\sigma_n - u_a)\tan\phi' + (u_a - u_w)\tan\phi^b\right)\beta$$

where:

s	=	effective shear strength of the soil at the base center of a slice
β	=	base length of a slice
σ_n	=	normal stress at base center of a slice

Similarly, the mobilized shear force of each slice is calculated by multiplying the mobilized shear stress (τ_m) at the base center of the slice with the base length.

$$S_m = \tau_m \beta$$

A local stability factor of a slice can also be obtained when the available resisting shear force of a slice is compared to the mobilized shear force of a slice.

$$Local\ S.F. = \frac{S_r}{S_m} = \frac{s\beta}{\tau\beta}$$

Of significance is the fact that both the normal stress (σ_n) and the mobilized shear stress (τ_m) are computable values from a SIGMA/W analysis. Therefore, the equations for computing the stability factors are linear; that is, no iteration is required to establish the stability factors as in the limit equilibrium method. Iterations may be required in the SIGMA/W analysis, but not in the SLOPE/W analysis.

Normal stress and mobilized shear stress

To use the Finite Element Stress method, you need to start by performing a SIGMA/W analysis.

The information required from the SIGMA/W analysis is the stress state as describe by σ_x, σ_y and τ_{xy} at each Gauss point within each element. These stress values are used to compute the normal stress and the mobilized shear stress at the base center of each slice. The procedure is as follows:

Step 1: Element Nodal Stresses

SIGMA/W calculates and stores the computed stresses at element Gauss points. To compute the stress state at the slice base center, it is first necessary to establish the stress state at the element nodes. This is done by projecting the Gauss values to the nodes and then averaging the nodal values obtained from each adjoining element.

The projection is done with the use of the interpolating functions. In equation form:

$$f = \langle N \rangle \{F\}$$

where:

f	=	stress at the element nodes
$<N>$	=	matrix of the interpolating functions
$\{F\}$	=	stress values at the Gauss points

The interpolating functions are the same as the standard functions used to describe a variable within an element in terms of nodal values, except that the local coordinates are the reciprocal of the standard Gauss point integration points.

Consider, for example, if the local coordinates of a Gauss integration point inside an element are (0.577, 0.577). When the Gauss points are projected outward from the Gauss point to the corner node, the local coordinates for the closest corner node are (1.73, 1.73). Figure 14-8 illustrates this projection scheme for a quadrilateral element.

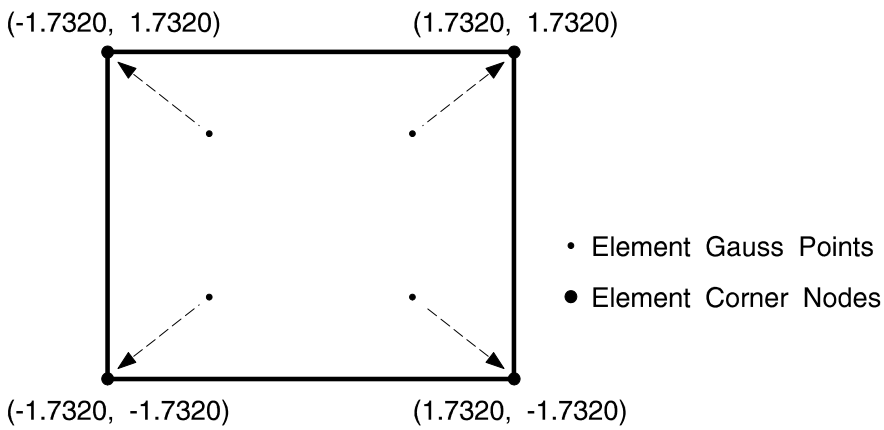

Figure 14-8 Projection from Gauss points to corners

The above projection is carried out for each element in a problem, and the values from each adjoining element are then averaged. Upon completing this procedure, σ_x, σ_y and τ_{xy} are known at each node in the entire mesh.

Step 3: Base Normal and Shear Stresses

The normal stress $\{\sigma_n\}$ and the mobilized shear stress (τ_m) at the base center are computed using the following Mohr circle-based equations:

$$\sigma_n = \frac{\sigma_x + \sigma_y}{2} + \frac{\sigma_x - \sigma_y}{2}\cos 2\theta + \tau_{xy}\sin 2\theta$$

$$\tau_m = \tau_{xy}\cos 2\theta - \frac{\sigma_x - \sigma_y}{2}\sin 2\theta$$

where:

σ_x	=	total stress in x-direction at the base center,
σ_y	=	total stress in y-direction at the base center,
τ_{xy}	=	shear stress in x- and y-directions at the base center, and
θ	=	angle measured from positive x-axis to the line of application of the normal stress.

The line of application of the normal stress is perpendicular to the base plane of the slice, whereas the line of application of the mobilized shear stress is parallel to the base plane.

14.17 Probabilistic slope stability analysis

Deterministic slope stability analyses compute the factor of safety based on a fixed set of conditions and material parameters. If the factor of safety is greater than unity, the slope is considered to be stable. On the contrary, if the factor of safety is less than unity, the slope is considered to be unstable or susceptible to failure. Deterministic analyses suffer from limitations; such as that the variability of the input parameters is not considered, and questions like "How stable is the slope?" cannot be answered.

Probabilistic slope stability analysis allows for the consideration of variability in the input parameters and it quantifies the probability of failure of a slope. SLOPE/W can perform probabilistic slope stability analyses using the Monte Carlo method.

SLOPE/W allows the following parameter variability distribution functions: Normal, Lognormal, Uniform, Triangular and Generalized Spline function. Details of these functions are discussed in the Probabilistic and Sensitivity Analyses Chapter.

Monte Carlo method

The Monte Carlo method is a simple, but versatile computational procedure that is suitable for a high speed computer. In general, the implementation of the method involves the following steps:

- The selection of a deterministic solution procedure, such as the Spencer's method or the finite element stress method.
- The decisions regarding which input parameters are to be modeled probabilistically and the representation of their variability in terms of a selected distribution model.
- The conversion of any distribution function into a sampling function, the random sampling of new input parameters and the determination of new factors of safety many times.
- The computation of the probability of failure based on the number of factors of safety less than 1.0 with respect to the total number of converged slip surfaces. For example, in an analysis with 1000 Monte Carlo trials, 980 trials produce a converged factor of safety and 98 trials produce a factor of safety of less than 1.0. The probability of failure is 10.0 %.

In SLOPE/W, one or more most critical slip surfaces are first determined based on the mean value of the input parameters using any of the limit equilibrium and finite element stress methods. Probabilistic analysis is then performed on these critical slip surfaces, taking into consideration the variability of the input parameters.

The number of Monte Carlo trials in an analysis is dependent on the number of variable input parameters and the expected probability of failure. In general, the number of required trials increases as the number

of variable input increases or the expected probability of failure becomes smaller. It is not unusual to do thousands of trials in order to achieve an acceptable level of confidence in a Monte Carlo probabilistic slope stability analysis.

Parameter variability

Soils are naturally formed materials; consequently their physical properties vary from point to point. This variation occurs even in an apparently homogeneous layer. The variability in the value of soil properties is a major contributor to the uncertainty in the stability of a slope. Laboratory results on natural soils indicate that most soil properties can be considered as random variables conforming to the normal distribution function.

In SLOPE/W, the variability of the following input parameters can be considered:

- Material parameters for the various material strength models, including unit weight, cohesion and frictional angles,
- Pore-water pressure conditions,
- The magnitude of the applied point loads, and
- The horizontal and vertical seismic coefficients.

Random number generation

Fundamental to the Monte Carlo method are the randomly generated input parameters that are fed into a deterministic model. In SLOPE/W, this is done using a random number generation function. The random numbers generated from the function are uniformly distributed with values between 0 and 1.0. The generated random number is then used to get a new parameter value for the sampling function.

Correlation coefficient

A correlation coefficient expresses the relative strength of the association between two parameters. Laboratory tests on a wide variety of soils (; and W) show that the shear strength parameters c and ϕ are often negatively correlated with correlation coefficient ranges from -0.72 to 0.35. Correlation between strength parameters may affect the probability distribution of a slope. SLOPE/W allows the specification of c and ϕ correlation coefficients for all soil models using c and ϕ parameters. Furthermore, in the case of a bilinear soil model, SLOPE/W allows the specification of correlation coefficient for ϕ and $\phi 2$.

Correlation coefficients will always fall between -1 and 1. When the correlation coefficient is positive, c and ϕ are positively correlated implying that larger values of c are more likely to occur with larger values of ϕ. Similarly, when the correlation coefficient is negative, c and ϕ are negatively correlated and reflects the tendency of a larger value of c to occur with a smaller value of ϕ. A zero correlation coefficient implies that c and ϕ are independent parameters.

In SLOPE/W, when estimating a new trial value for ϕ and $\phi 2$, the normalized random number is adjusted to consider the effect of correlation. The following equation is used in the adjustment:

$$N_a = N_1 k + \left(1 - |k|\right) N_2$$

where:

k	=	correlation coefficient between the first and second parameters,
N_1	=	normalized random number for the first parameter,

N_2 = normalized random number for the second parameter, and

N_a = adjusted normalized random number for the second parameter.

Number of Monte Carlo trials

Probabilistic slope stability analysis using the Monte Carlo method involves many trial runs. Theoretically, the more trial runs used in an analysis the more accurate the solution will be. How many trials are required in a probabilistic slope stability analysis? It has been suggested that the number of required Monte Carlo trials is dependent on the desired level of confidence in the solution, as well as the number of variables being considered. Statistically, the following equation can be developed:

$$N_{mc} = \left[\frac{\left(d^2\right)}{\left(4\left(1-\varepsilon\right)^2\right)} \right]^m$$

where:

N_{mc} = number of Monte Carlo trials,

ε = the desired level of confidence (0 to 100%) expressed in decimal form,

d = the normal standard deviate corresponding to the level of confidence, and

m = number of variables.

The number of Monte Carlo trials increases geometrically with the level of confidence and the number of variables. For example, if the desired level of confidence is 80%, the normal standard deviate will be 1.28; the number of Monte Carlo trials will be 10 for 1 variable, 100 for 2 variables and 1,000 for 3 variables. For a 90% level of confidence, the normal standard deviate will be 1.64; the number of Monte Carlo trials will be 67 for 1 variable, 4,489 for 2 variables and 300,763 for 3 variables. In fact, for a 100% level of confidence, an infinite number of trials will be required.

For practical purposes, the number of Monte Carlo trials to be conducted is usually in the order of thousands. This may not be sufficient for a high level of confidence with multiple variables; fortunately, in most cases, the solution is not very sensitive to the number of trials after a few thousands trials have been run. Furthermore, for most engineering projects, the degree of uncertainty in the input parameters may not warrant a high level of confidence in a probabilistic analysis.

References

Abramson, L.W., Lee, T.S., Sharma, S., and Boyce, G.M., 2002. Slope Stability and Stabilization Methods. John Wiley & Sons Inc. pp.712.

Budhu, M. 2007. Soil Mechanics and Foundations, 2nd Edition. John Wiley & Sons.

Bishop, A.W. and Morgenstern, N., 1960. Stability coefficients for earth slopes. Geotechnique, Vol. 10, No. 4, pp. 164 169.

Christian, J.T., Ladd, C.C. and Baecher, G.B., 1994. Reliability Applied to Slope Stability Analysis. Journal of Geotechnical Engineering, Vol. 120, No. 12. pp. 2180-2207.

Corps of Engineers (2003) "Appendix G - Procedures and Examples for Rapid Drawdown". Engineering Manual, EM 1110-2-1902. Department of the U.S Army Corps of Engineers.

Duncan, J.M.,Wright S.G. and Wong, K.S. (1990). "Slope Stability during Rapid Drawdown". Proceedings of H. Bolton Seed Memorial Symposium. Vol. 2.

El-Ramly, H., Morgenstern, N.R., Cruden, D.M. 2002. Probabilistic Slope Stability Analysis for Practice. Canadian Geotechnical Journal. Vol. 39. pp. 665-683.

Fellenius, W., 1936. Calculation of the Stability of Earth Dams. Proceedings of the Second Congress of Large Dams, Vol. 4, pp. 445-463.

Fredlund, D.G., 1974. Slope Stability Analysis. User's Manual CD-4, Department of Civil Engineering, University of Saskatchewan, Saskatoon, Canada.

Fredlund, D.G., and Krahn, J., 1977. Comparison of slope stability methods of analysis. Canadian Geotechnical Journal, Vol. 14, No. 3, pp. 429 439.

Fredlund, D.G., Krahn, J., and Pufahl, D. 1981. The relationship between limit equilibrium slope stability methods. Proc. 10th Int. Conf. Soil Mech. Found. Eng. (Stockholm, Sweden), Vol. 3, pp. 409-416.

Fredlund, D.G., Zhang, Z.M. and Lam, L., 1992. Effect of the Axis of Moment Equlibrium in Slope Stability Analysis. Canadian Geotechnical Journal, Vol. 29, No. 3.

Fredlund, D.G., Xing, A. Fredlund M.D., and Barbour, S.L., 1996. The Relationship of the Unsaturated Soil Shear Strength to the Soil-water Characteristic Curve. Canadian Geotechnical Journal, Vol. 33, pp. 440-448.

Greco, V.R. 1996. Efficient Monte Carlo Technique for Locating Critical Slip Surface. Journal of Geotechincal Engineering. Vol 122, No. 7. ASCE, pp.517-525.

Grivas, D.A., 1981. How Reliable are the Present Slope Failure Prediction Methods? Proceedings of the Tenth International Conference of Soil Mechanics and Foundation Engineering, Stockholm, Sweden, Vol. 3, pp.427-430.

Harr, M.E., 1987. Reliability-Based Design in Civil Engineering. McGraw-Hill Book Company. pp. 290.

Higdon A., Ohlsen, E.H., Stiles, W.B., Weese, J.A. and Riley, W.F., 1978. Mechanics of Materials. John Wiley & Sons. pp.752.

Hoek, E. 2000. Course Notes entitled Practical Rock Engineering (2000 ed., Chapter 11).

Hoek, E., Bray, J.W., 1974. Rock Slope Engineering – Appendix 3. Published for the Institute of Mining and Metallurgy., pp. 352 – 354.

Hoek, E., Carranza-Torres, C. and Corkum, B., 2002. Hoek-Brown Failure Criterion – 2002 Edition. Proc. North American Rock Mechanics Society meeting in Toronto in July 2002.

Janbu, N., Bjerrum, J. and Kjaernsli, B., 1956. Stabilitetsberegning for Fyllinger Skjaeringer og Naturlige Skraninger. Norwegian Geotechnical Publications, No. 16, Oslo.

Janbu, N. 1954. Applications of Composite Slip Surfaces for Stability Analysis. In Proceedings of the European Conference on the Stability of Earth Slopes, Stockholm, Vol. 3, p. 39-43.

Krahn, J., 2003. The 2001 R.M. Hardy Lecture: The Limits of Limit Equilibrium Analyses. Canadian Geotechnical Journal, Vol. 40. pp.643-660.

Krahn, J., Price, V.E., and Morgenstern, N.R., 1971. Slope Stability Computer Program for Morgenstern-Price Method of Analysis. User's Manual No. 14, University of Alberta, Edmonton, Canada.

Kramer, S.L. 1996. Geotechnical Earthquake Engineering. Prentice Hall, pp. 437.

Ladd, C.C., 1991. Stability evaluation during staged construction: 22nd Terzaghi Lecture. Journal of Geotechnical Engineering, ASCE, 117(4), pp. 537-615

Ladd, C.C. and Foott, R. 1974. New Design Procedure for Stability of Soft Clays. Journal of the Geotechnical Engineering Division, ASCE, Vol. 100, (GT7), pp. 763-786.

Lam, L., and Fredlund D.G., 1993. A general Limit Equilibrium Model for Three-Dimensional Slope Stability Analysis. Canadian Geotechnical Journal. Vol. 30. pp. 905-919.

Lambe, T.W. and Whitman, R.V., 1969. Soil Mechanics. John Wiley and Sons, pp. 359-365.

Lapin, L.L., 1983. Probability and Statistics for Modern Engineering. PWS Publishers. pp. 624.

Li, K.S. and Lumb, P., 1987. Probabilistic Design of Slopes. Canadian Geotechnical Journal, Vol. 24, No. 4, pp. 520-535.

Lumb, P., 1966. The Variability of Natural Soils. Canadian Geotechnical Journal, Vol. 3, No. 2, pp. 74-97.

Lumb, P., 1970. Safety Factors and the Probability Distribution of Soil Strength . Canadian Geotechnical Journal, Vol. 7, No. 3, pp. 225-242.

Malkawi, A.I.H, Hassan, W.F. and Sarma, S.K. 2001. Global Serach Method for Locating General Slip Surface Using Monte Carlo Technique. Journal of Geotechnical and Geoenvironmental Engineering. Vol 127, No. 8, pp. 688-698.

Morgenstern, N.R., and Price, V.E., 1965. The Analysis of the Stability of General Slip Surfaces. Geotechnique, Vol. 15, pp. 79-93.

Mostyn, G.R. and Li, K.S., 1993. Probabilistic Slope Stability Analysis - State-of-Play, Proceedings of the Conference on Probabilistic Methods in Geotechnical Engineering, Canberra, Australia. pp. 281-290.

Petterson, K.E. 1955. The Early History of Circular Sliding Surfaces, Geotechnique, Vol. 5, p. 275-296.

Sarma, S.K., 1973. Stability Analysis of Embankments and Slopes. Geotechnique, Vol. 23 (3), pp. 423-433.

Sarma, S.K., 1979. Stability Analysis of Embankments and Slopes. Journal of the Geotechnical Engineering Division. ASCE. Vol. 105, No. GT12. pp. 1511-1524.

Smith, G.N., 1974. Elements of Soil Mechanics for Civil and Mining Engineers. Crosby Lockwood Staples, London. pp. 126-144.

Spencer, E. 1967. A Method of Analysis of Embankments assuming Parallel Inter-slice Forces. Geotechnique, Vol 17 (1), pp. 11-26.

Soulié, M., Montes, P. and Silvestri, V. 1990. Modelling Spatial Variability of Soil Parameters, Canadian Geotechnical Journal, Vol. 27, No. 5, pp. 617-630.

Vanapalli, S.K., Fredlund D.G., Pufahl, D.E. and Clifton, A.W., 1996. Model for the Prediction of Shear Strength with respect to Soil Suction. Canadian Geotechnical Journal, Vol. 33, pp. 379-392.

Vanmarcke, E.H., 1983. Random Fields: Analysis and Synthesis. MIT Press, Cambridge, Mass.

Whitman, R.V. and Bailey, W.A., 1967. Use of Computer for Slope Stability Analysis. Journal of the Soil Mechanics and Foundation Division of ASCE, Vol. 93, No. SM4.

Wolff, T.F, 1985. Analysis and Design of Embankment Dams: A Probabilistic Approach. Ph.D. Thesis, Purdue University, West Lafayette, IN.

Index

ϕ^b.....226
Add-in 112
Anchors and nails.....152
anisotropic function.....120
Anisotropic strength 119
B-bar coefficients.....136
Bedrock.....117
Bilinear.....117
Bishop's simplified 34
Block slip surface 13
Block specified slip surface 73
C – ϕ correlation 200
Circular slip surface.....11
Closed form curve fits.....112
Composite slip surface.....13
Composite slip surfaces 68
Convergence 150
Corps of Engineers method 43
Correlation coefficient.....235
data-point strength envelope.....118
Deep-seated instability.....163
Definition of variables.....215
Distributing the reinforcement load148
Dynamic analysis 183
Dynamic Stability 177
Entry and exit specification 77
F of S dependent.....144
Factor of Safety contours 67
factor of safety error code.....89
Finite element computed pressures138
Finite element stress method.....231
Finite element stress-based method51
Force equilibrium.....220
Fully specified slip surfaces.....71
Functions 109
General limit equilibrium method7, 219
General Limit Equilibrium Method 27
Geometry.....95
Geosynthetic.....155
GLE formulation.....7
Grid and radius for circular slips 63
Ground surface line 99
Hoek & Brown.....124
Illustrative Examples.....236
Interslice assumption.....43
Interslice force functions 11
Interslice forces 223
Invalid slip surfaces.....89
Janbu generalized method 20
Janbu's simplified method.....36
Lambda (λ).....8
Limit Equilibrium Fundamentals.....5
line loads.....100
Liquefaction stability 187

Lowe-Karafiath method 46
M-alpha 221
Material Strength.....115
Method basics 6
Minimum depth.....86
Missing physics 21
Mobilization of reinforcement forces143
Mohr-Coulomb 115
Moment axis 231
Moment equilibrium.....220
Monte Carlo.....234
Monte Carlo trials.....201
Morgenstern-Price method 40
Multiple piezometric lines 134
Newmark procedure.....187
Optimization 79
Ordinary or Fellenius 31
Parameter variability 235
passive earth pressure.....163
Permanent deformation.....185
Phreatic correction 134
Piezometric surfaces.....133
Piles.....158
Planar slip surface.....12
Pore-water.....133
Pore-water pressures at discrete points.....137
probabilistic analyses.....191
Probabilistic slope stability analysis234
Probability density functions.....191
probability of failure 201
Pseudostatic analysis.....179
Rapid Drawdown 58
Regions 95
Reinforcement 143
reliability index 201
R_u Coefficients.....135
safety map 68
sampling distance 204
Sarma method 48
Seepage forces.....23
Seismic 177
Sensitivity analyses 207
Sheet pile walls 162
Slice discretization 97
Slip surface shapes.....11
Slip Surface Shapes 63
soil strength 82
Soil-structure interaction.....171
soil-water characteristic curve.....227
Spatial functions 112
Spatial variability 202
Spencer method 37
Spline 109
Stability factor 231
staged rapid drawdown method ...60
steady state strength 116, 187
Strength as a function of depth ...121
Stress distributions 15

Structural Components.....143
surcharge pressures.....102, 103
Tension cracks 86
Tie-back wall 168
Total Cohesion and Total Phi 116
Undrained strength.....84, 117
unit weight.....130
unsaturated shear strength 226
Unsaturated shear strength.....129
variogram.....206

A consistent set of units

		Example of	Example of
Property	**Units**	**Metric Units**	**Imperial Units**
Geometry	L	meters	feet
Unit Weight of Water	F/L^3	kN/m^3	p.c.f.
Soil Unit Weight	F/L^3	kN/m3	p.c.f.
Cohesion	F/L^2	kN/m^2	p.s.f.
Water Pressure	F/L^2	kN/m^2	p.s.f.
Pressure Head	L	m	ft.
Point Load	F/L	kN/m	lbs/ft.
acceleration	F/T^2	m/s^2	ft/s^2
velocity	F/L	m/s	ft/s
deformation	L	m	ft.